SCHOOL OF CIVIL ENGINEERING

JOINT HIGHWAY RESEARCH PROJECT

JHRP-75-17

EVALUATION OF CONTINUOUSLY REINFORCED CONCRETE PAVEMENTS IN INDIANA

Asif Faiz

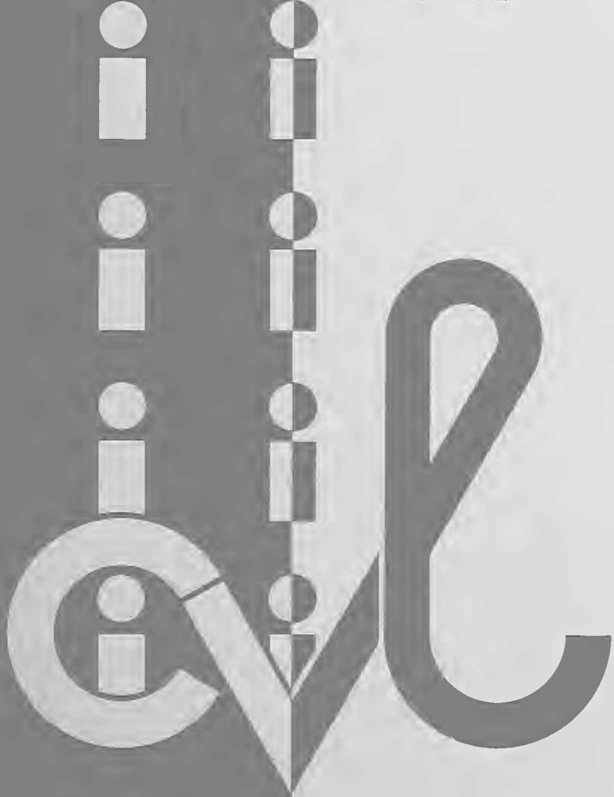

PURDUE UNIVERSITY
INDIANA STATE HIGHWAY COMMISSION

Digitized by the Internet Archive
in 2011 with funding from
LYRASIS members and Sloan Foundation; Indiana Department of Transportation

http://www.archive.org/details/evaluationofcont00faiz

Final Report

EVALUATION OF CONTINUOUSLY REINFORCED CONCRETE PAVEMENTS IN INDIANA

TO: J. F. McLaughlin, Director
Joint Highway Research Project

October 1, 1975

Project: C-36-52J

FROM: H. L. Michael, Associate Director
Joint Highway Research Project

File: 6-20-10

Attached is a Final Report on the JHRP Research Project titled "Evaluation of Continuously Reinforced Concrete Pavements in Indiana". The title of the Report is the same. It has been authored by Mr. Asif Faiz, Graduate Instructor in Research on our staff, who also used the Report as his thesis for the Ph.D. degree. Professor E. J. Yoder directed the study and preparation of the Report.

The findings reported herein will be useful in developing an improved design of CRC pavements for use in Indiana and should also be of value in other states. The research was performed in response to a problem encountered by Indiana with CRC pavements and provides much information valuable in the understanding and solution of that problem.

The Report is submitted as fulfillment of the objectives of the Research.

Respectfully submitted,

Harold L Michael

Harold L. Michael
Associate Director

HLM:sas

cc: W. L. Dolch
R. L. Eskew
G. D. Gibson
W. H. Goetz
M. J. Gutzwiller
G. K. Hallock
M. L. Hayes
C. W. Lovell
G. W. Marks
R. F. Marsh
R. D. Miles
P. L. Owens
G. T. Satterly
C. F. Scholer
M. B. Scott
K. C. Sinha
L. E. Wood
E. J. Yoder
S. R. Yoder

Final Report

EVALUATION OF CONTINUOUSLY REINFORCED CONCRETE PAVEMENTS IN INDIANA

by

Asif Faiz
Graduate Instructor in Research

Joint Highway Research Project

Project No.: C-36-52J

File No.: 6-20-10

Prepared as Part of an Investigation

Conducted by

Joint Highway Research Project
Engineering Experiment Station
Purdue University

in cooperation with the

Indiana State Highway Commission

Purdue University
West Lafayette, Indiana
October 1, 1975

ACKNOWLEDGMENTS

This report represents the culmination of three years of hard work, perseverance, and patience on part of many people who were instrumental in making this study a successful and worthwhile effort.

The study was conceived, developed, and conducted under the guidance of Professor Eldon J. Yoder. Without his interest and personal involvement in all phases of the work, it would have been difficult to conduct this investigation. The careful and thorough review of the manuscript by Professor Yoder helped in improving the quality of the work. The author's association with Professor Yoder has been a source of guidance and education, not only in the area of academic pursuit, but in the broader sphere of human relations, professional development, and personal conduct. It has been the author's good fortune to reap numerous benefits from this close association.

The responsibility of managing the detailed field study fell on the shoulders of Professor Donald G. Shurig. He performed an admirable task of coordinating the field work, which required close cooperation among personnel from Indiana State Highway Commission (ISHC) and Purdue University.

The generous help in funds, equipment and personnel provided by ISHC was invaluable to the success of this investigation. In particular, the assistance rendered, by the District Engineers and the staff of Crawfordsville, Greenfield, and LaPorte Districts; the Materials and Tests Division; and the Director and staff of the Research and Training Center (all of Indiana State Highway Commission),is duly acknowledged.

The author is grateful to Purdue University for the financial assistance to pursue graduate studies.

The help given by Professor Virgil L. Anderson in statistical experimental designs and data analysis, since the inception of this research, is gratefully acknowledged. The author is particularly indebted for the many hours spent with Professor Anderson in developing appropriate experimental design models and delving into the intricate world of restriction errors, inference space,and randomization.

Many other individuals made significant contributions to the study. Professor Harold L. Michael offered advice in developing the model for traffic load applications. Professor Charles H. Scholer and Mr. Robert Barnes helped in testing the concrete cores obtained during the field study. Professor James E. Newman of the Agronomy Department provided meterological data from which temperature variables were developed. Professor Robert D. Miles made available soil and airphoto strip maps for use in the study. Mr. Atef Gadallah, the author's close colleague, took an active part in various phases of the study. The author is also grateful to Professors Virgil Anderson, Harold Michael, and Robert Miles for their review of the manuscript.

A number of Civil Engineering undergraduates helped in the most tedious part of the work. Messrs. Tim Garland, Bill Dudley, John Tomko and Lou Dasaro deserve praise for their hard work.

Appreciation is due to Ms. Marian Foltz and Ms. Jan Smith for typing the manuscript.

Finally, the author is grateful for the moral support, affection,and care tendered by his wife, Surraya. There were numerous weekends when she painstakingly performed difficult and boring calculations to meet deadlines.

TABLE OF CONTENTS

Page

LIST OF TABLES ix

LIST OF FIGURES. xvii

ABSTRACT xxi

PART 1. PROBLEM DEFINITION

INTRODUCTION 1

  Use of Continuously Reinforced Concrete Pavements. 3
  Continuously Reinforced Concrete Pavements in Indiana 5

BACKGROUND OF THIS RESEARCH. 8

CRC PAVEMENT TECHNOLOGY - A REVIEW 10

  Theoretical Concepts. 12
    Reinforcement. 12
    Pavement Slab Thickness and Support Elements. 16
    Terminal Effects 21
  Structural Design of Continuously Reinforced Concrete Pavements 22
    Current Design Methods 23
    Reinforcement. 24
    Pavement Slab Thickness. 26
    Subbase and Subgrade 27
    Transverse Construction Joint. 27
    Terminal Provisions. 28
  Construction Practice 28
    Type of Steel. 28
    Method of Placement of Steel 29
    Method of Paving 30
    Subbase and Subgrade 30

TABLE OF CONTENTS (Continued)

Page

DESIGN OF THIS RESEARCH. 31

Study Objectives. 31
Scope of the Study. 31
Research Approach 33

PART II. STATEWIDE CRCP CONDITION SURVEY

STATEWIDE CONDITION SURVEY 35

Study Design. 35
  Sampling Procedure 36
  Data Collection. 37
  Statistical Design 39
  Independent Factors. 39
  Covariates or Concomitant Variables. 43
  Response or Evaluated Variables. 43
Analysis and Results. 44
  Factors Affecting Distress as Evaluated by Number of Defects per Section 52
  Factors Affecting Pavement Cracking. 52
  Detailed Study of Factors Influencing Performance of CRC Pavements. 53
  Distribution of Defects. 74
Summary of Results of Statewide Condition Survey. . 74
Postscript. 77

PART III. DETAILED EVALUATION OF SELECTED CRCP TEST SECTIONS-FIELD AND LABORATORY STUDIES

DESIGN OF DETAILED EVALUATION STUDY. 78

Study Design. 78
  Delineation of Test Sections 79
Collection of Field Data. 80
Laboratory Testing Program. 87
Approach to Data Analysis 88

FIELD AND LABORATORY TEST PROCEDURES 89

Field Test Procedures 89
  Equipment Used in the CRCP Field Study 98
Laboratory Test Procedures. 101
  Tests on Concrete Cores. 102
  Tests on Subbase and Subgrade Materials. 103
Presentation of Test Data 109

TABLE OF CONTENTS (Continued)

Page

COMPARISON OF FAILED TEST LOCATIONS WITH GOOD TEST LOCATIONS WITHIN TEST SECTIONS 111

Comparison of Material Properties 112
  Subgrade Properties. 112
  Properties of Granular Subbases. 118
  Properties of Bituminous Stabilized Subbases . 129
  Concrete Properties. 133
Comparison of Measures of Performance 139
  Dynamic Pavement Deflection. 139
  Surface Curvature Index. 146
  Crack Width. 156
  Crack Spacing. 161
  Crack Intersections. 163
Summary of Results. 165

TEST SECTIONS WITH FAILURES VS. TEST SECTIONS WITHOUT FAILURES: A COMPARISON 169

Comparison of Material Properties 170
  Subgrade Properties. 170
  Properties of Granular Subbases. 173
  Properties of Bituminous Stabilized Subbase. . 178
  Concrete Properties. 179
Comparison of Measures of Performance 186
  Dynamic Pavement Deflection. 186
  Surface Curvature Index. 201
  Crack Width, Spacing and Intersections 205
Analysis of Temperature Variables 205
Traffic Analysis. 207
Summary of Results. 209

EVALUATION OF CONSTRUCTION VARIABLES AND STEEL REINFORCEMENT REQUIREMENTS. 213

Effect of Construction Variables on Properties of Concrete. 213
Effect of Construction Variables on Pavement Cracking Parameters. 222
Minimum Steel Requirements for CRCP 229

DISCUSSION OF RESULTS. 238

Material Properties 238
  Subgrade Properties. 238
  Properties of Granular (Graded Aggregate) Subbases. 243
  Properties of Bituminous Stabilized Subbase. . 256
  Concrete Properties. 256

TABLE OF CONTENTS (Continued)

Page

Design Considerations 257
Construction Factors. 261
Temperature and Traffic Variables 262
Pavement Response Functions 263

PART IV. CONCLUSIONS AND RECOMMENDATIONS

CONCLUSIONS. 269

RECOMMENDATIONS. 273

CRCP Structural Design. 273
Material Specifications 274
Construction. 275

REFERENCES 276

APPENDICES

Appendix A. 282
Appendix B. 286
Appendix C. 303
Appendix D. 342
Appendix E. 347

VITA 356

LIST OF TABLES

Table		Page
1	Data Obtained During Statewide Condition Survey of CRC Pavements	38
2	Factorial Design for Study of Factors Influencing CRCP Performance.	40
3	Foster-Burr Test for Homogeneity of Variance.	47
4	Least Squares Analysis of Covariance - Number of Defects per Section	48
5	Least Squares Analysis of Covariance - Number of Asphalt Patches and Breakups per Section	49
6	Least Squares Analysis of Covariance - Length of Pavement Section Showing Random Cracks Plus Close Parallel Cracks	50
7	Least Squares Analysis of Covariance - Number of Spalled Cracks per Section.	51
8	Variation of Defects per Section with Type of Subbase	54
9	Variation of Asphalt Patches and Breakups per Section with Type of Subbase.	58
10	Effect of Subbase Type on CRC Pavement Pumping	59
11	Variation of Defects per Section with Type of Steel Reinforcement.	61
12	Variation of Asphalt Patches and Breakups per Section with Methods of Paving and Steel Placement	62
13	Variation of Length of Cracking in Feet per Section with Methods of Paving and Steel Placement	63

LIST OF TABLES (Continued)

Table Page

14 Effect of Method of Construction on Distribution of Defects and Length of Cracking Per Section. 65

15 Change in Number of Defects per Mile by Subbase Type (I-65). 67

16 Change in Number of Defects per Mile by Construction Type (I-65) 67

17 Equivalence Coefficient, F, for Classes of Truck Routes 69

18 Effect of Cumulative Load Applications on Distribution of Defects Among Sections . 73

19 Effect of Slump on Distribution of Defects Among Sections. 73

20 Permeability Relationships. 110

21 Summary of Analysis of Variance - Subgrade CBR (Percent) 114

22 Variation of Subgrade and Subbase CBR with Pavement Condition and Location of Test Points 116

23 Variation of Subgrade Characteristics with Pavement Condition 117

24 Summary of Analysis of Variance - Percent Passing #40 Sieve (Subgrade). 119

25 Summary of Analysis of Variance - Percent Passing #4 Sieve (Subgrade) 120

26 Summary of Analysis of Variance - Subbase CBR (Percent) 122

27 Summary of Analysis of Variance - Percent Compaction (Subbase). 124

28 Variation of Granular Subbase Characteristics with Pavement Condition . . 125

LIST OF TABLES (Continued)

Table		Page
29	Summary of Analysis of Variance - Permeability at 25°C (ft/day)	126
30	Variation of Subbase CBR, Permeability and Percent Compaction with Pavement Condition and Type of Subbase	130
31	Variation of the Properties of Asphalt-Treated Subbase Between Good and Failed Test Locations.	132
32	Summary of Analysis of Variance - Bulk Density of Concrete (lb/ft^3).	134
33	Summary of Analysis of Variance - Dynamic Modulus of Elasticity of Concrete (10^6 psi)	135
34	Summary of Analysis of Variance - Splitting Tensile Strength of Concrete (psi).	136
35	Relationship Between Pavement Condition and Concrete Properties	138
36	Concrete Characteristics Above and Below the Steel Reinforcement	138
37	Expected Mean Squares for Analysis of Variance of Deflection and Surface Curvature Index Data.	142
38	Summary of Analysis of Variance - Dynamic Pavement Deflection (milli-inches).	143
39	Relationship Between Pavement Deflection and Evaluated Factors	145
40	Newman-Keuls Sequential Range Test for Comparison of Mean Transverse Deflections .	147
41	Summary of Analysis of Variance - Surface Curvature Index (milli-inches).	152
42	Relationship Between Surface Curvature Index and Evaluated Factors	153

LIST OF TABLES (Continued)

Table Page

43 Newman-Keuls Sequential Range Test for Comparison of Mean Transverse SCI Values. 154

44 Summary of Analysis of Variance - Crack Width (in.) 159

45 Summary of Analysis of Variance - Mean Crack Spacing (ft.) 162

46 Summary of Analysis of Variance - Crack Spacing Variance (ft^2). 162

47 Relationship Between Statistical Measures of Crack Spacing, Crack Intersections, and Pavement Condition. 164

48 Summary of Analysis of Variance - No. of Crack Intersections per 100 ft. Length of Pavement. 166

49 ANOVA Summary - Subgrade CBR (Percent). . . 172

50 Summary of Results of One-Tailed T-Test on Subgrade Properties. 174

51 ANOVA Summary - Gravel Subbase CBR (Percent) 175

52 Effect of Subbase Type on Pavement Condition 177

53 Variation of the Properties of Asphalt-Treated Subbase with Pavement Condition . . 180

54 Summary of One-Tailed T-Test on Concrete Slump (in.) 182

55 ANOVA Summary - Dynamic Modulus of Elasticity of Concrete (psi). 183

56 ANOVA Summary - Splitting Tensile Strength of Concrete (psi) 184

57 Variation of Concrete Properties with Pavement Condition and Position Relative to the Steel Reinforcement. 185

LIST OF TABLES (Continued)

Table		Page
58	ANOVA Summary - Dynamic Pavement Deflection (milli-inches)	189
59	Variation of Pavement Dynamic Deflection and Surface Curvature Index with Condition of Test Sections and Distance from the Pavement Edge	191
60	ANOVA Summary - Dynamic Pavement Deflection (10^{-3} in.) at 100 ft. Intervals Along Test Sections	193
61	ANOVA Summary - Surface Curvature Index (milli-inches).	202
62	The Effect of the Interaction of Test Section Condition with Test Position (Crack vs. Midspan) on Pavement Surface Curvature Index	204
63	Summary of Results of T-Test on Pavement Cracking Parameters	206
64	Summary of Average Values of Temperature Variables and Cumulative Load Applications. .	208
65	Least Squares Analysis of Variance - Dynamic Modulus of Elasticity of Concrete (10^6 psi)	216
66	Variation of Concrete Dynamic Modulus of Elasticity with Method of Steel Placement and Position Relative to the Steel Reinforcement	217
67	Least Squares Analysis of Variance - Splitting Tensile Strength of Concrete (psi).	219
68	Variation of Concrete Splitting Tensile Strength with Type of Steel and Method of Steel Placement	220
69	Analysis of Variance Associated with Linear Multiple Regression Analysis of Crack Spacing Variance.	226
70	Summary of Step-wise Linear Multiple Regression Analysis - Crack Spacing Variance.	227

LIST OF TABLES (Continued)

Table Page

71 Effect of Subbase Type on Crack Spacing Variance. 228

72 Effect of Steel Type and Method of Steel Placement on Crack Spacing Variance 230

73 Analysis of Minimum Steel Requirements for CRCP. 231

74 Values of Pavement Response Functions Associated with 9 in. CRCP in Good Condition. . 265

Appendix A
Table

A1 Summary of Statewide Condition Survey Data. . . 282

Appendix B
Table

B1 Pavement Condition Data for Testing Variability Among Survey Parties. 288

B2 Summary of Analysis of Variance of Defects per Section (Survey Party Variability Study). . 289

B3 Summary of Analysis of Variance of Length of Random Cracking per Section (Survey Party Variability Study). 290

B4 Summary of Analysis of Variance of Spalled Cracks per Section (Survey Party Variability Study). 291

B5 Summary of Analysis of Variance of Spalled Cracks per Section (Survey Party Variability Study). 293

B6 Summary of Analysis of Variance of Length of Random Cracking per Section (Survey Party Variability Study). 294

B7 Hypothesis Tests for Non-Zero Regression Coefficients in Covariance Analysis of Statewide Condition Survey Data 298

B8 Test for Homogeneity of Regression Coefficients Within Groups. 299

LIST OF TABLES (Continued)

Appendix B
Table

Table		Page
B9	Least Squares Analysis of Variance - Time. . .	300
B10	Least Squares Analysis of Variance - Slump (in.).	301
B11	Variation of Concrete Slump with Method of Construction.	302

Appendix C
Table

Table		Page
C1	Section and Test Location Identification Data	303
C2	Construction Variables	305
C3	Traffic Data	307
C4	Temperature Data	309
C5	Summary of Dynamic Pavement Deflection Data (obtained along the lane center-line at 100 ft. intervals)	311
C6	Summary of Subgrade Grain Size Distribution and Consistency Limits Data.	314
C7	Summary of Subgrade CBR and Density Data . . .	317
C8	Summary of Subbase Grain Size Distribution and Consistency Limits Data.	320
C9	Summary of Subbase Characteristics, CBR and Permeability Data.	323
C10	Summary of Subbase Density Data.	326
C11	Summary of Concrete Data	330
C12	Summary of Pavement Cracking Data.	333
C13	Summary of Dynamic Deflection Data Obtained at Test Locations.	336
C14	Summary of Surface Curvature Index (SCI) Data Obtained at Test Location.	339

LIST OF TABLES (Continued)

Appendix D
Table

		Page
D1	Gravel Subbase Permeability Model.	343
D2	Crushed Stone Subbase Permeability Model . .	344
D3	Slag Subbase Permeability Model (Based on Data from Pavement Sections with No Distress	345
D4	Slag Subbase Permeability Model (Based on Data from Pavement Section with Failure) . .	346

Appendix E
Table

E1	Analysis of Variance Associated with Linear Multiple Regression Analysis of Maximum Slab Surface Temperature	352
E2	Analysis of Variance Associated with Linear Multiple Regression Analysis of Minimum Slab Surface Temperature	353
E3	Statistical Attributes of the Regression Equation for the Maximum Temperature of the Concrete Slab Surface.	354
E4	Statistical Attributes of the Regression Equation for the Minimum Temperature of the Concrete Slab Surface.	355

LIST OF FIGURES

Figure		Page
1	CRC Pavements in Indiana - Summer 1972	6
2	Use of CRCP in Indiana by Years.	7
3	Percentage of Trucks in Right Lane of a 4-Lane Divided Highway	72
4	Percentage of Trucks and Buses in Right Lane of a 6-Lane Divided Highway	72
5	Frequency Distribution of Defects Observed in the Statewide CRCP Survey	75
6	Active Pumping at the Pavement Edge.	81
7	Incipient Failure Condition Indicated by Heavy Spalled Cracks	81
8	Typical Layout of Test Sections.	82
9	Test Location - Failure Condition.	83
10	Test Location - Good Condition with a Uniform and Normal Crack Pattern	83
11	Test Location - Non-uniform, Closely Spaced Crack Pattern.	84
12	A Typical Bifurcated Crack with a Crack Intersection	84
13	Advance Signs Indicating Lane Closure Ahead. .	90
14	Flashing Arrow to Guide Vehicles to the Open Lane.	90
15	Test Section Barricaded and Ready for Testing.	91
16	View of Testing Operation. Note Heavy Traffic in Clear Lanes	91

LIST OF FIGURES (Continued)

Figure		Page
17	Deflection Measurement at a Mid-Span Position with the Dynaflect.	92
18	Measuring Crack Spacing Along the Pavement Edge	92
19	Removing Bituminous Shoulder to Expose the Subbase.	93
20	Test Pit at the Shoulder-Slab Interface. . . .	93
21	Nuclear Gauge for Measuring Moisture Content and Density.	94
22	Testing the Subbase with the High Load Penetrometer at the Shoulder Position.	94
23	Extracting a Concrete Core with a Pavement Coring Rig	95
24	Testing the Subbase with the High Load Penetrometer at the Core-Hole Position	95
25	Testing the Subgrade with Dynamic Cone Penetrometer	96
26	Obtaining a Subgrade Tube Sample	96
27	Sampling Subgrade Material	97
28	Crack Width Measurement with a Direct Measuring Microscope	97
29	Two Methods of Rapid CBR Tests	99
30	Density Control Curve for Gravel Subbases. . .	104
31	Typical Data from Failed and Good Locations within a Test Section with Gravel Subbase. . .	128
32	Effect of Position and Condition on Pavement Deflection	148
33	Typical Deflection Basin Reconstructed from Dynaflect Readings. Only One-Half of Basin is Measured.	149

LIST OF FIGURES (Continued)

Figure Page

34 Effect of Traverse Positions and Condition on Pavement Surface Curvature Index. 155

35 Effect of Test Position and Condition on Pavement Surface Curvature Index 157

36 Relationship of Crack Width with Position and Pavement Condition 160

37 Deflection Profiles of Test Sections with Gravel Subbase 195

38 Deflection Profiles of Test Sections with Crushed Stone Subbase. 197

39 Deflection Profiles of Test Sections with Bituminous-Stabilized Subbase. 198

40 Deflection Profiles of Test Sections with Slag Subbase 200

41 Variation of Percent Compaction for Subgrades. 240

42 Correlation Between Subbase CBR and Subgrade CBR (CBR Measured at the Core Hole). 241

43 Correlation Between Subbase CBR and Subgrade CBR (CBR Measured at the Pavement-Shoulder Interface) 242

44 Variation of Percent Compaction for Gravel Subbases 244

45 Effect of Densification on Permeability. . . . 247

46 Effect of Dust Ratio on Permeability of Gravel Subbases. 249

47 Effect of Percent Passing No. 4 Sieve on Permeability of Gravel Subbases. 250

48 Effect of Percent Passing No. 200 Sieve on Permeability of Slag Subbases 251

49 Effect of Subbase Strength and Permeability on CRCP Performance. 255

50 Effect of Pavement Slab Thickness on Dynamic Pavement Deflection. 260

LIST OF FIGURES (Continued)

Appendix E Figure		Page
E1	Air and Slab Temperature Data - 1936 and 1940.	349

ABSTRACT

Faiz, Asif. Ph.D., Purdue University, August 1975. Evaluation of Continuously Reinforced Concrete Pavements in Indiana. Major Professor: Eldon J. Yoder.

Continuously reinforced concrete pavements (CRCP) represent a relatively recent development in concrete pavement technology. Their widespread use in recent years has met with mixed success. This study reports the findings of a detailed field investigation of in-service CRC pavements in Indiana. One of the objectives of this evaluation was to recommend design and construction guidelines that would help to improve CRCP performance.

The study consisted of the following sequential steps:

1. Pavement condition surveys.
2. Detailed field testing and evaluation.
3. Laboratory testing program.

The CRC pavement condition survey was conducted on a statewide basis wherein every CRCP construction contract in Indiana was included in the survey. A total of 89 survey sections, each 5000 ft. in length, were used. These were obtained by random sampling, stratified over the following factors: construction contract, method of paving, method of steel placement, method of steel fabrication (type of reinforcement), subbase type and subgrade parent material.

A statistical analysis of the condition survey data showed that subbase type, methods of steel placement and steel fabrication, concrete slump, and age of pavement since opened to traffic were significant contributors to pavement performance.

Based on these results, a field investigation of CRC pavements was conducted. In this study, 31 test sections, each 1000 ft. in length, were used. As far as possible, each test section represented a unique combination of material, construction, traffic, and temperature variables. All the test sections were located on Interstate Highways in order to obtain a homogeneous set of test sections in terms of thickness (9-in.) and traffic intensity. Detailed field evaluation,including tests on all pavement layers and dynamic deflection measurements, was followed by a comprehensive laboratory testing program. The resulting data from these two phases were analyzed within the framework of statistical experimental designs.

The results of the detailed field and laboratory studies showed that failures in CRCP are a function of a number of interacting variables. Generally higher pavement deflection, decreased pavement stiffness, wider crack widths, and erratic, non-uniform crack patterns were associated with failed pavement condition. The support conditions under CRCP were of particular significance relative to performance. Well-compacted granular subbases with high stability and good permeability (internal drainage) showed excellent performance. Failures on CRCP were found to be correlated with concrete having a relatively low bulk density and modulus of elasticity. It was observed that paving concrete with a relatively higher slump (minimum of 1.5 in.) was more suited to CRCP with respect to good performance. An analysis of CRCP design revealed that use of 0.6 percent steel was, at best, marginal. There were further indications that current CRCP thickness design may be inadequate to withstand the traffic loads imposed on Interstate Highways.

Finally, the report contains a set of construction and design guidelines that should help to improve the performance of CRCP in Indiana.

PART I

PROBLEM DEFINITION

INTRODUCTION

The extensive use of continuous reinforcement in con- concrete pavement slabs is a relatively recent development in concrete pavement technology although they have been built experimentally since 1938. The earliest concrete pavements were poured without joints and were unreinforced. These pavements, over their service life, developed random cracks due to shrinkage, temperature and load stresses. Eventually this uncontrolled cracking led to impaired serviceability and structural integrity of the pavement.

One method of controlling random cracking is by the use of short slabs with pre-formed cracks or joints at a spacing of 12-15 ft. The use of joints helps to relieve internal stresses and controls cracking, that would otherwise occur randomly, due to volume changes resulting mainly from temperature and moisture variations in the concrete slab. Though the use of unreinforced slabs with closely spaced joints allows cracking to occur at pre-established locations, the joints can be a major source of maintenance problems if dowel bars are not used. Pumping, and faulted joints are major problems associated with the use of these joints. Many states have used short slabs with success especially when used in conjunction with stabilized bases and/or local transfer devices at the joints.

Joint spacing can be increased to 40-90 ft. by using longitudinal reinforcement up to 0.3 percent of the cross-sectional area of the slab. The function of steel in such simply reinforced concrete pavements is to hold the cracks together, thereby preserving granular interlock at the crack faces. Along with the use of longer slabs, use of dowels for load transfer at joints is essential.

The amount of steel required in simply reinforced concrete pavements is not directly proportional to the slab length for very long slabs. The actual relationship for these long slabs is a parabolic function with the required steel increasing at a progressively decreasing rate as the slab length increases, reaching a maximum at a slab length of 600-800 ft. Beyond this length, the steel requirement does not increase (19).* Hence, it becomes possible to attain a concrete pavement in which the continuity of the reinforcement is not interrupted except at abutting structures or at the ends of a project. Such a pavement is defined as a continuously reinforced concrete pavement (CRCP).

The continuously reinforced concrete pavement has no transverse joints other than expansion joints at bridges and other structures and construction joints that are used at the end of a day's pour. It contains relatively high amounts of steel normally ranging from 0.5 to 0.8 percent of the cross-sectional area. The function of steel in these pavements is to hold the cracks that occur tight and it also induces and controls crack formation. As the amount of reinforcement in the slab is increased, the number of cracks also increases. This is one of the aims of using this pavement since, ideally, stresses are evenly distributed among all the cracks and no single crack opens excessively. The optimum reinforcement for continuously reinforced concrete pavements should be such that it causes sufficient stress-relieving transverse cracks to occur and then holds these cracks tightly closed under service.

Transverse cracks develop in CRC pavements at an early age. Crack frequency is influenced by the amount of longitudinal steel, the temperature of the concrete at the time of placement, air temperature range and other environmental conditions during curing, the properties of concrete, and characteristics of steel reinforcement. Traffic load applications and temperature drops below the paving temperature also affect cracking. The optimal crack spacing is 4-10 ft. The average width of the cracks is generally in the range of 0.003 in. to .032 in.

---

*Numbers in parentheses refer to entries in the list of references.

If properly designed and constructed, CRC pavements have the following desirable properties (20,64):

1. Maintenance expenses are considerably reduced since very few joints are used. The transverse cracks are held tightly closed and do not require sealing.
2. The problems of spalling, faulting, and pumping commonly associated with transverse joints are minimized.
3. The original riding qualities of the pavement can be maintained over a longer service period. CRC pavements do not have the annoying and monotonous riding characteristics of jointed pavements.
4. Traffic delays and hazards associated with routine pavement maintenance, especially on high volume facilities are avoided, thereby improving traffic safety and quality of service.
5. The combination of reduced maintenance costs and longer service life results in lower equivalent annual costs.
6. CRC pavement has greater structural capacity than a jointed pavement of equal thickness.

Use of Continuously Reinforced Concrete Pavements

During the past several years, use of continuously reinforced concrete pavements has increased considerably. It is of interest to note that the first experimental continuously reinforced concrete pavement was built in 1938 on US 40 near Stilesville, Indiana. This was a cooperative research project between Indiana and the Bureau of Public Roads in a study dealing with joint spacing and required steel for various slab lengths. The purpose of the project was to obtain information on the possibilities of reducing the number of transverse joints in concrete pavements.

The percentages of steel used in the test sections varied from 0.07 to 1.82 percent. The higher percentages of steel were used for the longest slabs (1,310 feet in length).

The results of the study indicated that the use of heavier amounts of steel and longer slab lengths was practicable in what is now known as a "continuously reinforced concrete pavement". The sections containing higher percentages of steel are still giving excellent service although those sections with the lower steel percentages have failed and have been resurfaced (15).

Since 1938, a number of research oriented CRCP projects were built at various locations in the United States. Illinois and New Jersey constructed experimental test sections in 1947. Two years later California built a similar project. In 1951, portions of the Fort Worth freeways in Texas were constructed with continuously reinforced concrete. This was followed by other CRC pavements in Texas in 1955 and 1957. In addition, Pennsylvania constructed two continuously reinforced concrete projects in 1956 and 1957.

As of 1958, there were 79 miles of equivalent two-lane CRC pavement in the United States. In 1959, the U.S. Bureau of Public Roads (now FHWA) issued a memorandum to the effect that CRC pavements, meeting certain minimum design criteria would be approved for Federal-aid projects. This action changed the status of CRC pavement from experimental to functional. Since 1959 the use of CRC pavements has been on the increase with the result that more than 10,000 miles of equivalent two-lane pavement were in use or under contract in thirty-three states at the end of 1971 (33).

Outside the United States, a number of countries have built CRC pavements. Notable among these are Belgium, West

Germany, the Netherlands, Sweden and Switzerland. The Road Research Laboratory (U.K.) has investigated the use of CRC bases under asphalt surface courses (13). Belgium built its first experimental CRC pavement in 1950 and has recently undertaken such construction over a total of 81 miles of freeway (22).

Continuously Reinforced Concrete Pavements in Indiana

The use of CRC pavement in Indiana has followed the national trend. A substantial mileage of this pavement was constructed in Indiana between the years 1966-1971. Figure 1 shows the extent of continuously reinforced concrete pavement constructed in Indiana up to 1972. The first pavement, as was mentioned previously, was built on an experimental basis in 1938. Several short sections of pavement were constructed in the mid-60's. During the past several years many additional miles of continuously reinforced pavement have been built, primarily on the Interstate system. The increase in the use of CRC pavements in Indiana is shown in Figure 2.

Most of the CRC pavements in Indiana are nine inches thick (primarily on the Interstate system) although some have been constructed seven and eight inches in thickness. Generally, non-stabilized granular subbases have been used under the pavement, although in recent years the trend has been towards the use of bituminous-stabilized subbases.

The percentage of steel used has been 0.6 percent of the cross-sectional area, irrespective of the other design factors.

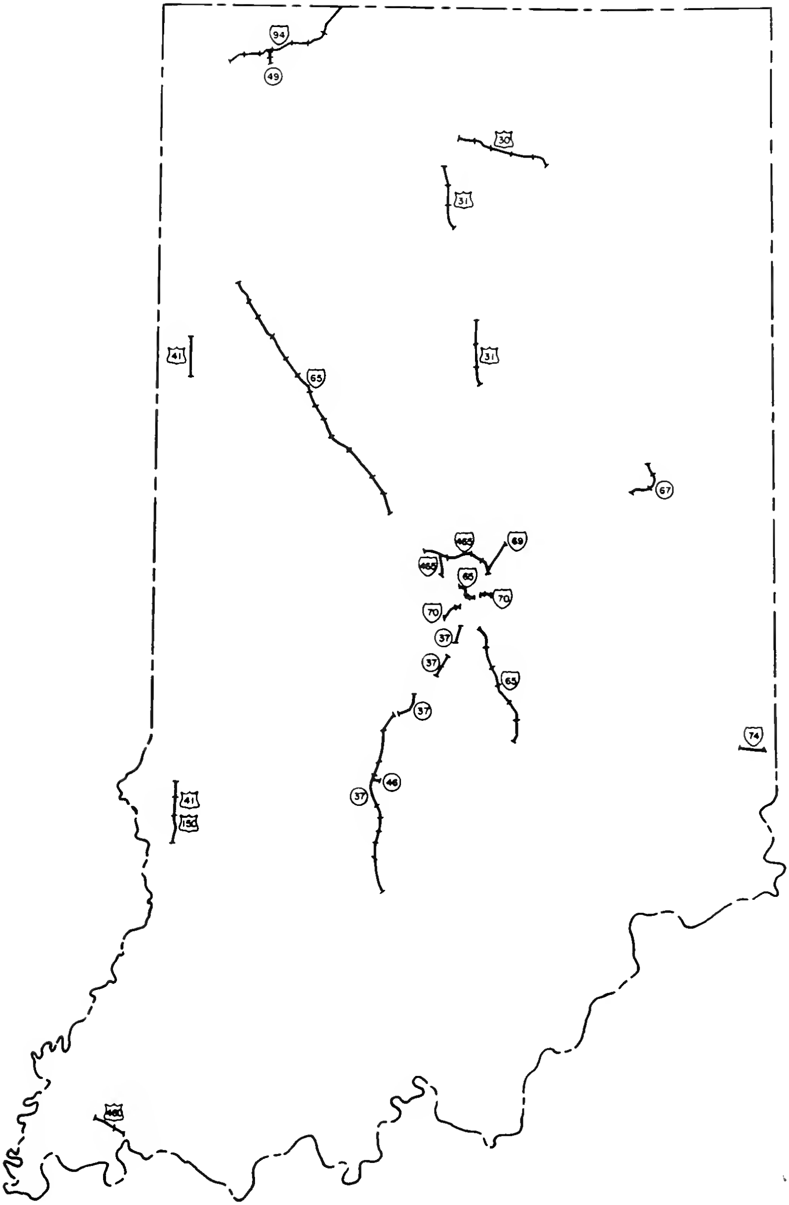
94
49
30
31
41
65
31
67
465
69
465
65
70
70
37
37
65
37
46
37
74
41
150
460

FIG.1 CRC PAVEMENTS IN INDIANA
SUMMER 1972

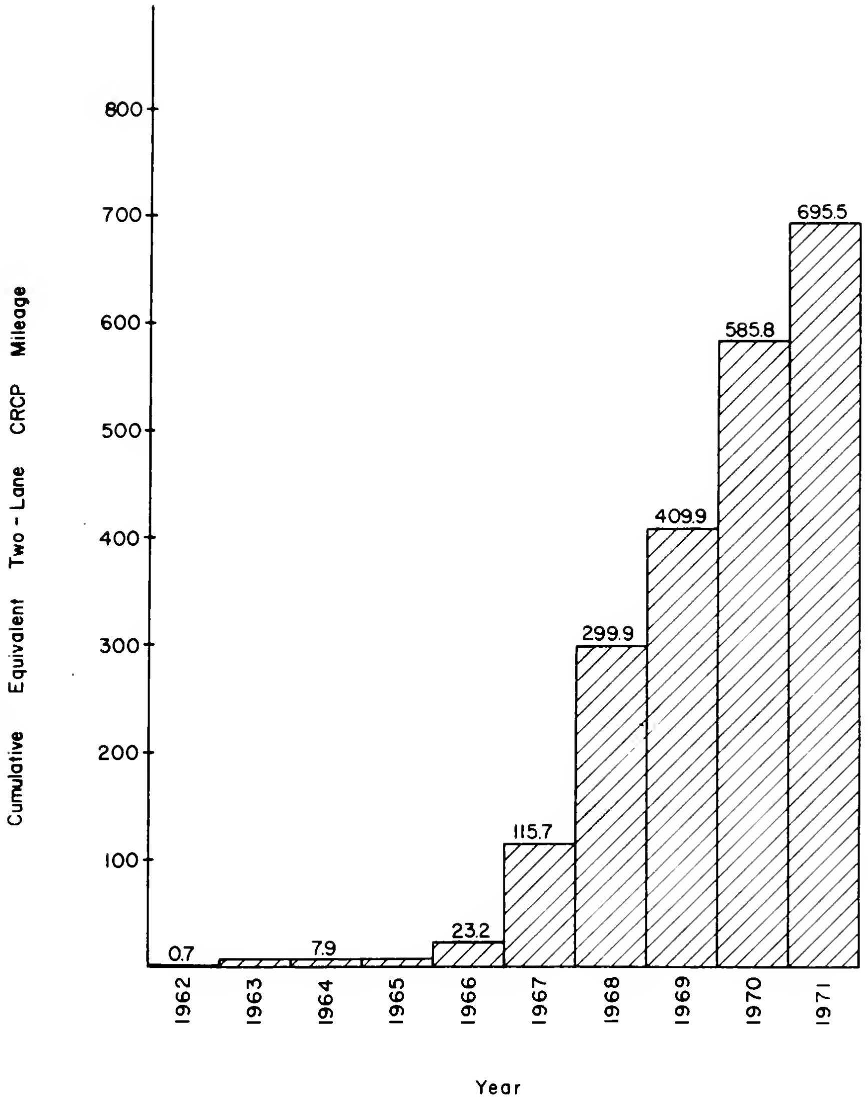

FIG. 2 USE OF CRCP IN INDIANA BY YEARS

BACKGROUND OF THIS RESEARCH

In Indiana, the use of CRCP has met with mixed success as regards service performance. Some pavement sections are in excellent condition though they have sustained over a million equivalent 18 kip, single-axle applications during a period of 3-4 years. On the other hand, some sections developed severe distress soon after they were opened to traffic.

Prior to the summer of 1972, the Indiana State Highway Commission investigated the performance of CRC pavements on Interstate Highway I-65. Though several reasons for poor performance were ascertained, the results were inconclusive. It was demonstrated that some distress had occurred because of poor consolidation of the concrete slab below the steel reinforcement. In some instances, it was shown that failures occurred at construction joints and at areas of steel overlap. There were, however, many other areas on I-65 that had shown distress, but the distress mechanism could not be determined.

In July 1972, engineers from the Indiana State Highway Commission asked the Joint Highway Research Project at Purdue University to evaluate the performance of CRC pavements with special reference to certain portions of I-65. In view of this request, a continuing study of the performance of CRC pavements was initiated during the summer of 1972 by the Joint Highway Research Project. The objective of this study was to evaluate and recommend design and construction techniques that would result in improved performance of continuously reinforced concrete pavements. A brief description of the sequence of this research program is as follows:

1. Detailed study of the performance of Interstate Highway I-65. This was conducted during July-August 1972.
2. Statewide condition survey of all CRC pavements in Indiana. This was completed in November 1972.
3. Field evaluation of selected pavement sections. This was conducted in May-June 1973.
4. Laboratory evaluation of materials obtained in the detailed field study (step 3). This phase was completed in December 1974.

CRC PAVEMENT TECHNOLOGY - A REVIEW

The design of continuously reinforced concrete pavements is based primarily on a consideration of:

1. Internal forces caused by the shrinkage of concrete and expansion and contraction due to temperature variations.
2. External forces imposed by traffic loads.

Net tensile stresses are set up in the concrete at initial shrinkage because of the restraint offered by the bonded reinforcement, the subbase friction, and adjacent pavement lanes. When the tension in the concrete exceeds the ultimate tensile strength of concrete, a crack occurs.

The effect of temperature is similar except that the cracking occurs due to contraction resulting from a drop in temperature.

Once a crack occurs because of environmental effects (shrinkage or temperature), the tensile stresses are transferred to the steel and any resulting strain is carried by the reinforcing steel in the immediate vicinity of the crack. At some distance from the crack, the stress in the reinforcement is transferred back to the concrete by bond between concrete and steel. For adequate performance, the amount of reinforcement should be such that the stresses in the steel remain below the elastic limit. If the steel is not sufficient in area, it will yield in tension, thus allowing a crack to open excessively. Further strain at the crack may cause the steel to break. If the tensile capacity of steel exceeds that of concrete, the tension at the mid-portion of the concrete section, between adjacent cracks, reaches the ultimate strength of concrete and another crack occurs. The narrow opening of another crack in the concrete helps to relieve the stress in the steel. This action continues (after initial cracking due to restrained shrinkage stresses has occurred) under the influence of periodic variation of temperature and moisture conditions in the slab, until the pavement contains a sufficient number of closely spaced (4-10 ft. spacing) narrow cracks to accommodate the strains caused by environmental effects. This explanation of the environmental cracking of CRC pavement assumes full restraint between cracks or that no change in the length of the slab section, between cracks, takes place. A corollary to this assumption is the presence of a uniform, stiff, durable, and rough support under the continuous slab. This mechanism applies to the interior portion of the CRC pavement slab approximately 300-500 ft. from each end. A simplified analysis of the environmental cracking of CRCP has been developed by Pasko (51).

In properly designed and constructed CRC pavement, good load transfer is obtained at the cracks because of aggregate interlock. As long as the continuity of slab is maintained, i.e. shear displacement between adjacent crack faces is prevented, the behavior of the CRC pavement under traffic loads differs from that of the conventional rigid pavement. As such,the performance of CRC pavement is affected by the quality of the support conditions. Under the action of traffic loads, poor quality subbases can induce excessive deflections and stresses in the pavement, leading to distress. Therefore for good performance, maintenance of adequate support is essential. If loss of support occurs due to a number of factors such as densification of the subbase, pumping, loss of strength due to presence of water in the subbase,or settlement of the embankment, the slab cannot conform to the non-uniform shape of the subbase because of high tensile stresses. Repeated load applications may then cause high deflections, resulting in spalling of the crack faces. Eventually under the combined action of traffic loads and loss of support the slab may disintegrate.

Theoretical Concepts

Theoretical concepts related to the analysis of CRC pavements treat the action of the concrete slab and steel reinforcement separately. The concrete slab together with the support elements (subbase and subgrade) are designed to withstand load stresses while the purpose of reinforcement is to control environmental cracking.

The purpose of this review is to examine the theoretical developments relating to:

1. Reinforcement
2. Pavement thickness and support elements
3. Terminal treatment

Reinforcement

Generally, CRC pavements are reinforced in both the longitudinal and transverse directions. Since the introduction of slipform paving and placement of the steel reinforcement by a depressor, transverse reinforcement has been omitted in many cases.

Longitudinal Reinforcement. The function of longitudinal steel in CRC pavement is to control cracking, so that crack spacing is neither too wide to permit the cracks to open to a degree that aggregate interlock is lost nor too close to result in disintegration of the slab.

Vetter (61) proposed the first theoretical relationships explaining the behavior of continuously reinforced concrete structures. These relationships are still used to design the longitudinal reinforcement for CRCP. From a consideration of the static equilibrium of a fully restrained continuously reinforced concrete member, he proposed that the minimum percentage of steel needed to control volume change due to shrinkage, in reinforced concrete, is equal to the ratio of the tensile strength of concrete to the yield strength of steel or,

$$p_s = \frac{f'_t}{f_y} \times 100 \qquad (1)$$

where p_s = percentage of steel = $\frac{A_s}{A_c} \times 100$

A_s = cross-sectional area of longitudinal steel (sq. in.)

A_c = cross-sectional area of pavement slab (sq. in.)

f'_t = tensile strength of concrete (psi)

f_y = yield strength of steel (psi)

The percentage steel needed to resist any shrinkage that may occur was given to be:

$$p_s = \frac{f'_t}{f_y + \delta E_s - nf'_t} \times 100 \qquad (2)$$

where δ = coefficient of shrinkage of concrete

E_s = modulus of elasticity of steel (psi)

n = modular ratio = $\frac{E_s}{E_c}$

E_c = modulus of elasticity of concrete (psi)

The minimum amount of steel required to resist volume changes caused by temperature was determined to be

$$p_s = \frac{f'_t}{f_y - nf'_t} \times 100 \qquad (3)$$

The minimum reinforcement given by equation 3 may be used as long as the total temperature drop from the temperature at time of construction does not exceed

$$\Delta T = \frac{f_y + nf'_t}{2 \varepsilon E_s} \qquad (4)$$

where ΔT = total temperature drop from the temperature at time of construction to some later date

ε = thermal coefficient of expansion of steel

Where the temperature drop is in excess of this limiting value, the amount of steel can be found from

$$p_s = \frac{f'_t}{2\ (f_y - \Delta T \epsilon E_s)} \times 100 \qquad (5)$$

These equations are based on the premise that the tensile stress in the steel must not exceed its yield point and, hence, no yielding of steel must occur at cracks formed by restrained volume changes.

The formulas developed by Vetter do not take into consideration the frictional stresses that might develop at the slab-subgrade interface. A modification of these equations was first proposed in the 1962 AASHO Interim Guide (1). If the coefficient of friction between the slab and the subbase is assumed to be 1.5, then equations 1, 2, 3 and 5 are valid. Otherwise, the percentage of steel determined by these formulas should be modified by a factor of (1.3 - 0.2F), where F is the coefficient of friction between the slab and the subbase. Appropriate friction coefficients for various types of subbases have been obtained by McCullough (40). The use of this factor implies that higher amounts of steel are needed for smooth subbases as compared to rough textured subbases.

According to Vetter's analysis the amount of steel required is directly proportional to the tensile strength of concrete. It has been suggested that the strength of concrete be specified by a range rather than a minimum value after an initial CRC design has been determined. The upper limit on the strength of concrete would restrict the use of excessive amount of reinforcement while the lower limit would ensure durability of the concrete (30). Such an approach obviously would lead to problems relating to construction quality control.

Another important observation that results from Vetter's analysis is that crack spacing is inversely proportional to the percentage of steel, the bond stress, and the perimeter of steel bar per unit area of steel. In order for cracks to occur at optimal spacing, a high percentage of steel, a relatively large perimeter of steel reinforcement compared to the area, and high bond stresses are required.

Friberg (29) also analyzed the formation of cracks in CRC pavements. His analysis shows that both the width and spacing of the cracks are directly proportional to the diameter of the reinforcement bars and are inversely related to bond stress. This agrees with the results derived by Vetter. In order to obtain high bond stresses, so that an optimal spacing of cracks is obtained, the use of deformed bars is recommended.

Transverse Reinforcement. The main function of transverse steel is to ensure adequate load transfer across random longitudinal cracks that might occur in the pavement. Transverse reinforcement as well as tie bars are designed by the use of the following equation:

$$p_s = \frac{LF}{2\ f_s} \times 100 \qquad (6)$$

where p_s = percentage of steel
L = width of slab (ft.)
F = coefficient of friction for the subbase
f_s = allowable working stress in steel (psi)

From the viewpoint of construction practice, transverse steel helps in supporting the longitudinal reinforcement where pre-set steel is used.

Zuk (71) proposed that transverse reinforcement in wire fabric helps in transferring load stresses by serving as anchors for the steel within the concrete. His analysis showed that crack spacing and crack width are influenced by the distance between transverse wires.

Treybig, et.al.(57) evaluated the effect of transverse steel in CRC pavement. They recommend that for soil types and support conditions, where a high probability of longitudinal cracking exists, transverse reinforcement is needed to hold the cracks together and maintain aggregate interlock for purpose of load transfer. In cases where construction equipment needed to position the longitudinal steel without the help of transverse reinforcement is available and there is a low probability of longitudinal cracking, transverse steel may be omitted. Among the causes contributing to longitudinal cracking in CRCP are: expansive clay foundations, differential loss of support and consolidation, transverse volume change due to variations in temperature and moisture within the slab, improper placement of longitudinal joints, exceptionally wide pavements, high friction subbase, concrete with a high thermal coefficient, or combinations of these factors.

Pavement Slab Thickness and Support Elements

Most thickness design methods for concrete pavements utilize either modifications of Westergaard's Theories or empirical relationships developed from the AASHO Road Test data. The thickness of the pavement slab is primarily a function of the magnitude of wheel loads and fatigue caused by load repititions.

Zuk (70) made the first attempt to develop a rational method for the thickness design of CRCP. His analysis based on cracked slab behavior, with the further assumption that the slab segment between cracks was essentially homogeneous, resulted in the following expression for thickness of CRCP:

$$t = \left[\frac{4.526\ E_c\ P^4}{(f_t)^4\ b^3\ (k_1 + k_2 + k_3)} \right]^{1/5} \tag{7}$$

where t = allowable thickness (in.)

E_c = modulus of elasticity of concrete

P = wheel load (lb.)

b = spacing between cracks (in.)

f_t = allowable tensile stress of concrete (psi)
k_1 = elastic subgrade modulus per width b, (psi)
k_2 = elastic restraint modulus of the adjacent segments transferred by longitudinal steel (psi)
k_3 = aggregate interlock modulus (psi)

From Equation 7, for a given wheel load (static analysis), the thickness of slab required varies directly with the modulus of elasticity of concrete and indirectly with the allowable tensile stress of the concrete, crack spacing, modulus of subgrade reaction, and degree of aggregate interlock. Earlier in the discussion on longitudinal reinforcement, it was observed that the amount of reinforcement is directly proportional to the tensile strength of concrete (Eq. 1, 2, 3 and 5). If a lower tensile strength of concrete is specified for the purpose of reducing the reinforcement requirements, then from Zuk's analysis, it would appear that a corresponding increase in thickness of the pavement slab may become necessary.

This analysis cannot be applied readily in determining slab thickness as moduli relating to aggregate interlock and elastic restraint are difficult to determine.

In 1960, McCullough and Ledbetter (41) presented one of the first studies, aimed at formalizing the design of continuously reinforced concrete pavements, by considering load, temperature, and shrinkage stresses. In this design system, a trial thickness, d, of the pavement slab is obtained by the use of Westergaard's theoretical equation for the interior loading case. The trial thickness is then reduced by an amount derived by the transformation of steel area to an equivalent area of concrete. The final thickness is, then, given by:

$$t = d - P_s nd = d(1 - P_s n) \qquad (8)$$

where t = design thickness (in.)

d = trial thickness (in.)

P_s = steel area ratio = $\frac{A_s}{A_c}$

A_s = area of steel (in^2)

A_c = area of concrete (in^2)

n = modular ratio = $\frac{E_s}{E_c}$

E_s = modulus of elasticity of steel (psi)

E_c = modulus of elasticity of concrete (psi)

The last step in this design procedure is a consideration of the effect of longitudinal edge stresses on slab thickness. If additional thickness is needed because of edge stresses, either it is converted into additional reinforcement to be placed over a 12 in. width from the longitudinal edge or the edge is thickened by the extra amount.

In this method, the matter of attributing a load-carrying capacity to the steel reinforcement appears questionable, since the interactions among load, temperature and shrinkage stresses were not considered in the development of the design procedure.

Another approach to determining the thickness of CRCP is the one used by the Continuously Reinforced Pavement Group (20). They use an approximate relationship between the thickness of CRC pavement and that of a structurally equivalent jointed pavement. This relationship assumes that the average stress at a doweled dummy groove joint, with a joint opening of .073 in., is 93 percent of the stress at a free edge carrying the entire load. It is further assumed that 100 percent shear transfer occurs at a transverse crack in CRCP for an interior loading condition or the maximum stress at a transverse crack is only 50 percent of that at a free edge. The relative thickness of jointed pavements and

CRC pavement for equal load carrying capacity is then given as:

$$\frac{t}{t_j} = \left[\frac{0.5S}{0.93S}\right]^{1/2} = 0.73 \qquad (9)$$

t_j = required thickness of a jointed pavement (in.)
t = required thickness of a CRC pavement (in.)
S = stress caused by a load placed at a free edge

This analysis shows that for a given load, the thickness required for CRC pavement is about 75 percent that of an equivalent jointed pavement.

Such a reduction in thickness has been questioned by both the Federal Aviation Administration and Portland Cement Association (27, 52). The thickness design procedures of these agencies, for airport pavements, do not permit any reduction in thickness of CRCP relative to the thickness requirements for an equivalent jointed concrete pavement.

The fatigue methods of thickness design (2, 3, 40) are based on AASHO Road Test Equations as extended by Hudson and McCullough (34). One form of this thickness design equation is given by (3):

$$\log L = -8.682 - 3.513 \log\left[\frac{J}{M_R h^2}\left(1 - \frac{2.61a}{Z^{0.25}h^{0.75}}\right)\right] - \frac{0.1612}{\beta'} \qquad (10)$$

where L = number of accumulated equivalent 18 kip single axle loads
J = a coefficient dependent on load transfer characteristics or slab continuity
M_R = third-point loading modulus of rupture or concrete at 28 days (psi)
h = nominal thickness of concrete pavement (in.)
$Z = \frac{E_c}{k}$

E_c = modulus of elasticity of concrete (psi)
k = modulus of subgrade reaction (psi per in.)
a = radius of equivalent loaded area = 7.15 for AASHO Road Test 9 kip. wheel.

$$\beta' = 1 + \frac{(1.624)\ 10^7}{(h + 1)^{8.46}}$$

The terminal serviceability in this expression is taken as 2.5. This relationship is used for determining the nominal thickness of both CRC and jointed pavements. For jointed pavements, the continuity or load transfer factor, J, is taken as 3.2 while for CRCP a J value of 2.2 is recommended. However, the use of a J-value of 2.2 for CRCP has not been evaluated adequately. It is based on limited performance data, using deflection measurements and comparisons with other design procedures (34). It is possible that the J-factor may change over the service life of a CRCP with variations in support conditions, fatigue due to load repetitions, and temperature drops above those normally assumed in the design of longitudinal reinforcement. In view of these uncertainties, any thickness design for CRCP should include an analysis of the sensitivity of slab thickness to variations in the load transfer factor J.

The use of large amounts of reinforcement in CRCP should undoubtedly add to the structural capacity of the pavement and the decrease in thickness of CRCP over an equivalent jointed pavement is perhaps justified. Data presented by Mellinger, et. al. (43) show that effective slab thickness of jointed concrete pavements is increased by 40 percent when 0.4 percent reinforcement is used in each of the longitudinal and transverse directions. However, such data cannot be directly applied to CRC pavements since the two pavement types have different service and performance characteristics. At the present time comprehensive performance data relating to slab thickness equivalencies between jointed and CRC pavements is not available. Hence any reduction in CRC pavement thickness over an equivalent jointed pavement is at best a judicious estimate.

Support conditions for CRCP are characterized by the modulus of subgrade reaction, k, which relates surface deflections to reactive pressure of the support. The assumption that k is constant implies an elastic support system. That is, the subbase-subgrade combination is assumed to exhibit elasticity. This assumption,however, is only valid through a limited range of stresses. Westergaard's analysis (62) of load stresses in concrete pavements shows that deflection is inversely proportional to the square root of the modulus of subgrade reaction. Hence, higher values of k (stronger support conditions) would result in smaller surface deflections under a given load. As excessive deflections impair the serviceability of concrete pavements, therefore higher values of k are associated with better performance.

To determine the effective supporting capability of both subgrade and subbase, nomographs are available that permit the estimation of a composite k-value, given the thickness of the subbase, the type or stiffness of the subbase and modulus of subgrade reaction (2, 40). The modulus of subgrade reaction k can be either determined from plate tests or estimated from correlations between k and other soil parameters such as CBR (52).

Terminal Effects

The interior portion of CRCP is completely restrained from movement but lengths about 300-500 feet from each end of the pavement will move, the amount of movement being a function of the friction between the slab and the subbase.

Gregory et. al. (30) have developed an equation in an attempt to explain this action. The length of pavement subject to movement can be calculated as:

$$L_{act} = \frac{\Delta T \, \varepsilon_c \, E_c}{F \, W} \tag{11}$$

where L_{act} = active length (in.)

ε_c = thermal coefficient of expansion of concrete

E_c = modulus of elasticity of concrete (psi)

F = coefficient of friction between the slab and subbase

W = weight of slab (lb.)

ΔT = total temperature drop (^{0}F)

The movement of one end of the slab can then be expressed as:

$$x = \frac{(\varepsilon_c \ \Delta T)^2 \ E_c}{2 \ F \ W} \tag{12}$$

where x = movement of one end of slab and other terms are as given for Equation 11.

According to Equation 11,the end movement varies directly with the elasticity of concrete and inversely with the friction factor. A rough subbase, consequently, not only reduced longitudinal reinforcement requirements but also restrains end movement.

Structural Design of Continuously Reinforced Concrete Pavements

The design methods for continuously reinforced concrete pavement require a number of inputs. These include:

1. Material Properties
    a) Concrete - tensile strength, modulus of elasticity, Poisson's ratio, modulus of rupture (flexural strength), coefficient of shrinkage, unit weight, thermal coefficient of expansion, bond strength between concrete and steel.

  - b) Steel - yield strength, allowable tensile strength, thermal coefficient of expansion, modulus of elasticity, size of reinforcement bars.
  - c) Subbase - type, stiffness value, coefficient of friction between subbase and slab.
  - d) Subgrade - modulus of subgrade reaction, coefficient of friction between subgrade and slab.

2. Temperature and Climate - magnitude and repetition of axle loads, maximum wheel loads, temperature, depth of frost.
3. Other Factors - load transfer or continuity factor, terminal serviceability, thickness reduction factor, impact factor.

Current Design Methods

The currently available design procedures for CRCP are as follows:

1. Highway Pavements
    - a) American Association of State Highway Officials (AASHO) Interim Guide, 1972 (2).
    - b) American Concrete Institute, (ACI), Design Procedure, 1972 (3).
    - c) United States Steel (USS) Design Manual, 1970 (40).
    - d) Continuously Reinforced Pavement Group (CRPG) Method, 1968 (20).
    - e) Wire Reinforcement Institute (WRI) Method, 1964 (64).

2. Airport Pavements
   - a) Federal Aviation Administration (FAA) Method, 1974 (27).
   - b) Portland Cement Association (PCA) Method, 1973 (50).
   - c) United States Steel Design Manual, 1970 (40).
   - d) Design Manual for Continuously Reinforced Concrete Pavements, Austin Research Engineers, 1974 (9).

In all these methods, pavement thickness and reinforcement requirements are determined separately. The following discussion will be confined to design methods for highway pavements.

Reinforcement

Longitudinal Reinforcement. Vetter's equations (61), as modified by a friction factor, are used in AASHO (alternate design), ACI, and USS methods to determine longitudinal steel requirements. The 1972 AASHO Interim Guide (2) suggests the use of longitudinal reinforcement between 0.5 to 0.8 percent of the cross-sectional area of the pavement slab depending on material properties and local experience. Values for all input factors can be easily determined, excepting the tensile strength of concrete. In the ACI procedure (3), it is recommended that a value of tensile strength (f_t) equal to 0.4 times the 28-day modulus of rupture may be used, provided a safety factor of 1.3 is applied to the percentage of steel (p_s) so obtained. The longitudinal steel should have a minimum yield strength of 60,000 psi.

The WRI method (64) recommends 0.5 to 0.7 percent longitudinal steel reinforcement while the CRPG method (20) suggests the use of 0.5 to 0.6 percent steel. These recommendations are based on performance data obtained from experimental pavements.

Transverse Reinforcement. Transverse steel area and tie bar requirements are determined in all methods by Equation 6.

Bond Area: The ratio of bond area of longitudinal bars to the concrete volume is generally checked by means of the following equation (40).

$$Q = \frac{4P_s}{D} > 0.03 \tag{13}$$

where Q = ratio of bond area to concrete volume, in^2/in^3

$P_s = \frac{\text{area of steel}}{\text{area of concrete}}$ = steel area ratio

D = diameter of reinforcing bars (in.)

Size and Spacing of Reinforcement (20, 64). According to recommendations by the Continuously Reinforced Pavement Group and Wire Reinforcement Institute the maximum size of longitudinal reinforcement should be No. 6 bars or its equivalent in deformed wire. Many engineers, however, believe this may be too restrictive. The minimum size of transverse steel is recommended to be No. 3 bars. They further recommend that spacing of longitudinal reinforcement should not exceed 9 in. and should be no less than 4 in. Transverse deformed bars needed to support and space the longitudinal bars should be limited to a maximum spacing of 48 in. For wire fabric, the recommendations are that spacing of longitudinal wires should be between 3 and 6 in., while the spacing of transverse wires should not exceed 16 in. The clearance between the longitudinal edge wire and the pavement edge and between the edge wire and center joint should be not less than 1 in. and not more than 6 in.

Position of Reinforcement. As regards position of reinforcement, the following controls are recommended by the CRP Group (20):

1. The steel should not be placed below the mid-depth of the slab.

2. A tolerance of about ± 0.5 in. should be permitted in the horizontal or vertical placing of longitudinal steel.

3. The minimum cover should be 2 in.

4. Minimum cover should be maintained where overlap of reinforcement occurs.

5. A tolerance of ± 2 in. should be allowed in the horizontal spacing of horizontal members.

Lap Requirements. American Concrete Institute recommendations (3) indicate a minimum overlap of 30 diameters with a minimum of 18 in. when the laps are in the same transverse section. When the laps are skewed, the minimum lap may be reduced to 25 diameters with a minimum of 16 in. provided no more than one-third of the bars are lapped within any 3 ft. length of pavement. In case of wire fabric, the mats should be lapped so that the end transverse wires of the two mats overlap a minimum of 4 in. center to center. Detailed diagrams and explanations regarding these lap requirements are provided by Refs. 20 and 64.

Pavement Slab Thickness

The design of slab thickness in ACI, AASHO, and USS methods is based on AASHO Road Test equations and the extensions developed by Hudson and McCullough (34). The required thickness is obtained by means of nomographs. Input variables include load repetitions, modulus of support, modulus of elasticity and modulus of rupture of concrete. The USS method also has provisions for design using the static wheel load method. The 1972 AASHO Interim Guide recommends that the reduction in thickness of CRCP over that of an equivalent jointed pavement should be based on local experience or performance studies.

The selection of pavement thickness in the WRI method is based on observations of CRC pavement performance under service conditions. It takes into consideration route classification, locality description, controlling vehicle type,and controlling single axle load. The recommended thickness on basis of these factors varies from 6-9 in.

In the CRPG design procedure, thickness is first determined using any of the methods for jointed pavement. The thickness used for CRCP is 70 to 80 percent of that found for the equivalent jointed pavement.

Subbase and Subgrade

Most design methods recommend that a granular subbase or a stabilized material be used under CRCP. Thickness requirements vary from 4-9 in. and have been determined largely on the basis of past experience. The USS Design Manual (40) provides a subbase thickness design guide for various combinations of subbase types and subgrade soils. The 1972 AASHO Interim Guide specifies gradation and strength requirements for various types of subbases. A nomograph is also provided to determine a composite support modulus, k, based on the modulus of subgrade reaction (or modulus of resilience of subgrade),the subbase thickness and stiffness of the subbase.

Transverse Construction Joint

A transverse construction joint is needed at the end of each day's pour or at any time when paving operations are stopped for a prolonged period. The following design details (2, 3) should be considered:

1. Construction joints should be of the butt type formed by a special type of header.
2. The reinforcement should be continued through the construction joint.
3. All end laps should occur beyond the construction joint and any other steel added at the joint.

Terminal Provisions

The terminal sections of CRCP are subject to longitudinal movements over a length of 250-500 ft. Terminal joints are provided to accommodate this movement. These fall into two broad categories:

1. Free end to allow movement by means of a joint capable of absorbing all the movement. Examples are finger type expansion joint, wide flange beam joint on a sleeper slab used with conventional doweled expansion joints in series, and use of sleeper slab with the space between pavements (4 ft.) filled with asphalt concrete.
2. Fixed or anchored end to resist the movement. This is in the form of lugs anchored in the subgrade. Anchorage for the lugs is provided by soil friction. Expansions joints are still provided.

Detailed designs of the terminal provisions are given in Refs. 3, 20, and 64.

Construction Practice

Except for the installation of reinforcement, CRC pavement is constructed in the same manner as jointed concrete pavements. The pavement may be constructed either by a site mixer or a central mixer. Similarly, either conventional paving using side forms or slipform paving may be utilized. Paving rates for slipformed concrete pavement are high, sometimes reaching 18 ft. a minute (30). The following discussion relates to some of the important construction aspects of CRCP.

Type of Steel

Reinforcement for CRCP may be fabricated in the form of loose bars, bar mats or welded wire fabric. Past performance and theoretical studies indicate that deformed wires or bars rather than plain reinforcement should be used because of bond considerations. In deformed bars, stresses are transferred by means of friction shear at the surface of the longitudinal bars, while in plain wire fabric, the stresses are carried though the transflexural anchorage provided by transverse wires.

Method of Placement of Steel

This factor comes into play when considering the consolidation of concrete below the plane of the reinforcement. The steel reinforcement may be installed by each of the following methods:

1. Pre-set on chairs.
2. Mechanical placement where the reinforcement is directly fed or depressed into the concrete up to the required depth. Another method of steel placement is by the two-lift technique where the reinforcement is placed between lifts.

Where steel is pre-set on chairs, it is possible that the reinforcement may dampen the vibrators and as a result poor consolidation of the lower portion of pavement may result. Good consolidation of concrete is essential in order to obtain full utilization of the full thickness of the concrete, as well as full and continuous bond between steel and concrete.

Concrete should be properly vibrated. It is recommended that vibratory compactors be used to ensure complete and uniform consolidation of the concrete and to prevent honeycombing around the loosely spaced reinforcement bars or wire fabric. This becomes especially critical at construction joints where extra reinforcement is added to provide continuity.

Placement of reinforcement needs careful attention at laps and construction joints. Laps should be tied to maintain the proper overlap during paving operation.

Method of Paving

The method of paving comes into consideration when comparing slipformed pavements with those that have been paved by the use of side forms. In slipforming a pavement, it is necessary to use a fairly stiff concrete with low slump. Since a stiff concrete mix is hard to compact, poor consolidation of concrete may result.

Subbase and Subgrade

When evaluating the effect of support conditions on performance, the primary factor is excessive deflection, which in turn may result in spalling and deterioration of cracks. Since CRCP is particularly sensitive to construction technique, extra care is required during construction to ensure that a uniformly stable and durable subbase and subgrade are obtained.

The primary concerns regarding subbase and subgrade construction are the matter of adequate compaction, sufficient shear resistance, and uniformity of compaction.

For subbases, both soil-aggregate and stabilized aggregate mixtures have been used. Graded aggregate subbases have given adequate performance where the subbase was sufficiently compacted and had good strength and internal drainage. Uniformity of these physical characteristics is of paramount importance in CRCP. The current trend, however, is towards the use of cement, lime,or bituminous stabilized subbases.

Construction practices and methods as applied to CRCP are described in detail in Refs. 20, 33, 48, and 64. The NCHRP Synthesis of Highway Practice No. 16 (33) contains a comprehensive survey of CRCP construction technology.

DESIGN OF THIS RESEARCH

This research study was designed to obtain a maximum amount of useful and pertinent information within the frame of reference of the study objectives. Extensive use of statistical experimental designs was made to obtain a wide inference space and to effect economy in the research effort.

Study Objectives

The primary objective of this research was to determine the causes of distress occurring on some portions of CRC pavements in Indiana. The ultimate purpose of the study is to evaluate and recommend design and construction techniques that would result in improved performance of continuously reinforced concrete pavements.

Scope of the Study

To be of greatest utility, research into the performance of any pavement must be based upon factors which are known to influence performance of that type of pavement construction. These factors include both the design and construction aspects.

The factors and their sub-categories, considered to be important and that were included in this study, are listed as follows:

1. Thickness and percentage of steel
    a. Percentage of steel; 0.6 percent on all pavements.
    b. Thickness of pavement; 7, 8 or 9 inches, depending on projected commercial traffic.

2. Type of Steel Reinforcement
    a. Wire fabric
    b. Bar mats
    c. Loose bars
3. Method of Steel Placement
    a. Pre-set on chairs
    b. Depressed
4. Concrete Properties
    a. Modulus of elasticity
    b. Tensile strength
    c. Unit weight
    d. Slump
5. Type of Construction
    a. Slipformed paving
    b. Paving by conventional side forms
6. Type and Properties of Subbase
    a. Subbase type (bituminous stabilized, slag, crushed stone and gravel)
    b. Strength
    c. Permeability
    d. Density, moisture content, and compaction
    e. Grain size distribution, consistency limits
    f. Percent asphalt content in bituminous stabilized subbases
7. Subgrade
    a. Subgrade type (fine grained, coarse grained)
    b. Strength
    c. Density, moisture content, compaction
    d. Grain size distribution, consistency limits
8. Traffic
    a. Time since opened to traffic
    b. Equivalent 18-kip. single-axle load applications

9. Climatic Factors
    a. Time since paved or opened to traffic
    b. Air and slab temperature at time of paving
    c. Temperature drop since time of paving

Many of these factors have been treated in the past in an empirical manner and no specific analytical analysis or recommendations have been available to the design engineer to incorporate these factors in the design process. Nevertheless, past performance of in-service pavements has indicated that these factors are of importance.

Research Approach

The study was conducted in a number of sequential phases. These were:

1. Pavement condition surveys
2. Detailed field evaluation
3. Laboratory testing program

Pavement Condition Surveys. The initial activity was confined to Interstate Highway I-65. The analysis of data obtained from this initial survey indicated the need to extend the study to include all CRC pavements in Indiana. The statewide condition survey was statistically designed. Pavement condition data were collected by visual observation of pavement sections. For each survey section, pavement surface defects such as patches, breakups, closely spaced and bifurcated transverse cracks, pumping, and spalled cracks were logged.

Detailed Field Evaluation. On basis of the factors,that were found in the statewide condition survey to significantly influence CRCP performance, a detailed field study of selected pavement sections was conducted. The study was set up within the framework of statistical experimental designs. This phase of the research included detailed field testing of various pavement components. Performance measures such as dynamic pavement deflection, surface curvature index, crack width, and crack spacing were also evaluated.

Laboratory Testing Program. Samples of subbase and subgrade materials and concrete cores obtained in the field study were tested by standard laboratory procedures to evaluate the engineering properties of these materials.

PART II

STATEWIDE CRCP CONDITION SURVEY

STATEWIDE CONDITION SURVEY

To evaluate the performance of CRC pavements in Indiana, a statewide condition survey was conducted in late 1972. The need for a statewide survey was dictated by the results of a preliminary survey of the northbound lanes of Interstate Highway I-65 between Lebanon and the northern terminus of CRCP near US Highway 24. The I-65 survey results indicated that the method of steel fabrication and the type of subbase significantly influenced the performance of CRCP. During the survey it was observed that the incidence of pavement defects, such as structural breakups, patches and heavily spalled cracks, was greater in cut sections than on fill sections. It was also noted that most of the heavy pumping occurred at the inside edge of horizontal curves turning to the right.

In order to arrive at more definitive conclusions and to include a larger range of construction and design variables, the scope of the condition survey was extended to include all the CRC pavements in Indiana. The statewide survey was a cooperative venture in which a study group from Purdue University was assisted by personnel from the Research and Training Center and the Crawfordsville District Office of Indiana State Highway Commission. A sampling procedure was used to design the field survey and statistical methods were used to analyze the resulting data.

Study Design

The intent of the study design was to insure the inclusion in the study of every CRCP contract that had been completed up to the time of the survey. A further purpose was to provide an inference space for the proposed analysis that would encompass all the factors under investigation.

Anderson and Mclean (7) define inference space as those limits of the investigated variables, within which, the results will apply.

Sampling Procedure

A stratified random sample of CRC pavements was used in the field survey. Stratified random sampling is a plan by which the population under consideration (in this case, all the CRCP contracts in Indiana) is divided into strata or classes according to some principle significant to the projected analysis. This is followed by sampling within each class as if it were a separate universe. The aim in stratification is to break up the population into classes that are fundamentally different in respect to the average or level of some quality characteristics (21).

Such a sampling scheme is superior to a simple random sample in that the inclusion of all independent factors to be evaluated in the study is guaranteed. This vastly improves the inference space of the desired analysis.

Only one simple random sample was obtained from each stratum or class. Such a sample or unit of evaluation was designated as a field survey section. Each field survey section was a 5,000 ft length of pavement. The location, relative to the direction of lanes, and beginning of each section were selected from the total length of CRC pavement in each stratum by the use of random number tables. Care was taken that a randomly selected pavement length was located approximately 200 to 300 ft away from the exact end or beginning of a construction contract.

The survey sections were stratified on the basis of the following factors: contract, method of paving, method of steel placement, method of steel fabrication, type of subbase, and type of subgrade. These factors are described in detail in the section on statistical design. Data relative to these factors were obtained from construction survey records.

In addition, information pertaining to concrete slump, date of paving, and date a section was opened to traffic was also taken from construction records.

Most of the pavement sections were 9 in. thick, although several were 8 in. thick and nine were 7 in. thick.

In certain cases, more than one survey section was sampled within a particular contract. This apparent duplication resulted whenever a contract crossed more than one level of any other stratification factor. For example, if two subgrade types occurred over one contract, two sections were included in the survey. Similarly, two sections were surveyed if two different methods of steel placement were used within a particular contract. Consequently, 89 CRCP sections were used in the survey.

A provision was made in the study design so that some of the sections would be surveyed a second time by a different survey party. This replication resulted in 95 sets of observations for use in the analysis.

Data Collection

Table 1 shows a listing of features that were logged by the five field survey parties. The survey sections were assigned at random to the parties. Owing to limitations of time and scheduling, it was not possible to assign an equal number of sections to each of the survey parties. The primary distress variables included close parallel cracks, random bifurcated and intersecting cracks, spalled cracks, edge pumping, and defects as noted by breakups, punchouts, and patches. A summary of the statewide condition survey data is presented in Appendix A.

Regarding parallel cracks, only those having a spacing closer than 30 inches were considered. Parallel cracks and random bifurcated and intersecting cracks were logged on the basis of linear feet of longitudinal pavement containing the particular type of crack under consideration. In addition,

Table 1. Data Obtained During Statewide Condition Survey of CRC Pavements.

Measures of Performance:

1. Defect: This term was used to define all pavement surface features indicative of a failure. The term included breakups, punchouts, asphalt patches,and concrete patches.

2. Breakups and Punchouts: These were counted and also estimated in terms of area.

3. Asphalt and Concrete Patches: These were counted and also estimated in terms of area.

4. Crack Counts: Number of spalled cracks per survey section were counted in terms of three qualitative categories: slightly spalled, moderately spalled, and excessively spalled.

5. Crack Patterns: Parallel cracks, with spacing less than 30 inches, and random bifurcated and intersecting cracks were evaluated in terms of linear feet of longitudinal length of pavement.

6. Pumping: Estimated in terms of linear feet of pavement section length that showed pumping. Pumping was identified by 1) observing discoloration (mudmarks) on the shoulder, 2) observing wet areas on the shoulder.

Supplementary Data:

1. Each breakup or a patch-together with its accompanying crack pattern and spalling characteristics was sketched on the survey form. Some of these defects were photographed.

2. Any dates marked on the pavement were recorded.

3. Joints (construction or expansion) were sketched and indicated by a station identification.

4. Identification features such as bridges, interchanges, etc. were indicated by a station identification. Remarks relative to unusual soil characteristics (subgrade) were also recorded.

cracks that showed spalling, were counted in three categories, depending upon the degree of spall. Defects were noted as breakups (obvious structural failures) or those areas that had been previously patched with asphalt or portland cement concrete. The defects were logged on the basis of total number observed per section. An estimate of the area of the defect was also made.

Information relating to grade, curvature, pumping, and general data on the physical features of the highway were also cataloged. The exact location of patches and breakups was noted on the log sheet. In addition, these locations were either sketched or photographed.

Statistical Design

A 2x2x3x4x2 factorial design with unequal subclass frequencies was used to study the factors influencing the performance of CRC pavements. A number of covariates or concomitant variables were superimposed on the factorial. The layout of the statistical design is shown in Table 2, which also indicates the independent factors and their corresponding levels selected for this investigation. Though a completely randomized factorial design was assumed for the analysis, this assumption may be questioned on the grounds that a restriction on randomization could have been caused by the use of five different survey teams. Procedures and tests for assessing the validity of the assumption of complete randomization are presented in Appendix B.

Independent Factors

The explanatory or independent factors used in the study were: method of paving, method of steel placement, method of steel fabrication (type of steel reinforcement), subbase type and subgrade type.

TABLE 2 FACTORIAL DESIGN FOR STUDY OF FACTORS INFLUENCING CRCP PERFORMANCE

	Method of Paving	Slipformed						Side Formed					
	Method of Steel Placement	Chairs			Depressor			Chairs			Depressor		
Type of Subgrade	Type of Subbase / Method of Steel Fabrication	Loose Bars	Bar Mats	Wire Fabric	Loose Bars	Bar Mats	Wire Fabric	Loose Bars	Bar Mats	Wire Fabric	Loose Bars	Bar Mats	Wire Fabric
Fine Grained	Bituminous Stabilized	9,8	8		9,8	8,8	8,8,8						
	Gravel	9,9,9,8	9,9,9,9,9,9,9,8,8,7,7	9,9,9,8,8,8		9	9,9,9,8			9,8,8,8		8	9,9,9,9,9,9,8
	Crushed Stone	9,7,7,7,7,7,7		9,9,8			9,8,8,7		9				9
	Slag					9,8,8,8	9						9
Granular	Bituminous Stabilized	8			8,8	8,8							
	Gravel		9	8		8	9			9		8	9,9
	Crushed Stone			9			9		9				9
	Slag					8,8							

Numbers in cells denote thickness of CRC pavement in inches.

A detailed breakdown of these factors is given below:

Method of Paving: This factor had two levels:

a. Sideformed
b. Slipformed

Method of Steel Placement: The method of placing steel reinforcement was subdivided into two categories:

a. Pre-set on chairs
b. Placed by mechanical means. This was usually accomplished by placing the reinforcement on top of plastic concrete and depressing it to the prescribed depth by a machine which imparts pressure and vibration.

Hence, the two levels of this factor were labeled as "chairs" and "depressor".

Method of Steel Fabrication: The three kinds of steel reinforcement used in CRC pavements formed the three levels of this factor:

a. Loose reinforcing bars
b. Tied bar mats
c. Welded deformed wire fabric

The amount of longitudinal steel used was 0.6 percent of the pavement cross-sectional area irrespective of other design factors.

In case of loose bars and tied bar mats, longitudinal reinforcement consisted of No. 5 bars with a c/c spacing of 5.5 in. for 9-in. thick pavements and a c/c spacing of 6.25 in. for 7- and 8-in. thick pavements. Use of No. 4 bars, with a c/c spacing of 4 in. for an 8 in. thick pavement and a c/c spacing of 4.5 in. for a 7 in. thick pavement, was also permitted. For transverse reinforcement, No. 4 bars with c/c spacing of 3 feet were used irrespective of pavement thickness. In some cases where steel reinforcement was mechanically placed, transverse steel was omitted. According to Indiana Specifications (35), welding of intersections is not permitted on tied bar mats. Furthermore, the mats may be assembled either inside or outside the forms. The reinforcement was required to be deformed billet steel bars.

The longitudinal reinforcement in welded deformed wire fabric consisted of wires of sizes D-16.8, D-19.2, and D-21.6 at 4 in. c/c spacing for 7 in., 8 in.,and 9 in. thick pavements respectively. For transverse reinforcement, wires of sizes D-4 to D-6 with a c/c spacing varying from 12 to 16 in. were used.

Type of Subbase: A variety of subbase materials have been used under CRC pavements in Indiana:

a. Gravel
b. Air cooled or granulated blast furnace slag
c. Crushed stone
d. Plant-mixed bituminous stabilized aggregate (crushed stone and gravel) with an asphalt content of 2.5 to 4.5 percent. Both asphalt cements and asphalt emulsions have been used as stabilizing agents.

The above materials constituted the four levels of this factor.

Type of Subgrade: Subgrades were classified into two types namely:

a. Fine grained
b. Granular

This information was obtained from aerial photographic strip maps and an engineering soils map of Indiana (37). The CRC pavements in Indiana traverse a variety of landforms. Of these physiographic units, ground moraines, ridge moraines, lacustrine lake-bed deposits, residual deposits, flood plains and alluvial deposits were classified as fine-grained parent materials. Gravel terraces, eskers, glacial outwash deposits, beach ridges and sand dunes were considered as granular parent materials.

Covariates or Concomitant Variables

Covariates or concomitant variables are used in statistical designs to increase the precision of the statistical experiment by removing additional sources of variations that could not be included in the stratification scheme, but had to be evaluated. Covariates are continuous variables in the sense that for each measurement of the response variable, there must be a corresponding value for the covariate. In this investigation it was considered necessary to incorporate some property of concrete and some measure of traffic load applications, for these variables have a considerable effect on distress in concrete pavements. The two covariates used in the statistical design were as follows:

a. Concrete slump measured in inches was obtained from construction survey records.
b. Traffic was evaluated using number of months since a pavement section was opened to traffic. This was used as a surrogate variable for traffic load applications. This also incorporates climatic effects such as annual temperature and frost cycles.

Response or Evaluated Variables

The following response variables obtained from the condition survey data, were used in the study:

a. Number of defects per survey section (5000 ft length of pavement).
b. Number of spalled cracks per survey section.
c. Linear feet of longitudinal pavement section with bifurcated and intersecting random cracks plus parallel cracks, having a spacing closer than 30 inches.
d. Linear feet of longitudinal pavement section where edge pumping was indicated.

Defect is a generic term used in this study to define all pavement surface features indicative of a failure. The term includes severely distressed locations such as breakups and punchouts or those locations that had been previously patched with asphalt or portland cement concrete.

Analysis and Results

The data obtained from the statewide CRCP condition survey were statistically analyzed by using a weighted least squares analysis of covariance procedure. This procedure was necessitated because of unequal subclass cell frequencies in the data. In this situation, the different comparisons with which the sums of squares are associated become nonorthogonal and usual analysis of covariance leads to biased test procedures.

The covariance analysis results reported in this study were obtained by using LSMLGP (Least Squares Maximum Likelihood General Purpose Program), a program at the Purdue University Computer Center. This program uses a general weighted least squares procedure (31) which can be applied to missing value problems where cell frequencies are unequal and also where data are not available for certain subclasses. The program can only handle main effects and 2-factor interactions, but has provisions for incorporating covariates (concomitant variables) in the analysis.

The following analysis of covariance model was used:

$$\begin{aligned} Y_{ijk\ell mp} = {} & \mu + A_i + B_j + C_k + D_\ell + F_m + AB_{ij} + AC_{ik} \\ & + AD_{i\ell} + AF_{im} + BC_{jk} + BD_{j\ell} + BF_{jm} + CD_{k\ell} \\ & + CF_{km} + DF_{\ell m} + \beta_1(S_{ijk\ell mp} - \overline{S}) \\ & + \beta_2(T_{ijk\ell mp} - \overline{T}) + \varepsilon_{(ijk\ell m)p} \end{aligned} \tag{14}$$

where

$Y_{ijk\ell mp}$ = dependent or response variable, e.g., number of defects per section;

μ = true mean effect for the population;

A_i = true effect of method of paving (slipformed versus sideformed);

B_j = true effect of method of steel placement (depressor versus chairs);

C_k = true effect of method of steel fabrication (bar mats versus wire fabric versus loose bars);

D_ℓ = true effect of type of subbase (bituminous-stabilized versus crushed-stone versus slag versus gravel);

F_m = true effect of subgrade soil (granular versus fine-grained);

$S_{ijk\ell mp}$ = linear effect of covariate, slump (in.);

$T_{ijk\ell mp}$ = linear effect of covariate, time (months of traffic);

β_1, β_2 = regression coefficients;

$\bar{S}, \bar{T}$ = mean values of slump and time respectively; and

$\varepsilon_{(ijk\ell m)p}$ = true error, NID (o, σ^2).

The other terms denote the 2-factor interactions among the factors A, B, C, D, and F. The subscripts assume the following values:

$i = 1, 2;$

$j = 1, 2;$

$k = 1, 2, 3;$

$\ell = 1, 2, 3, 4;$

$m = 1, 2;$ and

$p = 0$ (missing value) or $1, 2, \ldots, n_{ijk\ell m}$ (unequal subclass numbers).

The model does not take into consideration 3-factor and higher order interactions owing to computer program limitations. Consequently, these interaction effects are confounded with the error effect in this formulation.

The proposed covariance analysis assumes a completely randomized design (CRD). The assumptions underlying the analysis are discussed in Appendix B.

In analyzing some of the measured variables, a square root transformation was applied to the data to satisfy the requirement of homogeneity of variance, a usual assumption in covariance analysis. The results of the Foster-Burr Q-test (7, 14), used for testing homogeneity of variance, are given in Table 3.

Interaction effects and corresponding main effects that were non-significant at an α-level of 0.25 were pooled with the residual error term and tests of significance were made by using the pooled error term (7).

The analysis was first performed within the framework of the analysis of covariance model given by Equation 14. If a covariate effect did not show significance at an α-level of 0.05, the associated covariate term was deleted from the model and the analysis was repeated without the non-significant covariate. One exception was made to this rule in the analysis of spalled cracks per section. Here only the linear effect of the covariate time showed significance at an α-level of 0.05. The linear effect of the covariate slump, though only significant at an α-level of 0.10, was retained in the analysis as none of the main effects and interaction effects showed significance even at this level. Tables 4, 5, 6 and 7 summarize the results of the analysis of covariance.

The dependent variables shown in Tables 4 to 7 are as follows:

1. Square root of number of defects (asphalt patches, concrete patches and breakups) per section (Table 4).
2. Square root number of asphalt patches and breakups per section (Table 5).
3. Square root of number of spalled cracks per section, excluding slightly spalled and excessively spalled cracks (Table 6).
4. Length of pavement section showing random bifurcated and intersecting cracks plus parallel cracks with less than 30 in. spacing, in feet per section (Table 7).

The length of each section was 5000 ft. The number of observations used in the analysis were 95.

Table 3. Foster-Burr Test for Homogeneity of Variance

Response Variable	Avg. DF	No. of Samples	$Q_{(\text{calculated})}$	$Q_{3,20,0.001}$	Homogeneity of Variance at $\alpha = 0.001$
1. No. of Defects per Section	3	20	.4205	.146	Reject
2. Square Root of No. of Defects per Section	3	20	.1011	.146	Accept
3. No. of Asphalt Patches and Breakups per Section	3	20	.2273	.146	Reject
4. Square Root of No. of Asphalt Patches and Breakups per Section	3	20	.1308	.146	Accept
5. No. of Spalled Cracks per Section	3	20	.1609	.146	Reject
6. Square Root of No. of Spalled Cracks per Section	3	20	.0925	.146	Accept
7. L_{RC+PC} (ft. per Section)	3	20	.0913	.146	Accept

L_{RC+PC} = Length of Pavement Section showing random cracks plus parallel cracks with less than 30 in. spacing, in feet per section.

Table 4. Least Squares Analysis of Covariance - Number of Defects per Section

Source	DF	Sums of Squares	Mean Squares	F	$F_{.05}$	Significant at $\alpha = 0.05$
Total (uncorrected)	95	102.756				
Main Effects						
A_i (Paving)	1	1.315	1.315	2.29	3.96	---
B_j (Steel Placement)	1	0.235	0.235	0.41	3.96	---
C_k (Steel Type)	2	3.573	1.787	3.11	3.11	Yes*
D_ℓ (Subbase)	3	6.609	2.203	3.83	2.72	Yes
F_m (Subgrade)	1	0.307	0.307	0.54	3.96	---
Interaction Effects						
AB_{ij}	1	1.041	1.041	1.81	3.96	---
AC_{ik}	1	0.888	0.888	1.54	3.96	---
CF_{km}	2	2.750	1.375	2.39	3.11	---
Covariate Effect						
$S_{ijk\ell mp}$ (Slump,in.)	1	3.622	3.622	6.31	3.96	Yes
Remainder, $\varepsilon_{(ijk\ell m)p}$	81	46.553	0.575			

Dependent Variable = Square root of number of defects per section.
Regression Coefficient for covariate slump = β_1 = -0.582
Standard error of β_1 = 0.234
Overall mean for slump = $\overline{S}$ = 1.87 in.

*Borderline significance at α = .05.

Table 5. Least Squares Analysis of Covariance - Number of Asphalt Patches and Breakups Per Section

Source	DF	Sums of Squares	Mean Squares	F	$F_{.05}$	Significant at $\alpha = 0.05$
Total (uncorrected)	95	73.363				
Main Effects						
A_i (Paving)	1	0.617	0.617	1.52	3.96	---
B_j (Steel Placement)	1	0.816	0.816	2.01	3.96	---
C_k (Steel Type)	2	2.460	1.230	3.03	3.11	---
D_ℓ (Subbase)	3	6.782	1.261	5.57	2.72	Yes
F_m (Subgrade)	1	0.732	0.732	1.80	3.96	---
Interaction Effects						
AB_{ij}	1	2.732	2.732	6.73	3.96	Yes
AC_{ik}	1	1.530	1.530	3.77	3.96	---
CF_{km}	2	2.353	1.177	2.90	3.11	---
Covariate Effect						
$T_{ijk\ell mp}$ (time, mos.)	1	2.069	2.069	5.10	3.96	Yes
Remainder, $\varepsilon_{(ijk\ell m)p}$	81	33.353	0.406			

Dependent Variable = Square root of number of asphalt patches and breakups per section.
Regression coefficient for covariate, time = β_2 = 0.015.
Standard error of β_2 = 0.007
Overall mean for time = $\overline{T}$ = 15.45 months.

Table 6. Least Squares Analysis of Covariance - Length of Pavement Section Showing Random Cracks Plus Close Parallel Cracks.

Source	DF	Sums of Squares	Mean Squares		$F_{.05}$	Significant at $\alpha = 0.05$
Total (uncorrected)	95	11786182.5				
Main Effects						
A_i (Paving)	1	36828.7	36828.7	0.45	3.96	---
B_j (Steel Placement)	1	17021.3	17021.3	0.21	3.96	---
C_k (Steel Type)	2	5514.5	2757.3	0.03	3.11	---
D_ℓ (Subbase)	3	136454.2	45484.7	0.51	2.72	---
F_m (Subgrade)	1	439.9	439.9	0.01	3.96	---
Interaction Effects						
AB_{ij}	1	398123.7	398123.7	4.81	3.96	Yes
BF_{jm}	1	211012.5	211012.5	2.55	3.96	---
$CD_{k\ell}$	5	784707.5	156941.5	1.90	3.11	---
Covariate Effect						
$T_{ijk\ell mp}$, (Time,mos.)	1	358385.7	358385.7	4.33	3.96	Yes
Remainder, $\epsilon_{(ijk\ell m)p}$	78	6459082.8	82808.8			

Dependent Variable = Length of pavement section with random bifurcated and intersecting cracks plus parallel cracks with less than 30 in. spacing (ft/section).
Regression Coefficient for Covariate, Time = β_2 = 6.289.
Standard Error of β_2 = 3.159.
Overall Mean for Time = $\overline{T}$ = 15.45 months.

Table 7. Least Squares Analysis of Covariance - Number of Spalled Cracks per Section.

Source	DF	Sums of Squares	Mean Squares	F	$F_{.05}$	Significant at $\alpha = 0.05$
Total (uncorrected)	95	147.099				
Main Effects						
A_i (Paving)	1	0.460	0.460	0.51	3.96	---
B_j (Steel Placement)	1	0.078	0.078	0.09	3.96	---
Interaction Effects						
AB_{ij}	1	1.647	1.647	1.82	3.96	---
Covariate Effects						
$S_{ijk\ell mp}$ (slump, in.)	1	3.105	3.105	3.43	3.96	Yes*
$T_{ijk\ell mp}$ (Time, mos.)	1	4.414	4.414	4.88	3.96	Yes
Remainder, $\epsilon_{(ijk\ell m)p}$	89	80.460	0.904			

Dependent Variable = Square root of number of spalled cracks per section (excluding excessively and slightly spalled cracks).
Regression Coefficient for Covariate, Slump = β_1 = -0.543.
Standard Error of β_1 = 0.315.
Overall Mean for Slump = $\overline{S}$ = 1.87 in.
Regression Coefficient for Covariate, Time = β_2 = +0.222.
Standard Error of β_2 = 0.108.
Overall Mean for Time = $\overline{T}$ = 15.45 months.
* Significant at $\alpha = 0.10$.

The extent of pavement distress was evaluated primarily in terms of number of defects. Asphalt patches and breakups were considered separately from concrete patches in one analysis, for they manifested relatively recent pavement distress.

Factors Affecting Distress as Evaluated by Number of Defects Per Section

The results of analysis of covariance presented in Tables 4 and 5 indicate that:

1. The method of steel fabrication and subbase type together with concrete slump had a significant effect on pavement distress as evaluated by number of defects (concrete patches, asphalt patches and breakups) per section.
2. The type of subbase, time since the section was opened to traffic,and the interaction between methods of paving and placing steel reinforcement had a significant influence on pavement condition as determined by the number of asphalt patches and breakups observed per section.
3. Irrespective of the response variable, the subgrade type did not appear to have a significant effect on CRC pavement distress.

Factors Affecting Pavement Cracking

A study of results given in Tables 6 and 7 shows that:

1. The extent of parallel cracks with a crack spacing less than 30 in. and random cracking observed per section of pavement were significantly influenced by the age of pavement and the interaction between methods of paving and placing steel reinforcement.
2. Spalled cracks were primarily induced by traffic (indirectly measured by time since the section was opened to traffic). Concrete slump, was also shown to contribute to spalling of cracks.

Since physical properties of concrete were not evaluated in this phase of the study, the last result points to the effect that slump may have had on concrete properties,such as modulus of elasticity and tensile strength, which in turn could have influenced spalling of cracks.

Detailed Study of Factors Influencing Performance of CRC Pavements

This study further elucidates the results of analysis of covariance presented in Tables 4 through 7. Special emphasis is placed on estimation of factors, shown to be significant by the tests of hypotheses made in the covariance analyses.

Effect of Subgrade: The analyses indicate that type of subgrade parent material had no significant effect on pavement distress or the extent of observed cracking.

Effect of Subbase: The results of data analysis showed that subbase type had a major influence on pavement distress.

Table 8 gives the variation of defects per section with type of subbase. The dependent variable is the square root of number of defects per section. Mean values of the dependent variable for each subbase type are also given. Before the effect of subbase type could be evaluated, the response variable (sq. root of defects per section) had to be adjusted for the effect of slump. The adjusted mean values for various subbase types as shown in Table 8 were obtained by the following relationship:

$$\overline{Y'_\ell} = \overline{Y}_\ell - \beta_1(\overline{S}_\ell - \overline{S}) \qquad (15)$$

where $\overline{Y'_\ell}$ = mean value of response variable, for ℓ^{th} subbase type, adjusted for the effect of slump, $\ell = 1, 2, 3, 4$.

$\overline{Y}_\ell$ = mean value of response variable for ℓ^{th} subbase type.

Table 8. Variation of Defects Per Section with Type of Subbase.

Subbase Type D_ℓ	Number of Sections n_ℓ	Subbase Type Mean $(\overline{Y}_\ell)$	Mean Slump $(\overline{S}_\ell)$	Adjusted Subbase Type Mean $(\overline{Y}'_\ell)$	Standard Error $(s.e.)_\ell$
Gravel (D_1)	46	0.70	1.90	0.70	0.112
Slag (D_2)	8	0.50	1.91	0.52	0.268
Crushed Stone (D_3)	20	0.15	1.80	0.11	0.170
Bituminous Stabilized (D_4)	15	0.0	1.83	-0.02	0.196

Dependent Variable, $Y_{ijk\,mp}$ = Square root of number of defects per section.

$\overline{Y}_\ell$ = Mean value for ℓth subbase type; $\ell = 1,2,3,4$.

$\overline{S}_\ell$ = Mean value of slump, corresponding to $\overline{Y}_\ell$ (in.).

$\overline{Y}'_\ell = \overline{Y}_\ell - \beta_1(\overline{S}_\ell - \overline{S})$ = Mean value for the subbase type adjusted for the effect of slump.

β_1 = Regression coefficient for covariate, slump = -0.582.

$\overline{S}$ = Overall mean for slump = 1.87 in.

n_ℓ = Number of sections with the given type of subbase.

$\overline{S}_\ell$ = mean value of slump (in) corresponding to $\overline{Y}_\ell$

$\overline{S}$ = overall mean value for slump = 1.87 in.

β_1 = regression coefficient for covariate, slump = -0.582.

For purposes of estimation, the 95 percent confidence interval for the adjusted mean for any subbase type, ℓ may be obtained as:

$$\overline{Y}'_\ell - t_{(\alpha/2,df)} \cdot (s.e.)_\ell \leq \mu_{\sqrt{x_\ell}} \leq \overline{Y}'_\ell + t_{(\alpha/2,df)} \cdot (s.e.)_\ell \tag{16}$$

where

$\mu_{\sqrt{x_\ell}}$ = true adjusted mean value of square root of number of defects per section for subbase type, ℓ.

$\overline{Y}'_\ell$ = adjusted mean value for subbase type, ℓ.

$(s.e.)_\ell$ = standard error of mean value for subbase type, ℓ.

$t_{(\alpha/2,df)}$ = two-tailed t-value for a significance level, α, and degrees of freedom, df.

Note: 1. Standard error is approximately obtained as:

$$(s.e.)_\ell = \sqrt{\frac{S_E^2}{n_\ell}}$$

where,

S_E^2 = residual mean squares from analysis of covariance (in this case from Table 4).

n_ℓ = number of sections with subbase type, ℓ.

2. The degrees of freedom, df, correspond to the degrees of freedom for the residual error term (Table 4).

3. Significance level, $\alpha = 1 - \frac{\text{Percent Confidence}}{100}$

Finally the 95 percent confidence limits on the adjusted mean value as obtained in Equation 16 may be expressed in terms of the original, untransformed variable (number of defects per section) as follows:

$$(\overline{Y}'_\ell - t_{(\alpha/2,df)} \cdot (s.e.)_\ell)^2 \le \mu_{x_\ell} \le (\overline{Y}'_\ell + t_{(\alpha/2,df)} \cdot (s.e.)_\ell)^2 \qquad (17)$$

where μ_{x_ℓ} = true adjusted mean value of number of defects per section for subbase type, ℓ.

Applying equations 15, 16, and 17 to gravel subbase data presented in Table 8:

1. Adjusted mean value for the gravel subbase is:

   $\overline{Y}'_1 = 0.70 - (-0.582(1.90-1.87)) = 0.72$

2. The 95 percent confidence interval for the adjusted mean value of square root of number of defects per section for gravel subbase is:

   $$0.72 - (t_{0.025,81})0.112 \le \mu_{\sqrt{x_1}} \le 0.72 + (t_{0.025,81})0.112$$

or, $$0.72 - (1.990)0.112 \le \mu_{\sqrt{x_1}} \le 0.72 + (1.990)0.112$$

or, $$0.497 \le \mu_{\sqrt{x_1}} \le 0.942$$

3. In terms of the original variable (number of defects per section), the 95 percent confidence interval for the adjusted mean value, for gravel subbase, is given as:

   $(0.497)^2 \le \mu_{x_1} \le (0.942)^2$

   $0.247 \le \mu_{x_1} \le 0.887$ defects per section.

The procedures, used in developing Equations 15, 16, and 17 for obtaining the 95 percent confidence interval for subbase type means, can also be used for estimating confidence bands for treatment means relating to other significant main effects and interactions in this analysis. By using approproate values of the t-statistic, confidence intervals for the treatment means may be set at levels other than 95 percent.

For sake of simplicity, the variation of response functions with respect to significant explanatory factors is presented in terms of the transformed response variables, where applicable. The results presented for significant effects include treatment means, means adjusted for the covariate effect,and the corresponding standard errors.

The variation of asphalt patches and breakups per section with subbase type is shown in Table 9. A consideration of adjusted mean values given in Tables 8 and 9 shows that the use of crushed stone and bituminus stabilized subbases resulted in fewer defects per section than the use of gravel subbases. Slag subbases showed relatively poor performance. This conclusion needs a slight modification since the majority of defects related to slag subbases were confined to one construction contract.

Until the statewide condition survey, sections with bituminous-stabilized subbases did not show any significant distress and some sections with crushed-stone subbases showed minor distress. This conclusion should be viewed with caution as bituminous-stabilized subbases were used more recently (primarily 1972) and have not been exposed to the full range of environmental and traffic conditions. Since the time of the condition survey, severe distress has been reported on at least one contract with a bituminous-stabilized subbase.

The type and quality of subbases also have a significant influence on pavement pumping. Yoder (66) indicated that 3 basic conditions must be present to create pumping: frequent repetition of heavy loads, fine-grained material that will go into suspension with water, and free water under the pavement. The effect of subbase on pumping of CRC pavements is given in Table 10. Edge pumping was the primary mode of pavement pumping observed during the field survey, although

Table 9. Variation of Asphalt Patches and Breakups Per Section with Type of Subbase.

Subbase Type (D_ℓ)	Number of Sections (n_ℓ)	Subbase Type Mean ($\overline{Y}_\ell$)	Mean Time ($\overline{T}_\ell$)	Adjusted Subbase Type Mean ($\overline{Y}'_\ell$)	Standard Error $(s.e.)_\ell$
Gravel (D_1)	46	0.64	21.25	0.55	0.094
Slag (D_2)	8	0.38	8.75	0.48	0.225
Crushed Stone (D_3)	20	0.15	14.18	0.17	0.143
Bituminous Stabilized (D_4)	15	0.00	2.27	0.20	0.165

Dependent Variable, $Y_{ijk\ell mp}$ = Square root of nubber of asphalt patches and breakups per section.

$\overline{Y}_\ell$ = Mean value for ℓth subbase type, $\ell = 1,2,3,4$.

$\overline{T}_\ell$ = Mean value of time (months of traffic) corresponding to $\overline{Y}_\ell$.

$\overline{Y}'_\ell = \overline{Y}_\ell - \beta_2(\overline{T}_\ell - \overline{T})$ = Mean value of dependent variable for the ℓth subbase type, adjusted for the effect of time.

β_2 = Regression coefficient for covariate, time = 0.015.

$\overline{T}$ = Overall mean for time = 15.45 months.

Table 10. Effect of Subbase Type on CRC Pavement Pumping

Type of Subbase	Percentage of Survey Sections Showing		
	No Pumping	Minor Pumping*	Major Pumping**
Gravel	56.5	34.7	8.8
(46)	(26)	(16)	(4)
Crushed Stone	90.0	10.0	---
(20)	(18)	(2)	---
Bituminous Stabilized	93.3	6.7	---
(15)	(14)	(1)	---
Slag	100.0	---	---
(8)	(8)	---	---

Numbers in parentheses are number of sections falling in the category indicated.

* Pumping indicated on less than 10 percent of the section length.

** Pumping indicated on more than 10 percent of the section length.

pumping at cracks has been noted. The extent of observed pavement pumping was divided into 3 categories: no pumping; minor pumping, when pumping was indicated on less than 10 percent of the section length; and major pumping, when pumping was indicated on more than 10 percent of the section length.

Data given in Table 10 show that the highest incidence of pumping occurred where gravel subbases were used while no pumping was indicated on sections with slag subbases. Minor pumping was observed on sections with crushed stone and bituminous-stabilized subbases.

Effect of Type of Steel Reinforcement: Table 11 gives the variation of defects per section with method of steel fabrication. Compared to loose bars, the use of bar mats or wire fabric resulted in relatively greater distress. This statement should be qualified by the fact that bar mats and wire fabric were used in older CRCP construction contracts whereas loose bars have been used more recently (primarily 1972).

Effect of Methods of Paving and Steel Placement: The interaction between the methods of paving and steel placement was shown in the covariance analysis to have a significant effect on:

1. Number of defects per section.
2. Length of close transverse random cracking per section.

The variation of asphalt patches and breakups as a function of the interaction between methods of paving and steel placement is shown in Table 12, while the effect of this interaction on length of cracking is given in Table 13.

The least number of defects per section occurred where the steel reinforcement was placed by a depressor while the paving was accomplished by using conventional side forms. Hardly any practical difference in distribution of defects per section was indicated between pre-set steel or depressed

Table 11. Variation of Defects Per Section with Type of Steel Reinforcement

Type of Steel Reinforcement (C_k)	Number of Sections (n_k)	Steel Type Mean ($\overline{Y}_k$)	Mean Slump ($\overline{S}_k$)	Adjusted Steel Type Mean ($\overline{Y}'_k$)	Standard Error $(s.e.)_k$
Bar Mats (C_1)	29	0.58	1.87	0.59	0.141
Wire Fabric (C_2)	42	0.40	1.92	0.43	0.117
Loose Bars (C_3)	18	0.32	1.71	0.23	0.178

Dependent Variable, $Y_{ijk\ell mp}$ = Square root of number of defects per section.

$\overline{Y}_k$ = Mean value for kth type of steel reinforcement; k = 1,2,3.

$\overline{S}_k$ = Mean value of slump, corresponding to $\overline{Y}_k$ (in.)

$\overline{Y}'_k = \overline{Y}_k - \beta_1(\overline{S}_k - \overline{S})$ = Mean value of dependent variable for kth type of steel reinforcement adjusted for the effect of slump.

β_1 = Regression coefficient for covariate slump = -0.582.

$\overline{S}$ = Overall mean for slump = 1.87 in.

Table 12. Variation of Asphalt Patches and Breakups Per Section with Methods of Paving and Steel Placement.

Method of Paving (A_i)	Slipformed (A_1)		Sideformed (A_2)	
Method of Steel Placement (B_j)	Chairs (B_1)	Depressor (B_2)	Chairs (B_1)	Depressor (B_2)
Number of Sections (n_{ij})	38	30	7	14
Treatment Mean ($\overline{Y}_{ij}$)	0.45	0.35	0.74	0.21
Mean Time ($\overline{T}_{ij}$)	17.09	5.18	36.14	20.29
Adjusted Treatment Mean ($\overline{Y}'_{ij}$)	0.43	0.51	0.43	0.14
Standard Error $(s.e.)_{ij}$	0.103	0.116	0.241	0.170

Dependent Variable, $Y_{ijk\ell mp}$ = Square root of number of asphalt patches and breakups per section.

$\overline{Y}_{ij}$ = Mean value for the ith method of paving and the jth method of steel placement; $i = 1,2;\ j = 1,2$.

$\overline{T}_{ij}$ = Mean value of time (months of traffic), corresponding to $\overline{Y}_{ij}$.

$\overline{Y}_{ij} = Y_{ij} - \beta_2(\overline{T}_{ij} - \overline{T})$ = Mean value of dependent variable for the ith method of paving and the jth method of steel placement, adjusted for the effect of time.

β_2 = Regression coefficient for covariate, time = 0.015.

$\overline{T}$ = Overall mean for time = 15.45 months.

Table 13. Variation of Length of Cracking in Feet Per Section with Methods of Paving and Steel Placement.

Method of Paving (A_i)	Slipformed (A_1)		Sideformed (A_2)	
Method of Steel Placement (B_j)	Chairs (B_1)	Depressor (B_2)	Chairs (B_1)	Depressor (B_2)
Number of Sections (n_{ij})	38	30	7	14
Treatment Mean ($\overline{Y}_{ij}$)	557.8	245.5	610.3	632.6
Mean Time ($\overline{T}_{ij}$)	17.09	5.18	36.14	20.29
Adjusted Treatment Mean ($\overline{Y}_{ij}'$)	547.8	310.1	480.2	602.1
Standard Error $(s.e.)_{ij}$	46.7	52.5	108.8	76.9

Dependent Variable, $Y_{ijk\ell mp}$ = Longitudinal pavement length showing parallel cracks with less than 30 in. spacing plus longitudinal pavement length showing random cracking (ft.).

$\overline{Y}_{ij}$ = Mean value for the ith method of paving and the jth method of steel placement; $i = 1,2;\ j = 1,2.$

$\overline{T}_{ij}$ = Mean value of time (months of traffic), corresponding to $\overline{Y}_{ij}$.

$\overline{Y}_{ij}' = Y_{ij} - \beta_2(\overline{T}_{ij} - \overline{T})$ = Mean value of dependent variable for the ith method of paving and the jth method of steel placement, adjusted for the effect of time.

β_2 = Regression coefficient for covariate, time = 6.289.

$\overline{T}$ = Overall mean for time = 15.45 months.

steel, when the pavement was slipformed.

Similarly, the least amount of close transverse cracks occurred in sections, where a combination of slipformed paving and depressed steel was used. The largest amount of cracking was indicated in sections that were sideformed and where depressed steel was used.

By itself, neither the method of paving nor the method of steel placement had any significant effect on pavement distress or frequency of cracking. Nevertheless, it was suspected that the combined effect of method of paving, type of steel,and method of steel placement may have a significant influence on pavement distress. To evaluate this effect further, the data shown in Table 14 were developed. This table gives the variation, of the number of defects, the number of asphalt patches and breakups, and length of close random cracking per section, with various combinations of methods of paving, steel fabrication and steel placement. The response variables, where applicable, are the transformed variables adjusted for the effect of appropriate covariates.

A consideration of data presented in Table 14 shows that:

1. For various combinations of methods of paving and steel fabrication, a higher frequency of defects was indicated for sections where chairs were used for the placement of steel reinforcement. This trend breaks down in the case where side forms were used for paving and the steel reinforcement consisted of bar mats.

2. No specific trends were indicated for the distribution of asphalt patches and breakups. For slipformed sections fewest asphalt patches and breakups occurred where the reinforcement consisted of depressed loose bars. In case of sections paved with conventional side forms, the least number of asphalt patches and breakups per section were indicated for depressed wire fabric.

Table 14. Effect of Method of Construction on Distribution of Defects and Length of Cracking Per Section

Method of Paving	Slipformed				Side Formed					
Method of Steel Fabrication	Bar Mats		Wire Fabric		Loose Bars		Bar Mats		Wire Fabric	
Method of Steel Placement	CH	DP	CH	DP	CH	DP	CH	DP	CH	DP
No. of Sections	13	12	11	14	14	4	2	2	5	12
Adjusted Mean of Sq. Root of Defects Per Section*	0.52	0.39	0.32	0.28	0.26	0.11	1.16	1.37	0.99	0.45
Adjusted Mean of Sq. Root of Asphalt Patches and Breakups Per Section**	0.49	0.53	0.38	0.57	0.39	0.21	0.15	1.19	0.53	-0.04
Adjusted Mean of Length of Close Parallel Cracks and Random Cracking Per Section (feet)**	554.1	256.8	572.2	364.3	521.6	280.8	717.9	490.3	382.3	620.9
Mean Value of Slump (in.)	1.67	1.76	1.61	1.59	1.61	2.06	3.0	2.50	2.10	2.51
Mean Value of Time (months)	24.23	4.88	19.36	6.54	8.64	1.25	39.0	3.0	35.4	23.17

* Adjusted for the effect of concrete slump.
**Adjusted for the effect of time (months of traffic).
CH = Chairs
DP = Depressor

3. For various combinations of methods of paving and steel fabrication, more cracking was evidenced in sections where chairs were used for placing steel reinforcement. This relationship does not hold for one case where paving was done by conventional side forms and the reinforcement consisted of wire fabric.

The results deduced from the data presented in Table 14 are based on observed trends and do not have any statistical significance attached to them. For purposes of estimation, the three factor interaction can be further evaluated by a multiple regression technique using non-orthogonal dummy variables. The technique is described in Anderson and McLean (7).

Effect of Time: The time that a pavement has been under traffic had a significant effect on pavement distress. In the covariance analysis, asphalt patches and breakups and longitudinal random cracking were positively correlated with the linear effect of the covariate, time. This shows that the incidence of pavement distress and cracking increases with the time a pavement has been under traffic.

A study of selected CRCP sections on Interstate Highway I-65 was conducted to evaluate the effect of time on pavement distress in more detail. The change in number of defects per mile over time, for pavements with different types of subbase, is given in Table 15. A similar relationship for construction methods is shown in Table 16. These data indicate that over a period of 18 months, a significant increase in number of defects per mile occurred on sections where a bituminous stabilized subbase was used. The number of defects per mile also increased for gravel subbases, whereas for crushed stone subbases, no change was shown. A similar trend, showing increase in number of defects per mile was observed for various combinations of construction factors.

Table 15. Change in Number of Defects Per Mile by Subbase Type (I-65).

Subbase Type	Summer 1972	Fall 1973
Gravel	1.56	2.91
Crushed Stone	0.0	0.0
Bituminous Stabilized	0.21	1.44

Table 16. Change in Number of Defects Per Mile by Construction Type (I-65).

Construction Type			Number of Defects Per Mile	
Paving Method	Steel Type	Placement of Steel	Summer 1972	Fall 1973
Slipformed	Loose Bars	Chairs	4.13	8.51
Slipformed	Bar Mats	Chairs	1.50	1.85
Slipformed	Wire Fabric	Chairs	0.36	0.60
Slipformed	Wire Fabric	Depressor	1.25	2.08
Sideformed	Wire Fabric	Chairs	1.24	3.11
Sideformed	Wire Fabric	Depressor	0.26	0.52

Effect of Traffic: Since the effect of time included the influence of environmental factors such as annual temperature and frost cycles, a separate study was made to isolate the effect of traffic load applications.

In order to estimate the cumulative number of equivalent 18-kip, single-axle load applications for the critical traffic lane of each survey section, the following relationship was developed.

$$\Sigma L = (F)(ADT_{EQ})(N)(D/100)(T/100) \qquad (18)$$

where ΣL = cumulative number of equivalent 18-kip, single-axle load applications in the critical traffic lane.

F = equivalence coefficient

ADT_{EQ} = equivalent average daily traffic, both directions (veh/day)

N = number of days since opened to traffic (number of years, n x 365)

D = directional distribution factor (percent)

T = percent commercial vehicles in critical traffic lane (right lane)

The input variables used in the above equation may be obtained as follows:

1. F: This is an equivalence coefficient that permits the translation of traffic volumes expressed as ADT to equivalent 18-kip, single-axle applications. Ulbricht (59) derived values of this equivalence coefficient for three classes of truck routes in Indiana. These are given in Table 17. It should be noted that these equivalence coefficients are applicable only to traffic conditions in Indiana. For the purpose of this study, equivalence coefficients for Class I and Class II Truck Routes were used.

Table 17. Equivalence Coefficient, F, for Three Classes of Truck Routes.

Class of Truck Route	Equivalence Coefficient for Rigid Pavements
I	0.22
II	0.10
III	0.03

Class I Truck Routes = All Interstate routes and US-numbered routes connecting major population centers.

Class II Truck Routes = All other primary state highways.

Class III Truck Routes = All secondary state highways.

(Source: From Ulbricht)

2. ADT_{EQ}: This is the equivalent average annual daily traffic (both directions) for the study period and is given by:

$$ADT_{EQ} = \frac{1}{n} \left(ADT + \sum_{x=2}^{n} \frac{ADT(1+r)^{x} + ADT(1+r)^{x-1}}{2} \right) \tag{19}$$

where ADT_{EQ} = equivalent average annual daily traffic both directions (veh/day).

ADT = initial average daily traffic, both directions for year 1 (veh/day).

r = rate of annual traffic growth.

n = number of years since opened to traffic.

x = year under consideration.

The above expression may be simplified to:

$$ADT_{EQ} = \frac{ADT}{n} \left(1 + \frac{1}{2} \left(\sum_{x=2}^{n} (1+r)^{x} + (1+r)^{x-1} \right) \right) \tag{20}$$

For this study ADT_{EQ} was obtained by the following first order approximation of Equation 19.

$$ADT_{EQ} = \frac{ADT_i + ADT_f}{2} \tag{21}$$

where ADT_i = average daily traffic when pavement survey section was opened to traffic.

ADT_f = average daily traffic at time of condition survey.

Estimates of two-directional ADT_i and ADT_f were obtained from State of Indiana traffic maps for 1966, 1969, and 1972 (36).

3. N: Number of days since opened to traffic were obtained by determining the period in days between the time the pavement section was opened to traffic to the time of the condition survey.

4. D: The directional distribution was taken as 50 percent for purposes of this study.

5. T: The percentage of commercial vehicles in critical traffic lane of divided highways may be obtained by the use of Figures 3 and 4. In these figures, the percent of commercial vehicles in right lane is given as a function of the hourly traffic volume in one direction. The hourly traffic volume was obtained by dividing the ADT_{EQ} by 48. Figure 3 is taken from a study by Taragin on lateral placement of trucks (56), while Figure 4 was developed from data presented by Malo et.al. in their study related to traffic behavior on urban expressways (38). For two-lane highways with traffic in both directions, T is equal to 100 percent.

The distribution of defects for various ranges of accumulated 18-kip, single-axle load applications is given in Table 18. It is of interest to note that sections, that had sustained less than 30,000 equivalent 18-kip, single-axle applications in the traffic lane, did not show any apparent distress as indicated by patches or breakups. Beyond this level of load applications, 25-43 percent of the pavement sections developed structural failures. This conclusion is further substantiated by the evidence that almost all the defects were observed in the traffic lane of the survey seciions. Passing lanes which carry only 10-20 percent of truck traffic under normal traffic conditions were observed to be free of distress in the condition survey.

Effect of Concrete Slump: In the analysis of covariance of number of defects per section, the linear effect of concrete slump was found to be negatively correlated with the square root of number of defects per section. This indicates that pavements constructed with a relatively higher slump concrete should have a lower incidence of distress. The effect of slump on distribution of defects is demonstrated in Table 19. A higher percentage of sections had defects where the concrete slump was low. The optimum value of slump relative to good

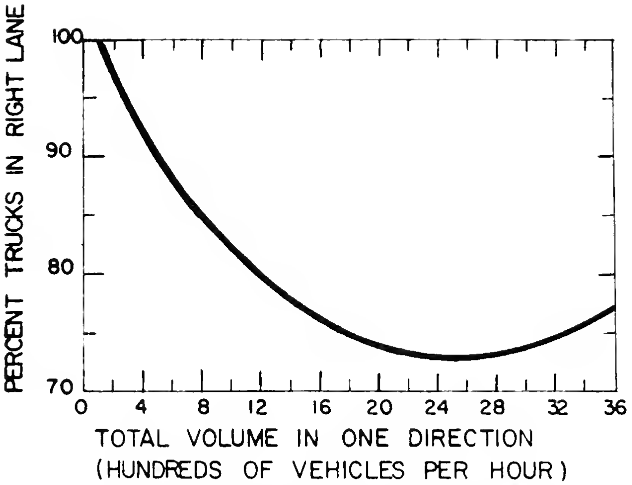

FIG.3 PERCENTAGE OF TRUCKS IN RIGHT LANE OF A 4-LANE DIVIDED HIGHWAY (FROM TARAGIN)

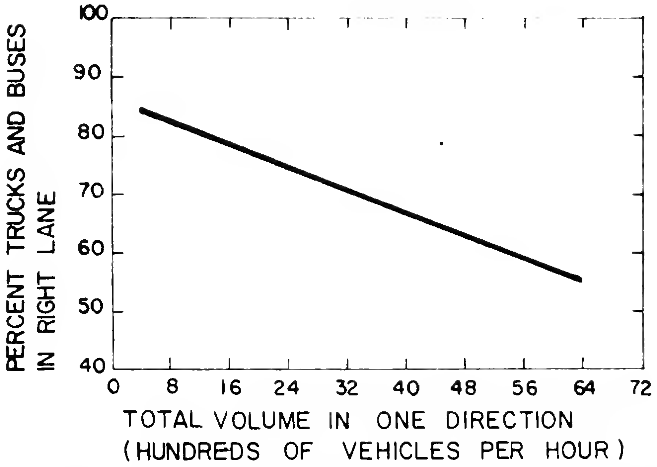

FIG.4 PERCENTAGE OF TRUCKS AND BUSES IN RIGHT LANE OF A 6-LANE DIVIDED HIGHWAY (ADAPTED FROM MALO ET.AL.)

Table 18. Effect of Cumulative Load Applications on Distribution of Defects Among Sections.

Log ΣL*	No. of Sections Surveyed	Sections With No Defects	Sections With Defects	
			Number	Percent
<3.5000	10	10	0	0.0
3.501 - 4.000	5	5	0	0.0
4.001 - 4.500	4	4	0	0.0
4.501 - 5.000	7	4	3	43.0
5.001 - 5.500	14	9	5	35.7
5.501 - 6.000	28	16	12	42.9
6.001 - 6.500	17	12	5	29.4
6.501 - 7.000	4	3	1	25.0

* ΣL = Cumulative equivalent 18-kip,single-axle load applications for the critical traffic lane.

Table 19. Effect of Slump on Distribution of Defects Among Sections.

Slump (in.)	No. of Sections Surveyed	Sections With No Defects	Sections With Defects		
			Number	Percent	No. Per Section*
1.0 - 1.5	31	17	14	42.2	2.9
1.5 - 2.0	39	29	10	25.6	3.2
2.0 - 2.5	13	11	2	15.4	1.0
2.5 - 3.0	4	3	1	25.0	1.0
>3.0	2	2	0	0.0	0.0

* Only sections with defects considered.

performance appears to be between 2.0 to 2.5 in. With increase in slump, a decrease in the number of defects per section was also indicated. The effect of slump values, greater than 2.5 in., on the occurrence of defects should be critically evaluated. There were only 6 sections having slump values greater than 2.5 in. and these may not be representative of the effect.

Distribution of Defects

Figure 5 shows the frequency distribution of defects (concrete patches, asphalt patches and breakups) observed during the statewide CRCP condition survey. This distribution indicates that:

1. 69.7 percent of CRCP sections surveyed did not show any defects.
2. 26.9 percent of CRCP sections had from one to five defects per section.
3. 3.4 percent of CRCP sections had more than five defects per section.

This information was based on 89 sections, each 5,000 ft. long, of equivalent two-lane or three-lane CRC pavement.

Summary of Results of Statewide Condition Survey

The analysis of data collected during a statewide survey of continuously reinforced concrete pavements in Indiana, revealed a number of significant results and correlations. The survey was statistically designed wherein each construction contract was required to be in the study. At least 1 survey section 5,000 ft. in length was sampled from each contract. In some cases, more than one 5,000 ft. section was evaluated within a construction contract because of the stratification of factors used in the statistical study. The results of the statewide survey provided some definite indications relative to causes of distress in CRC pavements.

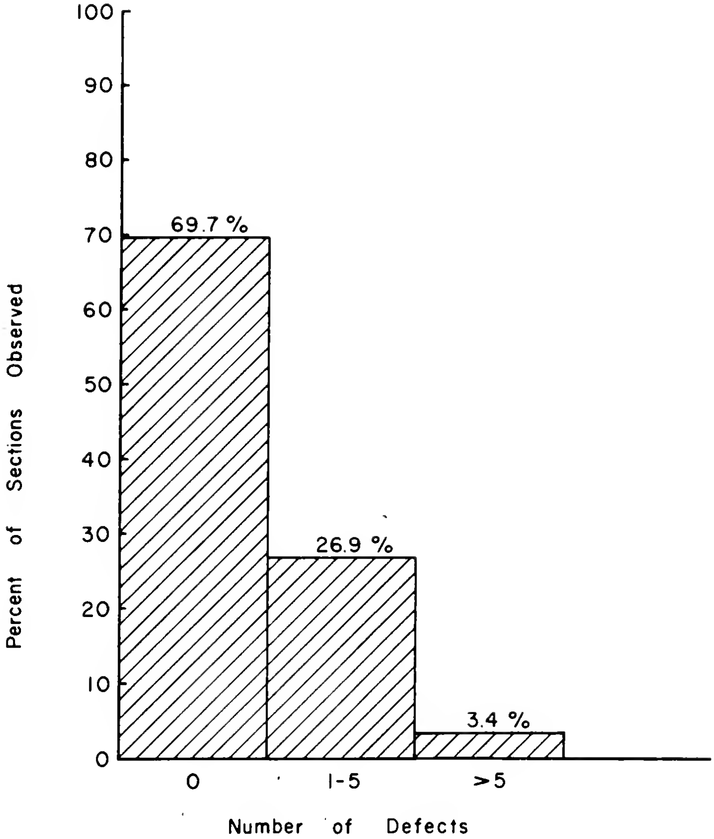

FIG. 5 FREQUENCY DISTRIBUTION OF DEFECTS OBSERVED IN THE STATEWIDE CRCP SURVEY

The following summary of results pertains to the effect of various factor influencing the performance of CRC pavements in Indiana.

1. Subbase type was found to be a significant contributor to the performance of CRC pavements; gravel subbases showed the poorest performance. Crushed stone and slag subbases have, in general, shown good performance, and at the time of the survey the bituminous-stabilized subbases showed little or no distress. Since the condition survey, some breakup has been encountered on at least one bituminous-stabilized subbase.
2. For most combinations of methods of paving and steel fabrication, depressed steel performed better than preset steel used on chairs.
3. All other factors being constant, loose bars showed good performance compared to the use of bar mats and wire fabric. Though relatively poorer performance was indicated for bar mats and wire fabric, they have been used mainly on some of the earlier projects. Thus, pavements with these types of steel have been exposed to a wider range of environmental and traffic conditions.
4. Concrete slump had a significant effect on pavement performance; the optimum slump range was between 2.0 and 2.5 in. Slump values of 1.5 in. and greater have generally shown good results.
5. Pavements that were sideformed performed the same as those that were slipformed.
6. Distress of CRC pavements is associated with traffic. Pavements exposed to a larger number of load applications have shown greater distress.
7. The primary mode of pumping of CRC pavements is edge pumping. The results of the condition survey indicate that pavements with gravel subbases are more

susceptible to pumping. Pavements with crushed-stone and bituminous-stabilized subbases have shown some indication of pumping, while pavements with slag subbases have not pumped.

8. Subgrade parent material type (granular or fine-grained) was not a significant contributor to performance of CRC pavements. This refers to type of subgrade and not to other factors such as degree of compaction.

Postcript

At the time of the condition survey, no defects were observed on the section located on construction Contract R-8001 on Interstate Highway I-65, south of Indianapolis. This contract had the following construction features:

a) Method of Paving: slipformed.
b) Method of Steel Placement: chairs.
c) Type of Steel Reinforcement: bar mats.
d) Type of Subbase: gravel.
e) Time Under Traffic: 6 months.

In the light of the results of the condition survey, it could be predicted that, over time, this section would develop distress.

A year later in November 1973, 11 defects (structural failures) were recorded over the 5,000 ft. length of the section. By August 1974, the number of defects had increased to 18.

PART III

DETAILED EVALUATION OF SELECTED CRCP TEST SECTIONS

FIELD AND LABORATORY STUDIES

DESIGN OF THE DETAILED EVALUATION STUDY

After the completion of the statewide condition survey, a detailed program of field and laboratory investigations was set up to evaluate by physical tests the parameters that were shown to contribute significantly to CRCP performance in the condition survey. With respect to the broad framework of the study, the detailed field investigation constituted the second phase of the research while the laboratory testing program was the third and the final step. These phases of the research are presented together because of the overlap of some of the results obtained from the two parts. The field study was conducted in May-June 1973 while the laboratory testing program was completed in December 1974.

Study Design

The field investigation was designed to include only the CRC pavements that are part of the Interstate Highway System in Indiana. As a result only 9-inch thick pavements were evaluated. This measure was taken for the purpose of obtaining a homogeneous set of pavement sections with respect to pavement thicknesses and percentage of steel reinforcement. The objective was to evaluate the factors that had contributed to non-uniform performance of CRCP in spite of maintaining the same design constants such as pavement thickness and amount of reinforcing steel.

The design of the detailed evaluation study was based on the results of the 1972 statewide condition. The factors that were found to be statistically significant in the condition survey were used as the stratification criterion for sampling the test sections for the field study. The stratification scheme consisted of the following factors:

1. method of paving (slipformed; sideformed)
2. method of steel placement (depressed steel, steel pre-set on chairs)
3. type of steel reinforcement (wire fabric, bar mats, loose bars)
4. type of subbase (gravel, slag, crushed stone, bituminous stabilized)

A total of 31 test sections were included in the field investigation. The test sections were located on Interstate Highways I-65, I-69, I-70, I-90 and I-465.

Delineation of Test Sections

The test sections used in the field investigation were delineated according to the following criteria:

1. The test section, 1000 ft. in length, was a tangent section with flat gradients (less than ± 1%) under uniform grade conditions, i.e., completely under fill, cut or at grade conditions.
2. It was required that the test section lie within the internal portion of the continuous slab, substantially removed from construction or expansion joints.
3. The test section was located wholly within one physiographic unit, e.g., ground moraine, glacial terrace, flood plain, etc.
4. Wherever possible, a test section was located to include at least one location where significant distress as indicated by a breakup or a patch was observed.
5. The structural components of the pavement section were required to conform to a combination of levels of factors comprising the stratification scheme.
6. The 1000 ft. test section was located within one of the randomly selected 5000 ft. survey sections used in the statewide conditions survey.

Fifteen sections were available that had at least one location where a breakup or a patch was observed. Pumping at the pavement edge was indicated in the vicinity of most of the failed locations. An example of this type of pavement pumping is illustrated in Figure 6. An additional section had one location with heavily spalled cracks indicative of an incipient failure condition. This condition is shown in Figure 7. The rest of the sections showed no apparent indication of distress. In a few instances the 1000 ft. test section could not be located within the 5000 ft. randomly selected survey sections used in the statewide condition survey, because some elements of the controlling criteria could not be satisfied. In such cases, a new randomly sampled 1000 ft. test section was used.

Collection of Field Data

The typical layout and the data collected at each test section are outlined in Figure 8. The first step in the data collection procedure was to divide the test section into 10 segments of 100 ft. length each. Where possible two test locations, corresponding to failed and good pavement conditions respectively, were selected within each test section. A failed test location was defined as one showing distress, indicated by a patch or a breakup. Conversely, a good test location was defined as one showing no apparent distress. Typical examples of these conditions are illustrated in Figures 9 and 10. Two test locations were also used in test sections, which did not show any indication of a failure. One location corresponded to an area with a uniform and evenly spaced crack pattern (see Figure 10) while the other was representative of an area with a relatively more dispersed and non-uniform transverse cracking (see Figures 11 and 12). These crack patterns were evaluated subjectively by visual examination. In

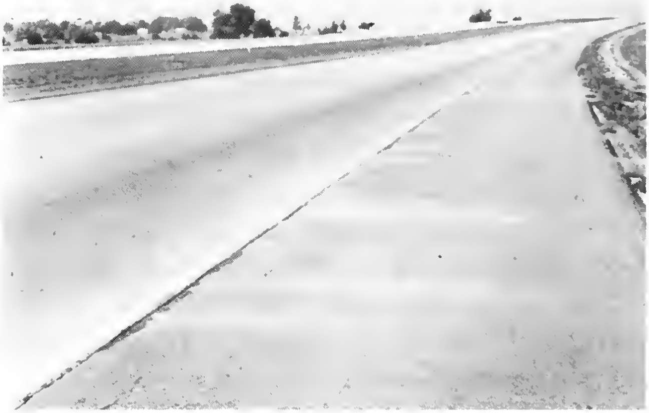

FIG. 6 ACTIVE PUMPING AT THE PAVEMENT EDGE

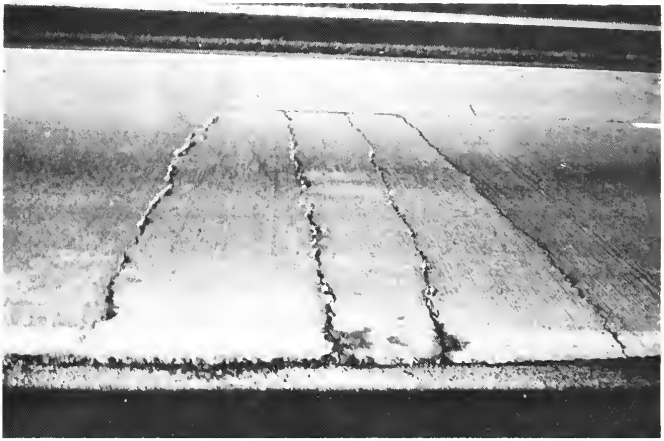

FIG. 7 INCIPIENT FAILURE CONDITION INDICATED BY HEAVILY SPALLED CRACKS

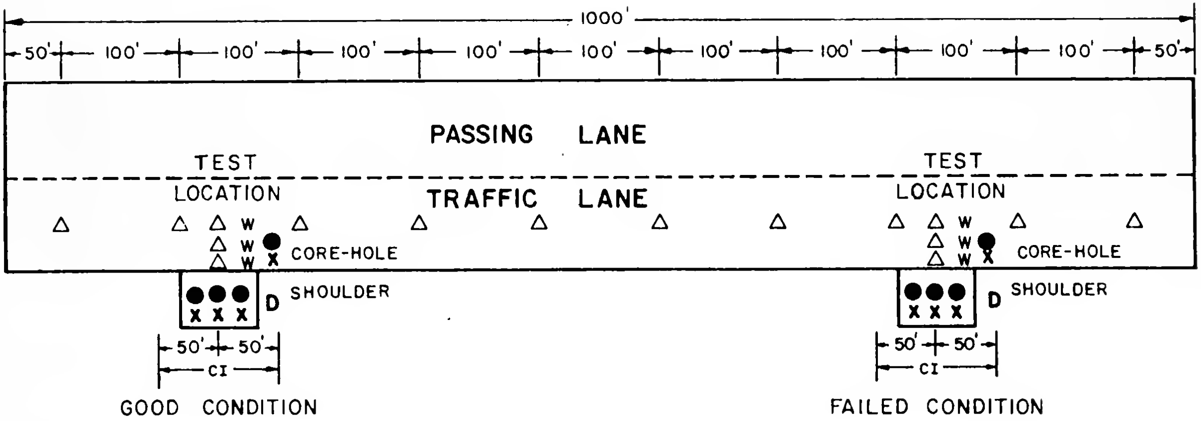
1000'
50'
100'
100'
100'
100'
100'
100'
100'
100'
100'
50'
PASSING LANE
TRAFFIC LANE
TEST LOCATION
TEST LOCATION
W
W
W
X
CORE-HOLE
D
SHOULDER
50'
50'
CI
GOOD CONDITION
FAILED CONDITION

LEGEND:

△ = DYNAFLECT MEASUREMENTS AT CRACK AND MID-SPAN POSITIONS

W = CRACK WIDTH MEASUREMENTS AT ONE CRACK

● = CONE PENETROMETER TEST FOR SUBBASE

X = DYNAMIC CONE PENETROMETER TEST FOR SUBGRADE

D = SUBGRADE AND SUBBASE DENSITY AND WATER CONTENT MEASUREMENTS

CI = 100ft. SECTION FOR CRACK INTERVAL MEASUREMENTS AND CRACK INTERSECTION COUNTS

FIG. 8 TYPICAL LAYOUT OF TEST SECTIONS (NOT TO SCALE)

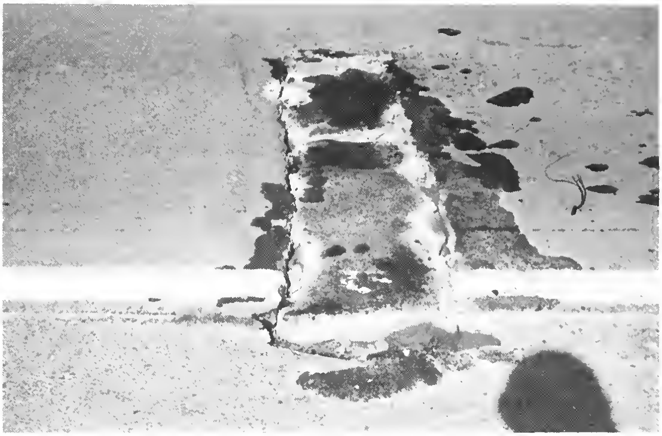

FIG. 9 TEST LOCATION – FAILURE CONDITION

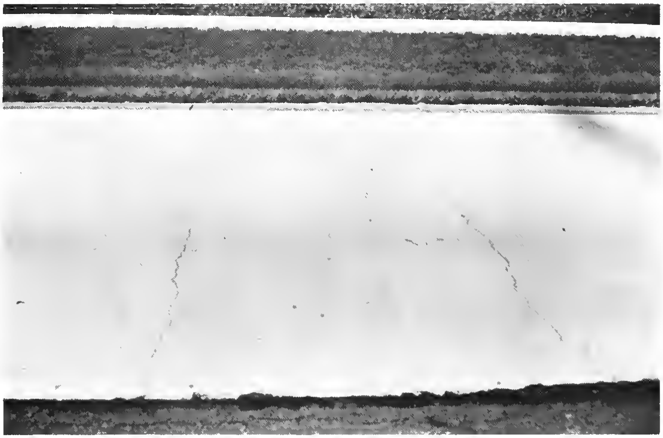

FIG. 10 TEST LOCATION – GOOD CONDITION WITH A UNIFORM AND NORMAL CRACK PATTERN

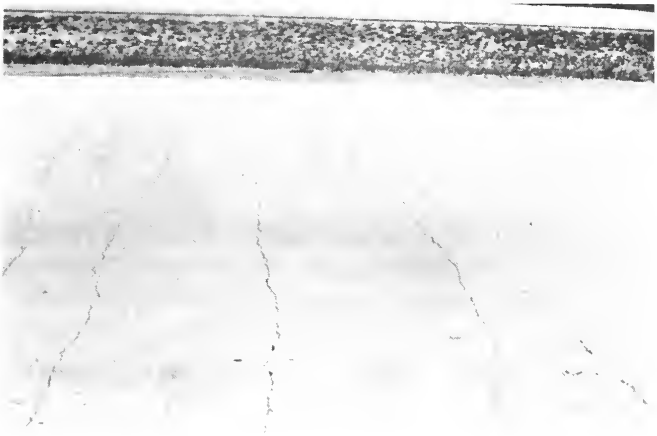

FIG.11 TEST LOCATION — NON-UNIFORM, CLOSELY SPACED CRACK PATTERN

FIG.12 A TYPICAL BIFURCATED CRACK WITH A CRACK INTERSECTION

certain sections without failures, tests were conducted only at one location because of limitations of time.

At a test location, tests on the subbase and the subgrade were made at two points. One test point, located at the pavement-shoulder interface, was designated as the shoulder position. The other test point was the hole through the pavement from which a concrete core had been extracted. This was designated as the core-hole position.

A series of tests performed at a test section consisted of the following:*

Deflection Measurements: Pavement deflections were evaluated with the Dynaflect (53, 54). At the center of each 100 ft. segment two deflection measurements were taken, one at a crack position, while the other at the mid-span position between two transverse cracks. These measurements were taken along the center line of the traffic lane, by using only the sensor between the steel wheels.

A second set of deflection measurements were made at the test locations. These measurements were obtained by using all the sensors and were taken, across the traffic lane, at 1.0 ft., 3.5 ft., and 6.0 ft. from the outside pavement edge, approximately corresponding to the outside edge, the right wheel path and the lane center line positions, respectively. The transverse deflections were determined at both a crack position and an adjacent mid-span position between two transverse cracks.

Some additional deflection measurements were made at close intervals (about 2.0 ft.) at a failed location along the center line of the traffic lane in order to delineate the extent of the failures. Hence, at a given test section, a minimum of 20 Dynaflect readings in the longitudinal direction and 12 Dynaflect readings in the transverse direction were recorded.

---

*Photographs illustrating the test methods and equipment are shown in Figures 13 to 28.

Crack Width Measurements: Crack widths were measured by means of a 50X, direct measuring pocket microscope. The points,where crack width measurements were made,corresponded to the positions along a crack where deflections were evaluated. This resulted in three crack width measurements at each test location or a total of six crack width measurements at each test section.

Crack Interval Measurements: Pavement segments 50 ft. in length were first measured on either side of a test location. This was followed by crack interval measurements along the pavement edge over the 100 ft. section centered on a test location. In addition, the number of crack intersections were counted over the 100 ft. section at each test location. Figure 12 shows a typical example of a crack intersection at a bifurcated crack.

Subgrade and Subbase Evaluation: In-place penetration tests were made on subbase and subgrade by means of the High Load Penetrometer (11) and the Dynamic Cone Penetrometer (60), respectively. These tests were performed at both core-hole and shoulder positions at each of the two test locations. In all, eight penetrometer tests, four each on subbase and subgrade were performed at each test location. The penetration test values were converted to in-place California Bearing Ratio (CBR) by the use of calibration charts. Before conducting the penetration tests, in-place nuclear density and water content determinations were made on the subbase and the subgrade. As a check on nuclear moisture content and density measurements, moisture content of the subbase and subgrade materials was determined by the standard procedure and subgrade density was measured by means of a thin-walled tube sampler. These tests were made at the shoulder position after the penetration tests. At the completion of a series of tests on the subbase or subgrade, material was sampled from under the pavement at the pavement-shoulder interface for laboratory testing. In case of failed locations, care was taken to sample the material some distance away (about 5 ft.) from the failed area. In most cases the subbase material directly under the failed area had densified to a degree that it could not be extracted by a pick.

Concrete Cores: Concrete cores were obtained from the two test locations within each test section. These cores were taken from the traffic lane, close to the point from where the subgrade and subbase material were sampled.

Laboratory Testing Program

The laboratory testing program consisted of:

Tests on Concrete Cores: Concrete cores obtained from the field were subjected to the following tests

a. Specific gravity and absorption tests
b. Pulse velocity measurements
c. Bulk density measurements

Next the cores were cut and segments without any steel from above and below the level of reinforcement were tested for specific gravity, water absorption, pulse velocity, bulk density,and splitting tensile strength.

Tests of Subbase and Subbase Materials: The series of tests on subgrade soils and granular subbase materials included standard classification and compaction tests. Permeability tests, utilizing a constant head permeameter, were made on selected samples of slag, crushed stone, and gravel subbases.

For bituminous stabilized subbase materials, the grain-size distribution and asphalt content were determined.

All laboratory tests were conducted in a random order, in order to distribute any random variation in test procedures or among testing personnel over all the measurements.

Approach to Data Analysis

The characteristics of the design of the field study offered two dichotomies that could be profitably used in data analysis. These were:

1. Comparison of failed test locations with good test locations, within test sections showing significant distress.
2. Comparison of test sections showing distress (as indicated by a breakup or a patch) with test sections in good condition and showing no apparent distress.

In the light of the significant results obtained from these comparisons, factors contributing to the distress of CRCP were further evaluated utilizing all the data obtained in the field study.

FIELD AND LABORATORY TEST PROCEDURES

The field and laboratory test procedures outlined in the design of the detailed study are described in this section.

Field Test Procedures

The detailed field study involved the following test measurements and sampling procedures:

1. Pavement deflection measurements by means of the Dynaflect.
2. Crack width and crack spacing measurements.
3. Penetrometer tests on the subbase and subgrade.
4. Subbase and subgrade density and moisture content measurements.
5. Sampling of subbase and subgrade materials.
6. Extraction of concrete cores by a truck-mounted pavement coring rig.

The sequence in which the tests were run had to be carefully organized, so that the tests could be made in as random a manner as possible but with a minimum expenditure of time. A typical sequence of events in running a battery of tests at a test location is illustrated in Figures 13 to 28. It should be noted that identical test procedures and sampling techniques for subgrade and subbase are not illustrated twice in this sequence. All the tests on the subbase and sampling of material had to be completed before the subgrade could be tested and sampled. The approximate amounts of subbase and subgrade samples taken at each test location were 80 and 50 lbs. respectively.

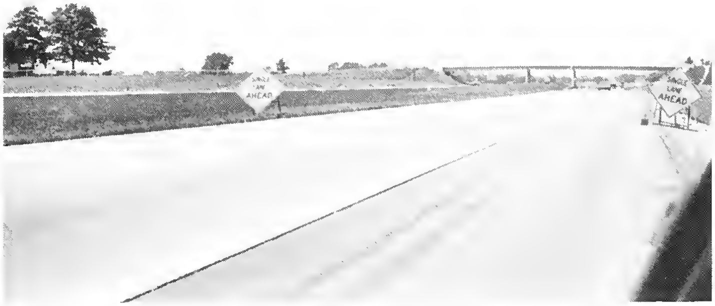
SINGLE LANE AHEAD
SINGLE LANE AHEAD

FIG. 13 ADVANCE SIGNS INDICATING LANE CLOSURE AHEAD

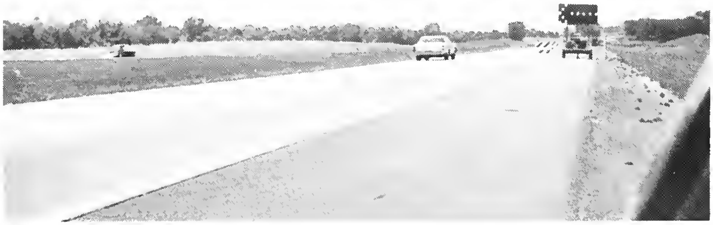

FIG. 14 FLASHING ARROW TO GUIDE VEHICLES TO THE OPEN LANE

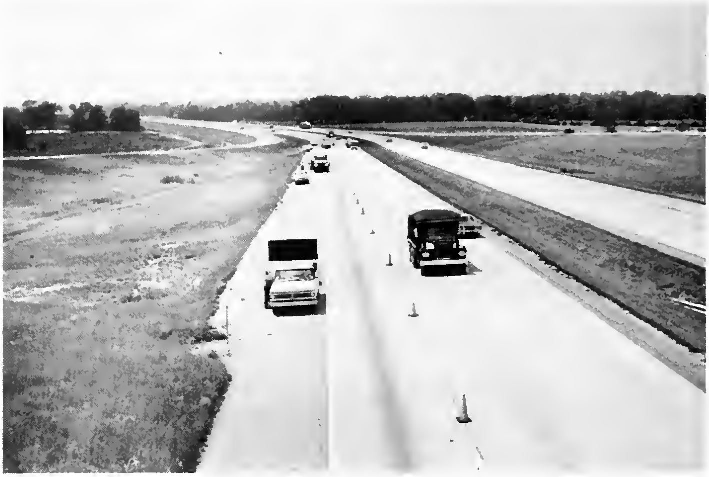

FIG. 15 TEST SECTION BARRICADED AND READY FOR TESTING

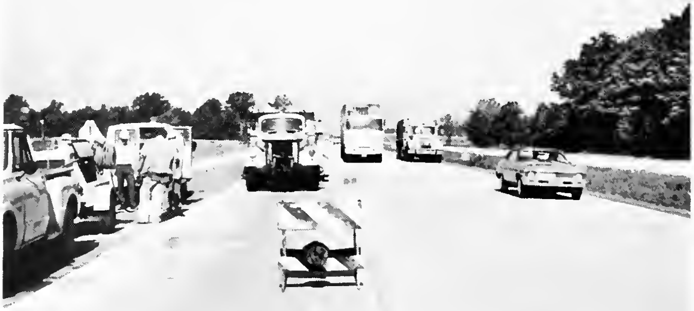

FIG. 16 VIEW OF TESTING OPERATION. NOTE HEAVY TRAFFIC IN CLEAR LANES

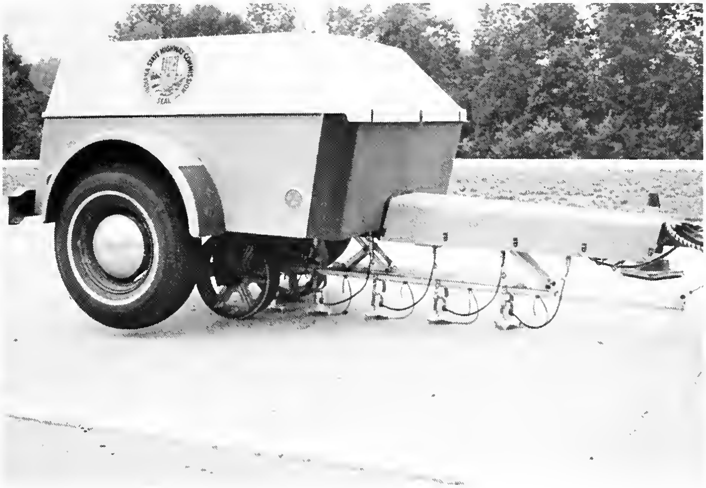

FIG.17 DEFLECTION MEASUREMENT AT A MID-SPAN POSITION WITH THE DYNAFLECT

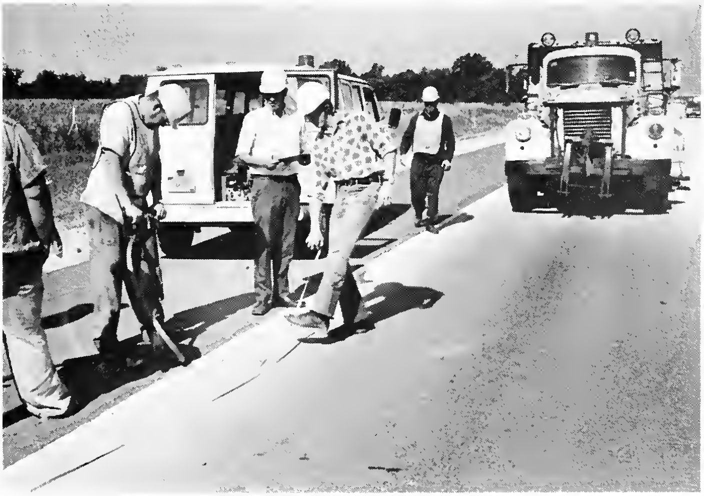

FIG.18 MEASURING CRACK SPACING ALONG THE PAVEMENT EDGE

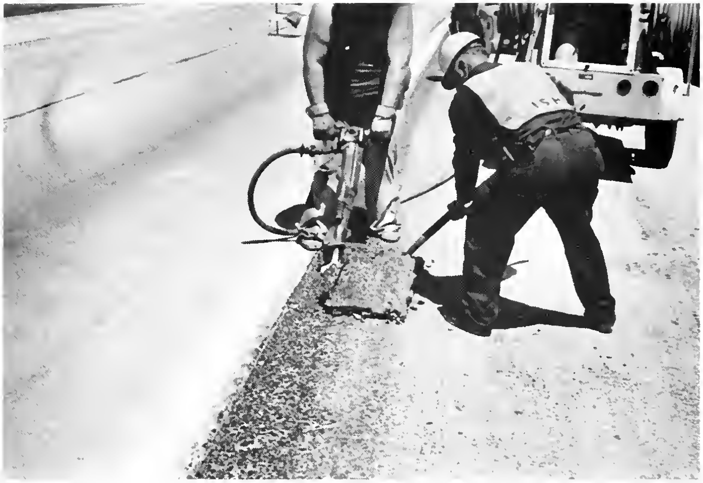

FIG.19 REMOVING BITUMINOUS SHOULDER TO EXPOSE THE SUBBASE

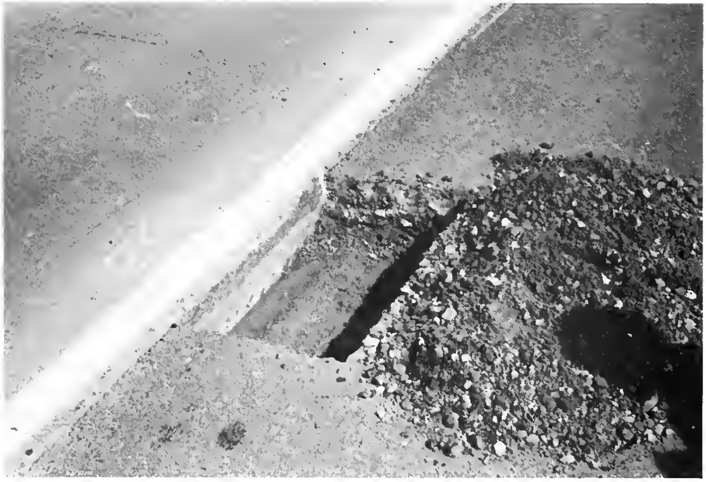

FIG.20 TEST PIT AT THE SHOUDER-SLAB INTERFACE

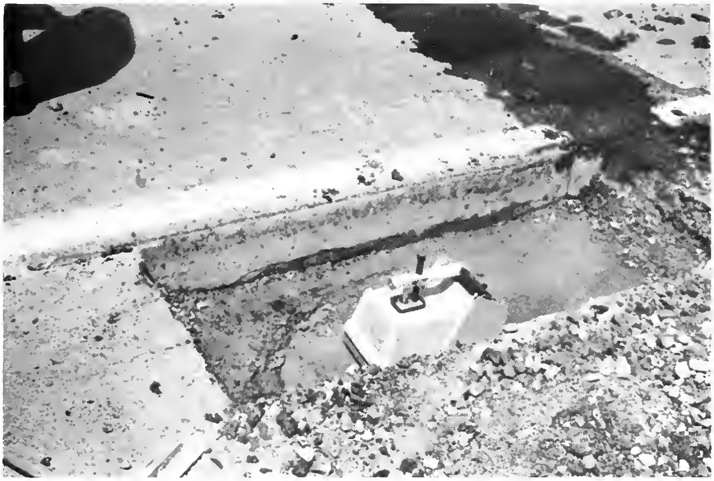

FIG. 21 NUCLEAR GAUGE FOR MEASURING MOISTURE CONTENT AND DENSITY

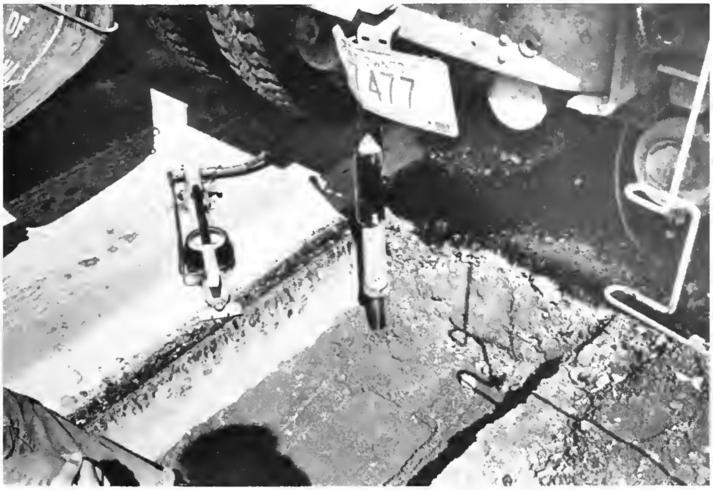

FIG. 22 TESTING THE SUBBASE WITH THE HIGH LOAD PENETROMETER AT THE SHOULDER POSITION

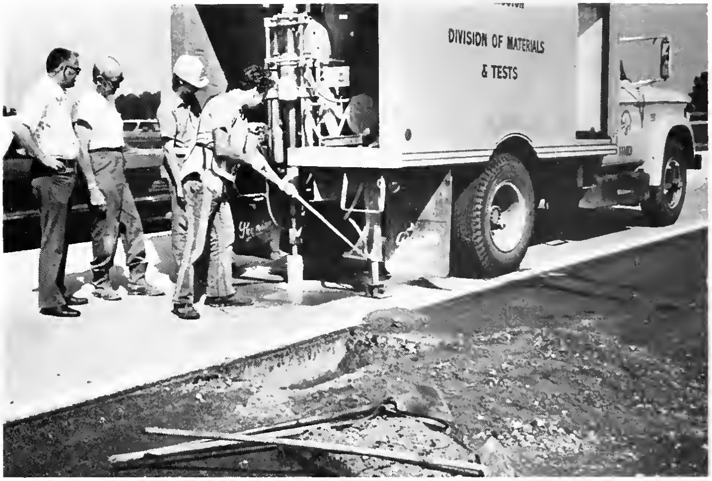
DIVISION OF MATERIALS
& TESTS

FIG.23 EXTRACTING A CONCRETE CORE WITH A PAVEMENT CORING RIG

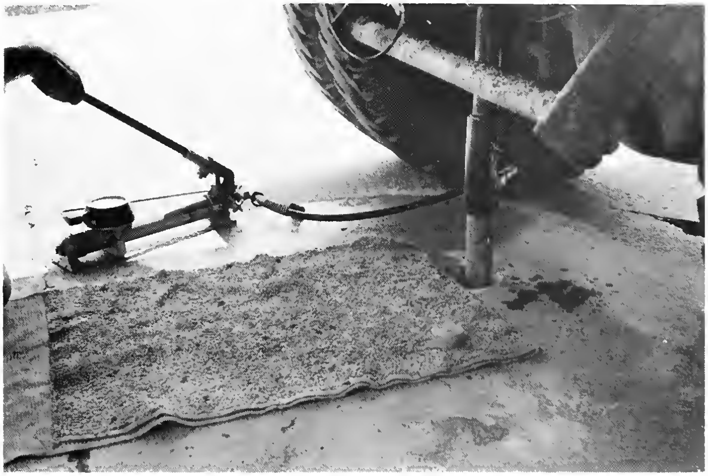

FIG.24 TESTING THE SUBBASE WITH THE HIGH LOAD PENETROMETER AT THE CORE-HOLE POSITION

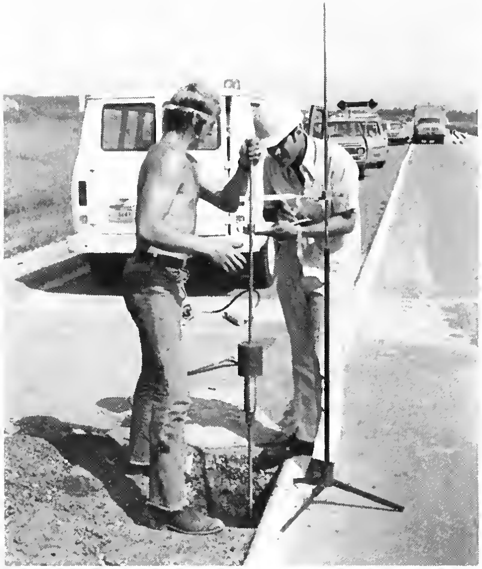

FIG.25 TESTING THE SUBGRADE WITH DYNAMIC CONE PENETROMETER

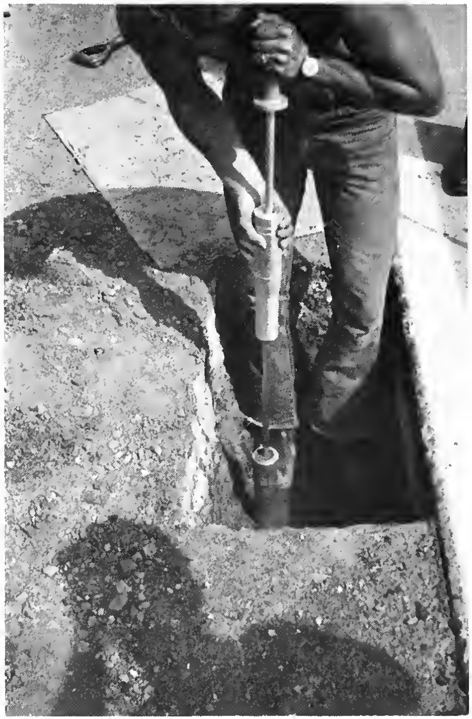

FIG.26 OBTAINING A SUBGRADE TUBE SAMPLE

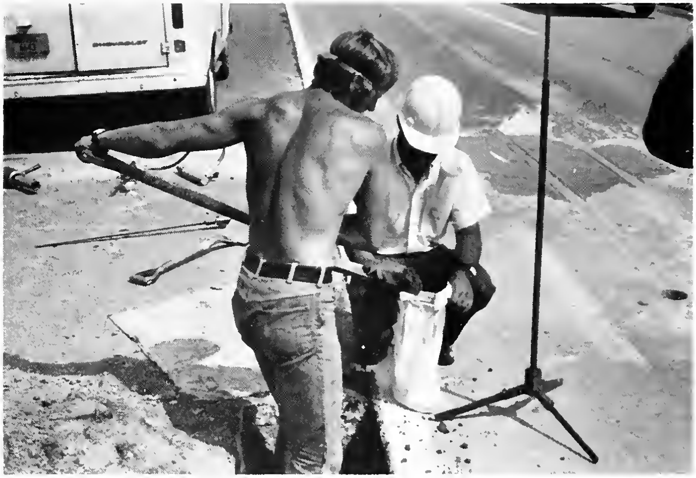

FIG.27 SAMPLING SUBGRADE MATERIAL

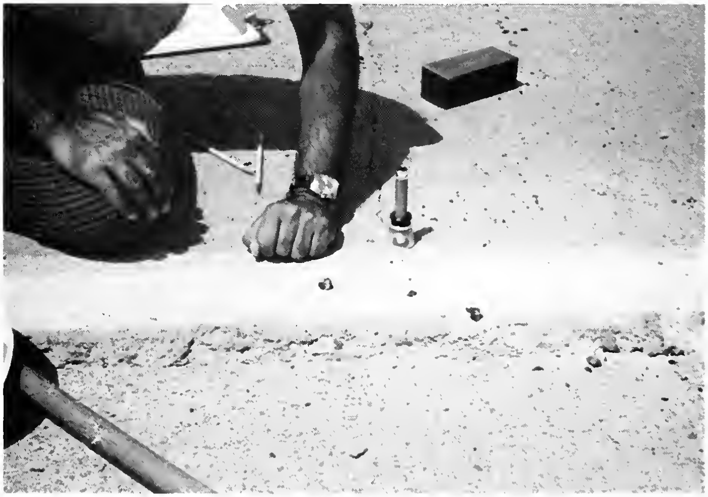

FIG.28 CRACK WIDTH MEASUREMENT WITH A DIRECT MEASURING MICROSCOPE

From one test location to another, the order of running some of the tests was varied to preclude restrictions on randomization. Nevertheless, in some instances, such restrictions were unavoidable and were accounted for in the statistical analysis of test data.

Equipment Used in the CRCP Field Study

High Load Penetrometer (Figure 29): This is a static soil strength tester. It consists of a two inch diameter cone point mounted at the rod end of a hydraulic cylinder. The hydraulic cylinder or jack is connected by a hose to a hand pump which provides the hydraulic pressure to extend the cylinder. This arrangement results in a large penetration force on the test probe. The test probe is sized so that the effect of gravel, in the range of sizes commonly found, can be included as part of the measured soil strength. The penetrometer is calibrated in terms of California Bearing Ratio (CBR). The CBR of soil can be determined as a function of soil failure pressure under the influence of the cone point. The relationship of CBR and the failure pressure is expressed as (11):

$$\text{CBR} = \frac{P_s}{25} - \frac{P_s^2}{416670} \qquad (22)$$

where CBR = California Bearing Ratio (percent)

P_s = Soil failure pressure in psi exerted on the projected area of the 2 in. diameter cone point (3.14 in.^{2})

Any friction and shear forces at the side of the cone point are included in the total force. The High Load Penetrometer was used for subbase evaluation in the field study.

Dynamic Cone Penetrometer (Figure 29): The Dynamic Cone Penetrometer (DCP) is a modified version of the penetrometer used by the Country Roads Board, Victoria, Australia. It consists basically of a 10 kg hammer sliding

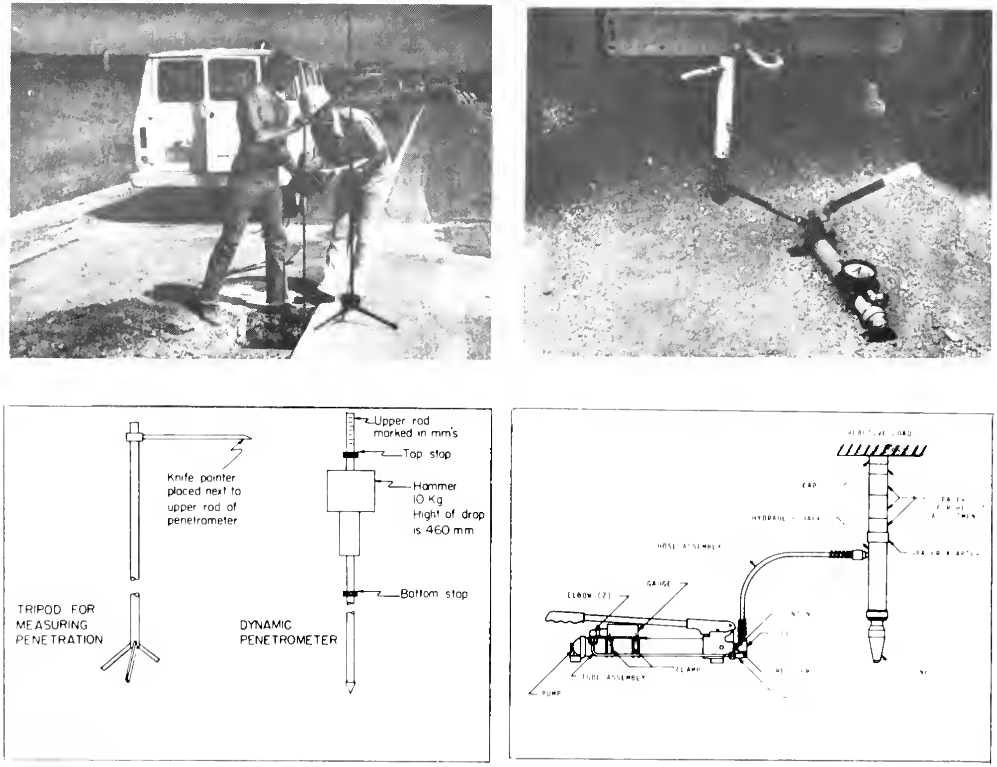
Upper rod marked in mm's
Top stop
Hammer 10 Kg Hight of drop is 460 mm
Bottom stop
Knife pointer placed next to upper rod of penetrometer
TRIPOD FOR MEASURING PENETRATION
DYNAMIC PENETROMETER
REACTIVE LOAD
CAP
HYDRAULIC JACK
HOSE ASSEMBLY
GAUGE
ELBOW (2)
CLAMP
TUBE ASSEMBLY
PUMP

(a) DYNAMIC CONE (FINE GRAINED SOILS)

(b) HIGH LOAD CONE (GRANULAR SOIL)

FIG. 29 TWO METHODS OF RAPID CBR TESTS
FROM YODER AND GADALLAH)

on a 16 mm rod dropping through a distance of 460 mm and striking an anvil at the lower end of that rod, on the end of which is a hardened steel cone, 20 mm in diameter. The penetrometer is driven by blows of the drop hammer and the penetration per blow in mm is measured on graduations on the upper rod. The CBR value of the in-situ soil, in the range of 1 to 50 CBR, may be obtained from:

$$\mathrm{CBR} = \frac{229.9}{P} \tag{23}$$

where CBR = California Bearing Ratio (percent)
P = Penetration (mm/blow)

The use of DCP permits the rapid determination of the bearing value of soils in the range of CBR of 1 to 50. It should be noted, however, that the DCP is not suitable for use in granular soils; coarse sands are probably the limit of usability of the device. In the field investigation the DCP was used for subgrade evaluation.

Direct Measuring Microscope (Figure 28): Crack widths were measured by means of a 50X, pocket size direct measuring microscope. This is a handy microscope with a precision glass reticle having a 0.1-in. scale calibrated in increments of 0.001 in. Estimates of up to 0.0005 in. can be made by this device.

Dynaflect (Figure 17): This is an electro-mechanical system for measuring the dynamic deflection, of a surface or structure, caused by an oscillatory load. Deflection measurements are independent of a fixed surface reference. The deflection readings obtained by this system range from 30 milli-inches (.03 in.) to ten micro-inches (.00001 in.).

The Dynaflect, mounted on a two-wheel trailer, is towed behind a panel truck. It has two sets of wheels, the outer pair consists of rubber tires while the inner set is a pair of steel load wheels. Between test sections, it travels on rubber tires at normal speeds. On arriving at a test section, the steel wheels are lowered to the pavement, lifting the rubber-tired wheels and transmitting to the pavement an oscillatory load, generated by eccentric weights rotating at a frequency of 8 revolutions per second. The deflection measurements are taken by lowering five motion sensors to the pavement surface and the voltage output of the sensors is read on a meter directly in milli-inches of vertical deflection of the pavement surface. The meter is located inside the tow-truck where it can be read directly by the operator (53).

The relationship between Dynaflect deflection and Benkelman Beam deflection can be approximated by:

$$Y = 20.09X \tag{24}$$

where Y = Benkelman Beam deflection (milli-inches)
X = Dynaflect deflection (milli-inches)

This relationship, reported by Scrivner et. al., was obtained by a regression analysis of 240 pairs of deflection measurements made by the use of the two instruments (53).

Laboratory Test Procedures

The laboratory testing program consisted of the following tests:

a. Concrete cores:
    1. Specific Gravity and Absorption tests.
    2. Bulk density.
    3. Pulse velocity measurements.
    4. Splitting tensile strength tests.

b. Granular subbase samples:
    1. Particle size analysis
    2. Consistency limits tests
    3. Compaction tests
    4. Permeability tests

c. Bituminous stabilized subbase samples:
   1. Asphalt extraction test
   2. Particle size analysis
   3. Consistency limits tests

The last two tests were conducted on residual aggregate from the asphalt extraction test.

d. Subgrade samples:
   1. Particle size analysis
   2. Consistency limits tests
   3. Compaction tests

Tests on Concrete Cores

Concrete cores, obtained during the field study, were prepared and tested in accordance with ASTM Standards (4). Specific Gravity and Absorption tests were performed according to ASTM Designation C642-69T (4). Bulk Unit Weight (Density) was calculated as follows:

$$\text{Bulk Unit Weight} = \frac{\text{Weight of concrete core sample at ambient moisture content}}{\text{Bulk volume of sample}}, \quad \text{lb/ft}^3 \tag{25}$$

Pulse velocity measurements were conducted according to ASTM Designation C 597-71 (4). Dynamic modulus of elasticity of concrete was estimated from pulse velocity determinations by the following relationship:

$$E_c' = (\text{Pulse velocity})^2 \times \text{Density} \tag{26}$$

The estimated value deviates from the exact definition of dynamic modulus of elasticity E_c, which is given by

$$E_c = (\text{Pulse velocity})^2 \times \text{Density} \times \frac{(1 + \mu)(1 - 2\mu)}{1 + \mu} \tag{27}$$

where μ = Poisson's ratio for concrete

In this study, Poisson's ratio was not determined and was assumed constant for all concrete samples.
Splitting tensile strength tests were performed according to ASTM Designation C496-71(4).

All these tests were conducted on portions of concrete core sawed from above and below the steel reinforcement. This procedure became necessary in order to obtain test samples free of embedded reinforcement.

Tests on Subbase and Subgrade Materials

The granular subbase and subgrade soil samples obtained during the field study were split and quartered to obtain the necessary amount of material for conducting the various tests.

Particle size distribution was determined by a wet sieve analysis procedure carried out in accordance with a combination of methods given in ASTM Designations D1140-54 and D422-63 (5).

Liquid limit and plastic limit tests were done according to ASTM Designations D423-66 and D424-59, respectively (5).

Compaction tests on subgrade soil samples complied with ASTM Designation D698-70, Method A (5), while those on crushed stone and slag subbase aggregate mixtures followed the procedure given in ASTM Designation D698-70, Method C (5). These test methods are identical to the Standard AASHTO (T-99) compaction tests. For gravel subbase aggregate mixtures, standard compaction tests were first run on a few samples. Next the density control curve shown in Figure 30 was developed by the method proposed by Yoder and Williamson (69). This control curve relates maximum dry density to material passing the No. 4 sieve. The maximum dry density of gravel subbase samples was determined by the use of this curve. This procedure permitted considerable time savings in evaluating maximum densities. To verify that maximum dry densities obtained from the control curve were

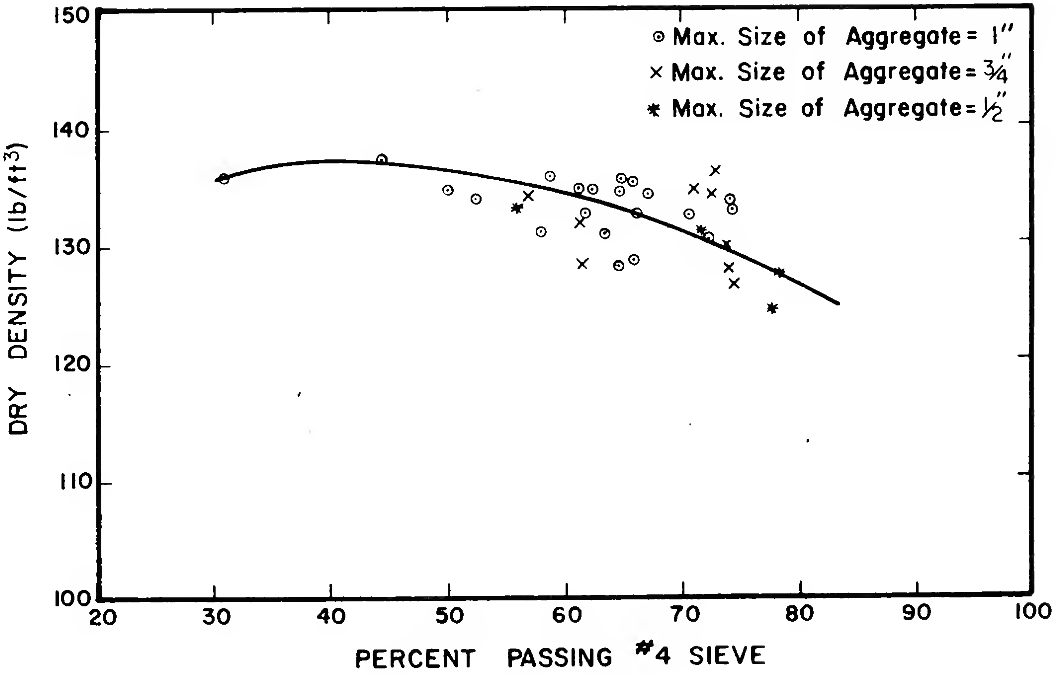

FIG.30 DENSITY CONTROL CURVE FOR GRAVEL SUBBASES

compatible with those obtained by the standard compaction test, a statistical paired comparison test (t-test) was made on the gravel subbase data. The results of the test showed no significant difference, at an α-level of 0.05, between the maximum dry densities obtained by the two procedures.

One aspect of the compaction test procedures on subbase samples varied from the standard test method. Though the compaction test was run on material passing the 3/4-in. sieve, the material retained on the 3/4-in. sieve was not replaced by an equal amount passing the 3/4-in. sieve and retained on the No. 4 sieve.

As the laboratory maximum dry density values were used as a standard for determining the percent compaction obtained in the field, the field density measurements were adjusted downward to compensate for the oversized material by the following procedure:

Let γ_f = measured field dry density (16/ft.^{3})
$P\ 3/4$ = percent passing the 3/4-in. sieve
G = specific gravity of aggregate retained on 3/4-in. sieve.

Then for 1 cu. ft. of subbase aggregate mixture,

Wt. of material retained on 3/4-in. sieve $= W_1 = \gamma_f \left(1 - \frac{P\ 3/4}{100}\right)$, lb

Wt. of material passing 3/4-in. sieve $= W_2 = \gamma_f - W_1$

$$= \gamma_f\left(\frac{P\ 3/4}{100}\right), \text{ lb}$$

Vol. of material retained on 3/4-in. sieve $= V_1 = \frac{W_1}{62.4G}$, ft^3

$$= \frac{\gamma_f \left(1 - \frac{P\ 3/4}{100}\right)}{62.4G}, \text{ ft}^3$$

$$\text{Vol. of material passing 3/4-in. sieve} = V_2 = 1 - V_1,\ \text{ft}^3$$

$$= 1 - \frac{\gamma_f(1 - \frac{P\ 3/4}{100})}{62.4G},\ \text{ft}^3$$

$$= \frac{62.4G - \gamma_f\ (1 - \frac{P\ 3/4}{100})}{62.4G},\text{ft}^3$$

Now let, $\gamma'_f = \frac{W_2}{V_2}$

Then
$$\gamma'_f = \frac{62.4G\ (\frac{P.3/4}{100})\ \gamma_f}{62.4G - \gamma_f\ (1 - \frac{P.3/4}{100})} \tag{28}$$

where γ'_f = field dry density adjusted for the effect of oversized subbase aggregate, lb/ft^3

γ_f = measured field dry density, lb/ft^3

$P\ 3/4$ = percent passing the 3/4-in. sieve

G = specific gravity of oversized material (retained on 3/4-in. sieve)

= 2.65 for gravel

= 2.76 for crushed stone

= 2.21 for slag, for this study

Percent Compaction was then obtained as:

$$\text{Percent Compaction} = \frac{\gamma'_f}{\gamma_{max}} \tag{29}$$

where γ'_f = adjusted subbase field dry density, lb/ft^3

γ_{max} = maximum lab. dry density, lb/ft^3

A similar correction based on material passing the No. 4 sieve was also applied to subgrade field densities. The expression for adjusted subgrade densities is given by:

$$\gamma''_f = \frac{62.4G\ (\frac{P\ 4}{100})\ \ \gamma_f}{62.4G - \gamma_f\ (1 - \frac{P\ 4}{100}\ )} \tag{30}$$

where γ_f'' = field dry density, adjusted for the coarse fraction (retained on No. 4 sieve) in the subgrade, lb/ft^3

γ_f = measured field dry density, lb/ft^3

P 4 = percent passing the No. 4 sieve

G = specific gravity of material retained on No. 4 sieve

= 2.65 for this study.

Percent compaction was then obtained as:

$$\text{Percent compaction} = \frac{\gamma_f''}{\gamma_{max}} \tag{31}$$

where γ_f'' = adjusted subgrade field dry density, lb/ft^3

γ_{max} = maximum lab. dry density, lb/ft^3

The results reported in this study are based on nuclear density and moisture content measurements. A statistical comparison of subgrade dry densities obtained by the nuclear gauge and the tube sampler showed no difference between the two methods at the 5 percent significant level. The moisture content values, for both the subbase and subgrade, as determined by the nuclear gauge were on the average 2-3 percentage points higher than the moisture contents obtained by the standard method.

Permeability tests on granular subbase aggregate mixtures (gravel, crushed stone and slag) were made by means of a constant head permeameter. In principle, the design of the equipment conformed to ASTM Designation D 2424-68 (5). However, the testing procedure described in the standard test was modified to some extent.

The permeameter had a 6-in. diameter and a 7-in. height. The effective height of the molded sample was 4.584 in., which corresponds to the height of the sample used in the standard compaction test. The test samples were molded dynamically by a 5-lb. sliding hammer with a free fall of 12-in. The aggregate mixture was placed in 3 layers, and 56 blows were applied to each layer. The test was repeated on newly molded samples of the same material but the compactive effort was varied by changing the number of blows applied per layer from 56 blows to 42, 28, or 14 blows. This procedure was adopted to study the effect of variations in density on permeability.

The tests were run on material as sampled in the field and oversized material (retained on 3/4-in. sieve) was not removed. This permitted a means of translating the permeability values obtained in the laboratory to field values.

A surcharge weight in the form of a stiff spring attached to a steel plate and equivalent to the pressure of the concrete slab was placed on the molded sample.

Other variations from the standard procedure were:

a. Use of tap water instead of de-aired water. The presence of air in the water tends to cause an unsteady flow of water. This was rectified by the design of the constant head tank, wherein stagnant conditions were created to remove turbulence and some of the air.

b. The samples were not compacted according to the prescribed procedure. Instead, a procedure essentially conforming to the standard AASHTO test method (T-99) was used, as explained earlier.

Other than these variations the test procedure followed the steps outlined in the standard test.

The coefficient of permeability was computed using the formula

$$k = \frac{QL}{Ath} \qquad (32)$$

where k = coefficient of permeability (cm/sec)

Q = quantity of water discharged (cm^3)

L = height of sample (cm)
A = cross-sectional area of sample (cm^2)
t = total time of discharge (sec)
h = total head lost (cm)

The permeability values so obtained were adjusted by a temperature correction to a base temperature of 25°C and then were converted to ft/day units.

Permeability tests were run only on a randomly selected group of samples of each subbase material, because the test is exceedingly time consuming. Each permeability test required 3-4 hours to complete.

The last step was to evolve statistical models from the permeability test data so that, given a number of input parameters such as dry density and grain-size distribution variables, permeability values could be predicted. The mathematical form, that is, the independent variables to be used in these relationships were obtained from the studies by Yoder (65) and Faiz (4). The permeability models for different types of subbases were obtained by a stepwise multiple regression procedure and are presented in Table 20. It would be observed that these statistical equations are highly significant (see Appendix D) and may be used for predictive purposes with confidence. Field permeability values were estimated by these relationships.

Asphalt Extraction tests were performed to determine the asphalt content of the bituminous stabilized subbase samples. The test procedure followed the method given by ASTM Designation D2172-67 (5).

Presentation of Test Data

A large amount of data were collected from the field and laboratory tests. These data were coded and transferred to computer cards, in order to maintain easy access to the data for purposes of analysis. A summary of these data is presented in Appendix C.

TABLE 20 PERMEABILITY RELATIONSHIPS

SUBASE TYPE	MODEL	NO. OF CASES	R^2	STANDARD ERROR
GRAVEL	$\mathrm{LOG}_{10} K = 16.05572 - 0.09884\,\gamma_d - 0.03435(P.4) + 1.10754(DR)$	23	0.802	0.236
CRUSHED STONE	$\mathrm{LOG}_{10} K = 12.56327 - 0.07464\,\gamma_d$	12	0.956	0.117
SLAG *	$\mathrm{LOG}_{10} K = 8.68635 - 0.05093\,\gamma_d - 0.11301(P.200)$	11	0.984	0.120
SLAG **	$\mathrm{LOG}_{10} K = 10.07609 - 0.08756\,\gamma_d$	4	0.974	0.057

K = COEFFICIENT OF PERMEABILITY AT 25° C (FT./DAY)
γ_d = DRY DENSITY (LB./FT^3)
P.4 = PERCENT PASSING NO. 4 SIEVE
P.200 = PERCENT PASSING NO. 200 SIEVE
DR = DUST RATIO = $\dfrac{\text{PERCENT PASSING NO. 200 SIEVE}}{\text{PERCENT PASSING NO. 4 SIEVE}}$
* = SECTIONS WITH NO FAILURE
** = SECTION WITH FAILURE

COMPARISON OF FAILED TEST LOCATIONS WITH GOOD TEST LOCATIONS WITHIN TEST SECTIONS

The objective of this phase of the analysis was to compare the material and performance characteristics of structurally failed locations with structurally sound (good) locations, within CRCP test sections showing significant distress. Structural distress was identified primarily by the presence of breakups and asphalt and concrete patches.

In the detailed study only 15 test sections were obtained that had at least one structural failure within the section. An additional section had a location with heavily spalled cracks which are a prelude to a structural failure (See Figure 7). This test section was included in the analysis of those variables that are known to influence or cause spalled cracks.

The variables evaluated in this analysis were grouped into two categories, namely, material properties and performance measures and are listed as follows:

Material Properties (Input Variables)

a) Subgrade Characteristics: CBR as measured by dynamic penetration resistance, percent compaction, consistency limits and grain size distribution.

b) Subbase Characteristics: CBR as measured by the High Load Penetrometer, percent compaction, estimated permeability, and grain size distribution (all granular subbases tested out to be non-plastic).

The properties of bituminous stabilized subbases included grain size distribution and percent asphalt content.

c) Concrete properties: Bulk density, dynamic modulus of elasticity, and splitting tensile strength.

Measures of Performance (Output Variables)

a) Dynamic pavement deflection
b) Surface curvature index
c) Crack width
d) Crack spacing - mean and variance
e) Crack intersections

Some of these variables are defined in more detail later in the analysis.

Comparison of Material Properties

The material properties were analyzed within the framework of a fixed-effect randomized complete block design (7). The main reason for using a randomized complete block design (RCBD) was to remove a source of variation, due to the effect of blocks, from the error term. The test sections of the field study design corresponded to the blocks of the RCBD. Since all the measurements had to be completed at a test section, before proceeding to another test section, a restriction on randomization* was caused. As a result of this restriction the effect of test sections on various evaluated variables could not be tested for significance.

Subgrade Properties

Subgrade CBR. Estimates of subgrade in-situ California Bearing Ratio (CBR) of the top 4 inches of subgrade were obtained from the Dynamic Cone Penetrometer test. The following analysis of variance (ANOVA) model was used to evaluate the subgrade CBR data.

---

*This concept has been developed by Anderson (6) as an aid to making correct statistical tests in the analysis of statistically designed experiments.

$$Y_{ijk} = \mu + S_i + \delta_{(i)} + C_j + SC_{ij} + P_k + SP_{ik} + CP_{jk} + \varepsilon_{(ijk)} \qquad (33)$$

$i = 1, 2, \ldots .14$

$j = 1, 2$

$k = 1, 2$

where

Y_{ijk} = estimated in-place CBR obtained at the k^{th} test point in j^{th} condition within the i^{th} test section (percent).

μ = overall true mean effect.

S_i = true effect of the i^{th} test section.

$\delta_{(i)}$ = restriction error, random; NID $(0, \sigma_\delta^2)$; completely confounded with the effect of the i^{th} test section, caused by running all tests at the i^{th} section before proceeding to the next test section.

C_j = true effect of the j^{th} pavement condition (failed location compared with good location).

SC_{ij} = true interaction effect of the i^{th} test section with the j^{th} pavement condition.

P_k = true effect of the k^{th} test point (shoulder vs. core-hole).

SP_{ik} = true interaction effect of the i^{th} test section with the k^{th} test point.

CP_{jk} = true interaction effect of the j^{th} pavement condition with the k^{th} test point.

$\varepsilon_{(ijk)}$ = true error, NID $(0, \sigma_\varepsilon^2)$. This term is estimated in the analysis of variance, from the interaction source assuming the interaction of the i^{th} test section, the j^{th} condition and the k^{th} test point is zero.

The results of the analysis of variance of subgrade CBR data, presented in Table 21, indicated that:

Table 21. Summary of Analysis of Variance - Subgrade CBR (Percent)

Source of Variation	DF	Sums of Squares	Mean Square	F	$F_{0.05, \text{crit.}}$
S_i (Test Sections)	13	3504.23	269.56	*	---
δ_i	0	---	---	---	---
Main Effect:					
C_j (Condition)	1	13.02	13.02	0.39	4.67
P_k (Test Points)	1	58.02	58.02	1.73	4.67
Interaction Effects:					
SC_{ij}	13	1174.23	90.33	2.69**	2.58
SP_{ik}	13	706.23	54.33	1.62	2.58
CP_{jk}	1	2.16	2.16	0.06	4.67
Error, $\epsilon_{(ijk)}$	13	437.09	33.62		
Total	55	5894.98			

*None available because of restriction on randomization due to the blocking effect of test sections

**Significant at $\alpha = 0.05$

1. There was no significant difference in subgrade CBR values between good and failed locations. Furthermore, the CBR values were not affected by the position at which the test was performed.

2. Subgrade CBR was significantly influenced by the interaction of test sections with pavement condition.

The variation of subgrade CBR with pavement condition and test points is shown in Table 22. These data indicate that the average subgrade CBR values did not vary appreciably with either the pavement condition or the position where the test was performed.

Percent Compaction. .Subgrade compaction data were analyzed by the following ANOVA model:

$$Y_{ij} = \mu + S_i + \delta_{(i)} + C_j + \varepsilon_{(ij)} \qquad (34)$$

$i = 1, 2, \ldots 13$

$j = 1, 2$

where

Y_{ij} = percent compaction of the subgrade at a test location in j^{th} condition within the i^{th} section.

$\varepsilon_{(ij)}$= true error, NID $(0, \sigma_\varepsilon^2)$

and all other terms are as defined in Equation 33.

The ANOVA results showed no significant difference in percent compaction between good and failed locations. Treatment means and partial data from the ANOVA results are shown in Table 23. Tests of significance were made by the error term obtained after removing, by Tukey's method (7), the sum of squares due to non-additivity with one degree of freedom from the estimate of interaction/error term, $\varepsilon_{(ij)}$, given in Equation 34. The average values of percent com-compaction in Table 23 are indicative of consistently low subgrade compaction (95.5 percent) at both good and failed locations. Although percent compaction values were shown not to be significantly different between failed and

Table 22. Variation of Subgrade and Subbase CBR with Pavement Condition and Location of Test Points

Pavement Condition	Good		Failed	
Test Point	Shoulder	Core	Shoulder	Core
*Average Subgrade CBR (Percent)	14.6	16.3	13.3	15.7
*Average Subbase CBR (Percent)	39.1	44.5	32.4	43.7

*Average of CBR data obtained from 14 test sections.

Table 23. Variation of Subgrade Characteristics with Pavement Condition

Variable	No. of Sections	Mean Value for Good Locations ($\overline{Y}_{.1}$)	Mean Value for Failed Locations ($\overline{Y}_{.2}$)	*Effect of Condition, C_j	*Error Mean Square, S_E^2
Percent Compaction	13	95.6	95.5	NS	71.3
Liquid Limit (LL)	14	25.4	24.2	NS	50.2
Plasticity Index (PI)	14	10.4	10.1	NS	19.6
Percent Passing					
No. 4 Sieve	14	92.7	95.3	S	7.71
No. 40 Sieve	14	74.6	81.4	S	37.26
No. 200 Sieve	14	59.3	62.2	NS	87.4

S = Significant
NS = Non-significant

* From ANOVA

good locations all of the observed values were low. Poor compaction of subgrade can create an inherently unstable layer in the pavement structure.

Grain Size and Consistency Limits. Data pertaining to these variables were evaluated by the ANOVA model given in Equation 34, except that the data were obtained from 14 sections ($i = 1, 2, \ldots 14$). Two of the grain size parameters showed a significant difference between good and failed locations. These were the percent passing the No. 4 and the No. 40 seives. The analysis of variance results for these variables, given in Tables 24 and 25, show that subgrade soils at good locations had a higher sand content (smaller percentage passing the No. 4 and the No. 40 seives). The significant interaction (SC_{ij}) can be interpreted to mean that grain-size characteristics of the subgrade soils varied significantly, depending upon the location of test sections and the pavement condition.

The liquid limit and plasticity index of subgrade soils and the amount of fines (minus No. 200 material) were found to be of the same order of magnitude at both failed and good locations.

The variation of selected subgrade characteristics with pavement condition is given in Table 23.

Properties of the Granular Subbases

In the comparison of the characteristics of granular subbases, it was not possible to stratify the data by subbase type (gravel, crushed stone, slag) as only one test section with a failed location was available for each of the crushed stone and slag subbase types. Even so, all the sections with at least one failed location, irrespective of subbase type, were included in the analysis. This was made possible by the use of the randomized complete block design, wherein any variation due to the subbase type is accounted for in the variation attributed to the test sections (blocks).

Table 24. Summary of Analysis of Variance - Percent Passing #40 Sieve (Subgrade)

Source of Variation	DF	Sums of Squares	Mean Square	F	$F_{.05, crit.}$
S_i (Test Sections)	13	3637.71	---	---	---
$\delta_{(i)}$	0	---	---	---	---
C_j (Condition)	1	320.97	320.97	8.61*	4.75
SC_{ij} (Non-additivity)	1	968.09	968.09	25.98*	4.75
Error, $\varepsilon'_{(ij)}$	12	447.13	37.26		
Total	27				

*Significant at $\alpha = 0.05$

Table 25. Summary of Analysis of Variance - Percent Passing #4 Sieve (Subgrade)

Source of Variation	DF	Sums of Squares	Mean Square	F	$F_{.05,\ \text{crit.}}$
S_i (Test Sections)	13	706.44	54.34	---	---
$\delta_{(i)}$	0	---	---	---	---
C_j (Condition)	1	46.03	46.03	5.97*	4.75
SC_{ij} (Non-additivity)	1	317.58	317.58	41.18*	4.75
Error $\varepsilon'_{(ij)}$	12	92.55	7.71		
Total	27	1162.61			

*Significant at $\alpha = 0.05$

Subbase CBR. In-place subbase CBR values were estimated from the High Load Penetrometer test data. The penetration CBR data were then analyzed by the use of the ANOVA model given in Equation 33. From the results of the analysis of variance of subbase CBR data, presented in Table 26, it is seen that:

1. There was a significant difference in subbase CBR between good and failed locations within a test section.

2. Subbase CBR values were significantly influenced by the position at which the test was performed. Tests made at the core-hole gave higher CBR values than those performed at the shoulder-pavement interface.

3. The interaction effect of test sections with pavement condition was found to be a significant factor in explaining the variation in subbase CBR.

4. The subbase CBR was also significantly affected by the interaction between pavement condition and the position at which the test was performed.

The variation of subbase CBR with pavement condition and test points is shown in Table 22. The tabulated data are the means of values obtained from 14 test sections with at least one structural failure. As expected subbase CBR values obtained at good locations were higher than the values tested at failed locations. The higher subbase CBR values obtained at core-hole points may be attributed to the surcharge effect of the pavement slab. In general, subbase CBR values were very low, pointing to instability of this layer in the pavement structure as a major factor influencing performance.

Percent Compaction. Only 11 sections were included in the evaluation as reliable data were not available for the other sections. The percent compaction values apply to the subbase material tested at the pavement-shoulder interface. The ANOVA model used in the analysis of compaction data is given by Equation 34 except that the measured variable is the

Table 26. Summary of Analysis of Variance - Subbase CBR (Percent)

Source of Variation	DF	Sums of Squares	Mean Square	F	$F_{.05,crit}$	$F_{.10,crit}$
S_i (Test Sections)	13	10838.81	833.75	---	---	---
$\delta_{(i)}$	0	---	---	---	---	---
Main Effects						
C_j (Condition)	1	196.88	196.88	4.64*	4.67	3.14
P_k (Test Points)	1	986.16	986.16	23.26**	4.67	3.14
Interaction Effects						
SC_{ij}	13	2824.38	217.26	5.12**	2.58	2.10
SP_{ik}	13	1420.09	109.24	2.58*	2.58	2.10
CP_{jk}	1	123.02	123.02	2.90	4.67	3.14
Error, $\varepsilon_{(ijk)}$	13	551.23	42.40			
Total	55	16940.55				

*Significant at $\alpha = 0.10$
**Significant at $\alpha = 0.05$

percent compaction of the subbase. The results of the analysis are presented in Table 27. No significant difference in percent compaction was shown between failed and good locations. However, mean values for good and failed locations, given in Table 28, demonstrate that subbases were not compacted sufficiently. Inadequate compaction can be a critical factor in subbase performance and a source of major problems. It has been demonstrated by a laboratory investigation that the stability of the subbase is a direct function of how well the subbase is compacted (24).

Permeability. The field permeability values were estimated by the subbase permeability models given in Table 20. Results of analysis of variance of permeability data may be seen in Table 29, while average values are presented in Table 28. These results show that the subbase was more permeable at good locations than at failed locations. It was further indicated that the interaction of section characteristics with pavement condition had a significant influence on subbase permeability. This is not unusual since the variation due to sections includes the differences in permeability characteristics of the three types of granular subbases used in the study.

In the detailed field study, the water content of the subbases (See Table 28) was observed to be considerably higher than the optimum water content for granular subbases (5-8 percent). This reveals that the subbases retained water and were not freely draining. At a number of test locations water was observed to drain from under the slab into the open test pit excavated at the shoulder-pavement interface. Similarly at other test locations the water in the core hole did not drain but maintained a constant level.

Grain-Size Distribution and Consistency Limits. For the sake of brevity, detailed analysis of variance results are not shown for grain-size distribution variables. Average

Table 27. Summary of Analysis of Variance - Percent Compaction(Subbase)

Source of Variation	DF	Sums of Squares	Mean Square	F	$F_{.05,crit}$
S_i (Test Sections)	10	1906.09	190.60	---	---
$\delta_{(i)}$	0	---	---	---	---
C_j (Condition)	1	12.23	12.23	0.37	5.12
SC_{ij} (Non-additivity)	1	33.96	33.96	1.02	5.12
Error, $\varepsilon_{(ij)}$	9	298.78	33.20		
Total	21	2251.01			

Table 28. Variation of Granular Subbase Characteristics with Pavement Condition

Variable	No. of Sections	Mean Value for Good Locations ($\overline{Y}_{.1}$)	Mean Value for Failed Locations ($\overline{Y}_{.2}$)	*Effect of Condition, C_j	*Error Mean Square, S_E^2
CBR (Percent)	14	42.0	38.0	S (α=.10)	42.4
Percent Compaction	11	94.2	95.7	NS(α=.10)	33.2
Permeability (ft/day)	11	946.8	245.0	S (α=.05)	252754.9
Percent Passing:					
3/4 in. sieve	14	89.0	91.8	S (α=.10)	14.7
1/2 in. sieve	14	80.5	84.4	S (α=.10)	26.0
3/8 in. sieve	14	75.4	79.4	NS	28.9
No. 4 sieve	14	62.1	66.9	S (α=.10)	54.7
No. 10 sieve	14	46.1	48.7	S (α=.10)	12.7
No. 40 sieve	14	14.9	18.1	S (α=.10)	22.3
No. 100 sieve	14	8.5	9.7	S (α=.05)	0.26
No. 200 sieve	14	6.9	7.9	S (α=.05)	0.28
Field Water Content (Percent)	12	11.3	11.3	NS	4.84

*From ANOVA

Table 29. Summary of Analysis of Variance - Permeability at 25°C (ft/day)

Source	DF	Sums of Squares	Mean Square	F	$F_{.05,crit}$
S_i (Test Sections)	10	14923001.7	1492300.2	---	---
$\delta_{(i)}$	--	---	---	---	---
C_j (Condition)	1	2708948.0	2708948.0	10.72*	5.12
SC_{ij} (Non-additivity)	1	9930998.7	9930998.7	39.29*	5.12
Error, $\varepsilon_{(ij)}$	9	2274794.1	252754.9		
Total	21	29837742.6			

*Significant at $\alpha = 0.05$

values obtained for these parameters at failed and good locations and some of the results of ANOVA are summarized in Table 28.

The results, most of which are only significant at an α-level of 10 percent point to an interesting observation. Subbase material at failed locations was found to be more fine-grained (i.e. had relatively more sand and fines) than the material at good locations. On the average, the material passing the various sieve sizes tested out 3-4 percent higher for samples obtained at failed locations than for those taken at good locations. Though the indicated difference in grain-size distribution between failed and good locations is within the range normally permitted by subbase aggregate specifications (35), it is quite possible that this consistent difference could be an outcome of degradation and the resultant densification of subbase under traffic.

Grain-size distribution functions at good and failed locations, within a typical section with a gravel subbase, are shown in Figure 31. The corresponding CBR, permeability, and density values for the two locations are also indicated. It would be observed that a relatively higher density was indicated at the failed location though density values at both good and failed locations were lower than the indicated maximum Standard AASHTO density

The estimated permeability of the subbase at the failed locations was also found to be lower than the permeability at the good location. If it is assumed that the subbase density at the good location approximately represents the as-compacted density at the test locations, then it may be safely stated that some densification of the subbase occurred at the failed location with a resultant loss in shear strength (CBR) and permeability.

Type of Subbase. In the statewide condition survey, it was indicated that subbase type had a significant influence

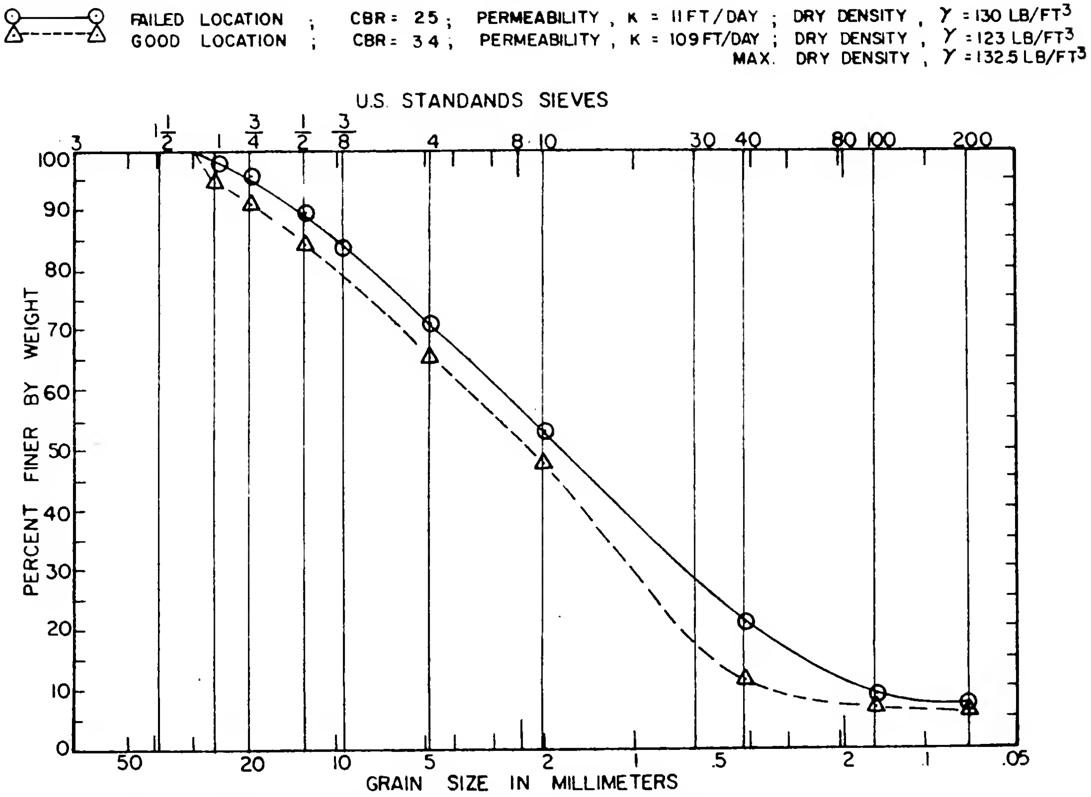

FIG.31 TYPICAL DATA FROM FAILED AND GOOD LOCATIONS WITHIN A TEST SECTION WITH GRAVEL SUBBASE
(DATA FROM I-65, CONTRACT R-8001, STATIONS 1037+00 — 1047+00 NBL)

on pavement performance. Table 30 summarizes the variation of subbase (CBR), permeability, and percent compaction with type of subbase and pavement condition. The tabulated data for slag and crushed stone subbases are relatively limited as they are based on only one test section for each of these subbase types. The failures on gravel subbase may be attributed primarily to poor strength and relatively low permeability of the subbase. A contributory cause of the failure at the section with slag subbase may be the relatively poor strength of the subbase at the failed location as compared with the strength at the good location. For the section with crushed stone subbase, though the values of CBR, permeability, and percent compaction were about the same at failed and good locations, the failure may be partly due to the low strength and poor compaction of the subbase.

Compared to gravel subbase, the better performance of crushed stone subbase may be attributed to the higher permeability characteristics of the crushed stone subbase; whereas for slag subbase, good compaction and higher strength (CBR) appear to be the reasons for better performance.

It should be noted that these results were obtained by comparing the subbase characteristics at failed locations with good locations, a pair of failed and good test locations being situated within a test section, 1000 ft. in length. It is therefore not surprising that the variability in the physical attributes of the subbase between good and failed test locations, though significant, is not too large. The results derived from this comparison point out the subbase characteristics contributing to localized CRCP failures.

Properties of Bituminous Stabilized Subbase

Although provisions were made in the proposed field testing program to obtain cores of the asphalt stabilized subbase for detailed laboratory tests, the cores could not

Table 30. Variation of Subbase CBR, Permeability,and Percent Compaction with Pavement Condition and Type of Subbase

Type of Subbase	Condition at Test Location	Subbase CBR (Percent)		Permeability,k (ft/day)	Percent Compaction
		Shoulder	Core		
Gravel*	Good	34.6	40.2	1001	93.3
	Failed	30.0	43.0	177	94.3
Slag**	Good	95	100	30	117.2
	Failed	56	58	26	115.8
Crushed** Stone	Good	32	41	1368.5	89.9
	Failed	33	38	1075.8	88.4

*CBR: mean values of data from 12 test sections.

*Permeability and Percent Compaction: mean values of data from 9 test sections.

**Data from only 1 test section.

be recovered at any of the field test locations. The subbase material was not sufficiently stable and crumbled on contact with the coring drill.

Only one test section with an asphalt stabilized subbase was available that had at least one failed location. The differences in subbase properties between the good and the failed test locations, as shown in Table 31, are based on test data obtained from this section. The materials used in the subbase course were found to be Indiana Specifications Size No. 73B aggregate cold mixed with asphalt emulsion. This is designated as Type I bituminous stabilized subbase in Indiana Standard Specifications (35).

Data presented in Table 31 show no apparent differences between the properties of the subbase at failed and good test locations.

The grain-size distributions of the subbase aggregate, however, were close to the maximum permissible limits for Size No. 73 Aggregate. The amount of fines (minus No. 200 material) in the aggregate exceeded the permissible maximum limit of 5 percent. The asphalt content was also slightly higher than the maximum specified (2.5-4.0 percent) for Type I bituminous stabilized subbase.

The instability of the subbase as indicated by the failure to obtain an intact core may be attributed to either partial curing of the emulsion or presence of water in the subbase. The second proposition pointing to poor subbase drainage appears more likely as a large amount of free water was observed to drain from under the slab into the test pit at the shoulder. The subgrade under the stabilized subbase was observed to be relatively dry. Though sufficient penetration CBR data could not be collected, the lone value obtained at the failed location (shoulder position) also pointed to the low stability of the subbase.

Table 31. Variation of the Properties of Asphalt-Treated Subbase Between Good and Failed Test Locations (Data from Contract R-8232, I-65)

Subbase Characteristic	Test Location	
	Good	Failed
Asphalt Content (Percent)	4.35	4.49
Percent Finer than Sieve Size:		
1 in.	100.0	100.0
3/4 in.	96.0	96.6
1/2 in.	80.4	81.8
3/8 in.	73.6	73.1
No. 4	59.2	58.7
No. 10	43.4	42.4
No. 40	20.8	19.2
No. 100	8.0	7.2
No. 200	5.6	5.1
Penetration CBR (Percent):	---	34*

*Measured at the shoulder portion.

Concrete Properties

Concrete test data were analyzed by using the following analysis of variance model:

$$Y_{ijk} = \mu + S_i + \delta_{(i)} + C_j + SC_{ij} + T_k + ST_{ik} + CT_{jk} + \varepsilon_{(ijk)} \qquad (35)$$

$i = 1, 2, \ldots 16$

$j = 1, 2$

$k = 1, 2$

where

Y_{ijk} = concrete test value (bulk unit weight in lb/ft^3; dynamic modulus of elasticity in psi; splitting tensile strength in psi) obtained from testing the kth segment of concrete core taken from a test location in jth condition within the ith test section.

μ = overall true mean effect.

S_i = true effect of the ith test section.

$\delta_{(i)}$ = restriction error, random; NID $(0, \sigma_\delta^2)$.

C_j = true effect of the jth pavement condition.

T_k = true effect of the kth segment of concrete core.

$\varepsilon_{(ijk)}$ = error, NID $(0, \sigma_\delta^2)$.

The other terms denote the two-factor interactions between the factors S_i, C_j, and T_k. The pavement condition factor, C_j implies a comparison of a good location with a failed location. Factor T_k refers to a comparison of the properties of the concrete core segment above the steel reinforcement with the segment below the steel.

Tables 32, 33, and 34 summarize the results of analysis of variance (ANOVA) of bulk density, dynamic modulus of elasticity and splitting tensile strength data, respectively.

Table 32. Summary of Analysis of Variance - Bulk Density of Concrete (lb/ft^3)

Source of Variation	DF	Sums of Squares	Mean Square	F	$F_{.05,crit}$
S_i (Test Sections)	15	475.30	31.67	---	---
$\delta_{(i)}$	0	---	---	---	---
Main Effects					
C_j (Condition)	1	22.68	22.68	10.87*	4.54
T_k (Core Segments)	1	9.38	9.38	4.49	4.54
Interaction Effects					
SC_{ij}	15	121.58	8.11	3.88*	2.40
ST_{ik}	15	80.80	5.39	2.58*	2.40
CT_{jk}	1	1.29	1.29	0.62	4.54
Error, $\varepsilon_{(ijk)}$	15	31.30	2.09		
Total	63	742.34			

*Significant at $\alpha = 0.05$

Table 33. Summary of Analysis of Variance - Dynamic Modulus of Elasticity of Concrete (10^6 psi)

Source of Variation	DF	Sums of Squares	Mean Square	F	$F_{.05,crit.}$
S_i (Test Sections)	15	7.592	0.506	---	---
$\delta_{(i)}$	0	---	---	---	---
Main Effects					
C_j (Condition)	1	1.134	1.134	16.93*	4.54
T_k (Core Segments)	1	0.107	0.107	1.60	4.54
Interaction Effects					
SC_{ij}	15	4.862	0.324	4.84*	2.40
ST_{ik}	15	2.251	0.150	2.24	2.40
CT_{jk}	1	0.031	0.031	0.46	4.54
Error, $\varepsilon_{(ijk)}$	15	1.005	0.067		
Total	63	16.982			

*Significant at $\alpha = 0.05$

Table 34. Summary of Analysis of Variance - Splitting Tensile Strength of Concrete (psi)

Source of Variation	DF	Sums of Squares	Mean Square	F	$F_{.05, crit.}$
S_i (Test Sectsion)	15	191352.21	12756.8	---	---
$\delta_{(i)}$	0	---	---	---	---
Main Effects					
C_j (Condition)	1	4347.8	4347.8	1.42	4.54
T_k (Core Segments)	1	8918.4	8918.4	2.92	4.54
Interaction Effects					
SC_{ij}	15	70136.8	4675.8	1.53	2.40
ST_{ik}	15	107813.1	7187.5	2.35	2.40
CT_{jk}	1	5067.7	5067.7	2.35	2.40
Error, $\varepsilon_{(ijk)}$	15	45874.4	3058.7		
Total	63	433510.4			

An examination of these ANOVA results shows that:

1. A significant difference in bulk density and dynamic modulus of elasticity of concrete was indicated between good and failed locations within a test section. The difference in splitting tensile strength at these locations was not significant.

2. No significant difference in bulk density, modulus of elasticity,or splitting tensile strength of concrete was detected between core segments above and below the steel reinforcement. In other words, properties of pavement concrete above and below the steel reinforcement were relatively uniform.

3. The interaction effect between the characteristics of the test sections (blocking affect) and the pavement condition was significant with respect to bulk density and modulus of elasticity of concrete.

4. Bulk unit weight was also shown to vary with the interaction between the test sections and the core segments.

These results were obtained from the analysis of concrete cores obtained from 16 test sections showing significant distress as evidenced by a breakup, a patch, or a potential failure condition as evidenced by heavily spalled cracks. Average values of bulk density, dynamic modulus of elasticity,and splitting tensile strength corresponding to failed and good pavement conditions are presented in Table 35. The difference in average bulk density of concrete does not reveal any practical significance. However, the statistical significance indicated in the analysis establishes that bulk unit weight of concrete at good locations was relatively higher than at failed locations.

From results given in Tables 32, 33,and 35 it may be concluded that pavement failures, at sections showing distress, were associated with concrete having a relatively low bulk density and modulus of elasticity.

Table 35. Relationship Between Pavement Condition and Concrete Properties*

*Concrete Properties	Pavement Condition	
	Good	Failed
Average Bulk Density, γ_c lb/ft^3	141.5	140.3
Average Dynamic Modulus of Elasticity, E_c(10^6psi)	5.03	4.76
Average Splitting Tensile Strength, f_{ts} (psi)	522.5	506.0

*Average of Test Data from 16 test sections.

Table 36. Concrete Characteristics Above and Below the Steel Reinforcement*

*Concrete Properties	Above the Steel Reinforcement	Below the Steel Reinforcement
Average Bulk Density γ_c (lb/ft^3)	140.6	141.3
Average Dynamic Modulus of Elasticity, E_c(10^6psi)	4.85	4.94
Average Splitting Tensile Strength, f_{ts}	502.4	526.0

*Average of test data from 16 test sections.

Comparison of Measures of Performance

Except for dynamic pavement deflections and surface curvature index, the performance variables were analyzed within the framework of a fixed-effect RCBD. In the case of deflection parameters a number of restrictions errors were caused by the order in which Dynaflect measurements were taken. The causes of the restrictions on randomization of Dynaflect measurements were:

1. All the measurements had to be completed on one test section before proceeding to the next one.(first restriction error)

2. A set of deflection measurements had to be completely recorded at one location before moving to another location. (second restriction error)

3. Because of the limitations of the test procedures, all readings at a given transverse position, such as the lane center line, had to be completed before the equipment could be moved to the next transverse position. (third restriction error)

These restriction errors necessitated the use of a split-split-split plot design (7) for dynamic deflection and surface curvature index data analysis.

Dynamic Pavement Deflection

Pavement deflections were measured, in mils (0.001 in.) by means of Dynaflect, at specified intervals across the outside lane (traffic lane) at two test locations within a test section. The two test locations corresponded to failed and good conditions respectively. Only 12 sections were used in the evaulation of pavement deflection characteristics.

The section with the bituminous stabilized subbase was excluded because exceedingly high deflections were reported for this section. The remaining sections were omitted because complete deflection data for these sections were not available.

The following ANOVA model was used for the analysis of deflection data:

$$Y_{ijk\ell} = \mu + S_i + \delta_{(i)} + C_j + CS_{ij} + \omega_{(ij)} + L_k + SL_{ik} + CL_{jk} + SCL_{ijk} + \eta_{(ijk)} + M_\ell + SM_{i\ell} + CM_{j\ell} + SCM_{ij\ell} + LM_{k\ell} + SLM_{ik\ell} + CLM_{jk\ell} + \varepsilon_{(ijk\ell)} \quad (36)$$

$i = 1, 2, \ldots .12$
$j = 1, 2$
$k = 1, 2, 3$
$\ell = 1, 2$

where

$Y_{ijk\ell}$ = deflection measurement in milli-inches made at the ℓ^{th} test position and the k^{th} transverse position on the outside lane, at a test location in j^{th} condition within the i^{th} test section.
μ = overall **true** mean effect.
S_i = true effect of the i^{th} test section.
$\delta_{(i)}$ = first restriction error, random; $NID(0,\sigma^2_\delta)$.
C_j = true effect of the j^{th} pavement condition (good vs. failed)
$\omega_{(ij)}$ = second restriction error, $NID\ (0,\sigma^2_\omega)$.
L_k = true effect of the k^{th} transverse position.
$\eta_{(ij)}$ = third restriction error, $NID\ (0,\sigma^2_\eta)$.
M_ℓ = true effect of the ℓ^{th} test position (crack position vs. mid-span position).
$\varepsilon_{(ijk\ell)}$ = within error, $NID\ (0,\sigma^2_\varepsilon)$

The other terms denote the interaction effects among the factors S_i, C_j, L_k and M_ℓ.

The factor L_k refers to transverse deflection measurements, made across the outside lane at 1.0 ft., 3.5 ft. and 6.0 ft. from the outside pavement edge. Essentially, this factor evaluates the variation of pavement deflection with distance from the pavement edge. The factor M_ℓ compares deflections obtained at a crack position with those measured at an adjacent mid-span position between two transverse cracks.

The results of applying the expected mean square algorithm (54) to the ANOVA model given by Equation 36 are shown in Table 37. The restriction errors pointed out earlier can be noticed clearly from the terms included in the expected mean squares. Owing to these restriction errors exact tests were not available for evaluating the significance of various effects.

The effect of sections (whole plot) could not be tested for significance as the whole plot error, $\delta_{(i)}$, could not be estimated. An estimate of variation due to the second restriction error was obtained by splitting the sum of squares for the interaction term SC_{ij} into one portion for SC_{ij} (non-additivity) with one degree of freedom and the remaining portion for the restriction error with 10 degrees of freedom (7).

Tests for the factor L_k and associated two-factor interaction terms were made by the three-factor interaction term, SCL_{ijk}. This is a conservative test, as the denominator of the F-test may be somewhat larger than it would be otherwise (7).

The factor M_k and its associated two and three-factor interaction terms were tested by the three-factor interaction term, $SCLM_{ijk\ell}$, used as an estimate of the within error term.

Table 38 gives a summary of the results of analysis of variance performed on deflection data. From these results, it may be concluded:

Table 37. Expected Mean Squares for Analysis of Variance of Deflection and Surface Curvature Index Data.

Source	Degrees of Freedom	Expected Mean Squares
S_i	11	$\sigma_\varepsilon^2 + 2\sigma_\eta^2 + 6\sigma_\omega^2 + 12\sigma_\delta^2 + 12\phi(S)$
$\delta_{(i)}$	0	$\sigma_\varepsilon^2 + 2\sigma_\eta^2 + 6\sigma_\omega^2 + 12\sigma_\delta^2$
C_j	1	$\sigma_\varepsilon^2 + 2\sigma_\eta^2 + 6\sigma_\omega^2 + 72\phi(C)$
SC_{ij}	11	$\sigma_\varepsilon^2 + 2\sigma_\eta^2 + 6\sigma_\omega^2 + 6\phi(SC)$
$\omega_{(ij)}$	0	$\sigma_\varepsilon^2 + 2\sigma_\eta^2 + 6\sigma_\omega^2$
L_k	2	$\sigma_\varepsilon^2 + 2\sigma_\eta^2 + 48\phi(L)$
SL_{ik}	22	$\sigma_\varepsilon^2 + 2\sigma_\eta^2 + 4\phi(SL)$
CL_{jk}	2	$\sigma_\varepsilon^2 + 2\sigma_\eta^2 + 24\phi(CL)$
SCL_{ijk}	22	$\sigma_\varepsilon^2 + 2\sigma_\eta^2 + 2\phi(SCL)$
$\eta_{(ijk)}$	0	$\sigma_\varepsilon^2 + 2\sigma_\eta^2$
M_ℓ	1	$\sigma_\varepsilon^2 + 72\phi(M)$
$SM_{i\ell}$	11	$\sigma_\varepsilon^2 + 6\phi(SM)$
$CM_{j\ell}$	1	$\sigma_\varepsilon^2 + 36\phi(CM)$
$SCM_{ij\ell}$	11	$\sigma_\varepsilon^2 + 3\phi(SCM)$
$LM_{k\ell}$	2	$\sigma_\varepsilon^2 + 24\phi(LM)$
$SLM_{ik\ell}$	22	$\sigma_\varepsilon^2 + 2\phi(SLM)$
$CLM_{jk\ell}$	2	$\sigma_\varepsilon^2 + 12\phi(CLM)$
$SCLM_{ijk\ell}$	22	$\sigma_\varepsilon^2 + \phi(SCLM)$
$\varepsilon_{(ijk\ell)}$	0	σ_ε^2
Total	143	

σ^2 = variance

ϕ = fixed component of the factor or interaction.

Table 38. Summary of Analysis of Variance - Dynamic Pavement Deflection (milli-inches)

Source of Variation	DF	Sums of Squares	Mean Square	F	$F_{.05,crit}$
S_i (Test Sections)	11	9.04	0.82	---	---
$\delta_{(i)}$	--	--	--	---	---
C_j (Condition	1	8.04	8.04	17.48*	4.96
SC_{ij} (Non-additivity)	1	3.40	3.40	7.39*	4.96
$\omega_{(ij)}$	10	4.64	0.46	---	---
L_k (Transverse Position)	2	3.22	1.61	14.64*	3.44
SL_{ik}	22	2.89	0.13	1.18	2.05
CL_{jk}	2	1.03	0.52	4.72*	3.44
SCL_{ijk}	22	2.41	0.11	---	---
$\eta_{(ijk)}$	0	--	--	---	---
M_ℓ (Test Position)	1	0.13	0.13	1.73	4.30
$SM_{i\ell}$	11	4.32	0.39	5.15*	2.27
$CM_{j\ell}$	1	0.27	0.27	3.52	4.30
$SCM_{ij\ell}$	11	4.22	0.28	5.02*	2.27
$LM_{k\ell}$	2	0.01	0.005	0.07	3.44
$SLM_{ik\ell}$	22	1.91	0.09	1.13	2.05
$CLM_{jk\ell}$	2	0.008	0.004	0.05	3.44
$\epsilon_{(ijk\ell)}$	22	1.68	0.076		
Total	143	44.82			

*Significant at $\alpha = .05$

1. There was a significant difference in pavement deflection between good and failed location.

2. The variation in pavement deflection at various points across the outside (traffic) lane was significant.

3. There was no significant difference between deflections measured at a crack as compared to deflections evaluated at a mid-span position between adjacent cracks.

In addition, the following interaction effects were also shown to have a significant influence on the variation in pavement deflection:

1. The interaction of pavement condition with the distance from the outside edge.

2. The interaction of test sections with pavement condition.

3. The interaction of test sections with test positions.

4. The three-factor interaction among test section characteristics, pavement condition and test positions.

Some of the significant trends indicated by the analysis of variance are further demonstrated in Table 39, which shows that:

1. Average pavement deflection at good locations was about 58 percent of average deflection at failed location.

2. Deflections decreased in magnitude with increasing distance from the outside pavement edge. On the average, deflection at the lane center line was 69 percent of that at 1.0 ft. from the outside edge.

3. Average deflection (0.87 milli-inch) at crack positions was not significantly different from the average deflection (0.93 milli-inch) at mid-span positions between transverse cracks. This could possibly be attributed to the time of the year (June), when the study was conducted. Because of higher temperatures, the cracks are held close together assuring greater granular interlock and good load transfer.

Table 39. Relationship Between Pavement Deflection and Evaluated Factors

*Average Dynamic Deflection (10^{-3}in.)						
Pavement Condition		Transverse Location (Distance from outside pavement edge, ft)			Test Position	
Good	Failed	1.0	3.5	6.0	At Crack	Mid-Span**
0.66	1.14	1.10	0.85	0.75	0.87	0.93

*Average of deflection measurements at 12 test sections.

**Mid-span between adjacent cracks.

The variation of deflections across the pavement was also evaluated by testing for significance the differences in the mean deflections obtained at 1.0, 3.5, and 6.0 feet from the pavement edge. Newman Keuls Sequential Range Test (7) was used for this purpose.

The results of this test (see Table 40) point out:

1. A significant difference between the mean deflection obtained at 1.0 ft. from the pavement edge and the mean deflection at the lane center-line (6.0 ft. from the outside edge).
2. A significant difference between the mean pavement edge deflection and the mean deflection observed 3.5 ft. from the edge.
3. No significant difference in deflections observed at 3.5 ft. and 6.0 ft. from the pavement edge, respectively.

These results correlate well with the field observation that most of the pavement breakups were found to occur at the pavement edge. In fact, pavement distress in the form of spalled cracks generally starts at the pavement edge.

Figure 32 depicts the effect of the interaction of pavement condition with the distance from the pavement edge on pavement deflection. The relative difference in average pavement deflection between good and failed locations was greater near the pavement edge than at more interior locations.

Surface Curvature Index

Surface curvature index is defined as the difference between the readings of the first two Dynaflect sensors (w_1 - w_2). A typical deflection basin reconstructed from Dynaflect readings and the concept of surface curvature index, SCI, is illustrated in Figure 33. SCI was calculated from Dynaflect readings taken with all the sensors at good and failed locations within each test section.

Table 40. Newman-Keuls Sequential Range Test for Comparison of Mean Transverse Deflections

Mean Values:

Distance from Outside Pavement Edge (ft)	Mean Dynamic Deflection, $\bar{Y}_{..k.}$ (milli-inches)	Rank of Mean
1.0	1.103	1
3.5	0.851	2
6.0	0.747	3

Tests of Differences Between the Means

	Means Spanned (k)	
Rank	3	2
1	0.356*	0.252*
2	0.104	

*Significant at $\alpha = 0.05$

Notes:

1. Critical range between means, $R_k = q_\alpha(k,df)\sqrt{\frac{\text{Mean Sq.(SCL)}}{48}}$
2. df = degrees of freedom for SCL.
3. Mean Square (SCL) = 0.11 from ANOVA, Table 38.
4. No. of observations included in each mean = 48
5. k = No. of means spanned.
6. Differencein means significant when $(\bar{Y}_{..p.} - \bar{Y}_{..q.}) > R_k$

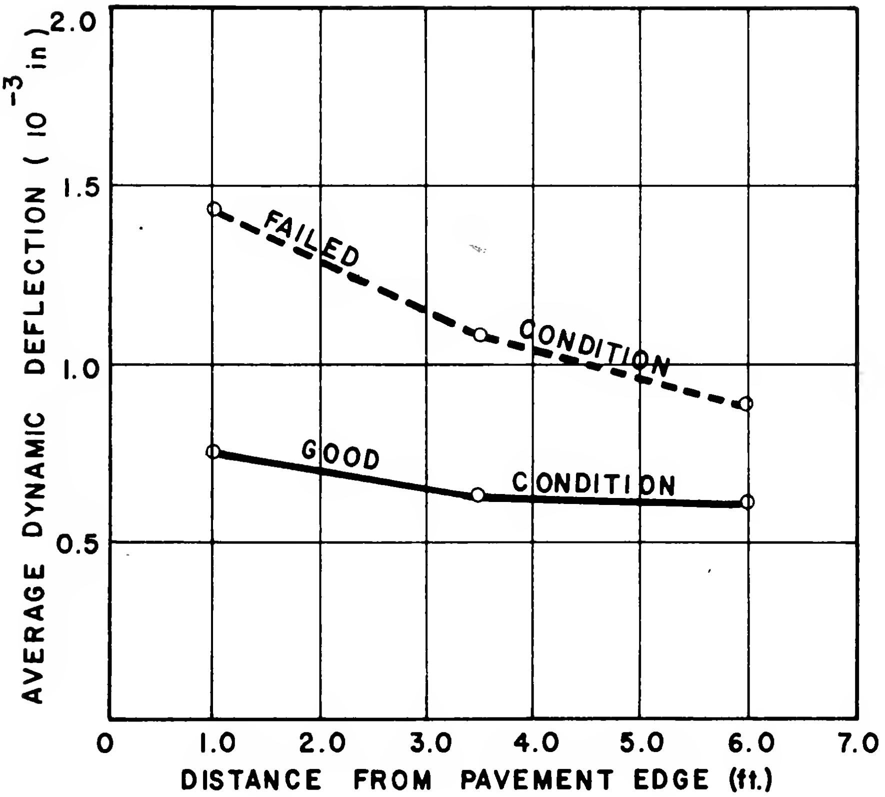

FIG. 32 EFFECT OF POSITION AND CONDITION ON PAVEMENT DEFLECTION

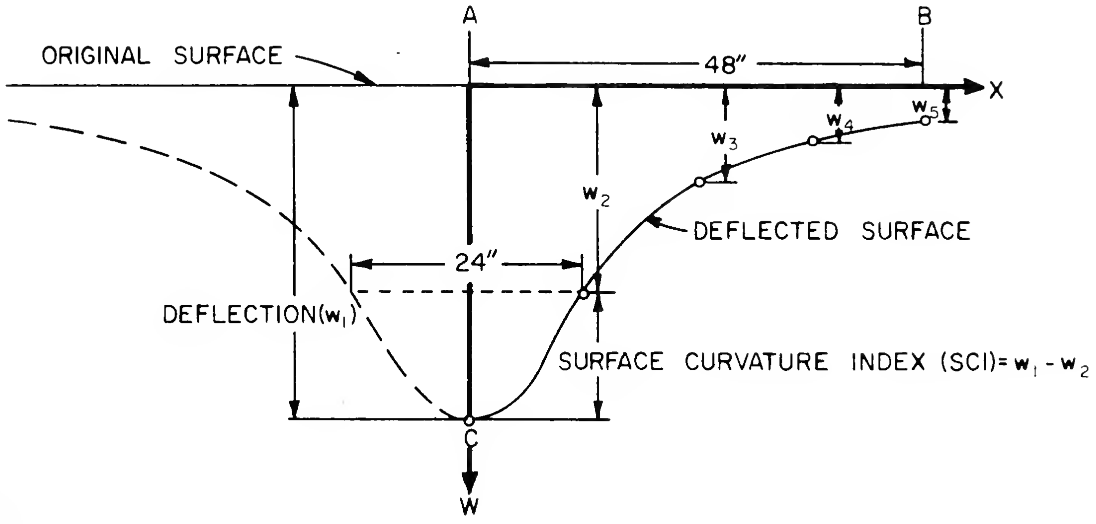
A
B
ORIGINAL SURFACE
48"
X
w_5
w_4
w_3
w_2
DEFLECTED SURFACE
24"
DEFLECTION(w_1)
SURFACE CURVATURE INDEX (SCI)= $w_1 - w_2$
C
W

w_x = Deflection reading of sensor x.

W = Applied load.

X = Distance from applied load.

FIG. 33 TYPICAL DEFLECTION BASIN RECONSTRUCTED FROM DYNAFLECT READINGS. ONLY ONE-HALF OF BASIN IS MEASURED (FROM SCRIVNER ET. AL.)

Scrivner and his group (53) were among the first to use the parameter, SCI, for evaluating seasonal changes in the load-carrying capabilities of flexible pavements. They state that the curvature at the point, C, in Figure 33 can be approximated by the derivative, $\frac{d^2w}{dx^2}$, where x is measured parallel to the line AC. Assuming a symmetrical deflection basin, the derivative, $\frac{d^2w}{dx^2}$, can be approximated as:

$$\frac{d^2w}{dx^2} \approx \frac{2(w_1-w_2)}{1000a^2} \tag{37}$$

or

$$\frac{d^2w}{dx^2} \approx \frac{SCI}{500a^2} \tag{38}$$

where, a, is the distance between sensor No. 1 and sensor No. 2 and the number 1000 in Equation 37 converts the unit of measurement from milli-inches to inches. The reciprocal of the derivative, $\frac{d^2w}{dx^2}$, is approximately equal to the radius of curvature of the deflected surface at the point C, or

$$\frac{d^2w}{dx^2} = \frac{1}{R} \tag{39}$$

where R is the radius of curvature of the deflected surface at the point, C, in inches.

The idea can be further extended to obtain an approximate relationship between the SCI and the pavement stiffness, a lower SCI being associated with a stiffer pavement. A stiff pavement, in turn, is defined as one offering a relatively greater resistance to imposed stresses.

The ANOVA model given by Equation 36 was used to analyze the SCI data with the exceptions that the response variable was SCI and data from only 10 test sections were used. One of the excluded test sections (with bituminous stabilized subbase), had exceedingly high SCI values while complete SCI data were not available for the remaining sections. The results are presented in Table 41. The following effects were shown to significantly influence the variation in SCI data.

1. Pavement condition; failed locations had a considerably higher SCI than good locations.
2. Transverse position; SCI varied significantly over positions between the pavement edge and the center line of the traffic lane.
3. The interaction effects between
    a) Section characteristics and pavement condition.
    b) Pavement condition and transverse positions across the pavement.
    c) Pavement condition and test position.
    d) Section characteristics and test position.

The analysis showed no significant difference in SCI between crack and mid-span positions. The relationship between SCI and the main effects is given in Table 42.

A Newman-Keuls Sequential Range Test (7) was made on the differences of mean SCI values indicated for the three transverse positions. The results of the test given in Table 43 show that the only significant difference in SCI occurred between the position, 1.0 ft. from the pavement edge and the lane center-line. Differences between other transverse positions were found to be non-significant.

The effect of the interaction of pavement condition with transverse positions on pavement SCI is illustrated in Figure 34. SCI values across the pavement were almost identical for locations in good condition whereas at failed locations, they increasedlinearly between the center-line of the right lane and the outside pavement edge. It may be deduced that the pavement test sections showed uniform stiffness characteristics at good locations whereas a significant decrease in stiffness was noted across the pavement at failed locations, the pavement edge being the most critical

Table 41. Summary of Analysis of Variance - Surface Curvature Index (milli-inches)

Source of Variation	DF	Sums of Squares	Mean Square	F	$F_{.05,crit}$
S_i (Test Sections)	9	5.938	0.660	---	---
$\delta_{(i)}$	0	---	---	---	---
C_j (Condition)	1	4.933	4.933	38.54*	5.32
SC_{ij} (Non-additivity)	1	4.744	4.744	37.06*	5.32
$\omega_{(ij)}$	8	0.946	0.128	---	---
L_k (Transverse Position)	2	0.611	0.306	8.05*	3.55
SL_{ik}	18	0.742	0.041	1.08	2.23
CL_{jk}	2	0.533	0.267	7.03*	3.55
SCL_{ijk}	18	0.682	0.038	---	---
$\eta_{(ijk)}$	0	---	---	---	---
M_ℓ (Test Position)	1	0.180	0.180	3.51	4.41
$SM_{i\ell}$	4	4.434	0.493	9.67*	2.46
$CM_{j\ell}$	1	0.226	0.226	4.41**	4.41
$SCM_{ij\ell}$	9	4.450	0.494	9.63*	2.46
$LM_{k\ell}$	2	0.095	0.048	0.94	3.55
$SLM_{ik\ell}$	18	0.910	0.051	0.994	2.23
$CLM_{jk\ell}$	2	0.083	0.042	0.819	3.55
$\varepsilon_{(ijk\ell)}$	18	0.923	0.0513		
Total	119				

*Significant at $\alpha = 0.05$

**Significant at $\alpha = 0.05$, on pooling interaction terms LM, SLM and CLM with the error term, $\varepsilon_{(ijk\ell)}$

Table 42. Relationship Between Surface Curvature Index and Evaluated Factors

*Average Surface Curvature Index (10^{-3} in.)						
Pavement Condition		Transverse Location (Distance from Outside Pavement Edge, ft.)			Test Position	
Good	Failed	1.0	3.5	6.0	At Crack	Mid-Span
0.049	0.455	0.340	.250	0.166	0.213	0.291

*Average of SCI values from 10 test sections.

Table 43. Newman-Keuls Sequential Range Test for Comparison of Mean Transverse SCI Values

Mean Values:

Distance from Outside Pavement Edge (ft)	Mean Square Curvature Index SCI(milli-inches)	Rank of Mean
1.0	0.340	1
3.5	0.250	2
6.0	0.166	3

Tests of Differences Between the Means

	Means	Spanned (k)
Rank	3	2
1	0.174*	0.090
2	0.089	

*Significant at α = 0.05

Notes:

1. Critical range between means, $R_k = q_\alpha(k,df)\sqrt{\frac{\text{Mean Sq.(SCL)}}{40}}$
2. df = degrees of freedom for SCL.
3. Mean Squares (SCL) = .038 from ANOVA, Table 41.
4. No. of observations included in each mean = 40
5. K = No. of means spanned.
6. Difference in means significant when $(\overline{Y}_{..p.} - \overline{Y}_{..q.}) > R_k$

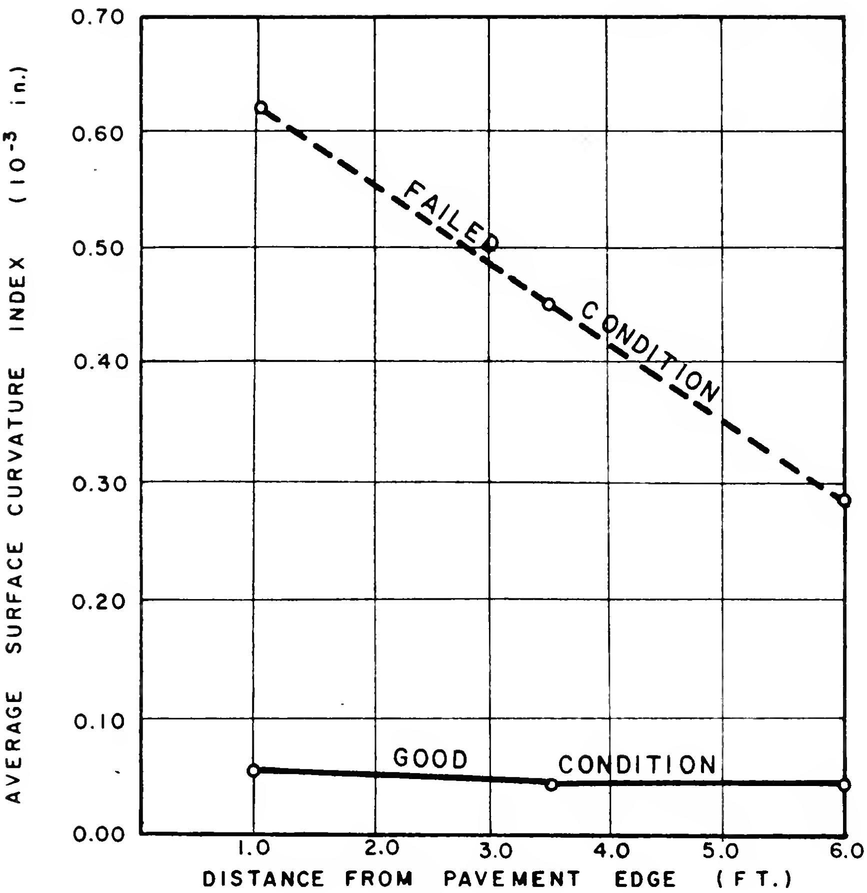

FIG. 34 EFFECT OF TRAVERSE POSITION AND CONDITION ON PAVEMENT SURFACE CURVATURE INDEX.

position. This again points to the presence of a critical condition at the pavement edge under imposed stresses.

Though no difference in SCI values was indicated between crack and mid-span test positions, Figure 35 shows the effect of the interaction of test positions and pavement condition on SCI. At good locations the difference in SCI values between crack and mid-span positions was practically negligible, whereas at failed locations higher SCI values were shown for mid-span positions than for crack positions. These results basically point to lack of uniformity in pavement stiffness at failed locations. Although it is indicated to the contrary, one would expect a higher SCI value at a crack position rather than at a mid-span position between adjacent cracks. The contra indication may be a function of the structural failure and reflects loss of support under the pavement slab.

Crack Width

A total of 16 test sections were included in this analysis. The additional test section was the one having a test location showing heavily spalled cracks (incipient failure condition).

The following ANOVA model, based on a RCBD, was used for the analysis of crack width measurements:

$$Y_{ijk} = \mu + S_i + \delta_{(i)} + C_j + SC_{ij} + L_k + SL_{ik} + CL_{jk}$$

$$\varepsilon_{(ijk)} \qquad (40)$$

$i = 1, 2, \ldots .16$

$j = 1, 2$

$k = 1, 2, 3$

where

Y_{ijk} = crack width (in) measured at the k^{th} transverse position on the outside lane, at a test location in j^{th} condition within the i^{th} test section.

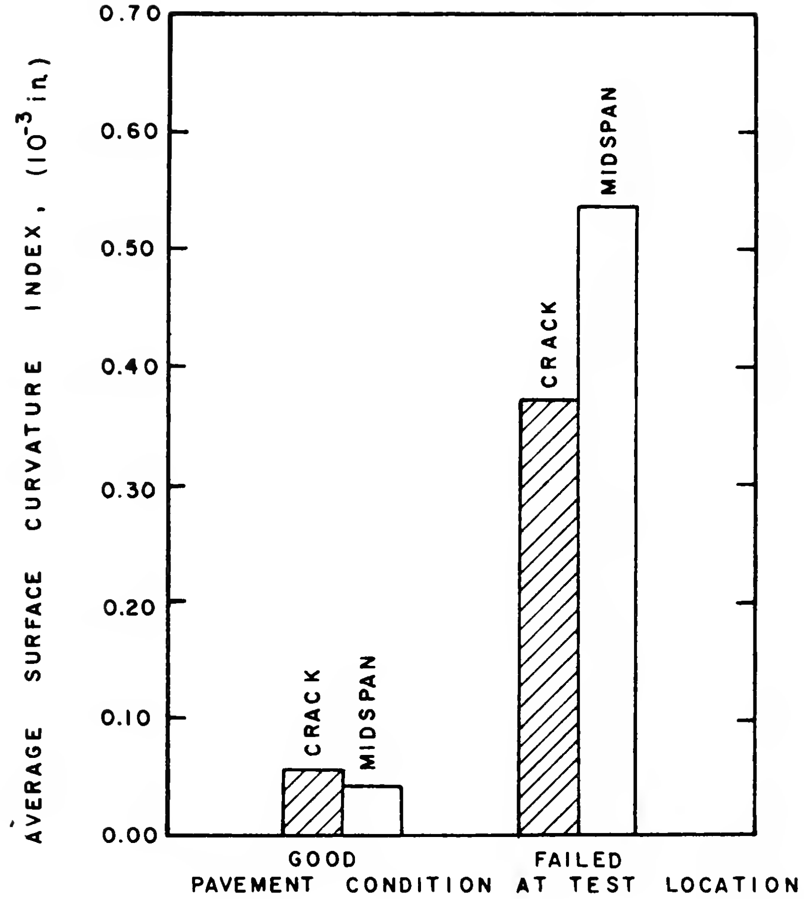

FIG. 35 EFFECT OF TEST POSITION AND CONDITION ON PAVEMENT SURFACE CURVATURE INDEX.

μ = overall true mean effect.

S_i = true effect of the ith test condition.

$\delta_{(i)}$ = restriction error, NID $(0,\sigma_\delta^2)$.

C_j = true effect of the jth pavement condition.

SC_{ij} = true interaction effect between the ith test section and the jth pavement condition.

L_k = true effect of kth transverse position.

SL_{ik} = true interaction effect between the ith test section and the kth transverse section.

CL_{jk} = true interaction effect between the jth pavement condition and the kth transverse location.

$\varepsilon_{(ijk)}$ = true within error, NID $(0,\sigma_\varepsilon^2)$ confounded with the true factor interaction, SCL_{ijk}.

The results of the ANOVA are given in Table 44, from which it may be concluded:

1. A significant difference in crack width was indicated between good and failed locations.

2. The variation of crack width across the outside traffic lane, between the outside edge and the lane center line, was not significant.

3. The interaction between the characteristics of test sections and pavement condition had a significant influence on crack width.

Further analysis of data showed that the mean crack width at good locations was 0.013 in. while at failed locations, the mean crack width was .032 in. Some of the other relationships resulting from the analysis of variance are presented in Figure 36. The plotted data are average crack widths obtained at 16 test sections. It is indicated that crack widths at failed locations were consistently greater than crack widths at good locations irrespective of the transverse position across the outside lane.

Table 44. Summary of Analysis of Variance - Crack Width (in.)

Source of Variation	DF	Sums of Squares	Mean Square	F	$F_{.05}$ crit.
S_i (Test Sections)	15	0.1229	0.00082	---	---
$\delta_{(i)}$	0	---	---	---	---
Main Effects					
C_j (Condition)	1	0.00851	0.00851	44.79*	4.17
L_k (Transverse Location)	2	0.00063	0.00032	1.68	3.32
Interaction Effects					
SC_{ij}	15	0.00698	0.00047	2.47*	2.01
SL_{ik}	30	0.00366	0.00012	0.63	1.84
CL_{jk}	2	0.00124	0.00062	3.26	3.32
Error, $\varepsilon_{(ijk)}$	30	0.00579	0.00019		
Total	95	0.3911			

*Significant at $\alpha = 0.05$

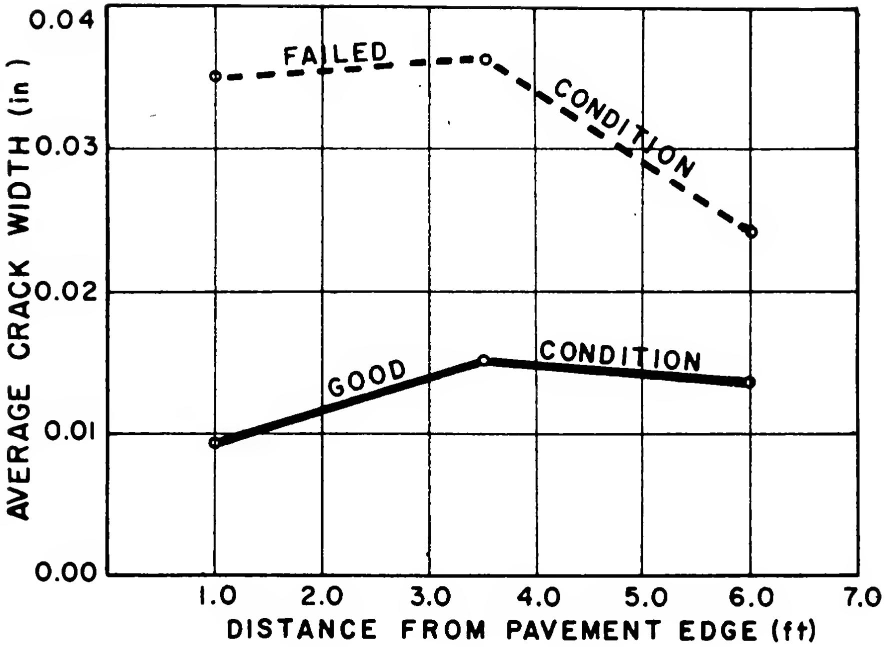

FIG.36 RELATIONSHIP OF CRACK WIDTH WITH POSITION AND PAVEMENT CONDITION

Crack Spacing

Crack spacing was measured along the pavement edge over a distance of 100 ft at each test location within a test section. The measures of crack spacing used in the analysis are:

1. Mean crack spacing, $\overline{X}_c$(ft)
2. Variance of crack intervals, V_c(ft^2)

The variance of crack intervals was obtained by:

$$V_c = \frac{\sum_{i=1}^{n} (X_{ic}-\overline{X}_c)^2}{n - 1} \tag{41}$$

where

V_c = variance of crack intervals (ft^2)

X_{ic} = individual crack interval, i = 1, ...n

$\overline{X}_c = \frac{\sum_{i=1}^{n} X_{ic}}{n}$ = mean crack interval (ft)

n = number of crack intervals per 100 ft. length of pavement at a test location

These variables were analyzed by ANOVA procedures using the following model:

$$Y_{ij} = \mu + S_i + \delta_{(i)} + C_j + \varepsilon_{(ij)} \tag{42}$$

$i = 1, 2, \ldots 15$

$j = 1, 2$

where

Y_{ij} = measure of crack spacing, e.g. $\overline{X}_c$, V_c obtained at the test location in jth condition within the ith test section

$\varepsilon_{(ij)}$= true error, NID $(0,\sigma^2_\varepsilon)$

and other terms are as defined in Equation 40.

ANOVA results for mean crack interval, $\overline{X}_c$, and variance of crack intervals, V_c, are presented in Tables 45 and 46

Table 45. Summary of Analysis of Variance - Mean Crack Spacing (ft.)

Source of Variation	DF	Sums of Squares	Mean Square	F	$F_{.05,crit.}$
S_i (Test Sections)	14	71.351	5.097	---	---
$\delta_{(i)}$	0	---	---	---	---
C_j (Condition)	1	4.937	4.937	3.20	4.67
SC_{ij}(Non-additivity)	1	0.0169	0.017	0.01	4.67
Error, $\varepsilon_{(ij)}$	13	20.054	1.543		
Total	29	96.359			

Table 46. Summary of Analysis of Variance - Crack Spacing Variance (ft^2)

Source of Variation	DF	Sums of Squares	Mean Square	F	$F_{.05,crit.}$
S_i (Test Sections)	14	150.67	10.76	---	---
$\delta_{(i)}$	0	---	---	---	---
C_j (Condition)	1	66.01	66.01	9.61*	4.67
SC_{ij}(Non-additivity)	1	41.44	41.44	6.04*	4.67
Error, $\varepsilon_{(ij)}$	13	89.26	6.87		
Total	29	347.38			

*Significant at $\alpha = 0.05$

respectively. These results show that:

1. There was no significant difference in average crack spacing between good and failed locations.

2. The difference in the variance of crack intervals, V_c, between good and failed locations was significant.

3. Crack spacing variance was also significantly influenced by the interaction of pavement condition with test sections.

Table 47 shows the relationship between pavement condition and the evaluated statistical measures of crack spacing. It would be observed that mean crack interval was not a reliable indicator of pavement condition. A measure of uniformity of crack spacing would be more appropriate from the viewpoint of ascertaining pavement condition. The data presented in Table 47 indicate that pavement sections in good condition had a more uniform and evenly spaced crack pattern than failed sections , a smaller variance of crack intervals being indicative of greater uniformity in crack spacing.

Crack Intersections

It was observed in the condition surveys that good pavement condition was associated with cracks that had a parallel transverse trend with relatively few or no intersections. Consequently, in the field study, this aspect was ≠ investigated in more detail. At each test location in a test section the number of crack intersections observed per 100 ft. length of pavement were counted. These counts were made in the traffic lane.

The ANOVA model given in Equation 42 was used for analyzing the crack intersections data, the dependent variable being the number of crack intersections per 100 ft. length of pavement.

Table 47. Relationship Between Statistical Measures of Crack Spacing, Crack Intersections, and Pavement Condition

Pavement Condition	Mean Crack Spacing $\overline{X}_c$		Variance of Crack Spacing V_c		Average Number of Crack Intersections Per 100 ft. Length of Pavement
	Average (ft)	Range(ft)	Average(ft^2)	Range(ft^2)	
Good	6.0	3.0 - 8.3	5.53	3.33 - 9.65	2.1
Failed	5.1	2.8 - 9.6	8.49	3.49 - 16.08	4.9

Note: Average and range values obtained from 15 test sections.

The results of analysis of variance are given in Table 48. It would be observed that there was a significant difference in number of crack intersections per 100 ft. length of pavement between good and failed locations within a test section. Average values of this variable at good and failed locations are given in Table 47. These results show that random and irregular crack patterns are indicative of poor pavement condition whereas uniform, evenly spaced crack patterns with relatively few intersecting cracks are representative of good pavement condition.

Summary of Results

The results summarized herein were obtained from a comparison of material properties and performance characteristics of failed test locations with structurally sound (good) test locations, within test sections showing significant distress. The following are the significant findings:

Subgrade Properties: No difference in subgrade CBR was indicated between good and failed locations. Subgrade compaction, however, was consistently low. Good pavement condition was associated with subgrades that were relatively more coarse-grained (sandy) than subgrades at failed locations.

Subbase Properties: CBR values of granular subbases at good locations were higher than the values obtained at failed locations. Higher CBR values were also obtained at the core-hole than at the shoulder. The higher values at the core-hole positions were no doubt due to the surcharge effect of the pavement slab. In any case, the CBR values of the gravel subbases were consistently lower than would be expected for well graded and adequately compacted materials of this type.

Although no significant difference in percent compaction was shown between good and failed locations, the compaction values were quite low. Pavement condition was found to be a

Table 48. Summary of Analysis of Variance - No. of Crack Intersections per 100 ft. Length of Pavement.

Source of Variation	DF	Sums of Squares	Mean Square	F	$F_{.05,crit.}$
S_i (Test Sections)	14	146.00	10.43	---	2.49
$\delta_{(i)}$	0	---	---	---	---
C_j (Condition)	1	61.63	61.63	14.41*	4.60
Error, $\varepsilon_{(ij)}$	14	59.87	4.28		
Total	29	267.50			

*Significant at $\alpha = 0.05$

function of subbase permeability, higher premeability characteristics being correlated with good condition. There was indication that distress in CRCP was partly an outcome of the densification of the subbase under traffic. As regards subbase type, failures on gravel subbases were due to the combined effect of poor strength (CBR), compaction,and permeability. On the section with slag subbase, the observed failure appeared to be due to the poor strength of the subbase. The highest permeability was noted for the crushed stone subbase. In the case of the bituminous stabilized subbase, both the asphalt content and the amount of filler (ninus No. 200 material) were slightly in excess of the specified values.

Concrete Properties: Pavement failures were associated with concrete having relatively low bulk density and modulus of elasticity. No significant difference in splitting tensile strength was indicated between good and failed locations. Also, no significant difference was found in the uniformity of concrete above and below the steel reinforcement with respect to bulk density, tensile strength,and modulus of elasticity.

Dynamic Pavement Deflection: Average pavement deflection at good locations was about 58 percent of average deflection at failed locations. Higher deflections were observed at the pavement edge than at the interior of the outside lane. Deflections decreased in magnitude with increasing distance from the pavement edge. Deflections at crack positions were not significantly different from deflections at mid-span positions between transverse cracks. From the standpoint of pavement condition, deflections close to the pavement edge were more critical than deflections at the interior of the outside lane.

Surface Curvature Index: Surface curvature index (SCI), was used as a measure of pavement stiffness, lower values of SCI indicating a stiffer pavement. Lower values of SCI were found to be correlated with pavement in good condition. SCI was observed to vary with the distance from the pavement edge for failed locations; higher SCI values occurring closer to the pavement edge. For good locations surface curvature indices were found to be uniformly low across the pavement.

Crack Width: Mean crack width at good locations (0.013 in.) was found to be significantly smaller than the mean crack width at failed locations (0.032 in.).

Crack Spacing: No significant difference in mean crack spacing was indicated between good and failed locations. However, the variance of crack intervals, indicative of uniformity of crack spacing, yielded more promising results. It was shown that the variance of crack intervals at good locations was significantly less than that at failed locations.

Crack Intersections: More intersecting cracks were observed at failed locations than at good locations, thereby indicating that good pavement condition is associated with non-intersecting, uniform, evenly spaced,transverse crack patterns.

TEST SECTIONS WITH FAILURES VS. TEST SECTIONS WITHOUT FAILURES: A COMPARISON

The aim of this comparative analysis was to identify material properties and performance characteristics that are indicators of potential distress in CRCP. Only data from structurally sound locations were included in the study. The objective of using such data was to isolate inherent deficiencies in the pavement structure even where no superficial evidence of distress was present.

For failed test sections, the data were obtained from structurally sound (good) test locations within test sections showing significant distress (see the comparison between failed and good test locations). Where two test locations were sampled within a test section without distress, data from only one randomly selected test location were used.

This comparison also includes test properties representative of the whole test section such as concrete slump, temperature variables, load repetitions, and deflection measurements taken at 100 ft. intervals along the length of the test section.

For most evaluated variables, the test sections were grouped into two categories, relative to the pavement condition:

1. sections with failures, that is, having no apparent distress (adequate condition).

2. sections with at least one failed location (poor condition).

The number of test sections in each of the "without" and "with" failure categories were 15 and 16 respectively.

Differences between the two categories with respect to material properties and performance characteristics were tested by the t-test. Sample variances were pooled where homogeneity of variance was indicated by the F-test; otherwise, the t-test was based on estimates of separate variances for the two categories. The hypotheses for the statistical tests were developed on basis of the results of the previous comparison between good and failed test locations.

In other cases, where a factorial arrangement was used, the data were analyzed within the framework of a nested factorial design (7). An equal number of randomly selected test sections were nested within each of the pavement condition categories.

All data were analyzed by appropriate computer programs at the Purdue University Computer Center. Where possible, the reported results emphasize only the significant findings.

Comparison of Material Properties

The results reported in this part are based on a comparative analysis of subgrade, subbase, and concrete properties between sections with failures and sections with no apparent distress.

Subgrade Properties

Subgrade CBR data were analyzed by the following ANOVA scheme:

$$Y_{ijk} = \mu + C'_i + S_{(i)j} + \delta_{(ij)} + P_k + C'P_{ik} + SP_{(i)jk} + \varepsilon_{(ijk)} \qquad (43)$$

$i = 1, 2$

$j = 1, 2 \ldots\ldots 14$ for $i = 1$

$15, 16 \ldots\ldots 28$ for $i = 2$

$k = 1, 2$

Y_{ijk} = estimated in-place CBR obtained at the k^{th} test position at the good test location in j^{th} test section, nested within the i^{th} pavement condition.

μ = overall true mean effect.

C'_i = true effect of the i^{th} pavement condition.

$S_{(i)j}$ = true effect of the j^{th} test section (random value) in the i^{th} condition, NID $(0, \sigma_s^2)$.

$\delta_{(ij)}$ = restriction error, NID $(0, \sigma_\delta^2)$.

P_k = true effect of the k^{th} test point (core hole vs. shoulder).

CP'_{ik} = true effect of the interaction of the i^{th} pavement condition with the k^{th} test point.

$SP_{(i)jk}$ = true effect of the interaction of the j^{th} test section in the i^{th} condition with the k^{th} test point, NID $(0, \sigma_{sp}^2)$.

$\varepsilon_{(ijk)}$ = within error, NID $(0, \sigma_\varepsilon^2)$; since the CBR test was not replicated at each test point, the error term has no degrees of freedom.

The ANOVA results of Table 49 show no significant effect. There was no difference in subgrade CBR values between failed and non-failed sections. The CBR values averaged 15 percent for each of the two categories.

Other Subgrade Properties: The results of t-test indicated no significant difference between the two test section groups with respect to percent compaction and material finer than No. 4 and No. 40 sieve sizes. The

Table 49. ANOVA Summary - Subgrade CBR (Percent)

Source of Variation	DF	Mean Square	Expected Mean Square	F	$F_{.05,\ crit.}$
C'_i (Condition)	1	0.018	$\sigma_\varepsilon^2+2\sigma_\delta^2+2\sigma_s^2+28\phi(c)$	.0002	4.23
$S_{(i)j}$ (Test Sections)	26	95.012	$\sigma_\varepsilon^2+2\sigma_\delta^2+2\sigma_s^2$	-----	----
δ_{ij}	0	-------	$\sigma_\varepsilon^2+2\sigma_\delta^2$	-----	----
P_k (Test Points)	1	161.161	$\sigma_\varepsilon^2+\sigma_{sp}^2+28\phi(P)$	2.37	4.23
$C'P_{ik}$	1	42.875	$\sigma_\varepsilon^2+\sigma_{sp}^2+14\phi(CP)$	0.63	4.23
$SP_{(i)jk}$	26	68.056	$\sigma_\varepsilon^2+\sigma_{sp}^2$	----	----
$\varepsilon_{(ijk)}$	0	-------	σ_ε^2		

average percent compaction at sections with failures was 94 percent whereas, at adequate sections with no apparent distress, it was 91 percent. These values point to consistently low subgrade compaction, irrespective of pavement condition.

The analysis, however, revealed that the liquid limit of subgrade soils and the amount of fines (minus the No. 200 sieve fraction) in the soil were significantly different between the sections comprising the two categories. A summary of the significant results is presented in Table 50. These results further substantiate the earlier finding that relatively better pavement condition was observed at sections where the subgrades were more sandy and had a higher proportion of coarse particles.

Properties of Granular Subbases

In view of the earlier analyses that brought to light significant differences among the properties and behavior of crushed stone, slag, and gravel subbases, the subbase data was first segregated by subbase type. The properties of the gravel subbases were comparatively analyzed,relative to poor and adequate pavement condition. Such an analysis could not be done on the other subbase types owing to paucity of data. Finally the variation of important subbase characteristics with subbase type was tabulated.

Gravel Subbases: The CBR data for gravel subbases was analyzed in the light of the ANOVA model given by Equation 43. Only ten test sections were used for each condition type. Results derived from this analysis (see Table 51) indicated little difference in subbase CBR relative to pavement condition. On the other hand, the CBR values obtained at the core-hole (an average CBR of 44 percent) were significantly larger than those measured at the shoulder (an average CBR of 35 percent).

Table 50. Summary of Results of One-Tailed T-Test on Subgrade Properties

Null Hypothesis, H_o: $\mu_1 = \mu_2$ Alternate Hypothesis, H_1: $\mu_1 > \mu_2$

Subgrade Variable	Condition of Test Sections	No. of Test Sections	Mean	Standard Error	Degrees of Freedom (ν)	$t_{calc.}$	$t_{(\alpha=.05,\nu)}$
Liquid Limit	With Failures (μ_1)	15	25.0	2.13	27	2.05*	1.703
	Without Failures (μ_2)	14	17.0	3.29			
Percent Passing No. 200 Sieve	With Failures (μ_1)	15	58.1	4.97	27	2.29*	1.703
	Without Failures (μ_2)	14	38.9	6.82			

*Significant at $\alpha = 0.05$; reject null hypothesis.

Note: Data from structurally sound test locations.

Table 51. ANOVA Summary - Gravel Subbase CBR (Percent)

Source of Variation	DF	Mean Square	Expected Mean Square	F	$F_{.05,\ crit.}$
C'_i (Condition)	1	75.63	$\sigma^2_\varepsilon+2\sigma^2_\delta+2\sigma^2_s+20\phi$ (C)	0.31	4.44
$S_{(i)j}$(Test Sections)	18	241.18	$\sigma^2_\varepsilon+2\sigma^2_\delta+2\sigma^2_s$	----	----
$\delta_{(ij)}$	0	------	$\sigma^2+2\sigma^2_\delta$	----	----
P_k (Test Points)	1	893.03	$\sigma^2_\varepsilon+\sigma^2_{sp}+20\phi$ (P)	16.33*	4.44
$C'P_{ik}$	1	0.23	$\sigma^2_\varepsilon+\sigma^2_{sp}+10\phi$ (CP)	0.004	4.44
$SP_{(i)jk}$	18	54.68	$\sigma^2_\varepsilon+\sigma^2_{sp}$	-----	
$\varepsilon_{(ijk)}$	0	------	σ^2_ε		

*Significant at $\alpha = 0.05$.

The grain-size distribution, percent compaction, and permeability of gravel subbases were essentially the same at both the sections with and without failures, as was shown by the results of t-tests on these properties. Even so, the degree of compaction achieved for the gravel subbases was uniformly low (about 93 percent of standard AASHTO on the average).

Comparison of Subbase Types: Table 52 describes the variation of subbase CBR, permeability, and degree of compaction with subbase type. Though no clear differences in the properties of the gravel subbase were evident between sections with failures and sections showing no apparent distress, the gravel subbases were not sufficiently compacted and had relatively low permeability and strength.

The failure on the section with slag subbase appears to have been caused by an isolated distress condition. The slag subbase at the failure (see Table 30) had low CBR values whereas at the good location on the same section, CBR values of 95-100 percent were measured. The permeability of the slag subbase at the section with the failure was lower than the average permeability values estimated at the other three sections with no failures. Hence the failure on the slag subbase can be attributed to an isolated location having subbase with poor strength and low permeability characteristics.

The crushed stone subbase at the section which had a failure was found to have a considerably smaller strength (CBR of 32 vs. 90 percent) and lower permeability than the subbase at the section with no distress.

These results also bring to light important differences among the properties of the different subbase types. Crushed stone subbases were the most permeable while slag subbases had the lowest permeability. The relatively poor water transmission characteristics of the slag subbase were more than balanced by its high strength, as indicated by CBR.

Table 52. Effect of Subbase Type on Pavement Condition

Type of Subbase	Condition of Test Sections	No. of Test Sections	Subbase CBR (percent)		Permeability, k (ft/day)	Percent Compaction
			Shoulder	Core		
Gravel	With Failures	13	33.5	38.0	978.9*	91.5*
	Without Failures	10	35.9	45.2	702.6**	93.2**
Slag	With Failures	1	95.0	100.0	30.0	117.2
	Without Failures	3	81.0	96.6	142.9	100.6
Crushed Stone	With Failures	1	32.0	41.0	1369.7	89.9
	Without Failures	1	90.0	59.0	2497.1	85.3

* Average of values from 9 test sections.

**Average of values from 10 test sections

Note: Data from structurally sound test locations.

Irrespective of pavement condition, the lowest strength was noted for gravel subbases. This is believed to be primarily a function of inadequate subbase compaction. The highest degree of compaction was indicated for the slag subbase whereas gravel and crushed stone subbases were found to have been insufficiently compacted (approximately only 90 percent of the specified minimum).

From the considerations noted above, in order to ensure good performance of the subbase, the subbase should be well compacted (minimum of 100 percent standard AASHTO), it should have high stability (CBR of 90-100 percent) and it should drain well (minimum permeability, k, of 1000 ft/day). Pavement sections showing the poorest performance were the ones constructed on subbases that had poor internal drainage and low stability.

Properties of Bituminous Stabilized Subbase

Evaluation of the bituminous-stabilized subbase was based on a comparison of one test section (on Contract R-8440) having no failures with another one (on Contract R-8232) that had significant distress. One striking difference between the two sections was the thickness of the asphalt stabilized layer observed during the detailed field study. The section without failures had a 6 in. stabilized subbase while the section with failures had a 4 in. subbase. In both cases, the asphalt-stabilized subbase was underlain by a 3 in. layer of gravel. This means that an effective subbase layer of 7-9 in. was used between the pavement slab and the subgrade. In terms of occurrence of failures, pavements on asphalt-stabilized subbase have performed no better than pavements placed on slag or crushed stone subbase.

On the section without failures, the materials used in the subbase were found to be Indiana Specification Size No. 53B aggregate cold-mixed with asphalt emulsion. The properties of the failed section have been reported earlier (see Table 31).

A comparison of the characteristics of the subbase material obtained from structurally sound locations at these sections is reported in Table 53. At the section without failures, the grain-size distribution of the aggregate and the asphalt content were within the limits specified for Type I bituminous-stabilized subbase (35). These data show that filler material (minus No. 200 sieve fraction) and/or asphalt content in excess of the specified values had a detrimental effect on the stability of the bituminous stabilized subbase. This conclusion is based on very limited data and deserves further investigation.

The stability of the bituminous stabilized subbases was found to be low. At the test section without failures, the average penetration CBR was 44.5 and 38 percent for core and shoulder positions,respectively. The shoulder value measured at a failed location on another section was only 34 percent. These stability values are in the same range as those measured for gravel subbases and are considerably lower than the ones for slag and crushed stone subbases at test sections without failures (see Table 52).

Concrete Properties

Bulk density of the concrete was excluded from the analysis as information on the source and type of aggregate used in the concrete was not available. Significant differences in bulk density could result from variations in the source and type of concrete aggregate. This would be particularly applicable where slag was used in the concrete mix. Hence, the analysis was confined to an evaluation of the modulus of elasticity, tensile strength,and slump of concrete.

Table 53. Variation of the Properties of Asphalt-Treated Subbase with Pavement Condition

Subbase Characteristics	Test Section			
	With Failures	Without Failures		
		Test Location 1	Test Location 2	Mean
Asphalt Content (Percent)	4.25	3.80	3.68	3.74
Percent Finer Than Sieve Size:				
1"	100.0	96.9	98.6	97.8
3/4"	96.0	90.5	93.4	92.0
1/2"	80.4	79.4	80.2	79.8
3/8"	73.6	70.2	72.7	71.5
No. 4	59.2	54.0	57.2	55.6
No. 10	43.4	38.9	43.0	41.0
No. 40	20.8	12.4	14.4	13.4
No. 100	8.0	3.1	3.3	3.2
No. 200	5.6	2.0	2.2	2.1
Penetrometer CBR (percent)				
Core*	-----	52	37	44.5
Shoulder*	34**	46	30	38.0

* Test position.

**Measured at failed test location; all other data from structurally sound locations.

Concrete Slump: Test sections without failures had an average concrete slump of 2.1 in. while an average slump of 1.7 in. was obtained for sections with failures. This difference was shown to be statistically significant by a t-test,based on separate variance estimates for the two data groups (see Table 54).

Modulus of Elasticity and Tensile Strength: These concrete properties were analyzed by the following ANOVA model:

$$Y_{ijk} = \mu + C'_i + S_{(i)j} + \delta_{(ij)} + T_k + C'T_{ik} + ST_{(i)mk} + \varepsilon_{(ijk)} \tag{44}$$

$i = 1, 2$

$j = 1, 2 \; .... \; 15$ for $i = 1$

$\; = 16, 17 \; .... \; 30$ for $i = 2$

where Y_{ijk} = concrete test value obtained from testing the k^{th} segment of concrete core taken from a good test location in j^{th} test section, nested within the i^{th} pavement condition category.

T_k = true effect of the k^{th} segment of concrete core,and

other terms are as defined in Equation 43. $C'T_{ik}$ and $ST_{(i)jk}$ denote the interactions between the main effects given by Equation 44.

The results of the analysis are summarized in Tables 55, 56, and 57. It is seen from these results that:

1. The modulus of elasticity of the concrete was significantly higher at test sections without failures than at sections with failures. No difference in splitting tensile strength of concrete was indicated, with respect to pavement condition.

Table 54. Summary of One-Tailed T-Test on Concrete Slump (in.)

Null Hypothesis, H_o: $\mu_1 = \mu_2$ Alternate Hypothesis, $H_1 = \mu_1 > \mu_2$

Condition of Test Sections	No. of Test Sections	Mean	Standard Deviation	Standard Error	Degrees of Freedom (ν)	$t_{calc.}$	$t_{(\alpha = .05,\nu)}$
Without Failures (μ_1)	15	2.13	.770	.199	21.03*	2.00**	1.73
With Failures (μ_2)	16	1.69	.409	.102			

* Based on separate variance estimate.

**Significant at $\alpha = .05$; reject null hypothesis.

Table 55. ANOVA Summary - Dynamic Modulus of Elasticity of Concrete (psi)

Source of Variation	DF	Mean Square	Expected Mean Square	F	$F_{.05}$
C'_i (Condition)	1	20.86	$\sigma^2_\varepsilon+2\sigma^2_\delta+2\sigma^2_s+30\sigma^2_c$	17.38*	4.20
$S_{(i)j}$ (Test Sections)	28	1.20	$\sigma^2_\varepsilon+2\sigma^2_\delta+2\sigma^2_s$	------	----
$\delta_{(ij)}$	0	-----	$\sigma^2_\varepsilon+2\sigma^2_\delta$	------	----
T_k (Core Segments)	1	1.33	$\sigma^2_\varepsilon+\sigma^2_{ST}+30\sigma^2_T$	4.43*	4.20
$C'T_{ik}$	1	0.48	$\sigma^2_\varepsilon+\sigma^2_{ST}+15\sigma^2_{CT}$	1.60	4.20
$ST_{(i)jk}$	28	0.30	$\sigma^2_\varepsilon+\sigma^2_{ST}$	------	
$\varepsilon_{(ijk)}$	0	-----	σ^2_ε		

*Significant at $\alpha = 0.05$.

Table 56. ANOVA Summary - Splitting Tensile Strength of Concrete (psi)

Source of Variation	DF	Mean Square	Expected Mean Square	F	$F_{.05}$
C'_i (Condition)	1	873.3	$\sigma_\varepsilon^2+2\sigma_\varepsilon^2+2\sigma_s^2+30\sigma_c^2$	0.07	4.20
$S_{(i)j}$ (Test Sections)	28	12230.8	$\sigma_\varepsilon^2+2\sigma_\delta^2+2\sigma_s^2$	----	----
$\delta_{(ij)}$	0	-------	$\sigma_\varepsilon^2+2\sigma_\delta^2$	----	----
T_k (Core Segments)	1	21671.4	$\sigma_\varepsilon^2+\sigma_{ST}^2+30\sigma_T^2$	5.44*	4.20
$C'T_{ik}$	1	1150.2	$\sigma_\varepsilon^2+\sigma_{ST}^2+15\sigma_{CT}^2$	0.29	4.20
$ST_{(i)jk}$	28	3981.4	$\sigma_\varepsilon^2+\sigma_{ST}^2$		
$\varepsilon_{(ijk)}$	0	-------	σ_ε^2		

*Significant at $\alpha = 0.05$.

Table 57. Variation of Concrete Properties with Pavement Condition and Position Relative to the Steel Reinforcement

Concrete Properties	Condition of Test Sections		Position	
	With Failures (15)	Without Failures (15)	Above the Steel Reinforcement (30)	Below the Steel Reinforcement (30)
Average Dynamic Modulus of Elasticity, E_c (psi)	4.97	6.15	5.41	5.71
Average Splitting Tensile Strength, f_{ts} (psi)	518.3	510.7	495.5	533.5

Note: 1. Data from structurally sound test locations.

2. Figures in parentheses denote the number of test sections included in the average.

2. Concrete above the steel reinforcement was found to have somewhat lower modulus of elasticity and splitting tensile strength than concrete below the steel reinforcement. This applies only to concrete cores obtained from structurally intact pavement locations. These differences, though statistically significant, were not large from a practical viewpoint.

3. There was no indication that the variation in concrete properties above and below the steel reinforcement had any influence on pavement condition. The interaction effect between pavement condition and core segments was not significant.

Comparison of Measures of Performance

Sections with failures were compared with sections with no apparent distress relative to dynamic pavement deflection, surface curvature index, crack width, crack spacing, and number of intersecting cracks per 100 ft. length of pavement. The data pertaining to these variables were obtained at a structurally intact test location within each test section. Furthermore, a detailed study of deflection measurements, taken at 100 ft. intervals over each test section, was also conducted.

Dynamic Pavement Deflection

Dynamic deflection measurements made at structurally intact locations were analyzed by the ANOVA model given as follows:

$$\begin{aligned} Y_{ijk} &= \mu + C'_i + S_{(i)j} + \delta_{(ij)} + L_k + C'L_{ik} \\ &\quad + SL_{(i)jk} + \omega_{(ijk)} + M_\ell + C'M_{i\ell} + SM_{(i)j\ell} \\ &\quad + LM_{k\ell} + C'LM_{ik\ell} + SLM_{(i)jk\ell} + \varepsilon_{(ijk)} \end{aligned} \tag{45}$$

$i = 1, 2$
$j = 1, \ldots 14$ for $i = 1$
$= 15, \ldots 28$ for $i = 2$
$k = 1, 2, 3$
$\ell = 1, 2$

where Y_{ijk} = deflection measurement (or surface curvature index) in milli-inches made at the ℓ^{th} test position and k^{th} transverse position on the outside lane at a good test location in the j^{th} section, nested within the i^{th} pavement condition.
μ = overall true mean effect.
C'_i = true effect of the i^{th} pavement condition, compares sections with failures vs. sections without failures.
$S_{(i)j}$ = true effect of the j^{th} test section (random) within i^{th} pavement condition, NID $(0, \sigma_s^2)$.
$\delta_{(i)}$ = first restriction error, NID $(0, \sigma_\delta^2)$, resulting from making all deflection measurements at one test section before proceeding to the next.
L_k = true effect of the k^{th} transverse position.
$\omega_{(ijk)}$ = second restriction error NID $(0, \sigma_\omega^2)$, caused by taking all deflection readings at one transverse position (e.g. outside edge), before moving to the next transverse position.
M_ℓ = true effect of the ℓ^{th} test position.
$\varepsilon_{(ijk\ )}$ = within error, NID $(0, \sigma_\varepsilon^2)$.

The other terms denote the interactions between the main effects C'_i, $S_{(i)j}$, L_k and M_ℓ. A mixed interaction effect (Fixed x Random) is considered random NID $(0, \sigma^2)$. A description of the levels of the fixed factors has been presented previously. The test data analyzed by this model were obtained from one structurally sound location within each test section. The properties of such a test location were considered representative of the non-failed areas of the pavement test section.

The results of the analysis (given in Table 58) indicated a significant variation in pavement deflection with distance from the pavement edge. As expected, the deflections (measured at structurally sound test locations) were not different at sections with failures compared to sections without failures. Also, no difference in deflections was indicated between crack and midspan positions. Average deflection values associated with these trends are presented in Table 59. The average edge deflection was about 30 percent larger than the deflection at the center-line of the traffic lane.

In the detailed field evaluation, additional deflection measurements were made along the center-line of the traffic lane at 100 ft. intervals. Restrictions on randomization were caused by the order in which these pavement deflections were measured. One obvious restriction resulted from completing all the field measurements at one test section before moving to the next test section. Another restriction was caused by taking sequential deflection measurements at crack and mid-span positions after every 100 ft. along the test section.

The ANOVA model used to analyze the data was derived from a nested factorial and is given by:

$$\begin{aligned} Y_{ijk} &= \mu + C'_i + S_{(i)j} + \delta_{(ij)} + I_{(ij)k} + \omega_{(ijk)} \\ &\quad + M_\ell + C'M_{i\ell} + SM_{(i)j\ell} + IM_{(ij)k\ell} \\ &\quad + \varepsilon_{(ijk\ell)} \end{aligned} \tag{46}$$

Table 58. ANOVA Summary - Dynamic Pavement Deflection (milli-inches)

Source of Variation	DF	Mean Square	Expected Mean Square	F	$F_{.05,\ crit.}$
C'_i (Condition)	1	0.0357	$\sigma_\varepsilon^2+\sigma_\omega^2+6\sigma_\delta^2+6\sigma_s^2+84\phi$ (C')	0.25	4.23
$S_{(i)j}$ (Sections)	26	0.1443	$\sigma_\varepsilon^2+2\sigma_\omega^2+6\sigma_\delta^2+6\sigma_s^2$	----	
$\delta_{(ij)}$	0	------	$\sigma_\varepsilon^2+2\sigma_\omega^2+6\sigma_\delta^2$	----	
L_k(Transverse Position)	2	0.5553	$\sigma_\varepsilon^2+2\sigma_\omega^2+2\sigma_{SL}^2+56\phi$ (L)	55.53*	3.19
$C'L_{ik}$	2	0.0029	$\sigma_\varepsilon^2+2\sigma_\omega^2+2\sigma_{SL}^2+28\phi$ (C'L)	0.29	3.19
$SL_{(i)jk}$	52	0.0100	$\sigma_\varepsilon^2+2\sigma_\omega^2+2\sigma_{SL}^2$	----	
$\omega_{(ijk)}$	0	------	$\sigma_\varepsilon^2+2\sigma_\omega^2$	----	

Table 58. Continued

Source of Variation	DF	Mean Square	Expected Mean Square	F	$F_{.05,crit.}$
M_{ℓ} (Test Position)	1	0.0013	$\sigma_{\varepsilon}^{2}+3\sigma_{SM}^{2}+84\phi$ (M)	0.56	4.23
$C'M_{i\ell}$	1	0.0035	$\sigma_{\varepsilon}^{2}+3\sigma_{SM}^{2}+42\phi$ (C'M)	1.52	4.23
$SM_{(i)j\ell}$	26	0.0023	$\sigma_{\varepsilon}^{2}+3\sigma_{SM}^{2}$	----	
$LM_{k\ell}$	2	0.0002	$\sigma_{\varepsilon}^{2}+\sigma_{SLM}^{2}+28\phi$ (KL)	0.22	3.19
$C'LM_{ik\ell}$	2	0.0001	$\sigma_{\varepsilon}^{2}+\sigma_{SLM}^{2}+14\phi$ (C'LM)	0.11	3.19
$SLM_{(i)jk\ell}$	52	0.0009	$\sigma_{\varepsilon}^{2}+\sigma_{SLM}^{2}$	----	
$\varepsilon_{(ijk\ell)}$	0	------	σ_{ε}^{2}	----	

*Significant at $\alpha = 0.05$.

Table 59. Variation of Pavement Dynamic Deflection and Surface Curvature Index with Condition of Test Sections and Distance from the Pavement Edge

	Test Sections		Distance From Pavement Edge(ft)**			Test Position	
Variable	With Failures*	Without Failures*	1.0	3.5	6.0	Crack	Midspan
Average Pavement Dynamic Deflection (10^{-3} in.)	0.66	0.69	0.79	0.63	0.61	0.68	0.67
Average Surface Curvature Index, SCI (10^{-3} in.)	0.051	0.047	0.060	0.045	0.043	0.053	0.046

* Average of test data from 14 test sections.

**Average of test data from 28 test sections.

Note: Data from structurally sound test locations.

$i = 1, 2$

$j = 1, \ldots 14$ for $i = 1$ (Test sections are nested within pavement condition)
$15, \ldots 28$ for $i = 2$

$k = 1, \ldots 10$ for $j = 1$ (Test intervals are nested within test sections)
$11, \ldots 20$ for $j = 2$
.
.
.
.
$271, \ldots 280$ for $j = 28$

$\ell = 1, 2$

where $Y_{ijk\ell}$ = deflection measurement in milli-inches made at the ℓ^{th} test position at the k^{th} interval along the j^{th} test section within i^{th} condition group.

$I_{(ij)k}$ = true effect of the k^{th} interval (random) along the j^{th} test section within i^{th} condition group, NID $(0, \sigma_I^2)$.

$IM_{(ij)k\ell}$ = true effect of the interaction of test interval with test position, NID $(0, \sigma_{IM}^2)$.

$\omega_{(ijk)}$ = second restriction error, NID $(0, \sigma_\omega^2)$.

and all other terms are as defined in Equation 45.

As would be evident, the experimental design associated with section-wide deflection measurements was poorly conceived, as most effects cannot be tested due to restriction errors.

The major interest in the analysis of deflection measurements, taken over the total extent of each test section at 100 ft. intervals, was to determine if pavement condition, as indicated by the presence or absence of failures, could be differentiated by such section-wide measurements.

The results of the analysis of variance are shown in Table 60. The only factors found to be significant were:

Table 60. ANOVA Summary - Dynamic Pavement Deflection (10^{-3} in.) at 100 ft. Intervals Along Test Sections

Source of Variation	DF	Mean Square	Expected Mean Square	F	$F_{.05,crit.}$
C'_i (Condition)	1	0.1495	$\sigma_\varepsilon^2+2\sigma_\omega^2+2\sigma_j^2+20\sigma_\delta^2+20\sigma_s^2+280\phi$ (C')	0.24	4.23
$S_{(i)j}$ (Test Sections)	26	0.6211	$\sigma_\varepsilon^2+2\sigma_\omega^2+2\sigma_I^2+20\sigma_\delta^2+20\sigma_s^2$	----	----
$\delta_{(ij)}$	0	------	$\sigma_\varepsilon^2+2\sigma_\omega^2+2\sigma_I^2+20\sigma_\delta^2$	----	----
$I_{(ij)k}$ (Test Intervals)	52	0.0118	$\sigma_\varepsilon^2+2\sigma_\omega^2+2\sigma_I^2$	----	----
$\omega_{(ijk)}$	0	------	$\sigma_\varepsilon^2+2\sigma_\omega^2$	----	----
M_ℓ (Test Positions)	1	0.1601	$\sigma_\varepsilon^2+\sigma_{IM}^2+10\sigma_{SM}^2+280\phi$ (M)	50.03*	4.23
$C'M_{i\ell}$	1	0.0006	$\sigma_\varepsilon^2+\sigma_{IM}^2+10\sigma_{SM}^2+140\phi$ (C'M)	0.19	4.23
$SM_{(i)j\ell}$	26	0.0032	$\sigma_\varepsilon^2+\sigma_{IM}^2+10\sigma_{SM}^2$	1.68*	1.50
$IM_{(ij)k\ell}$	252	0.0019	$\sigma_\varepsilon^2+\sigma_{IM}^2$	----	----
$\varepsilon_{(ijk\ell)}$	0	------	σ_ε^2		

*Significant at $\alpha = 0.05$.

1. The effect of test position, with the indication that the average deflection at crack positions (0.66 milli-inch) was significantly different from the average deflection at midspan positions (0.63 milli-inch). Though statistically significant, this difference is inconsequential from a practical viewpoint.

2. The interaction effect of test sections with test positions.

The results also showed that section-wide pavement deflections were not a good indicator of the pavement condition dichotomy used in this analysis (i.e. sections with failures vs. sections without failures). Since this did not appear reasonable, deflection profiles of selected pavement test sections were graphically analyzed to determine why pavement condition, as defined in the analysis of variance (Equation 44) did not explain the variation in pavement deflection.

Figure 37 shows the deflection profiles developed from deflection measurements made at 100 ft. intervals on three test sections with gravel subbases. The values shown are the average of crack and midspan deflections, measured 6.0 ft. from the pavement edge. Profiles No. 1 and No. 2 apply to two test sections, separated by the median strip, on Construction Contract R-7677, Interstate Highway I-65. At the time of the field study, the test section with deflection profile No. 2 had four concrete patches and four breakups and substantial edge pumping was indicated over the section. The test section on the opposite lanes, illustrated by deflection Profile No. 1 had no breakups, patches or any other indication of significant distress, although extensive edge pumping was observed. Yet the deflection Profile No. 1 exhibits higher overall deflections than the Profile No. 2. This is explained with reference to the Profile No. 3, obtained at a test section on Contract R-7913 (I-65). This latter contract has been completely free of distress inspite of having been under traffic since 1970. Deflection Profile

NOTES

CURVE NO.	HWY.	CONTRACT	STATIONS
①	I-65	R-7677	976+00 - 985+00 EBL
②	I-65	R-7677	976+00 - 985+00-NBL
③	I-65	R-7913	731+00 - 760+00 SBL

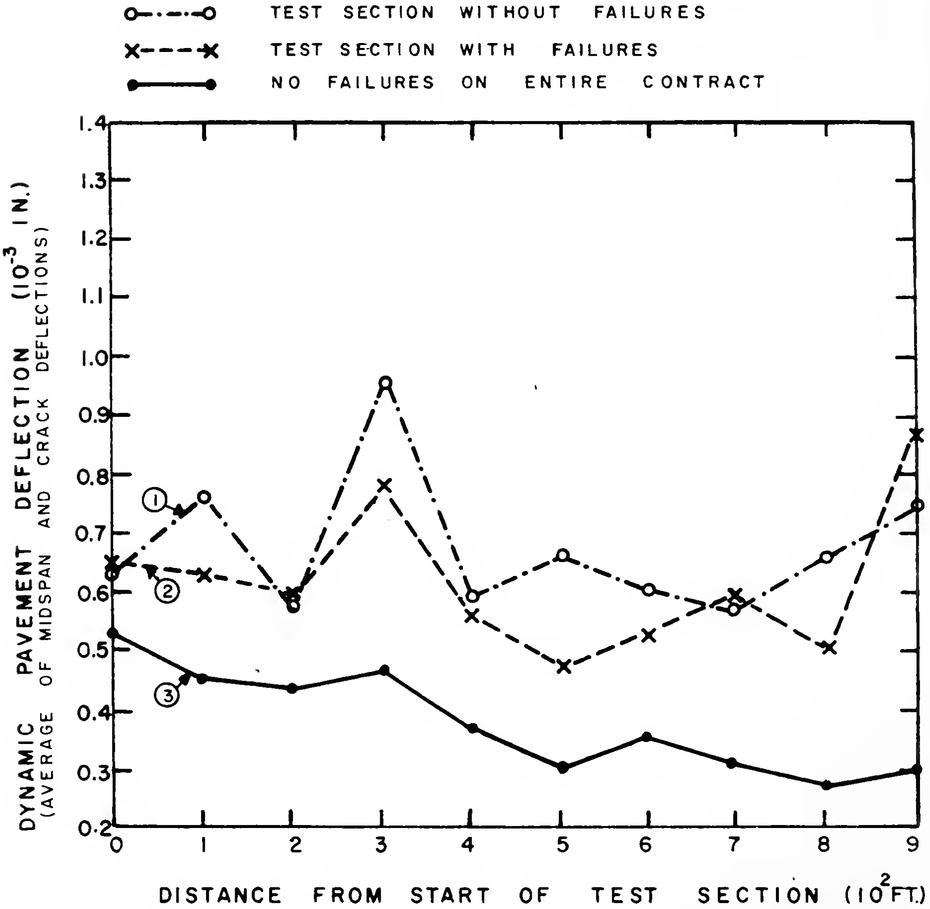

FIG.37 DEFLECTION PROFILES OF TEST SECTIONS WITH GRAVEL SUBBASE.

No. 3 represents excellent pavement condition as indicated by deflections of a relatively small magnitude (less than 0.50 milli-inch). This should be the deflection pattern of a pavement giving good performance. The deflection pattern given by Profile No. 1 signifies potential trouble, although no physical distress was indicated at the time of the field study. The high deflections reflect loss of support caused by the erosive action of pavement pumping. Under the action of repeated loads, it is only a matter of time before distress will be manifested in the form of breakups. Recently, this test section has experienced some breakup. The next stage in the cycle is extensive pavement distress. At this point, the discrete segments of the broken continuous slab tend to conform to the shape of the pumped subbase that had developed voids earlier. This settlement of the pavement slab can be observed by visual inspection of failed locations. The deflections observed at this stage are smaller than those before the breakup because now the slab is again in contact with the subbase and has regained some of the lost support. This is the condition shown in Profile No. 2. This analysis shows that low deflections are synonymous with good pavement condition as long as there are no apparent distress manifestations such as breakups, spalled cracks, and pumping. It is interesting to note that at 400 ft. from the start of test sections on Contract R-7677 (Profiles 1 and 2) very high deflections were measured on both sets of lanes. This reveals either a localized drainage problem across the right of way and/or an unstable condition in the subgrade.

Similar deflection profiles were drawn for test sections with other subbase types. The trend of lower deflections at sections without failures was also indicated for crushed stone and bituminous stabilized subbase (see Figures 38 and 39, respectively). This relationship was significantly pronounced for sections with the crushed stone subbase. The

NOTES

CURVE NO.	HWY.	CONTRACT	STATIONS
①	I - 94	R-8476	1788+00- 1797+00 EBL
②	I - 65	R-7634	699+00-708+00 NBL

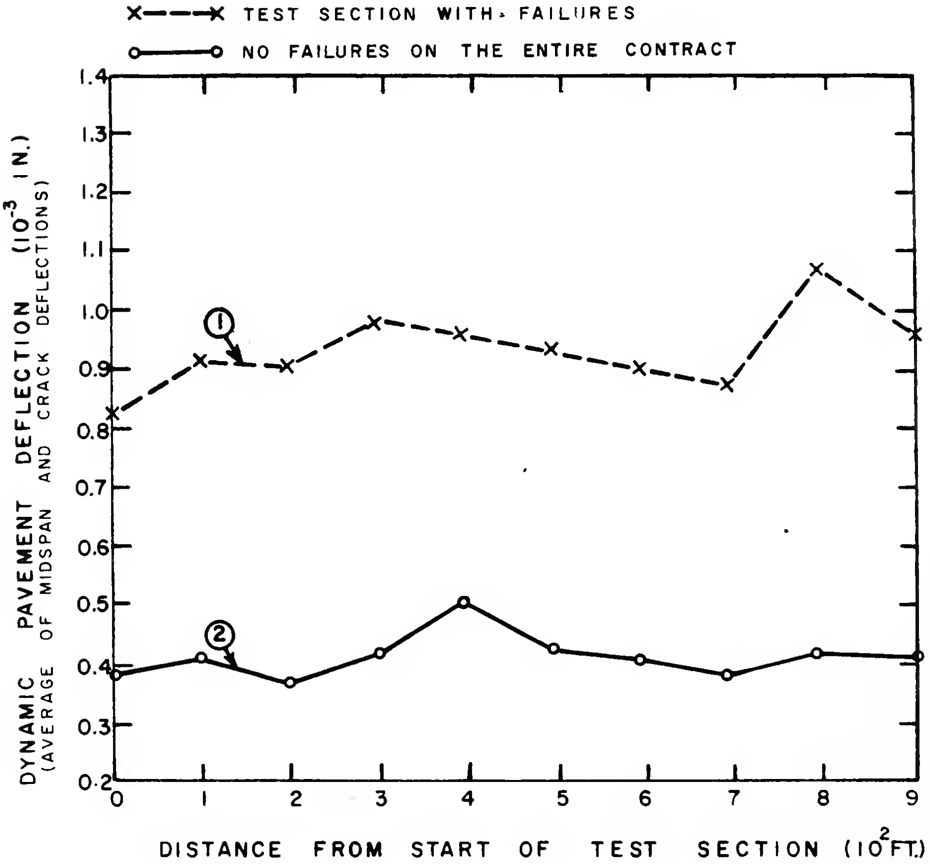

FIG. 38 DEFLECTION PROFILES OF TEST SECTIONS WITH CRUSHED STONE SUBBASE

NOTES

CURVE NO.	HWY.	CONTRACT	STATIONS
①	I-65	R-8232	203+00 - 212+00 NBL
②	I-65	R-8440	1318+00 - 1328+00 NBL

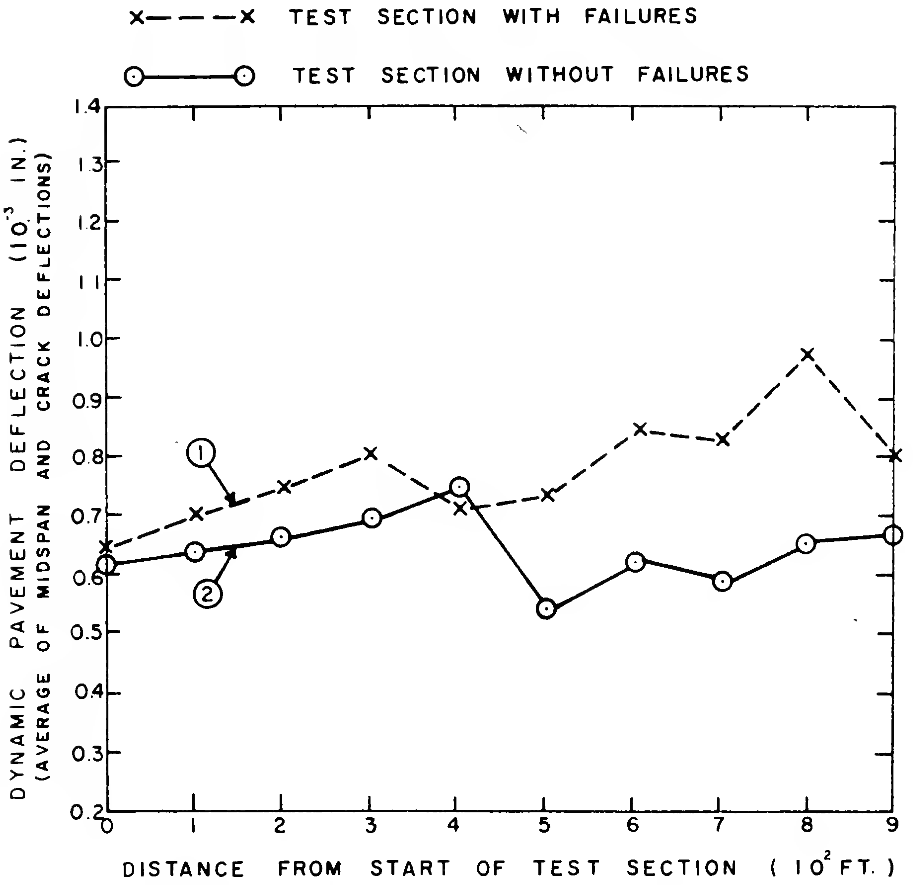

FIG.39 DEFLECTION PROFILES OF TEST SECTIONS WITH BITUMINOUS-STABILIZED SUBBASE

trend was not so strong in case of the bituminous stabilized subbase. Pavement deflection profiles obtained at test sections with slag subbase (see Figure 40) showed substantial variation from the trend for other subbase types. In Figure 40 the deflection Profile No. 2 for the section with a failure plotted considerably lower than Profile No. 1 for a section that had no failures. The deflections noted at another good section (Profile No. 3) were about the same as the pattern for the section with a failed location (Profile No. 2). It is quite possible that the observed failure was due to isolated pavement problems at the failed location rather than any section-wide deficiency in the subbase. There is indication that this was the case (cf. comparisons of failed test locations with good test locations).

An important deduction resulting from this analysis is that pavement deflections vary considerably with subbase type. For good pavement condition, lower pavement deflections were noted at sections with gravel and crushed stone subbase than for sections with slag and bituminous stabilized subbase. This may imply that allowable deflections are comparatively higher for bituminous-stabilized or slag subbases than for gravel or crushed stone subbases.

It becomes clear that pavement deflections are symptomatic rather than causative as far as CRC pavement performance is concerned. Any evaluation of CRCP, based on deflection measurements should be done with care and rigor as many extraneous factors affect deflections. Insofar as performance is concerned good pavement condition is assured where deflections, as measured by the Dynaflect, are less than 0.50 milli-inch. Deflections in the range of 0.60-0.90 milli-inch indicate a potential distress condition, whereas, values above 1.00 milli-inch reflect severe distress and high probability of breakups. These criteria apply to CRCP with 9-in. slab thickness, deflections measured at 6.0 ft. from the pavement edge. Development of

NOTES

CURVE NO.	HWY.	CONTRACT	STATIONS
①	I-94	R-8553	255+00 - 264+00 EBL
②	I-94	R-7883	1486+00 -1495+00 WBL
③	I-94	R-7525	983+00 - 992+00 EBL

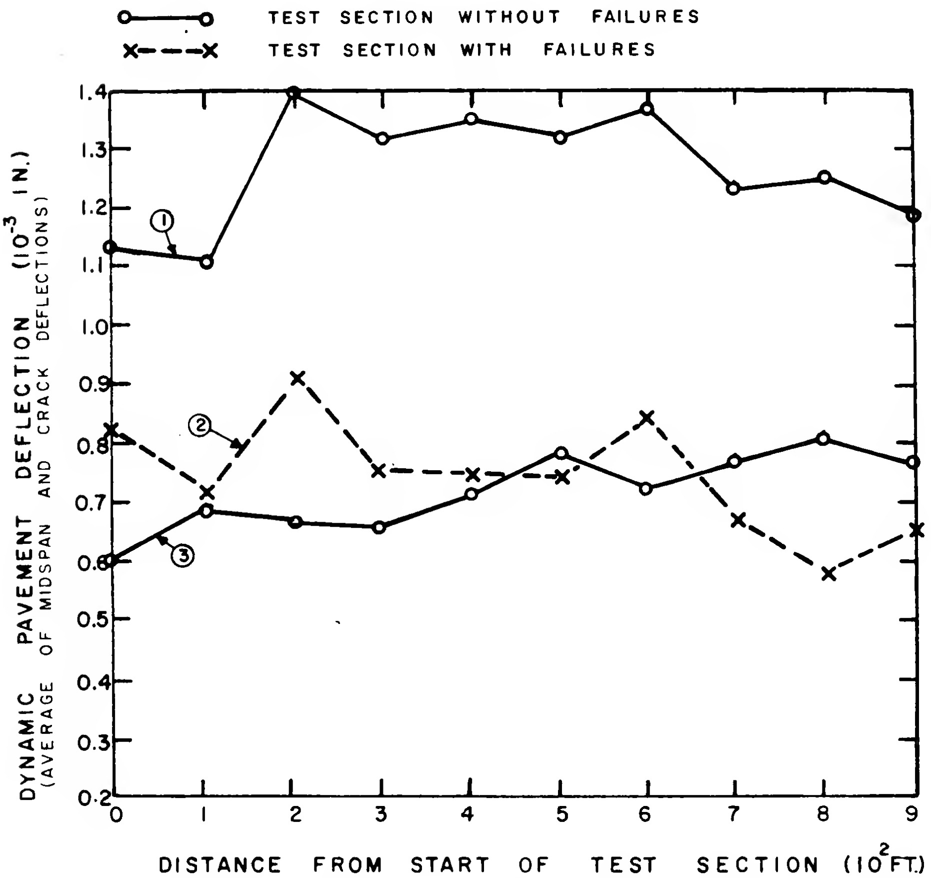

FIG.40 DEFLECTION PROFILES OF TEST SECTIONS WITH SLAG SUBBASE.

expected ranges of deflection values for various subbase types was beyond the scope of this study as sufficient test sections with slag, crushed stone,and bituminous stabilized subbases were not available.

Surface Curvature Index

Surface curvature index (SCI) data obtained at good test locations were analyzed by using the ANOVA model given in Equation 44. The analysis results, presented in Table 61 revealed:

1. A significant variation in SCI values across the pavement slab.
2. A significant interaction between condition of test section and test positions relative to the variation in SCI data.
3. No difference in SCI values with respect to section condition or test position.

Mean values corresponding to these trends are given in Table 59. Though the average SCI at 1.0 ft. from the pavement edge was significantly larger than the average SCI at the center-line of the traffic lane, this difference compared to the SCI noted at failed test locations (see Figure 34) was relatively small. This trend was independent of the effect of pavement condition as no significant interaction between pavement condition and transverse positions was detected in the analysis. Nevertheless, SCI values at the pavement edge were higher and represent decreased pavement stiffness at the edge.

The interaction between pavement condition and test positions requires further evaluation. Table 62 shows the mean values associated with this interaction effect.

It would be seen that the difference in SCI between crack and mid-span positions at sections with failures was 0.0159 milli-in. whereas at sections without failures, a

Table 61. ANOVA Summary - Surface Curvature Index (milli-inches)

Source of Variation	DF	Mean Square	Expected Mean Square	F	$F_{.05,\ crit.}$
C'_i (Condition)	1	0.0005	$\sigma_\epsilon^2+2\sigma_\omega^2+6\sigma_\delta^2+6\sigma_s^2+84\phi(C')$	0.56	4.23
$S_{(i)j}$ (Sections)	26	0.0009	$\sigma_\epsilon^2+2\sigma_\omega^2+6\sigma_\delta^2+6\sigma_s^2$	----	----
$\delta_{(ij)}$	0	------	$\sigma_\epsilon^2+2\sigma_\omega^2+6\sigma_\delta^2$	----	----
L_k (Transverse Position)	2	0.0047	$\sigma_\epsilon^2+2\sigma_\omega^2+2\sigma_{sL}^2+56\phi(L)$	9.40*	3.19
$C'L_{ik}$	2	0.0008	$\sigma_\epsilon^2+2\sigma_\omega^2+2\sigma_{sL}^2+28\phi(C'L)$	1.60	3.19
$SL_{(i)jk}$	52	0.0005	$\sigma_\epsilon^2+2\sigma_\omega^2+2\sigma_{sL}^2$	----	----
$\omega(ijk)$	0	------	$\sigma_\epsilon^2+2\sigma_\omega^2$	----	----
M_ℓ (Test Position)	1	0.0017	$\sigma_\epsilon^2+3\sigma_{sM}^2+84\phi(M)$	2.83	4.23
$C'M_{i\ell}$	1	0.0038	$\sigma_\epsilon^2+3\sigma_{sM}^2+42\phi(C'M)$	6.33*	4.23
$SM_{(i)j\ell}$	26	0.0006	$\sigma_\epsilon^2+3\sigma_{sM}^2$	-----	----
$LM_{k\ell}$	2	0.0005	$\sigma_\epsilon^2+\sigma_{sLM}^2+28\phi(LM)$	1.25	3.19

Table 61. Continued.

Source of Variation	DF	Mean Square	Expected Mean Square	F	$F_{.05,\ crit.}$
$C'LM_{ik\ell}$	2	0.0009	$\sigma^2_\varepsilon+\sigma^2_{sLM}+14\phi(C'LM)$	2.25	3.19
$SLM_{(i)jk\ell}$	52	0.0004	$\sigma^2_\varepsilon+\sigma^2_{sLM}$	----	
$\varepsilon_{(ijk\ell)}$	0	------	σ^2_ε		

*Significant at $\alpha = 0.05$.

Table 62. The Effect of the Interaction of Test Section Condition with Test Position (Crack vs. Mid-span) on Pavement Surface Curvature Index

Test Sections	Test Position	Mean Surface Curvature Index, SCI (10^{-3} in.)*	
With Failures	Crack	0.0590	Difference = 0.0159
	Mid-span	0.0431	
Without Failures	Crack	0.0462	Difference = 0.0031
	Mid-span	0.0493	

*Average of data from structurally sound locations at 14 test sections.

considerably smaller difference of only 0.0031 milli-in. was indicated. The higher difference at sections with failures points to lower pavement stiffness resulting from wider crack widths and inferior granular interlock at the crack faces on such sections. This result is quite important as it brings to light a deficient element in the pavement even when no specific distress condition was indicated at the test location. It should be noted that SCI values, reported in this section ,were obtained from structurally sound locations.

Crack Width, Spacing, and Intersections

Variables relating to pavement cracking were analyzed by the t-test. The results are presented in Table 63. Mean crack width at sections without failures (.0087 in.) was found to be significantly smaller than the average crack width (0.0127 in.) measured at sections with failures. No difference in crack spacing variables and number of crack intersections per 100 ft. length of pavement was indicated between the sections falling in the two condition categories.

Analysis of Temperature Variables

The temperature variables of interest were maximum air temperature on the day of paving, the minimum air temperature the following day, the drop in air temperature during the 24 hours after paving (difference of the previous two values), the maximum drop in air temperature (difference between maximum air temperature at the time of paving and the subsequent minimum temperature up to the time of the detailed field evaluation study).

The above temperature variables for each test section were estimated from the climatological data recorded at the nearest meterological station and published by the National Oceanic and Atmospheric Administration (45).

Table 63. Summary of Results of T-Test on Pavement Cracking Parameters***

Null Hypothesis, H_o: $\mu_1 = \mu_2$

Variable	Condition of Test Section	No. of Test Sections	Mean	Std. Error	Alternate Hypothesis (H_1)	$t_{calc.}$	$t_{crit.}$ ($\alpha = 0.05$)
Crack Width (in.)	With Failures, μ_1	16	0.0127	0.0013	$\mu_1 > \mu_2$	1.72* (29)	1.70
	Without Failures, μ_2	15	0.0087	0.0016			
Crack Spacing							
Mean (ft)	With Failures, μ_1	16	5.97	0.458	$\mu_1 \neq \mu_2$	1.07 (29)	± 2.04
	Without Failures, μ_2	15	5.34	0.349			
Variance (ft^2)	With Failures, μ_1	16	5.96	0.669	$\mu_1 \neq \mu_2$	-0.82** (18.17)	± 2.10
	Without Failures, μ_2	15	7.48	1.719			
Crack Intersec. per 100ft. Pavement Length	With Failures, μ_1	16	2.2	0.61	$\mu_1 \neq \mu_2$	-0.75 (29)	± 2.04
	Without Failures, μ_2	15	3.1	1.01			

* Significant at $\alpha = 0.05$; reject null hypothesis.

**T-test based on separate variance estimate.

***Data from structurally sound test locations.

Note: Numbers in parentheses are degrees of freedom associated with T-test.

Temperatures at the surface of the pavement slab, corresponding to the above air temperature variables were estimated from the slab temperature models given in Appendix E.

The results of a t-test on the temperature variables showed no significant difference between the mean values obtained at sections with failures as compared to the values for sections without failures.

A summary of average values is given in Table 64 while a detailed breakdown of temperature variables is tabulated in Appendix C.

An examination of these data indicates that maximum air temperature drops experienced on CRCP test sections up to the time of the field study averaged about 100°F, the largest estimated drop being 111°F. The corresponding largest drop in slab temperature was estimated by the equations given in Appendix E to be 117°F.

Maximum air temperature at the time of paving approximately ranged between 50°and 92°F, while the temperature drop during the 24 hours after paving was estimated between 15°and 35°F. This corresponded to a 24-hour drop of 26-40°F in the slab temperature.

The effect of temperature on steel requirements for CRCP is evaluated in a later section of the study.

Traffic Analysis

Cumulative 18 kip, single-axle load repetitions for each test section were estimated by the procedures developed for the analysis of CRCP statewide condition survey data. After transforming the estimated cumulative load repetitions so obtained to a common log base, the data were analyzed by a t-test. The results of this test showed no significant difference in load applications at sections with failures compared to sections without failures. This was not unexpected as most test sections used in the detailed field study

Table 64. Summary of Average Values of Temperature Variables and Cumulative Load Applications

Condition of Test Sections	No. of Test Sections	Average Air Temperature			Average Estimated Slab Temperature			ΣL (millions)
		Max.*	24-Hr.** Drop	Max.*** Drop	Max.*	24-Hr.** Drop	Max.*** Drop	
With Failures	16	78.6	22.7	99.6	100.1	29.5	102.8	1.34
		(1.96)	(0.85)	(1.82)	(2.84)	(0.65)	(2.70)	(0.15)
Without Failures	15	76.8	24.0	96.0	96.6	29.6	98.4	1.10
		(2.79)	(1.29)	(2.58)	(3.43)	(1.15)	(3.18)	(0.23)

* Estimated maximum temperature at time of paving.

** Temperature drop during 24-hours after paving.

***Maximum temperature drop from the temperature at time of paving to a subsequent minimum upto the time of detailed field study.

Note: 1. L = equivalent 18-kip, single-axle application.

2. Figures in parentheses are standard errors of the means to which they are appended.

had similar traffic characteristics. The average traffic applications at sections with failures were slightly higher than at sections with no distress (see Table 64). Detailed estimates of the cumulative 18 kip, load applications are tabulated in Appendix C.

Summary of Results

The comparison of test sections with failures as opposed to sections without failures, relative to material properties and performance characteristics evaluated at structurally sound test locations, resulted in a number of significant results. Similarly the evaluation of section-wide pavement characteristics also established some significant trends. These findings have brought to light inherent deficiencies in the pavement structure that eventually lead to distress.

The following is a summary of the significant results:

Subgrade Properties: The only significant result in the analysis of subgrade properties showed that subgrade soils at sections without failures were relatively more coarse grained and sandy than sections where failures had occurred. It is possible that sandy subgrades help in the internal drainage of the pavement structure, thereby reducing the incidence of pavement distress. Generally, subgrades were found to be poorly compacted, irrespective of the condition of the test sections. Unstable subgrades, especially when they are fine-grained, can be a source of potential problems as regards CRCP performance.

Subbase Properties: This analysis clarified the reasons for the better performance of certain subbase types. Crushed stone subbase at the section without failures was found to possess a high strength (CBR of 90 percent) and excellent internal drainage (over 2000 ft/day). The failure on another section with a crushed stone subbase was a function of poor stability (very low CBR), resulting from inadequate compaction.

The good condition of pavements on slag subbases was due to the very high stability (CBR of over 100 percent) of this subbase. The failure that was encountered on a section with slag subbase was caused by isolated distress conditions. At structurally sound locations, gravel subbases were found to have a moderately high permeability but showed poor stability characteristics, probably a function of insufficient compaction.

There are ample indications that pavement condition is influenced by an interaction of the stability and permeability characteristics of the subbase. For good CRCP performance, the subbase should be compacted to a minimum of 100 percent standard AASHO density; it should have high stability (a CBR of 90-100 percent); and it should be well draining (a minimum k of 1000 ft/day).

Conditions that are primarily responsible for poor performance of granular subbases are poor compaction at the time of construction and use of densely graded aggregate mixtures that have very low permeability.

As regards bituminous stabilized subbases, there was some evidence that the poor performance of this type of subbase at one test section could be attributed to the presence of a relatively large amount of asphalt binder and filler material (minus No. 200 fraction), in excess of the specified values. The stability of the bituminous stabilized subbases, as measured by the High Load Penetrometer, was low. The CBR values were in the same range as those obtained for gravel subbases.

Concrete Properties: It was shown that sections showing no failures were paved with a higher slump concrete. This result further substantiated a similar conclusion obtained from the analysis of statewide condition survey data.

The results of data analysis further indicated that the modulus of elasticity of concrete had a significant bearing on pavement condition. Concrete cores obtained from sections without any distress were tested to have an average dynamic modulus of elasticity of 6.15 million psi whereas cores, obtained from good locations on sections that had failures, had an average dynamic modulus of 4.97 million psi. The difference of a million psi in the dynamic moduli of elasticity of concrete is quite significant. This clearly indicates that poor performance of CRCP is to a large degree a function of deficiencies in the pavement structure caused by the use of relatively poor quality material. To ensure good performance, the paving concrete should be designed to have a high modulus of elasticity. No difference in splitting tensile strength was evident between poorly and adequately performing test sections.

Dynamic Pavement Deflection and Surface Curvature Index (SCI): Dynamic pavement deflections were shown to be a good indicator of pavement condition if used judiciously. Once the continuous slab breaks up into discrete segments, the usefulness of deflections measurements is impaired. As expected at good test locations, no difference in dynamic deflections and SCI was observed between sections with failures and sections without failures. Higher deflection and SCI values were noted at the pavement edge than at more interior locations irrespective of the pavement condition. The observed differences were negligible compared to the deflections and SCI values noted at failed test locations. These results indicate that a significant loss in pavement stiffness occurs only with the initiation of severe distress.

An evaluation of section-wide deflection measurements taken at 6.0 ft. from the pavement edge showed that for 9-in. CRCP, dynamic deflections less than 0.5 milli-inch, as measured by Dynaflect, are indicators of good pavement condition. Deflections in the range of 0.6-0.9 milli-inch spell a potential distress condition while values above 1.0 milli-inch are indicators of severe distress with a high probability of pavement breakup. These deflection measurements also indicated differences among subbase types. It was noted that deflections measured on sections with slag and bituminous stabilized subbases were higher than the deflections evaluated on sections with gravel and crushed stone subbases. This result applies only to sections that had no failures.

An important observation resulted from the analysis of SCI data. It was found that even at structurally sound test locations the difference in SCI values between crack and midspan positions was significantly higher at sections with failures than at sections without distress. This result points to a relative loss in granular interlock (associated with wider crack widths) and a resultant decrease in pavement stiffness at sections with failures, even at locations with no evidence of distress (presence of failures). It should be borne in mind that the deflection measurements were made in the warmer part of the year (May-June), and do not reflect the most critical pavement condition.

Crack Width: It was noted that crack widths observed at test sections with failures were significantly wider than those measured at good test sections, even though crack widths at only structurally intact locations were measured. The average crack width at good sections was 0.0087 in.

Crack Spacing: No difference in either the mean crack spacing or the variance of crack intervals was observed between sections falling in the two categories. Likewise the number of crack intersections at good locations in either type of test sections was essentially the same.

This result reveals that measures of crack spacing are useful as an indicator of pavement condition only where the pavement is already experiencing severe distress as manifested in some form of failure.

EVALUATION OF CONSTRUCTION VARIABLES AND STEEL REINFORCEMENT REQUIREMENTS

The results of the statewide condition survey revealed a significant relationship between construction variables and pavement condition. In the detailed field study, the effect of construction techniques on material properties and pavement response functions, such as crack width and crack spacing, was further explored. The construction variables of interest were the methods of paving, fabrication of steel reinforcement ,and placement of steel. A detailed stratification of test sections by construction type is given in Table C2, Appendix C. A study of the effect of construction variables on properties of concrete and pavement cracking parameters is presented in this chapter. In addition, the minimum steel requirements for CRCP, commensurate with Indiana conditions and using the concrete and temperature data presented previously, are also analyzed.

Effect of Construction Variables on Properties of Concrete

The properties of concrete evaluated in this analysis were the dynamic modulus of elasticity and tensile strength of concrete. Bulk density data could not be analyzed as the source and type of aggregate used in the concrete were not known. Since sufficient data were not available to permit the development of a complete factorial arrangement, only data from slipformed test sections were included in the study. This permitted the use of a nested factorial design with unequal number of test sections within various combinations of methods of steel fabrication and placement of steel.

The ANOVA model associated with the nested factorial design is given by:

$$Y_{ijk} = \mu + B_i + C_j + BC_{ij} + S_{(ij)k} + \delta_{(ijk)} + T_\ell + BT_{i\ell} + CT_{j\ell} + BCT_{ij\ell} + ST_{(ij)k\ell} + \epsilon_{(ijk\ell)} \qquad (47)$$

$i = 1, 2$

$j = 1, 2, 3$

$k = 1 \ldots n_{ij}$ (Unequal number of test sections within ij^{th} cell.

$\ell = 1, 2$

where $Y_{ijk\ell}$ = concrete test value obtained by testing the ℓ^{th} concrete core segment taken from a good test location in the k^{th} test section with j^{th} type of steel placed by the i^{th} method.

μ = overall true mean effect.

B_i = true effect of the i^{th} method of steel placement (chairs vs. depressor)

C_j = true effect of the j^{th} type of steel (loose bars vs. bar mats vs. wire fabric)

$S_{(ij)k}$ = true effect of the k^{th} test section nested within the combination of j^{th} st steel and i^{th} method of placement, NID $(0, \sigma_s^2)$.

$\delta_{(ijk)}$ = restriction error, NID $(0, \sigma_\delta^2)$ caused by completing the pavement coring operation at one test section before proceeding to the next.

T_ℓ = true effect of the ℓ^{th} core segment.

$\epsilon_{(ijk\ell)}$ = within error, NID $(0, \sigma_\epsilon^2)$.

and other terms are the interaction effects between the factors B_i, C_j, $S_{(ij)k}$ and T_ℓ. $ST_{(ij)k\ell}$ is assumed to be random, NID $(0, \sigma^2_{ST})$ while other interaction effects are fixed.

Estimates for the various effects were obtained by a least squares analysis of variance procedure. NBMD5V, a computer program at the Purdue University Computer Center was used for this purpose. The analysis was performed in two steps according to the following models:

$$Y_{ijk} = \mu + B_i + C_j + BC_{ij} + T_\ell + BT_{i\ell} + CT_{j\ell} + BCT_{ij\ell} + \varepsilon'_{(ij\ell)k} \tag{48}$$

$$Y_{ijk} = \mu + B_i + C_j + BC_{ij} + S_{(ij)k} \tag{49}$$

where $\varepsilon'_{(ij\ell)k}$ = within error NID $(0, \sigma^2_{\varepsilon'})$ and is approximately equivalent to $(S_{(ij)k} + ST_{(ij)k\ell})$.

and other terms are as defined in Equation 47.

Results obtained by the use of Equations 48 and 49 were combined to give analysis of variance results, approximately conforming to the ANOVA model given by Equation 47.

The ANOVA results for dynamic modulus of elasticity data in Tables 65 and 66 show that:

1. The method of steel placement had a significant effect on the dynamic modulus of elasticity. Concrete cores, obtained from pavement sections where the steel reinforcement was depressed into the plastic concrete, were found to have a significantly higher average modulus of elasticity (5.83 million psi) than concrete cores obtained from sections where reinforcement was pre-set on chairs, average modulus of elasticity being 5.13 million psi for the latter sections.

Table 65. Least Squares Analysis of Variance - Dynamic Modulus of Elasticity of Concrete (10^6 psi)

Source of Variation	DF	Sum of Squares	Mean Square	F	$F_{.05,crit.}$	DF for F-test
B_i (Placement)	1	3.830	3.830	5.81*	4.54	(1, 15)
C_j (Steel)	2	0.187	0.093	0.14	3.68	(2, 15)
BC_{ij}	2	1.963	0.981	1.49	3.68	(2, 15)
$S_{(ij)k}$	15	9.887	0.659	----	----	-------
$\delta_{(ijk)}$	0	-----	-----	----	----	-------
T_ℓ (Core Segments)	1	1.153	1.153	2.10	4.54	(1, 15)
$BT_{i\ell}$	1	3.919	3.919	7.76*	4.54	(1,15)
$CT_{j\ell}$	2	0.692	0.346	0.69	3.68	(2, 15)
$BCT_{ij\ell}$	2	0.552	0.276	0.50	3.68	(2, 15)
$ST_{(ij)k\ell}$	15	8.253	0.550	----	----	-------
$\varepsilon_{(ijk\ell)}$	0	-----	-----			
Total	41	30.435				

*Significant at $\alpha = 0.05$.

Table 66. Variation of Concrete Dynamic Modulus of Elasticity with Method of Steel Placement and Position Relative to the Steel Reinforcement

Steel Placement	Position of Core Segment	Mean Dynamic Modulus of Elasticity (10^6 psi)	
Chairs	Above Reinforcement	4.90 (14)*	5.13 (28)**
	Below Reinforcement	5.36 (14)	
Depressor	Above Reinforcement	6.28 (7)	5.83 (14)**
	Below Reinforcement	5.37 (7)	

* Numbers in parentheses are the number of test values on which the mean is based.

**Mean value for method of steel placement.

Note: Data from structurally intact test locations.

2. Modulus of elasticity of concrete was also found to be a function of the interaction of the method of placement with the position of the core segment relative to the steel reinforcement. This relationship is further elaborated in Table 66. It can be seen from these data, that the core segments taken from below the steel reinforcement had essentially similar elasticity properties (E'_c = 5.36 million psi) irrespective of the method of steel placement. A striking difference emerges in the core segments taken from above the steel reinforcement. It was found that concrete above the steel reinforcement had a significantly higher modulus of elasticity when the steel reinforcement was depressed as compared to pre-set steel on chairs. This can be attributed to the fact that depressed steel is vibrated into the concrete from the top. The average modulus of elasticity values for the two methods of steel placement in this case were 6.28 million and 4.90 million psi respectively.

The results of a similar analysis on splitting tensile strength (see Tables 67 and 68) revealed that:

1. The method of fabrication of the steel reinforcement influenced the tensile strength of the concrete. It was found that concrete cores obtained from sections where loose bars were used had a lower tensile strength than the cores taken from sections where bar mats or wire fabric were used. Concrete cores from sections with wire fabric were found to have the highest splitting tensile strength.

2. Tensile strength of concrete was also shown to be influenced by the interaction of steel type with the method of placement. This relationship, shown in Table 68, is particularly evident in the case of loose bars and wire fabric. For loose bars, lower tensile strength was indicated where a depressor was employed to place the steel reinforcement, as compared to steel placement with chairs.

Table 67. Least Squares Analysis of Variance - Splitting Tensile Strength of Concrete (psi)

Source of Variation	DF	Sum of Squares	Mean Square	F	$F_{.05,crit.}$	DF for F-test
B_i (Placement)	1	1273.1	1273.1	0.36	4.54	(1, 15)
C_j (Steel)	2	66674.5	33337.3	9.33*	3.68	(2, 15)
BC_{ij}	2	50495.1	25247.6	7.06*	3.68	(2, 15)
$S_{(ij)k}$	15	53610.9	3574.1	----	----	-------
$\delta_{(ijk)}$	0	-------	-------	----	----	-------
T (Core Segments)	1	4548.0	4548.0	0.84	4.54	(1, 15)
$BT_{i\ell}$	1	134.1	134.1	0.02	4.54	(1, 15)
$CT_{j\ell}$	2	20690.0	10345.0	1.90	3.68	(2, 15)
$BCT_{j\ell}$	2	35599.3	17799.6	3.28	3.68	(2, 15)
$ST_{(ij)k\ell}$	15	81502.7	5433.5	----	----	
$\epsilon_{(ijk\ell)}$	0	-------	-------			
Total	41	314527.7				

*Significant at $\alpha = 0.05$.

Table 68. Variation of Concrete Splitting Tensile Strength with Type of Steel and Method of Steel Placement

Type of Steel	Method of Steel Placement	Mean Splitting Tensile Strength (psi)	
Loose Bars	Chairs	480 (6)*	447 (8)**
	Depressor	350 (2)	
Bar Mats	Chairs	481 (14)	483 (18)**
	Depressor	489 (4)	
Wire Fabric	Chairs	495 (8)	536 (18)**
	Depressor	578 (8)	

* Figures in parentheses are the number of test values on which the mean is based.

**Mean values for steel type.

Note: Data from structurally sound test locations.

In contrast, this trend is reversed for wire fabric, a lower tensile strength of concrete being indicated where the steel was placed on chairs. Tensile strength of cores from sections with bar mats was essentially the same, irrespective of the method of placement.

As splitting tensile strength of concrete, within the range obtained in this investigation, was not found to be a significant factor affecting the condition of CRCP, these results are primarily of analytical interest. It should, however, be noted that the low tensile strength values, associated with a section where depressed loose bars were used, are based on data from only one test section and should be viewed with caution.

The above results apply only to slipformed pavement and are based on tests of concrete cores obtained from structurally intact locations at 21 test sections. Only seven of these sections had depressed steel. Though the inference space for these results is limited, they offer an explanation for the better performance of pavements where the steel reinforcement was depressed into the concrete. The higher modulus of elasticity of concrete at sections with depressed steel could be attributed to the superior vibration of concrete achieved by this construction technique.

The effect of method of paving was analyzed by a stepwise multiple regression analysis using dummy variables (23) to define the qualitative construction variables (methods of paving, steel fabrication and placement,and their interactions). The coefficient of determination (R^2) associated with the significant variables in the regression was less than 0.40. The dummy variable defining the method of paving did not enter the regression even at an α-level of 0.25,showing that the method of paving had no significant effect on the properties of concrete.

Effect of Construction Variables on Pavement Cracking Parameters

The incidence of cracking in CRCP is a function of a complex interaction among variables relating to:

1. Properties of concrete and steel.
2. Temperature and other environmental factors.
3. Subbase characteristics.
4. Method of construction.
5. Traffic load applications.

The last three factors are possibly secondary in importance. Their effect on CRCP cracking has not been investigated comprehensively in past performance studies.

In view of the complex interaction among these variables it was not possible to isolate the effect of construction methods without reference to the other variables. Therefore, it was first postulated that CRCP cracking parameters are related to the variables listed above by the following conceptual model:

$$c_p = f\,(x_{1i},\ x_{2j},\ x_{3k}, x_{4\ell},\ x_{5m},\ x_{6p}) \qquad (50)$$

where c_p = pavement cracking parameter - crack width, crack spacing (mean and variance), number of crack intersections per 100 ft. length of pavement.

x_{1i} = properties of concrete $i = 1, \ldots .\ n_1$

x_{2j} = properties of steel $j = 1, \ldots .\ n_2$

x_{3k} = temperature variables $k = 1, \ldots .\ n_3$

$x_{4\ell}$ = subbase characteristics $\ell = 1, \ldots .\ n_4$

x_{5m} = construction variables $m = 1, \ldots .\ n_5$

x_{6p} = traffic variables $p = 1, \ldots .\ n_6$

n_a = number of levels of the independent factor, x

The next step was to test the various hypotheses underlying the conceptual model. This was accomplished by linear multiple regression analysis. A step-wise regression procedure was used with the aid of the SPSS Statistical Package (47) at the Purdue University Computer Center. For each pavement cracking parameter, a number of regression runs were made with different independent variables in order to build a regression model that would be structurally and statistically correct.

For the variables: crack width, crack intersections and mean crack spacing, the regression analysis did not yield fruitful results. The resultant regression equations had low coefficients of determination (R^2 in the range of 0.2 to 0.4 with 7-8 variables in the model). Of the variables included in the regression equation only 2-3 were statistically significant as tested by the sequential F-test.

Multiple regression analysis of data on crack spacing variance (V_c) gave more promising results. The regression model associated with the best equation, obtained from regression runs on several combinations of independent variables, is given as follows:

$$V_c = b_0 + b_1 TD + b_2 D1 + b_3 D2 + b_4 B + b_5 C1 + b_6 C2 + b_7 BC1 + b_8 BC2 + \qquad (51)$$

where V_c = crack spacing variance (ft^2), defined in Equation 41.

TD = estimated air temperature drop during the 24-hr. period following paving (^{o}F).

D1, D2, D3 = dummy variables to define effect of subbase type;

gravel subbase: D1 = -1, D2 = -1, D3 = -1

bituminous stabilized subbase: D1 = 1, D2 = 0, D3 = 0

crushed stone subbase: $D1 = 0$,
$D2 = 0$,
$D3 = 1$

slag subbase: $D1 = 0$, $D2 = 1$,
$D3 = 0$

(D3 did not enter the regression because the F-level was insufficient)

B = effect of method of steel placement;
pre-set on chairs: $B = -1$
depressed steel: $B = 1$

C1, C2 = dummy variables to define effect of steel reinforcement
bar mats: $C1 = -1$, $C2 = -1$
loose bars: $C1 = 1$, $C2 = 0$
wire fabric: $C1 = 0$, $C2 = 1$

B·C1, B·C2 = interaction effects of method of steel placement with steel type

ε = residual NID $(0, \sigma_\varepsilon^2)$

It was assumed:

1. The random errors are normally distributed with mean equal to zero.
2. The random errors are independent of the x's (independent variables) and have a constant variance (σ_ε^2).

Note: The dummy variables in the regression analysis signify contrasts between the levels of the qualitative independent variables, given as follows:

1. D1: contrast between gravel and bituminous stabilized subbases.
2. D2: contrast between gravel and slag subbases.
3. D3: contrast between gravel and crushed stone subbases.
4. B: contrast between pre-set steel on chairs and depressed steel.
5. C1: contrast between bar mats and loose bars.
6. C2: contrast between bar mats and wire fabric.

7. B.C1: interaction of contrasts B and C1.

8. B.C2: interaction of contrasts B and C2.

The last two interaction terms affect any inferences obtained from the contrasts B, C1, and C2, as these terms are not orthogonal and are correlated.

The use of dummy variables permitted the evaluation of differences between the levels of various construction variables relative to crack spacing variance. The ANOVA associated with the regression analysis is given in Table 69 while the statistical properties of the regression equation are shown in Table 70. An examination of these results reveals:

1. Crack variance was directly related to the drop in air temperature immediately after paving; the larger the temperature drop during the 24-hour period after paving (approximately the curing time), the greater the crack variance. This result gives credence to the observation that the crack patterns in CRCP are established at an early stage in the life of the pavement and this is partly a function of temperature and other environmental conditions at the time of paving.

2. Crack variance (that is, lack of uniformity in crack spacing) was also influenced by type of subbase. A consideration of the contrast D1 in Table 70, shows that crack spacing on pavements with a bituminous stabilized subbase was more irregular (higher variance) than on pavements with a gravel subbase. Similarly contrast D2 shows that pavements on slag subbase had a smaller variance in crack spacing than the pavements on gravel subbase. The contrast D3 was not significant (it did not enter the regression even at an α-level of 0.25) indicating that crack spacing on gravel and crushed stone subbases had similar variances. The effect of subbase type on crack spacing variance is demonstrated in Table 71.

Table 69. Analysis of Variance Associated with Linear Multiple Regression Analysis of Crack Spacing Variance

Source of Variation	DF	Sum of Squares	Mean Square	F
Regression	8	1278.10	159.76	13.58*
TD**	1	219.59	219.59	18.67*
D1	1	204.16	204.16	17.36*
D2	1	151.18	151.18	12.86*
B.C1	1	148.98	148.98	12.67*
B	1	180.05	180.05	15.31*
B.C2	1	147.90	147.90	12.58*
C1	1	156.23	156.23	13.29*
C2	1	69.61	98.82	5.92*
Residual	44	517.48	11.76	

*Significant at $\alpha = 0.05$ as tested by the sequential F-test.

**Variables are listed in the order they entered the step-wise regression.

Table 70. Summary of Step-wise Linear Multiple Regression Analysis - Crack Spacing Variance

Dependent Variable = V_c = crack spacing variance (ft^2)

Mean response = 7.94

Standard error (square root of residual mean square) = 3.43

No. of cases = 53

Coefficient of determination = R^2 = 0.71

Step Number	Variable Name	Regression Coefficient	Standard Error	R^2	Increase in R^2
	Regression Const.	7.485	-----	-----	-----
1	TD	0.124	0.128	0.123	0.123
2	D1	0.884	2.056	0.236	0.113
3	D2	-1.235	1.418	0.320	0.084
4	B.C1	8.472	1.218	0.403	0.083
5	B	3.956	0.719	0.504	0.101
6	B.C2	-3.822	0.834	0.586	0.082
7	C1	7.280	1.737	0.673	0.087
8	C2	-2.450	1.007	0.712	0.039

Table 71. Effect of Subbase Type on Crack Spacing Variance

	Type of Subbase			
	Gravel	Crushed Stone	Slag	Bituminous Stabilized
Average Crack Spacing	7.35	7.76	5.21	18.60
Variance, V_c (ft^2)	(39)	(3)	(7)	(4)

Note: Numbers in parentheses are test locations included in the average.

3. Both the main contrasts and their interactions relative to method of steel placement and the type of steel were found to have a significant effect on crack variance. Average values associated with these effects are given in Table 72. It is indicated that the highest crack variance occurred at test locations where depressed loose bars were used. This result should be considered with caution as only one test section was available in the field study that had these construction features. It was further indicated in the case of both bar mats and wire fabric that depressed steel was associated with a smaller crack variance than pre-set steel on chairs.

Minimum Steel Requirements for CRCP

Longitudinal steel equal to 0.6 percent of the cross-sectional area of the pavement slab, has been used as the standard reinforcement design for CRCP in Indiana. Considering the temperature drops in Indiana, from extreme highs during the construction season in mid-summer to the sub-zero winter temperatures, and variability in concrete properties, there were indications that the designed reinforcement was not adequate. To evaluate this factor in more detail, the ACI reinforcement design equations (3) were used to calculate the minimum longitudinal steel requirements for CRCP in Indiana. First, an analysis of percent steel requirements as a function of temperature and material variables was made. Then using the values of maximum temperature drop and concrete properties determined in the previous parts of this study, the minimum reinforcement requirements were estimated.

Sections A, B, C and D of Table 73 show the results of a sensitivity analysis of percent steel requirements determined by the use of the ACI equations. Data from the detailed field study are tabulated in Section E of Table 73.

Table 72. Effect of Steel Type and Method of Steel Placement on Crack Spacing Variance

Type of Steel	Method of Steel Placement	No. of Test Locations	Average Crack Spacing Variance, V_c (ft^2)
Bar Mats	Chairs	15	8.33
	Depressor	3	4.67
Wire Fabric	Chairs	11	8.33
	Depressor	15	7.81
Loose Bars	Chairs	7	5.75
	Depressor	2	31.79*

*Data from one test section.

Table 73. Analysis of Minimum Steel Requirements for CRCP

A. Equation No. 1 of ACI Report (3)

$$p_s = \frac{f'_t}{f_y}(100)(FS)$$

f_y = 60,000 psi

FS = safety factor

Safety Factor = 1.0

f'_t (psi)	200	300	350	400	500
p_s (%)	0.33	0.50	0.58	0.67	0.83

Safety Factor = 1.3 (Recommended in ACI report)

f'_t (psi)	200	300	350	400	500
p_s (%)	0.43	0.65	0.75	0.87	1.08

Table 73. Continued

B. Equation No. 2 of ACI report

$$p_s = \frac{f'_t}{f_y + \delta E_s - nf'_t} (100(FS)$$

f_y = 60,000 psi

E_s = 29,000,000 psi

δ = 0.0006 for concrete with modulus of rupture of 650 psi (assumed constant for all concrete strengths)

FS = safety factor

Safety Factor = 1.0

f'_t (psi)	200			300			400			500		
n	5	7.5	10	5	7.5	10	5	7.5	10	5	7.5	10
p_s (%)	0.26	0.26	0.27	0.395	0.400	0.403	0.53	0.54	0.55	0.67	0.68	0.69

Safety Factor = 1.3 (Recommended in ACI report)

f'_t (psi)	200			300			400			500		
n	5	7.5	10	5	7.5	10	5	7.5	10	5	7.5	10
p_s (%)	0.34	0.34	0.35	0.51	0.52	0.52	0.69	0.70	0.72	0.87	0.88	0.90

Table 73. Continued

C. Equation No. 3 of ACI report

$$p_s = \frac{f'_t}{f_y - nf'_t}(100)(FS)$$

f_y = 60,000 psi

FS = safety factor

Safety Factor = 1.0

f'_t (psi)	200			300			400			500		
n	5	7.5	10	5	7.5	10	5	7.5	10	5	7.5	10
p_s (%)	0.34	0.34	0.35	0.51	0.52	0.53	0.69	0.70	0.71	0.87	0.89	0.91

Safety Factor = 1.3

f'_t (psi)	200			300			400			500		
n	5	7.5	10	5	7.5	10	5	7.5	10	5	7.5	10
p_s (%)	0.44	0.45	0.46	0.66	0.68	0.69	0.90	0.91	0.92	1.13	1.16	1.18

Table 73. Continued

D. Equation No. 4 of ACI report

$$p_s = \frac{f'_t}{2(f_y - \Delta T \varepsilon \ E_s)} (100)(FS)$$

f_y = 60,000 psi

= 0.0000065 in/in/$^{\circ}$F

E_s = 29,000,000 psi

FS = safety factor

Safety Factor = 1.0

f'_t (psi)	200			300			400			500		
ΔT ($^{\circ}$F)	75	100	125	75	100	125	75	100	125	75	100	125
p_s (%)	0.22	0.24	0.27	0.33	0.36	0.41	0.44	0.49	0.55	0.55	0.61	0.69

Safety Factor = 1.3

f'_t (psi)	200			300			400			500		
ΔT ($^{\circ}$F)	75	100	125	75	100	125	75	100	125	75	100	125
p_s (%)	0.29	0.31	0.35	0.43	0.47	0.53	0.57	0.64	0.72	0.72	0.79	0.90

Table 73. Continued

E. Concrete and temperature data from detailed field study

1. Average splitting strength data for:

Sections with failures		
a. Failed locations	506 psi	(359 psi)*
b. Good locations	523 psi	(371 psi)*
Sections without failures	511 psi	(362 psi)*

*Estimated design tensile strength (f'_t)

2. Average dynamic modulus of elasticity data for:

Sections with failures		
a. Failed locations	4.76×10^6 psi	n = 6.1
b. Good locations	5.03×10^6 psi	n = 5.8
Sections without failures	6.15×10^6 psi	n = 4.7

Note: Static modulus of elasticity is about 0.55-0.75 times the dynamic modulus of elasticity, depending upon concrete strength (see Neville, Ref. 46). Use of the static modulus of elasticity would result in larger n values than shown above and consequently higher percent steel than calculated in Parts A, B, C and D of this table.

3. Average maximum temperature drop from time of paving to the time of detailed field study:

	Air Temperature (°F)	Estimated Slab Temperature (°F)
a. Sections with failures	99.6	102.8
b. Sections without failures	96.0	98.4

Design tensile strength of concrete was estimated, from the recommendations given in the ACI report, as follows:

$$\text{Splitting tensile strength, } f_{ts} = (0.564)(MR) \tag{52}$$

$$\text{Design tensile strength, } f'_t = (0.40)(MR) \tag{53}$$

Combining Equations 52 and 53:

$$\text{Design tensile strength, } f'_t = \left(\frac{0.40}{0.564}\right) f_{ts}$$

$$= 0.70\ f_{ts} \tag{54}$$

Design tensile strength values are shown in Table 73, Sec. E.

The modular ratio (n) values are based on the dynamic modulus of elasticity of concrete. It is to be noted that dynamic modulus of elasticity reflects only the purely elastic characteristics of concrete and is not affected by creep. The dynamic modulus is approximately equal to the initial tangent modulus but is appreciably larger than the secant (static) modulus. The ratio of static and dynamic moduli varies from approximately 0.5 to 0.8 depending upon the strength of the concrete (46). Use of n values corresponding to the dynamic modulus of elasticity results in a slightly lower percentage of steel than would be obtained if the static modulus of elasticity values were used.

It is seen from Table 73, that the critical steel requirements are those given by the ACI Equations 1 and 3, to control restrained volume changes due to shrinkage and temperature,respectively.

To control restrained volume changes due to shrinkage (ACI, Equation 1), the minimum steel requirements using estimated design tensile strength (359-371 psi) are in the range of 0.59-0.61 percent steel without any allowance for safety. Using a safety factor of 1.3, as recommended in the ACI report, the minimum steel requirements increase to a range of 0.77-0.79 percent.

For the control of restrained volume change due to temperature (ACI Equation 3), the minimum requirements are in the range of 0.62-0.64 percent steel with no allowance for safety. These minimum requirements increase to 0.81-0.83 percent if a safety factor of 1.3 is used.

This analysis shows that, at best, the longitudinal reinforcement design for CRCP in Indiana (0.6 percent) was marginal. Without any allowance for safety, it was barely sufficient to control shrinkage stresses and was 0.02 to 0.04 percent less than the minimum needed to counter restrained volume change due to temperature. If a factor of safety (1.3) is considered, as recommended by the ACI design procedure, then one cannot escape the conclusion that the designed steel was less than the minimum needed (0.77 to 0.83 percent). The estimates of minimum steel requirements are on the low side being based on:

1. An average temperature drop of 100°F.
2. Dynamic modulus of elasticity of concrete (rather than the static modulus).
3. A lower tensile strength than indicated by the splitting tensile strength test.

DISCUSSION OF RESULTS

The detailed field evaluation study has provided substantial evidence, regarding the reasons for the relatively poor performance of some CRCP sections in Indiana as well as reasons for the good performance of other sections. Though significant explanations for poor performance have been found, it should be recognized that failures in CRCP are a function of a number of interacting variables relating to factors of construction, material variability, design, climate, and traffic. The purpose of this discussion is twofold, first to examine the critical variables relating to CRCP performance and second, to specify material, construction,and performance characteristics found to be associated with CRCP in good structural condition.

Material Properties

The material properties discussed in this section are those of subgrade soils, subbases,and paving concrete.

Subgrade Properties

From a theoretical viewpoint, thickness design of concrete pavements is relatively insensitive to the properties of subgrade as long as pumping, frost action, etc.,are accounted for in the design. Nevertheless, being the foundation of the pavement structure, the subgrade influences the behavior of the upper pavement layers. This appears to be of particular relevance to CRCP because of its continuity characteristics, as compared to conventional jointed concrete pavement.

There is evidence that CRC pavements on coarse-grained and sandy subgrades experienced significantly less distress than pavements on fine-grained subgrades.

Subgrades with a relatively higher sand content assist in the internal drainage of the pavement. This result acquires added significance, considering that subgrades at most test locations were found to have been poorly compacted, irrespective of the pavement condition.

The percent compaction for subgrades, ranged between 65 to 120 percent of the standard AASHTO (T-99) values, with an average of 92 percent. A distribution of subgrade compaction values is illustrated in Figure 41. At 76 percent of the test locations, the degree of compaction for the subgrades was below the specified minimum.

Inadequate compaction of the subgrade can also affect the stability of the subbase. The influence of the subgrade on subbase strength is demonstrated in Figures 42 and 43. In these figures, field CBR values of gravel subbases are plotted against the corresponding subgrade field CBR, recalling that CBR values in both cases were obtained by Penetrometer tests. For both the core hole and shoulder positions (see Figures 42 and 43, respectively) higher CBR values for the gravel subbase were associated with higher subgrade CBR. This points to the necessity of achieving adequate subgrade compaction, as this would add to the stability of the subbase.

It has been known for many years that the relative strength or load bearing capacity of the subgrade soil influences the degree of compaction that can be achieved for a graded aggregate base placed on the soil. This has recently been documented by Marek and Jones (39). In view of these considerations, the data show that relatively stiff subgrades are desirable and hence, it is possible that for very weak subgrades some form of stabilization other than mechanical compaction may be needed. It is worthwhile to note that one of the best performing CRCP sections in Indiana (Contract R-7634, I-65) was built on a shale rock subgrade with a crushed stone subbase.

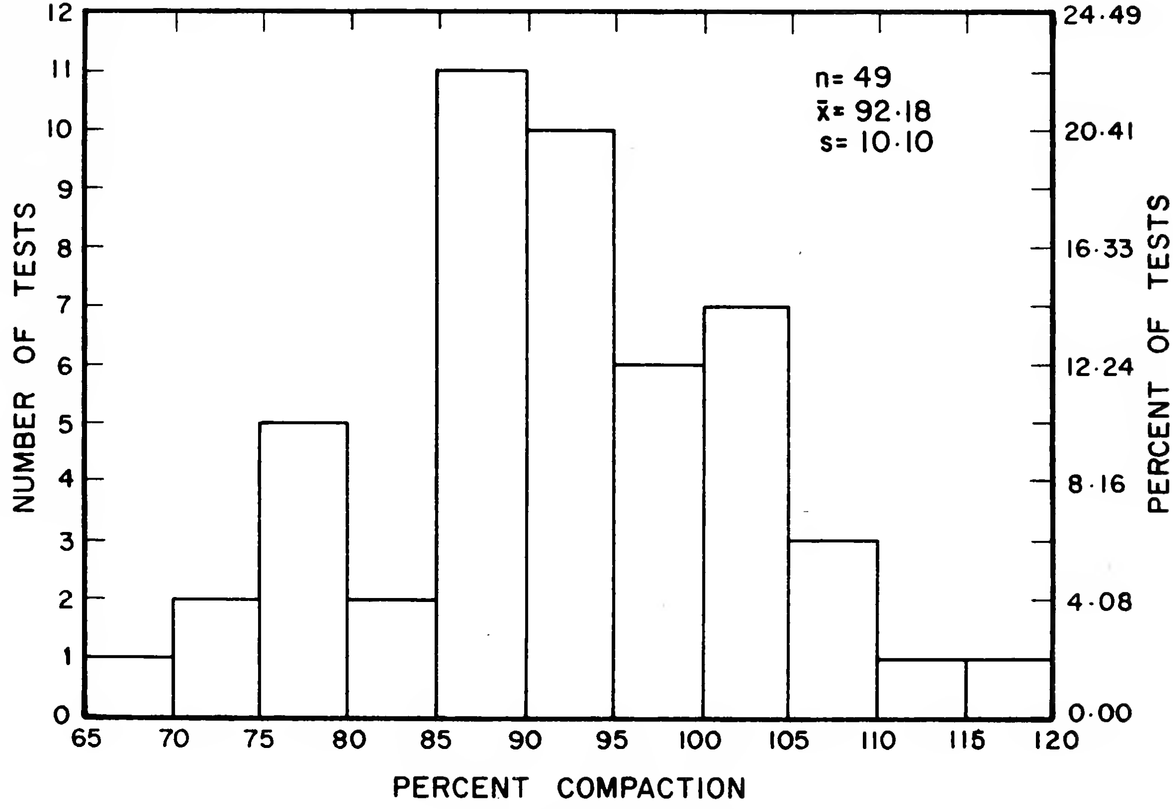

FIG. 41 VARIATION OF PERCENT COMPACTION FOR SUBGRADES

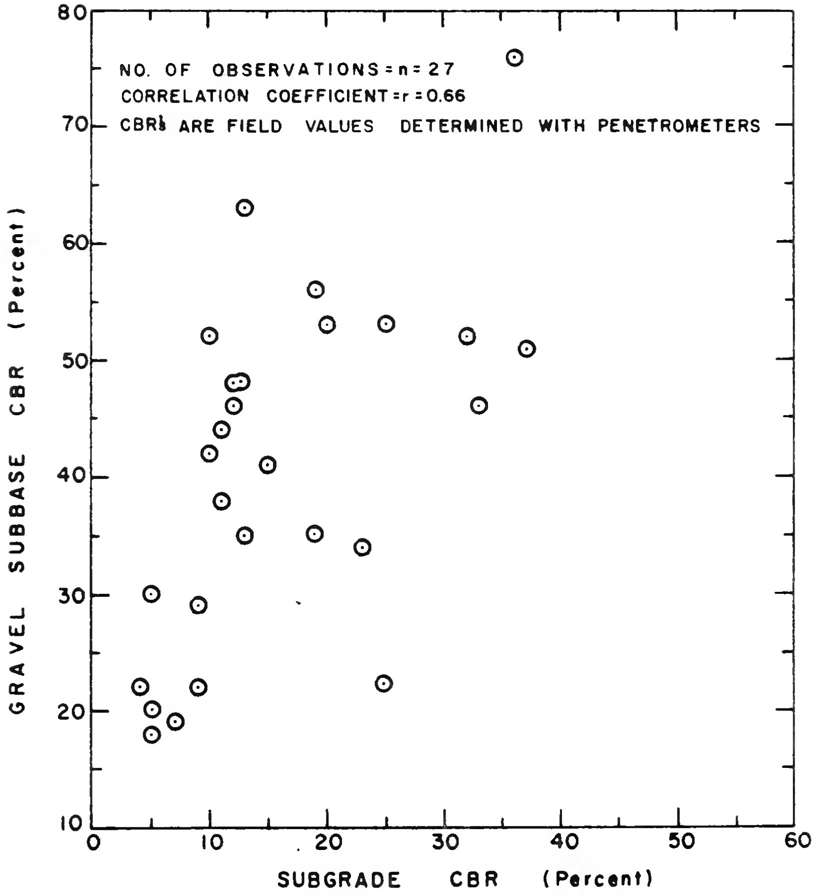

FIG. 42 CORRELATION BETWEEN SUBBASE CBR AND SUBGRADE CBR.

(CBR MEASURED AT THE CORE HOLE)

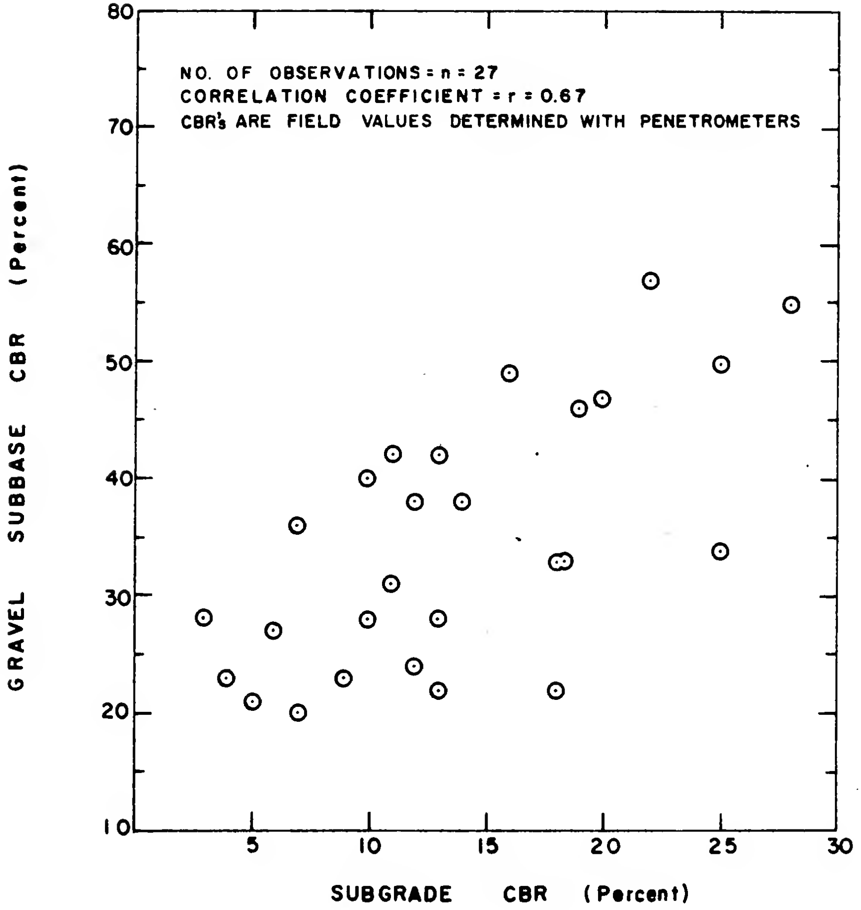

FIG. 43 CORRELATION BETWEEN SUBBASE CBR AND SUBGRADE CBR.

(CBR MEASURED AT THE PAVEMENT-SHOULDER INTERFACE)

Properties of Granular (Graded Aggregate) Subbases

Subbase, the major element of the support system for CRCP, was found to be a primary factor influencing CRCP performance. In all studies, ranging from visual condition surveys to detailed field and laboratory testing programs, subbase was shown to be a significant determinant of CRCP condition. This is not surprising as continuity requirements of CRCP presuppose the existence of a stable, firm, and non-erodible subbase.

In general, subbase-related distress in CRCP has been associated with gravel subbases, although there are pavement sections on gravel subbase that have performed admirably. In most cases, crushed stone and slag subbases have performed better than gravel subbases.

At test locations, where distress in CRCP could be attributed to graded aggregate subbases, the causes for the poor performance of subbase were found to be inadequate compaction, poor stability (as evaluated by penetrometer CBR), and low permeability.

Compaction: A distribution of percent compaction for gravel subbases is plotted in Figure 44. The average percent compaction was found to be 93.6 percent varying from a low of 75 to a high of 110 percent. This variation in subbase compaction is similar to the one determined by Williamson and Yoder, in their 1967 study of compaction variability for selected highway projects in Indiana (63). These data clearly show that a sizeable amount of the gravel subbases under CRCP were placed in a relatively loose state, with obvious implications of densification under traffic. Dynamic deflection measurements, evaluation of subbase density data, and grain-size distribution considerations indicate that gravel subbases have a tendency to densify under traffic, with the related loss in pavement support. Slag subbases in comparison were found to be extremely well compacted, while crushed stone subbases had the same degree of compaction as gravel subbases.

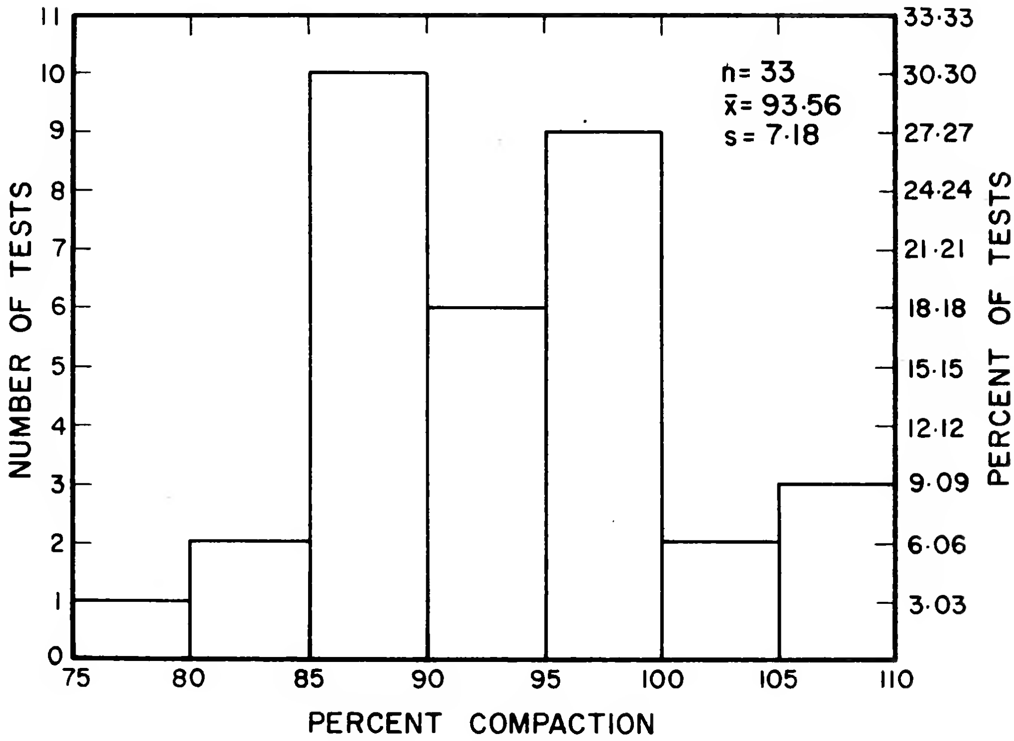

FIG.44 VARIATION OF PERCENT COMPACTION FOR GRAVEL SUBBASES

The stability of graded aggregate subbases is a function, in part,of how well the subbase is compacted. One recent publication recommends that a subbase compaction requirement based on AASHTO T-180 density is most realistic for modern traffic types and loads (39). It is further shown that the number of states, requiring AASHTO T-180 method as the basis of compaction control, increased from ten to sixteen from 1966 to 1971. From a viewpoint of practicality, modern compaction equipment can produce densities in granular base course materials in excess of AASHTO T-180. The need for establishing and adhering to adequate compaction control techniques is strongly indicated. As a minimum, proof-rolling may be required to ensure that adequate compaction of the subbase has been attained.

Strength (CBR): The stability of gravel subbases, as indicated by a field penetrometer test, was found to be in the range of 20-60 percent CBR with the majority of the CBR values less than 40 percent. For slag and crushed stone subbases, at test sections that had no apparent distress, CBR values of 90-100 percent were obtained. One of the reasons for the better performance of CRCP sections on crushed stone and slab subbases was, no doubt, the better stability characteristics of these latter subbases.

Permeability: Another important element governing subbase performance is the permeability of the subbase. The permeability characteristics of graded aggregate mixtures depend upon grain-size distribution, the type of coarse aggregate, the quality and amount of binder (minus No. 200 sieve fraction), and density. The permeability of porous media is governed by Darcy's Law, given as:

$$v = ki \tag{55}$$

where v = discharge velocity
i = hydraulic gradient (loss in head/unit length)
k = coefficient of permeability

The coefficient, k, has the units of velocity (ft/day) and depends on the properties of the permeable mass. It is also a function of density and viscosity of water. It is important to note that dense well-graded materials are less porous than open graded aggregates with a small amount of soil binder. Crushed materials in general have higher permeability rates, for a given gradation, than most common gravels (65). The above permeability relationship is only valid for laminar flow conditions within the porous media.

Permeability of subbases becomes an important consideration regarding pavement performance because it reflects the water-retaining ability of the subbase. It has been demonstrated by Cedergren that 80-90 percent of severe and premature damage to pavements is caused primarily by excess water. There are further indications that free water in granular base courses can easily reduce their strength by 25 percent or more under dynamic loads (18). Recent FHWA Guidelines (17) recommend that an adequate internal pavement drainage system should consist of a drain course, a filter course, trenches, and pipes. In the design of a drainage course, equivalent to the subbase under concrete pavements, the emphasis is on permeability rather than on particle size. According to the Guidelines, the permeability of the drain course as tested in the laboratory should not be less than 20,000 ft/day in areas with frost penetration to the depth of the drainage layer. To achieve this high permeability, essentially one-sized (3/4 in. to No. 4) crushed aggregate is recommended for use (17).

An appraisal of the permeability characteristics of graded aggregate subbases under CRCP in Indiana leaves much to be desired in view of these guidelines. Figure 45 presents permeability functions for gravel, crushed stone, and slag subbase material sampled during the detailed field study. These functions were obtained from permeability equations developed for these subbases (see Appendix D). It is quite

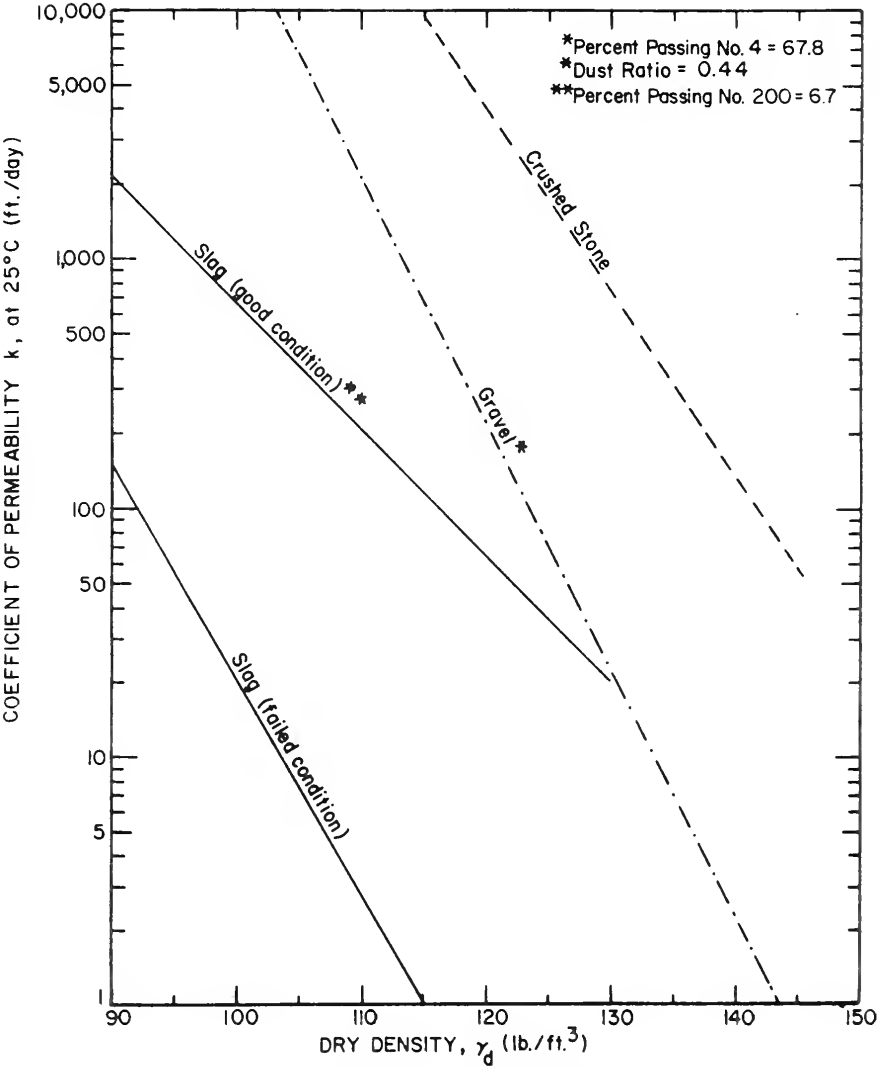

FIG. 45 EFFECT OF DENSIFICATION ON PERMEABILITY

clear from these data that crushed stone subbases had markedly better permeability than gravel or slag subbases. In the density range, normally encountered for well-compacted gravel and crushed stone subbases (130-140 lb/ft^3), the permeability of the crushed stone subbases was estimated to be 50 to 100 times higher than that for the gravel subbases.

The permeability curves illustrated in Figure 45 also show the effect of subbase densification on permeability. An increase in the density of gravel subbase from 120 lb/ft^3 to 130 lb/ft^3 resulted in a ten-fold decrease in permeability from 250 ft/day to 25 ft/day. The effect of densification on permeability was less significant for crushed stone and slag (good condition) subbases, as evidenced by the flatter slopes of the permeability functions for these subbase types.

There are possibilities for improving the permeability characteristics of the existing Indiana subbase aggregates by effecting modifications in the subbase specifications. Possible approaches are illustrated in Figures 46 to 48. For gravel subbases, higher permeabilities may be obtained by:

1. Permitting higher dust ratios (reducing the amount retained between no. 30 and No. 200 sieves).
2. Lowering the material passing the No. 4 sieve (obtaining a more open-graded aggregate).

The net effect of these approaches is to increase the water draining ability of gravel subbases as shown in Figures 46 and 47. It is pertinent to note that most aggregate specifications limit the dust ratio (the ratio of material passing the No. 200 sieve to the material passing the No. 40 sieve) to about 0.66. It has been proven in a laboratory study by Faiz (24) that for the extreme case, where the dust ratio was approximately 1.0 for a gravel subbase (i.e., skip-graded between No. 30 and No. 200 sieves), there was a marked increase in both stability and permeability over an equivalent densely-graded soil-gravel aggregate. Even otherwise, higher dust ratios were associated with better

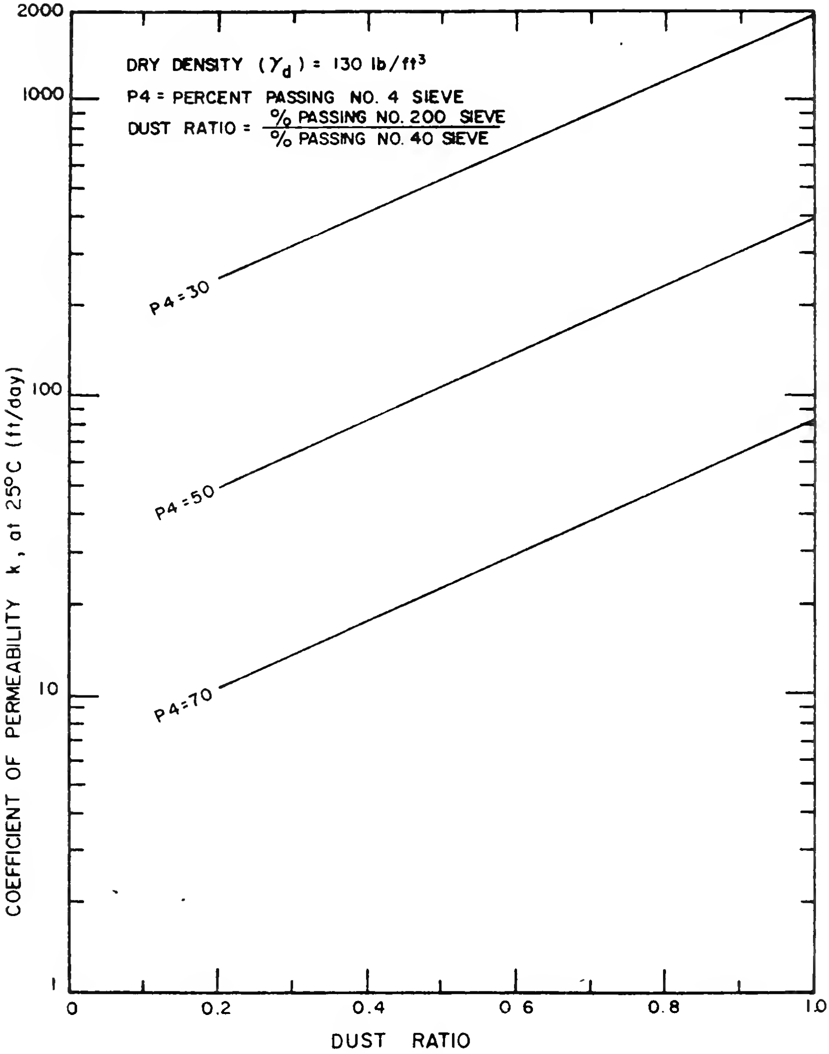

FIG. 46 EFFECT OF DUST RATIO ON PERMEABILITY OF GRAVEL SUBBASES

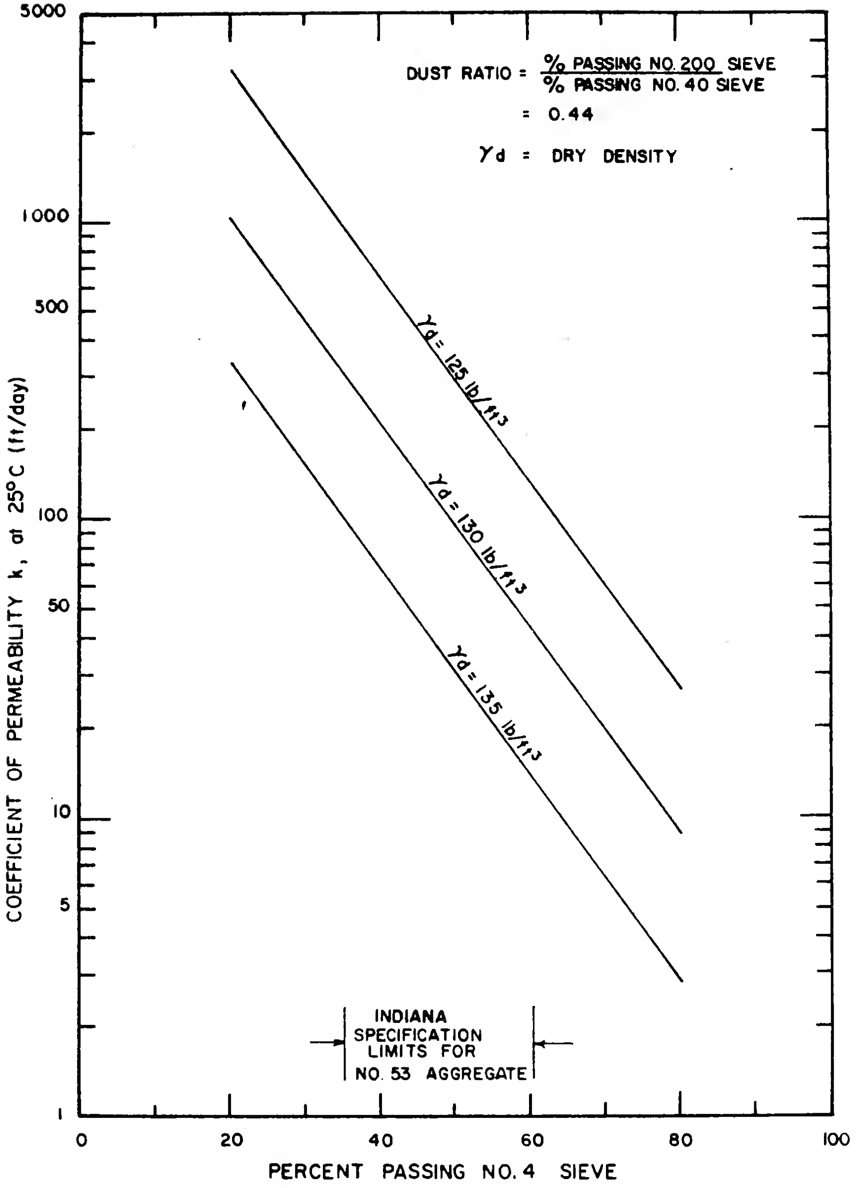

FIG.47 EFFECT OF PERCENT PASSING NO. 4 SIEVE ON PERMEABILITY OF GRAVEL SUBBASES

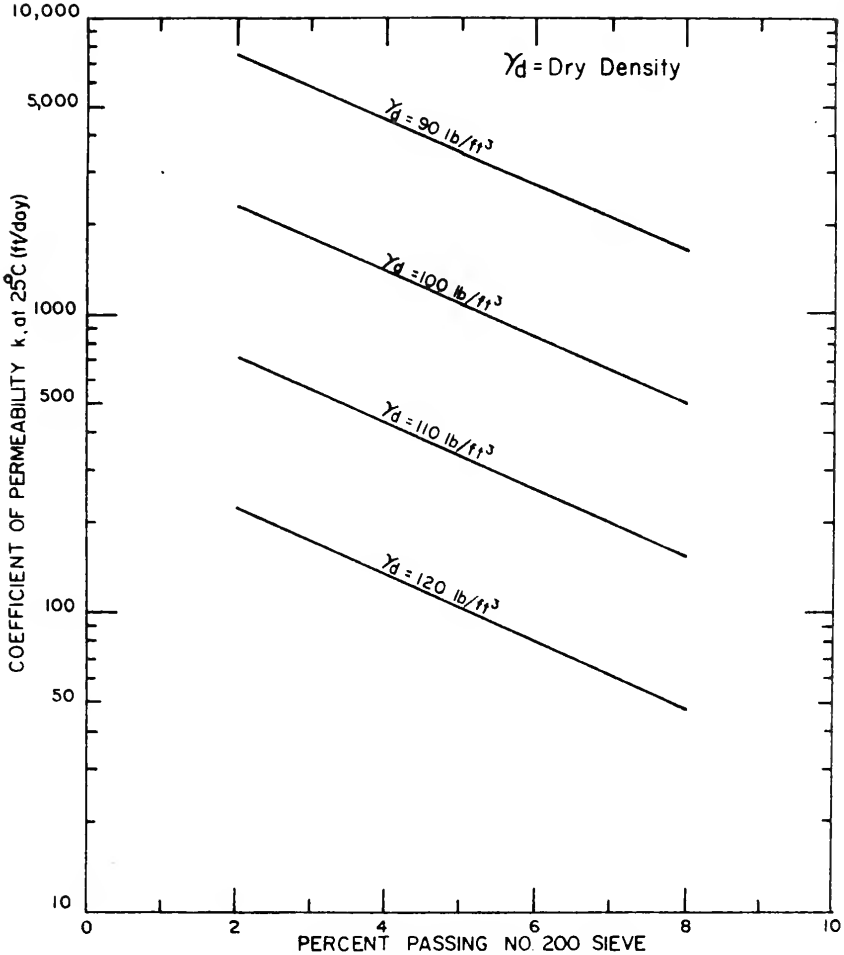

FIG. 48 EFFECT OF PERCENT PASSING NO. 200 SIEVE ON PERMEABILITY OF SLAG SUBBASES
(BASED ON PERMEABILITY MODEL FOR SECTIONS WITH NO FAILURE)

stability and permeability characteristics of soil-aggregate mixtures (24).

Similarly, the permeability of slag subbases can also be improved by allowing fewer fines in the aggregate mix (see Figure 48).

From a viewpoint of what can be achieved practically, without substantial changes in the existing specifications, the results of this study show that well compacted stable subbase materials must be required to have a minimum permeability of 1000 ft/day. It was observed in the detailed study that subbases with permeability above this limit showed good performance.

The time required for 50 percent drainage of the subbase may be calculated from the following relationship (16).

$$t_{50} = \frac{n_e \; D^2}{2k \; H_o} \tag{56}$$

where t_{50} = time for 50 percent drainage of a sloping base course with an edge drain along its lower edge (indicates the rate of fall of saturation of the base course).

n_e = effective porosity of the base.

D = sloping width of the base (ft.).

k = coefficient of permeability (ft/day).

H_o = $H + SD$

H = thickness of the base (ft.)

S = cross slope of the base.

The effect of improved permeability on drainage of the subbase is demonstrated by applying the above equation to the following cases:

a. Subbase with drains along both edges located 1.0 ft. from the pavement edge:

Considering a typical subbase, 6 in. (1/2 ft.) thick with a 13 ft. sloping width, 1.0 percent cross-slope ($S = 0.01$), and 30 percent effective porosity, it is seen that for:

$k = 10$ ft/day, $t_{50} = 4.021$ days

$k = 100$ ft/day, $t_{50} = 0.402$ day (9.7 hr.)

$k = 1000$ ft/day, $t_{50} = 0.040$ day (0.97 hr.)

An increase in permeability from 10 ft/day to 1000 ft/day reduces the 50 percent drainage time from 4 days to about one hour. For a permeability of 100 ft/day, the corresponding 50 percent drainage time would be about 10 hours.

b. Subbase with drainage through the shoulder:

In this case, the drainage outlet at the shoulder edge is considered as the equivalent of an edge drain. Repeating the above calculations for a 6 in. thick subbase, with a 28 ft. effective sloping width (from the center line of the pavement to the drainage outlet), 1.0 percent cross slope, and 30 percent effective porosity, it is found that for:

$k = 10$ ft/day, $t_{50} = 15.08$ days

$k = 100$ ft/day, $t_{50} = 1.51$ days (36 hr.)

$k = 1000$ ft/day, $t_{50} = 0.15$ day (3.6 hr.)

With drainage across the shoulder, an increase in permeability from 10 ft/day to 1000 ft/day approximately reduces the 50 percent drainage time from 15 days to about 4 hours. Similarly an increase in permeability from 100 ft/day to 1000 ft/day effects a reduction of 32 hours (from 36 hrs. to 4 hrs.) in the 50 percent drainage time.

It should be recognized that the 50 percent drainage time reflects the time for fall of saturation after stop of inflows and indirectly measures the ability of the subbase to retain water.

This presentation shows that the use of a minimum subbase permeability of 1000 ft/day is a reasonable step in the right direction.

Interaction Between Permeability and Strength: It is worthwhile to note that concrete pavement performance is also a function of the interaction between subbase permeability and strength (CBR). In Figure 49, the estimated field permeability values are plotted against field subbase CBR values measured at the shoulder-slab interface. These values pertain to 46 test locations of the detailed field study. Test data for crushed stone and slag subbases are shown with separate indicators. In addition, values obtained at failed test locations are differentiated from the values at good test locations. The data were grouped in nine categories corresponding to three levels each of subbase CBR and permeability. For low subbase strength (CBR < 40 percent), mainly gravel subbases, the percentage of failed test locations decreased from 53 percent in the low permeability group (k < 100 ft/day) to 25 percent in the high permeability group (k > 1000 ft/day). For medium subbase strength (40 percent < CBR < 80 percent), no failures were observed where permeability was greater than 1000 ft/day. Where subbase strength (CBR > 80 percent) was high (applies only to slag and crushed stone subbases) no failures were indicated, irrespective of permeability. The last result is based on limited data and may be misleading.

Recommended Criteria: To ensure adequate subbase performance under CRCP, it is recommended in the light of the results of the detailed field evaluation study, that the subbase must meet the following requirements:

1. Adequate compaction; an effective minimum of AASHTO T-99 density, preferable AASHTO T-180 density (in both cases, corrected for oversized material i.e. material retained on 3/4 in. sieve).
2. High stability; a minimum of 100 percent CBR.
3. Sufficient permeability; a minimum coefficient of permeability, k, of 1000 ft/day.

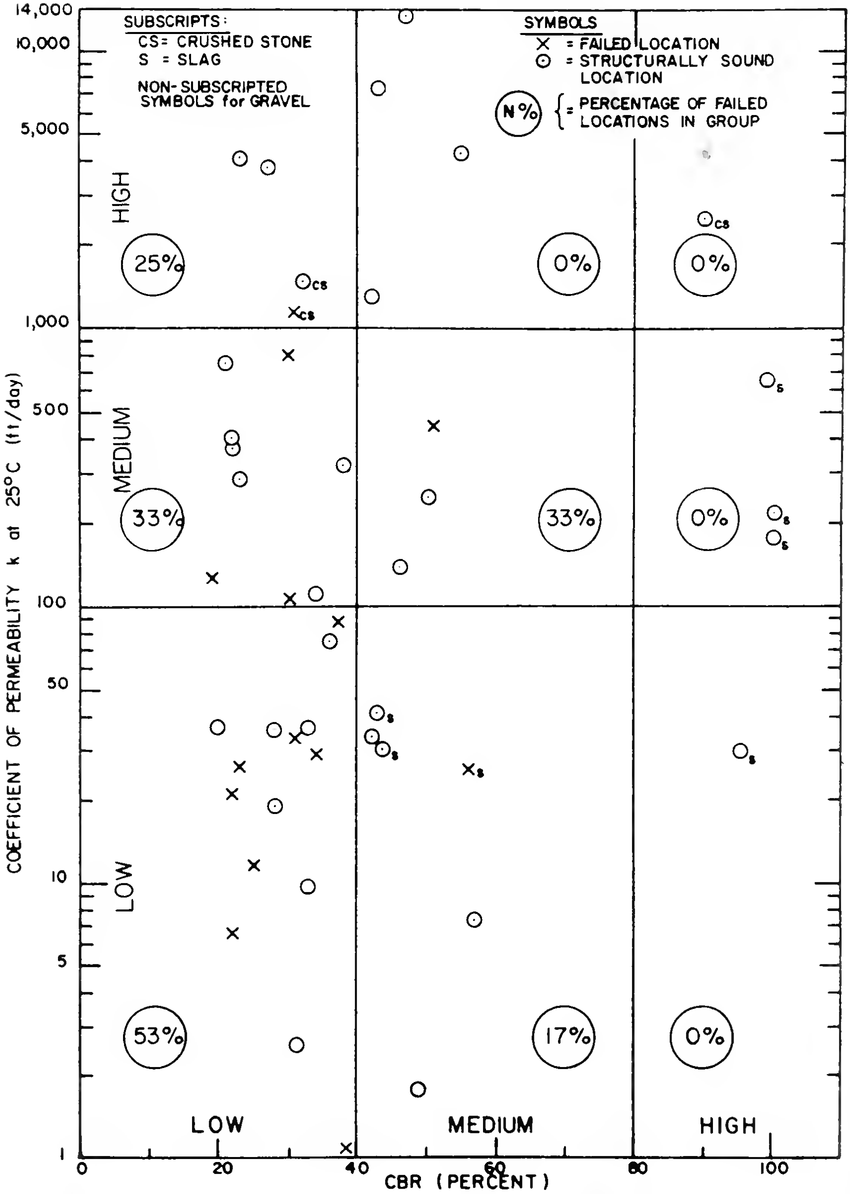

FIG.49 EFFECT OF SUBBASE STRENGTH AND PERMEABILITY ON CRCP PERFORMANCE

Properties of Bituminous Stabilized Subbase

The type of bituminous-stabilized subbase evaluated in this study was a graded gravel aggregate cold-mixed with an asphalt emulsion. One of the test sections with this subbase showed extensive failures. In general, field tests on this subbase indicated a relatively low stability similar to that obtained for the gravel subbases, the measure of stability being the penetrometer CBR. The asphalt content and minus No. 200 sieve fraction of the subbase at the failed test section were in excess of the amounts specified for Indiana Type 1 Subbase (35). To draw any conclusions relating to long range performance of these subbases would be premature as these subbases have been used recently (since 1972) and have not been exposed to the full range of traffic and environmental conditions. There is a need to evaluate the characteristics of these subbases in greater depth.

Concrete Properties

An analysis of test properties of concrete cores obtained during the field study showed:

1. Dynamic modulus of elasticity of concrete was of prime importance relative to pavement condition, higher moduli values being associated with good condition.
2. Splitting tensile strength had a minimal influence on pavement condition, within the range of values observed in the field study.
3. On sections that had failures, a relatively lower bulk density of concrete was obtained at the failed locations than at locations with no apparent distress.
4. No significant difference in concrete properties was evidenced above and below the steel reinforcement.
5. Higher concrete slump was associated with better pavement condition.

The dynamic modulus of elasticity as evaluated from pulse velocity determinations is a measure of concrete quality, lower values reflecting deterioration of the concrete.

Although modulus of elasticity is not directly proportional to strength, concretes of higher strength usually have higher moduli. An effective way of increasing the modulus of elasticity is by decreasing the water-cement ratio. This also helps in increasing the bulk density, for a constant amount of entrained air (12). However, the increase in modulus of elasticity must not be achieved at the expense of workability, as measured by concrete slump. It has been shown that concrete slump must be greater than 1.5 in. to ensure good CRCP performance.

The modulus of elasticity of concrete is also influenced by the type of aggregate, hard flinty type aggregates having high values. Soft limestone on the other hand has relatively low values. As long as the mix is workable, modulus of elasticity increases with fineness modulus. In general, longer mixing times and curing periods tend to increase the modulus of elasticity (58).

Design Considerations

The two basic considerations in the design of continuously reinforced concrete pavements are the amount of longitudinal reinforcement and the thickness of the pavement slab.

Percent Reinforcement: An analysis of longitudinal reinforcement requiements for Indiana conditions, using the ACI design equations, indicated that the use of 0.6 percent steel is marginal even where no allowance for safety is applied to the calculated values. Where a safety factor of 1.3, as recommended in the ACI design procedure, is applied to the calculated percent steel values, the minimum steel required to control restrained volume changes due to temperature and shrinkage is in the range of 0.77 to 0.83 percent. These values are based on an average temperature drop of 100^{o}F, which in many cases is lower than the estimated variation in temperature. Similarly the design tensile strength used in the analysis was only 71 percent of the recorded splitting tensile strength.

In view of these results, it becomes clear that the minimum amount of longitudinal reinforcement should be 0.7 percent of the cross-sectional area of the pavement slab. This is in agreement with the recent recommendations outlined in the report of the National Cooperative Highway Research Program (33), which mentioned that 0.7 percent steel should be used where temperature drop from time of placement is great. Also the FHWA memoranda of August 31, 1973 encourages the use of 0.7 percent steel in areas of large seasonal temperature changes or where extreme low temperatures occur (28).

Thickness Design: The Continuously Reinforced Concrete Pavement Group (20) recommended in 1968 that the thickness of CRCP could be reduced about 20-30 percent over conventional jointed pavement. As a result, it has been commonly accepted that pavement slab thickness may be reduced if the pavement is continuously reinforced. The major support for this contention comes from a deflection study wherein the deflection characteristics of CRCP were compared with those of jointed concrete pavements (42). In this study, it was demonstrated that a 10 in. jointed concrete pavement deflects 1.6 times more than an 8 in. CRCP. This result was based on a comparison of the actually measured deflections on jointed pavement with estimated deflections on CRCP computed from regression equations that had coefficients of determination (R^2) in the range of 0.307 to 0.486. This means that the estimation equations for CRCP deflection explained just 31-49 percent of the variability in the measured CRCP deflection data. In addition, the estimated deflections for CRCP were based on an 8-ft. average crack spacing and a 0.014 in. crack width. In-service CRC pavements are seldom found to have an average crack spacing of 8-ft. and only pavements in excellent condition have the indicated crack width. In view of these limitations and other anamolies in the reported data, any equivalence between the thicknesses of jointed pavement and continuously reinforced concrete pavements, based on deflection measurements, is subject to debate. An even more fundamental question is whether the allowable deflections for jointed pavements are the same as those for CRCP. If, as some researchers contend, CRCP is inherently more flexible than jointed pavement, then thickness equivalences between the two pavement types based on deflections are highly questionable.

Most failures in both the statewide condition survey and the detailed field study were noted in the traffic lane. From this study the data show that distress in CRCP began at a relatively early stage in the pavement life - approximately after 30,000 equivalent 18 kip, single-axle applications in the critical traffic lane. Furthermore, it has been found that CRCP is subject to a critical edge condition relative to stresses and deflections. These considerations question the validity of current thickness design for CRCP (9-in. pavement slabs on Interstate Highways in Indiana). There is a need to re-evaluate the present thickness design criteria for CRCP from a more fundamental and theoretical standpoint. It is possible that current CRCP thickness design procedures may be entirely inadequate in terms of providing structurally adequate pavements that can withstand the heavy load repetitions on highly trafficked highways.

As regards the relevance of deflection measurements, the data in Figure 50 provide an interesting insight into factors which must be considered. Deflection profiles are shown for 1000 ft. long test sections on two identical CRC

NOTES:

CURVE NO.	SLAB THICKNESS	SUBBASE TYPE	HWY.	CONTRACT	STATIONS
(1)	8"	GRAVEL	I-465	R-7529	236+00-245+00EBL
(2)	9"	GRAVEL	I-465	R-7841	914+00-924+00EBL

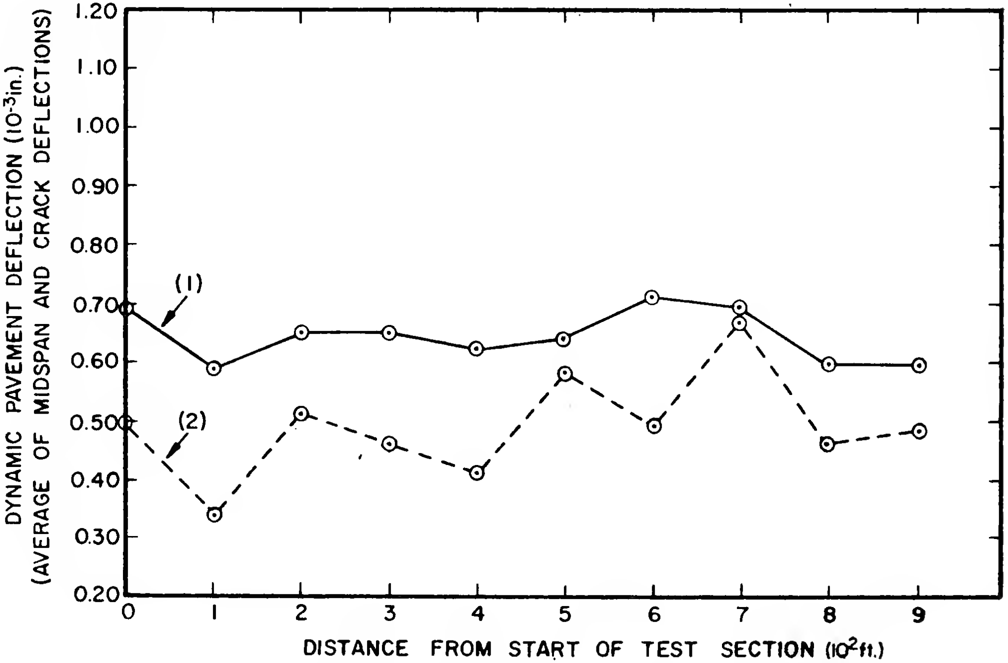

FIG. 50 EFFECT OF PAVEMENT SLAB THICKNESS ON DYNAMIC PAVEMENT DEFLECTION.

pavements; the only difference being the thickness of the pavement slab. Profile 1 applies to an 8 in. thick CRCP while Profile 2 is for a 9 in. thick CRCP with identical construction features. The deflection measurements were made under similar conditions at the same time of the year. The variation in the dynamic deflections (made with Dynaflect) of the 8 in. CRCP was between 0.59 and 0.70 milli-inch whereas deflection measurements on the 9 in. CRCP ranged between 0.33 and 0.69 milli-inch. Though the deflections on the 8-in. CRCP were higher on the average, there was at least one point where the measured deflections were the same for the two sections. This points that deflection data must be critically examined before any valid deductions can be drawn from such data.

Construction Factors

The detailed field study further substantiated the findings of the statewide condition survey that the method of construction had a significant effect on future pavement behavior. An evaluation of construction variables showed that the methods employed for CRCP construction influenced both the properties of concrete and pavement response functions.

The major findings were:

1. All other factors being equal, method of paving had no significant effect on either the properties of concrete or pavement features such as crack width or crack spacing.

2. At slipformed test sections where the steel was depressed into the concrete,it was found that the concrete had a higher modulus of elasticity than at test sections, where the steel was pre-set on chairs. This effect was particularly significant for the concrete layer above the steel reinforcement. It is possible that chairs impede the effective vibration of concrete.

3. As regards the type of steel reinforcement in slip-formed CRCP, it was observed that concrete cores from sections with loose bars had a lower splitting tensile strength compared to the strength of concrete cores taken at sections with bar mats or wire fabric. The highest tensile strength was indicated for concrete cores from sections with wire fabric. It was further shown that tensile strength of concrete was also influenced by the interaction of method of steel placement with the type of steel reinforcement. However, splitting tensile strength of concrete, within the range obtained in this study, was not a significant determinant of pavement performance.

Construction variables were also found to affect crack spacing characteristics. It was revealed that variance in crack spacing (lack of uniformity) was partly a result of the interaction between the type of steel reinforcement and the method of steel placement. The highest variance was indicated for a test section that had loose bars. Incidently, this section also had a bituminous-stabilized subbase. For bar mats and wire fabric, a higher dispersion in crack spacing was indicated at locations where the steel was preset on chairs instead of being placed with a depressor.

Since only non-destructive tests were made on CRCP test sections for the most part, it was not possible to ascertain the causes for the poor pavement response associated with some construction techniques. This aspect needs to be evaluated in more detail in future CRCP field studies.

Temperature and Traffic Variables

Temperature: It was found from an appraisal of air and slab temperatures that CRCP in Indiana has been subject to a wide variation in temperatures both at the time of construction and in the subsequent service life of the pavement. It was shown that crack patterns in CRCP are established at an early stage in the life of the pavement. Variance in crack spacing was found to be a function of the air temperature drop during the initial curing period of the concrete slab. The maximum temperature drops from the base temperature at the time of paving to a later date were found to be in range of 95 to 105°F with the highest recorded air temperature drop being 111°F. This corresponded to a drop of 117°F in the slab temperature. The temperature data, on which these results are based, spans a four-year period from 1969 to 1973. Considering the stochastic nature of temperature variables, even higher temperature drops over the entire life of the pavement may be reliably expected. Maximum air temperatures at the time of paving were estimated between 52-92°F.

Traffic: It was estimated that most of the test sections had received more than one million equivalent 18 kip, single-axle applications in the critical traffic lane. Test sections with failures were found to have received slightly more load applications than sections that had no failures. The incidence of structural failures in the traffic lane at most test locations points to the deleterious effect of heavy truck traffic and raises doubts about the structural adequacy of 9-in. thick CRCP to withstand the imposed loadings on Interstate Highways.

Pavement Response Functions

The response of continuously reinforced concrete pavement to the interaction of input variables related to design, materials, construction, climate, and traffic was evaluated in terms of dynamic deflection, surface curvature index (inversely related to pavement stiffness), crack width, crack spacing,and bifurcated cracks. The primary measure of performance was the incidence of structural distress as identified by the presence of breakups and asphalt and concrete patches. Secondary distress phenomena were manifested in pavement pumping and spalling of cracks.

For each pavement response function evaluated in this study, the values associated with good pavement condition are presented in Table 74.

The major findings resulting from the analysis of pavement response functions are summarized as follows:

Dynamic Pavement Deflection: Pavement deflections, if used with care, offer an excellent means of defining pavement condition even where no apparent distress is evident. Higher deflections were indicated at failed test locations than at good test locations. As regards section-wide deflections, higher deflections were observed at sections with potential failure rather than at sections where failures had already occurred.

Deflections tended to decrease with the distance from the pavement edge. The relative difference, between edge deflections and deflection measured at the center line of the traffic lane, was far more pronounced at failed test locations than at good test locations. This result correlates well with the observation that distress in CRCP generally starts at the pavement edge. To counteract this weakness at the pavement edge, at least one state has initiated the use of concrete shoulders tied to the traffic lane of the continuous pavement (18). No significant difference was indicated between deflections measured at cracks as compared with deflections at the midspan position between cracks, indicating relatively good granular interlock at the crack faces.

Deflection of pavements without failures on bituminous stabilized and slag subbases were generally higher than pavement deflections measured on good sections with gravel and crushed stone subbase. This may point to higher permissible deflections for bituminous stabilized and slag subbases than for the other two types.

Table 74. Values of Pavement Response Functions Associated with 9 in. CRCP in Good Condition

Pavement Response Function	Values Associated with Good Pavement Condition
Dynamic Deflection*	Less than 0.90 milli-inch at 1.0 ft. from the pavement edge. Less than 0.60 milli-inch at 6.0 ft. from the pavement edge.
Surface Curvature Index*	Less than 0.07 milli-inch at 1.0 ft. from the pavement edge. Less than 0.05 milli-inch at 6.0 ft. from the pavement edge.
Crack Width*	Less than 0.015 in.
Average Crack Spacing	4.0 to 10.0 ft.
Crack Spacing Variance**	Less than 9 $ft.^2$
No. of Crack Intersections per 100 ft. length of Pavement	No more than 4-5

* Based on summer measurements (June) at an average temperature of 77°F.

** Variance, $V_c = \dfrac{\sum_{i=1}^{n} (X_{ic} - X_c)^2}{n - 1}$

where X_{ic} = individual crack intervals, $i = 1, \ldots. n$.

X_c = mean crack interval (spacing).

n = number of crack intervals per 100 ft. length of pavement.

For 9-in. thick CRCP, dynamic deflections less than 0.5 milli-inch, as measured by Dynaflect, are indicators of good pavement condition. Potential distress is given by deflections in the range of 0.6-0.9 milli-inch, whereas deflections in excess of 1 milli-inch are indicators of severe distress. These criteria were determined from deflections measured at 6.0 ft. from the pavement edge and apply to measurements made in summer (June) at an average temperature of 77°F.

Surface Curvature Index, (SCI): Surface curvature index is an inverse function of pavement stiffness, higher values indicate higher stresses in the pavement slab. This parameter is obtained as the difference in deflections measured by the first two sensors of the Dynaflect. At failed test locations, a significant loss in pavement stiffness was noticed between the pavement edge and interior locations. On the contrary, good test locations retained uniform stiffness across the pavement. An important indicator of pavement condition became apparent when it was observed that, even at good test locations, higher SCI values were indicated at crack positions than at mid-span positions where the pavement section had experienced some failures. This was not the case at sections that were free of distress. This result points to the loss of some granular interlock at cracks in sections that had experienced distress.

Crack Width: Crack width was found to be a very sensitive indicator of CRCP condition. Test locations, that were structurally sound and in apparently good condition but within test sections that had experienced some form of distress, were found to have wider crack widths than test locations that had no manifestation of distress whatsoever.

Friberg's theoretical analysis (29) shows that crack width in long reinforced slabs may be derived as:

$$w = \frac{d}{4 E_s u} f^2 \tag{57}$$

where w = crack width
f = steel stress at crack
u = bond stress over an active bond length, c
E_s = modulus of elasticity of steel
d = diameter of steel bar
$c = \frac{f\ d}{4u}$

In the light of this relationship, crack widths in CRCP may be effectively decreased by decreasing the diameter of reinforcing bars to increase effective bond area, and/or by lowering the stress in steel at cracks with the provision of a larger amount of reinforcement.

Crack Spacing: Average crack spacing was not found to be correlated with pavement condition, within the range of values obtained for 9-in. CRC pavements in this study.

A measure of the dispersion or lack of uniformity of crack spacing was found to be correlated with pavement condition. It was observed that a higher variance in crack spacing was indicated at failed test locations than at good test locations. It is to be noted that irregular and nonuniform crack patterns signify poor pavement condition where other manifestations of distress (failures, pumping, or spalling) are already present.

The study also revealed that variance in crack spacing varied with subbase type: highest variance at sections with bituminous stabilized subbase; lowest at sections with slag subbase; no difference in crack variance at sections with gravel and crushed stone subbases.

Proper curing of paving concrete would result in more uniform crack patterns, as this would minimize the effects of temperature differentials immediately after paving. One way of accomplishing this would be to require that the paving be done late in the afternoon to reduce the effect of temperature drops during the critical curing period.

Crack Intersections: It had been indicated in earlier surveys that pavement failures were generally associated with bifurcated cracks. This was found to be so in the detailed field evaluation of CRCP, more crack intersections being associated with failed test locations than good locations.

It is hypothesized that bifurcated cracks possibly result from:

1. slippage of reinforcement at lap areas.
2. use of pre-set steel on chairs.
3. use of transverse wires.
4. combination of above factors.

Unfortunately this hypothesis could not be evaluated in the detailed field study. One possible approach to studying this phenomenon could be by means of a "Packometer", an instrument used for detecting the position and size of steel reinforcement embedded in concrete.

PART IV

CONCLUSIONS AND RECOMMENDATIONS

CONCLUSIONS

A composite picture of the condition and performance of continuously reinforced pavements in Indiana has been obtained by this investigation. Before any specific conclusions are presented, it must be recognized that distress in CRCP has been an outcome of a complex array of factors pertaining to design, material variability, construction, climate, and traffic. No single element in this array can be considered to be the primary cause of structural distress; it is an interaction of these elements that creates conditions leading to pavement failure.

Initially, marginal design together with certain construction methods created intrinsic deficiencies in the pavement structure. These weaknesses were further compounded by widespread material variability, resulting primarily from inadequate construction control. Continuously reinforced pavement, being less forgiving of such deficiencies, responds unfavorably under the action of traffic and environmental conditions, when inherent imperfections are present in the pavement. The result has been uneven performance, punctuated by severe structural distress in some cases. Inherently, CRCP is a good pavement; poor performance in some instances is not sufficient cause to relegate this pavement back to an experimental status. If properly designed and constructed, CRCP can adequately serve its intended functions.

At this point, it is more important to consider that there are many miles of CRCP in Indiana that are in good condition, irrespective of the marginal design and construction of uncertain quality.

The significant findings, resulting from a statistical analysis of data obtained from a comprehensive field evaluation of in-service CRC pavements in Indiana, are as follows:

1. Subbase and Subgrade: Unstable support conditions were found to be a primary contributor to CRCP distress. The subbase and, to a lesser extent, the subgrade were shown to exert a significant influence on the condition of CRCP. It was found that well compacted, permeable, and stable subbases lead to good pavement condition. The importance of the internal drainage of the pavement structure was underlined by the observation that pavements on coarse-grained (sandy) subgrades had significantly fewer failures than pavements on fine grained soils. There was significant evidence to suggest that granular subbases placed in a loose state densified under the action of traffic with a resultant loss of pavement support. In general, crushed stone and slag subbases performed better than gravel subbases. The major problems with graded aggregate subbases were inadequate compaction, poor stability, and low permeability. As regards Indiana Specification Type 1 bituminous stabilized subbases (cold mixed with asphalt emulsion) the observed trends suggest that the stability of these subbases is questionable. Further studies are needed to permit a more specific evaluation of bituminous stabilized subbases.

2. Concrete Properties: Higher concrete slump was found to be correlated with better CRCP performance. Concrete cores taken from good CRCP sections were tested to have a higher modulus of elasticity and bulk density than concrete cores obtained at failed locations. Splitting tensile strength, within the range observed in this study, was not found to be a significant performance factor.

3. Percent Steel: An analysis of CRCP longitudinal steel requirements using the characteristics of the evaluated CRCP test sections as input parameters, showed that,at best,the designed reinforcement of 0.6 percent steel was marginal. The data suggest the use of 0.7 percent steel.

4. Method of Pavement Construction: The properties of concrete and pavement response functions were significantly influenced by the method of pavement construction. It was observed that the use of chairs as a method of steel placement generally resulted in poor pavement condition. Concrete, at locations where chairs were used, was tested to have a lower modulus of elasticity in the layer above the steel reinforcement, as compared to the uniform moduli of concrete cores taken from sections with depressed steel. No significance differences were indicated in the uniformity of concrete from above and below the steel reinforcement.

Variance in crack spacing patterns (erratic crack spacing) was indicated to be partly a function of the interaction of type of steel with method of placement. For bar mats and wire fabric, a higher variance in crack spacing was associated with the use of pre-set steel on chairs as compared to depressed steel.

The method of paving (slipform vs. paving with side forms) had no effect on pavement condition. The use of bar mats was generally associated with more pavement failures than the use of wire fabric or loose bars.

5. Dynamic Pavement Deflection and Surface Curvature Index: Higher values for both these parameters were indicated at failed pavement sections than at good test sections. Deflections were observed to decrease in magnitude with increasing distance from the pavement edge. At failed test locations, the surface curvature index, SCI (inversely related to pavement stiffness) decreased linearly with the distance from the pavement edge. At good test locations, uniform SCI values were observed.

Gravel and crushed stone subbases had lower section-wide deflections than slag and bituminous-stabilized subbases. No significant difference was indicated between crack and midspan deflections, pointing to relatively good granular interlock at crack faces.

6. Crack Width: Pavement crack widths were found to be a sensitive indicator of pavement condition. Even at structurally sound locations, crack width on pavement sections with failures was greater than the width of cracks on sections with no distress.

7. Crack Spacing: Average crack spacing was about the same irrespective of pavement condition. The variance of crack spacing at failed test locations was significantly higher than the variance at good test locations. Frequent incidence of bifurcated cracks was also observed to be associated with failures. For good pavement condition it is necessary to have uniform, evenly spaced crack patterns with a small variance in crack spacing.

8. Temperature: Temperature drops both immediately after paving and during the service life of the pavement were noted to influence CRCP behavior. High temperature drops during the initial curing period of concrete resulted in a more dispersed and erratic crack pattern. Temperature variations during the service life affected the steel reinforcement requirements.

9. Traffic: Distress of CRC pavements was found to be associated with traffic. There is some evidence that the current CRCP thickness design does not provide pavements that are structurally adequate to withstand the traffic loadings on heavily trafficked Interstate Highways.

RECOMMENDATIONS

One of the main objectives of this investigation was to develop design and construction guidelines that would result in better performance of CRCP in Indiana.

As a fulfillment of this objective, recommendations covering the design and construction aspects of CRCP, are presented in the following sections.

CRCP Structural Design

1. Percent Steel: In view of the material variations and range of temperatures encountered in Indiana, it is recommended that the amount of minimum longitudinal reinforcement be increased to 0.7 percent.

2. Pavement Slab Thickness: The currently used "80-percent rule" regarding CRCP thickness (CRCP thickness = .80 x equivalent jointed pavement) should be re-evaluated. There are strong indications that the pavements obtained by the current designs are not adequate to withstand the traffic loadings on Interstate Highways. It is suggested that CRCP thickness be the same as that needed for an equivalent jointed pavement.

3. Subbase Thickness: Minimum thickness of bituminous stabilized subbases should be increased to 6-in. from the current standard practice of a 4 in. subbase. On weak subgrades, increase in thickness of both the graded aggregate and bituminous stabilized subbases may be warranted.

Material Specifications

1. Subgrade: Subgrades should be compacted to a minimum of 100 percent standard AASHTO (T-99) density, with proof-rolling. The density should be corrected for material retained on the No. 4 sieve. To effect adequate compaction control, the one-point compaction curve method (65) is recommended. Adoption of quality control procedures is also recommended.

2. Subbase (Graded Aggregate): For gravel, crushed stone and slag subbases the following recommendations are offered relative to:

a.	Compaction:	1.	100 percent Standard AASHTO (T-99) effective minimum.
		2.	100 percent Modified AASHTO (T-180) - desirable.
		3.	Density values to be corrected for material retained on 3/4 in. sieve).
		4.	Use of control curves and quality control techniques.
b.	Stability:		Minimum CBR of 100 percent.
c.	Permeability:		Minimum k = 1000 ft/day. Provision of effective sub-drainage (collector drains, filter courses as needed, trenches, and marked pipe outlets), in accordance with FHWA Guidelines (17).

3. Subbase (Bituminous Stabilized): Definitive criteria was not obtained in this study. There were indications that Type 1 subbase (cold mixed with asphalt emulsion) does not have sufficient stability.

4. Concrete: Paving concrete should have:
    a. Dynamic modulus of elasticity: 5.0-6.0 million psi.
    b. Splitting tensile strength: greater than 450 psi.
    c. Slump: a minimum slump of 1.5 in.; a 2-in. minimum slump would be more desirable.

5. Reinforcement: To ensure adequate vibration of concrete it is recommended that size No. 6 deformed bars or equivalent sizes in deformed wire fabric be used for longitudinal steel. Transverse steel may be omitted if conditions warrant.

Construction

As regards method of construction, the following recommendations are in order:

1. Use of pre-set steel on chairs should be discontinued.

2. Performance of tied bar mats should be critically examined by further field observations. There are indications that this type of steel fabrication is related to a higher incidence of failures than wire fabric or loose bars.

3. Sufficient vibration and compaction of concrete is essential to good performance of CRCP.

4. To permit good construction control, slower paving rates should be used.

5. Construction joints are points of weakness in CRCP, needing considerable care in their construction.

REFERENCES

REFERENCES

1. American Association of State Highway Officials, "AASHO Interim Guide for Design of Rigid Pavement Structures", Appendix F, Washington, D. C., 1962, pp. F1-F3.

2. American Association of State Highway Officials, "AASHO Interim Guide for Design of Pavement Structures", Washington, D. C., 1972, 125 pp.

3. American Concrete Institute, "A Design Procedure for Continuously Reinforced Concrete Pavements for Highways", ACI Journal, Report Title No. 69-32, Detroit, June 1972, pp. 309-319.

4. American Society for Testing and Materials, "Concrete and Mineral Aggregates", Annual ASTM Standards Part 10, Philadelphia, 1970, pp. 1-548.

5. American Society for Testing and Materials, "Bituminous Materials; Soils; Skid Resistance", Annual ASTM Standards, Part 11, 1970, pp. 1-978.

6. Anderson, V. L., "Restriction Errors for Linear Models (An Aid to Develop Models for Designed Experiments)", Biometrics, 26, June 1970, pp. 255-268.

7. Anderson, V. L., McLean, R. A., Design of Experiments - A Realistic Approach, Marcel Dekker Inc., New York, 1974, 418 pp.

8. Arndt, W. J., "Temperature Changes and Duration of High and Low Temperatures in a Concrete Pavement", Proceedings, Highway Research Board, Washington, D. C., Vol. 23, 1943, pp. 273-275.

9. Austin Research Engineers, "Design Manual for Continuously Reinforced Concrete Pavements", Continuously Reinforced Concrete Airfield Pavement, Vol. III, Technical Report AFWL-TR-73-229, Vol. III, DOT and DOD, Washington, D. C., 1974, 98 pp.

10. Barber, E. S., "Calculations of Maximum Pavement Temperatures from Weather Reports", Bulletin 168, Highway Research Board, pp. 1-8, 1957.

11. The Boeing Company, "High Load Penetrometer Soil Strength Tester", Document No. D6-24555, The Boeing Company, Commercial Airplane Division, Renton, Washington, 1971, pp. 1-16.

12. Bureau of Reclamation, Concrete Manual, U. S. Department of the Interior, Denver, Colorado, 1966, pp. 27-43.

13. Burks, E., "Continuously Reinforced Paving as a Base for Asphalt Running Surface", 1st European Symposium on Concrete Pavements, Paris, Vol. 2, July 1969, pp. 141-150.

14. Burr, I. W. and Foster, L. A., "A Test for Equality of Variances", Department of Statistics, Purdue University, Mimeo Series 282, April 1972.

15. Cashell, H. D. and Teske, W. E., "Continuous Reinforcement in Concrete Pavements", Proceedings, Highway Research Board, Vol. 34, 1955, pp. 34-56.

16. Cedergren, H. R., Drainage of Highway and Airfield Pavements, John Wiley and Sons, New York, 1974, pp. 157-158.

17. Cedergren, H. R., et. al., "Guidelines for the Design of Subsurface Drainage Systems for Highway Structural Sections", Offices of Research and Development, Federal Highway Administration (FHWA), Washington, D. C., 1972, 25 pp.

18. Cedergren, H. R. and Godfrey, Jr., K. A., "Water: Key Cause of Pavement Failure", Civil Engineering, ASCE, Vol. 44, No. 9, Sept. 1974, pp. 78-82.

19. Concrete Construction Publications Inc., "Continuously Reinforced Pavements", Concrete Construction, Reprint, Elmhurst, Illinois, June 1965.

20. Continuously Reinforced Pavement Group, "Design and Construction - Continuously Reinforced Concrete Pavement", Chicago, 1968, 79 pp.

21. Deming, W. E., Some Theory of Sampling, Dover Publications, Inc., New York, 1950, pp. 213-214.

22. Doyen, A., et. al., "Pavements of Continuous Reinforced Concrete in Belgium", 1st European Symposium on Concrete Pavements, Vol. 2, Paris, 1969, pp. 162-163.

23. Draper, N. R., and Smith, H., Applied Regression Analysis, John Wiley and Sons, Inc., New York, 1968, pp. 134-142.

24. Faiz, A., "The Effect of Skip-Grading on Stability of Soil-Aggregate Mixtures", Joint Highway Research Project, Purdue University, Report No. 10, July 1971, 101 pp.

25. Faiz, A. and Yoder, E. J., "Factors Influencing the Performance of Continuously Reinforced Concrete Pavements", Record 485, Transportation Research Board, Washington, D. C., 1974, pp. 1-13.

26. Faiz, A. and Yoder, E. J., "Evaluation of Parameters Significantly Influencing the Performance of CRC Pavements", presented at the 1974 Annual Convention of American Concrete Institute, San Francisco, April 1974 (to be published).

27. Federal Aviation Administration, "Airport Pavement Design and Evaluation", Advisory Circular, AC150/5320-6B, FAA, Department of Transportation, 1974, 124 pp.

28. Federal Highway Administration, "Continuously Reinforced Concrete Pavement", FHWA Notice, Aug. 31, 1973.

29. Friberg, B. F., "Frictional Restraint Under Concrete Pavements and Restraint Stresses in Long Reinforced Slabs", Proceedings, Highway Research Board, Vol. 33, 1954, pp. 167-182.

30. Gregory, J. M., et. al., "Continuously Reinforced Concrete Pavements: A Report of the Study Group", TRRL Laboratory Report 612, Transport and Road Research Laboratory, Crowthorne, England, 1974, 50 pp.

31. Harvey, W. R., "Least Squares Analysis of Data with Unequal Subclass Frequencies", Agriculture Research Service, U.S. Department of Agriculture, ARS 20-8, 1960.

32. Hicks, C. R., Fundamental Concepts in the Design of Experiments, Holt, Rinehart and Winston, New York, 1973, pp. 173-187.

33. Highway Research Board, "Continuously Reinforced Concrete Pavement", NCHRP Synthesis of Highway Practice, No. 16, 1973, pp. 1-18.

34. Hudson, W. R., and McCullough, B. F., "An Extension of Rigid Pavement Design Methods", Record 60, Highway Research Board, 1964, pp. 1-14.

35. Indiana State Highway Commission, Standard Specifications, Indianapolis, Indiana, 1971, 562 pp.

36. Indiana State Highway Commission, "Traffic Maps - State of Indiana", 1966, 1969, and 1972.

37. Joint Highway Research Project, "Engineering Soil Parent Material Areas of Indiana", Revised Edition of 1943 Map of Bulletin No. 87, Purdue University, 1950.

38. Malo, A. F., et. al., "Traffic Behavior on an Urban Expressway", Bulletin 235, Highway Research Board, 1960, p. 26.

39. Marek, C. R., and Jones Jr., T. R., "Compaction - An Essential Ingredient for Good Base Performance", Proceedings from a Conference on Utilization of Graded Aggregate Base Materials in Flexible Pavements, Oakbrook, Illinois, March 1974, pp. IX-1 to IX-38.

40. McCullough, B. F., "Design Manual for Continuously Reinforced Concrete Pavement", United States Steel Corporation, Pittsburgh, Penn., 1970, pp. 1-62.

41. McCullough, B. F., and Ledbetter, W. B., "LTS Design of Continuously Reinforced Concrete Pavement", Transactions ASCE, Vol. 127, Part IV, 1962, pp. 358-382.

42. McCullough, B. F., and Treybig, H. J., "A Statewide Deflection Study of Continuously Reinforced Concrete Pavement in Texas", Record 239, Highway Research Board, 1968, pp. 150-174.

43. Mellinger, F. M., et. al., "Heavy Wheel Load Traffic on Concrete Airfield Pavements", Proceedings, Highway Research Board, Vol. 36, 1957, pp. 175-189.

44. Moulton, L. K., and Schaub, J. H., "Estimation of Pavement Surface Freezing Indices", Transportation Engineering Journal ASCE, Vol. 95, No. TE4, Nov. 1969, pp. 587-604.

45. National Oceanic and Atmospheric Administration, "Climatological Data - Indiana", U.S. Department of Commerce, Asheville, North Carolina, Vols. 74-78, 1969-1973.

46. Neville, A. M., Properties of Concrete, John Wiley and Sons, New York, 1973, pp. 309-382.

47. Nie, N., et. al., Statistical Package for the Social Sciences (SPSS), McGraw-Hill Book Co., New York, 1970, pp. 174-195.

48. Olateju, O. T., "Techniques in Slip-form Paving and Continuously Reinforced Concrete Pavement Construction", Joint Highway Research Project, Purdue University, Report No. 6, March 1971.

49. Ostle, B., Statistics in Research, The Iowa State University Press, Ames, Iowa, 1963, pp. 438-439.

50. Packard, R. G., "Design of Concrete Airport Pavement", Engineering Bulletin, Portland Cement Association, Skokie, Illinois, 1973, p. 30.

51. Pasko, T. J., "A Simplified Analysis of Environmental Cracking of CRCP", NCHRP Synthesis of Highway Practice, No. 16, Appendix B, Highway Research Board, 1973, pp. 21-22.

52. Portland Cement Association, "Thickness Design for Concrete Pavements", Skokie, Illinois, 1966, p. 3.

53. Scrivner, F. H., et. al., "Detecting Seasonal Changes in Load-Carrying Capabilities of Flexible Pavements", NCHRP, Report 76, Highway Research Board, 1969, 37 pp.

54. Scrivner, F. H., et. al., "A New Research Tool for Measuring Pavement Deflection", Record 129, Highway Research Board, 1966, pp. 1-11.

55. Snedecor and Cochran, Statistical Methods, Iowa State University Press, Ames, Iowa, 1967, 593 pp.

56. Taragin, A., "Lateral Placement of Trucks on Two-Lane and Four-Lane Divided Highways", Public Roads, Bureau of Public Roads, Washington, D. C., Vol. 30, No. 3, 1958, pp. 71-75.

57. Treybig, H. J., et. al., "Effect of Transverse Steel in Continuously Reinforced Concrete Pavement", Special Report No. 116, Highway Research Board, 1971, pp. 138-150.

58. Troxell, G. E., Davis, H. E., and Kelly, J. W., Composition and Properties of Concrete, McGraw-Hill Book Co., New York, 1968, pp. 321-331.

59. Ulbricht, E. P., "A Method of Comparing Alternate Pavement Designs", Joint Highway Research Project, Purdue University, Report No. 28, 1967, pp. 67-73.

60. Van Vuuren, D. J., "Rapid Determination of CBR with the Portable Dynamic Cone Penetrometer", The Rhodesian Engineer, Paper No. 105, Salisbury, 1969.

61. Vetter, C. P., "Stresses in Reinforced Concrete Due to Volume Changes", Transactions, ASCE, Vol. 98, 1933, pp. 1039-1080.

62. Westergaard, H. M., "Computation of Stresses in Concrete Roads", Proceedings, Highway Research Board, Vol. 6, 1926, pp. 90-112.

63. Williamson, T. G., and Yoder, E. J., "An Investigation of Compaction Variability for Selected Highway Projects in Indiana", Record 235, Highway Research Board, 1968, pp. 1-12.

64. Wire Reinforcement Institute, "Continuously Reinforced Concrete Pavement - Deformed Welded Wire Fabric", Manual No. CRD5, Washington, D. C., 1964, 47 pp.

65. Yoder, E. J., Principles of Pavement Design, John Wiley and Sons, 1959, 569 pp.

66. Yoder, E. J., "Pumping of Highway and Airfield Pavements", Proceedings, Highway Research Board, Vol. 36, 1957, p. 388.

67. Yoder, E. J., and Faiz, A., "Design and Performance of Continuously Reinforced Concrete Pavements", Proceedings, 59th Annual Road School, Purdue University, Indiana, 1973, pp. 131-147.

68. Yoder, E. J., and Gadallah, A. A., "Design of Low Volume Roads", Conference on Low Cost Roads, Kuwait Society of Engineers, 1974, 57 pp.

69. Yoder, E. J., and Williamson, T. G., "Techniques for Compaction Control", Proceedings, 53rd Annual Road School, Purdue University, 1967, pp. 179-193.

70. Zuk, W., "Analysis of Special Problems in Continuously Reinforced Concrete Pavements", Bulletin 214, Highway Research Board, 1959, pp. 1-21.

71. Zuk, W., "Bond and Transflexural Anchorage Behavior of Welded Wire Fabric", Bulletin 238, Highway Research Board, 1960, pp. 78-92.

APPENDIX A

SUMMARY OF STATEWIDE CONDITION SURVEY DATA

TABLE A I. SUMMARY OF STATEWIDE CONDITION SURVEY DATA

NOTATION

LANE DIRECTION

EBL= Eastbound Lane
WBL= Westbound Lane
NBL= Northbound Lane
SBL= Southbound Lane

METHOD OF PAVING

SF= Slipformed
F = Sideformed

METHOD OF STEEL PLACEMENT

CH= Chairs
DP= Depressor

TYPE OF STEEL REINFORCEMENT

LB= Loose Bars
BM= Bar Mats
WF= Wire Fabric

TYPE OF SUBBASE

BS= Bituminous Stabilized
GR= Gravel
ST= Crushed Stone
SL= Slag

SUBGRADE PARENT MATERIAL

F= Fine-grained
C= Coarse-grained

OTHER SYMBOLS

NT= Not Opened To Traffic
✱ = Replicated Section (Re-evaluated By A Second Survey Party)
✱✱ = Found To Be 8 in. Thick In Detailed Field Study
$\frac{\text{ST}}{\text{SL}}, \frac{\text{ST}}{\text{GR}}, \frac{\text{SL}}{\text{GR}} : \frac{\text{Subbase Type Recorded In Construction Survey}}{\text{Subbase Type Found In Detailed Field Study}}$

TABLE A 1, contd.

		1	2	3*	4	5	6	7	8	9	10	11	12	13	14	15*	16
SECTION IDENTIFICATION	SECTION NO	1	2	3*	4	5	6	7	8	9	10	11	12	13	14	15*	16
	HIGHWAY	I-65	I-65	I-65	I-465	I-465	I-94	I-65	I-65	I-65	I-465	I-465	I-70	I-65	I-65	I-65	I-65
	CONTRACT	R8232	R7935	R7935	R7529	R7841	R8476	R7677	R7858	R8001	R7391	R7391	R7487	R7876	R7677	R7677	R7635
	START OF SECTION	190+00 NBL	700+00 NBL	700+00 NBL	224+00 EBL	1251+00 NBL & WBL	1718+00 EBL	980+00 NBL	1130+00 SBL	1005+00 NBL	826+00 EBL	708+00 WBL	663+30 WBL	480+00 SBL	836+00 SBL	836+00 SBL	1210+00 SBL
	END OF SECTION	240+00 NBL	750+00 NBL	730+00 NBL	274+00 EBL	1042+00 NBL & WBL	1768+00 EBL	1030+00 NBL	1180+00 SBL	1055+00 NBL	879+00 EBL	757+00 WBL	717+00 WBL	530+00 SBL	900+00 SBL	900+00 SBL	1260+00 SBL
	DATE OF CONDITION SURVEY	10/30/72	11/2/72	11/2/72	11/8/72	11/22/72	11/17/72	11/1/72	11/2/72	11/8/72	11/6/72	11/6/72	11/14/72	11/13/72	10/26/72	10/26/72	11/3/72
CONSTRUCTION VARIABLES	SLAB THICKNESS (in)	9	9	9	9**	9	9	9	9	9	9	9	9	9	9	9	9
	METHOD OF PAVING	SF	SF	SF	SF	SF	SF	SF	SF	SF	SF	SF	SF	SF	SF	SF	SF
	METHOD OF STEEL PLACEMENT	CH	CH	CH	CH	CH	CH	CH	CH	CH	CH	CH	CH	CH	CH	CN	CN
	TYPE OF STEEL REINFORCEMENT	LB	LB	LB	LB	LB	LB	BM	BM	BM	BM	BM	BM	BM	BM	BM	WF
	TYPE OF SUB-BASE	BS	GR	GR	GR	GR	ST	OR	GR	GR	GR	GR	GR	GR	GR	GR	GR
	SUBGRADE PARENT MATERIAL	F	F	F	F	F	F	F	F	F	F	F	F	F	C	C	F
	SLUMP (in)	1.56	1.0	1.0	1.625	1.25	1.5	1.5	1.375	2.05	1.5	1.5	1.75	1.5	1.5	1.5	1.5
	NO OF LANES	4	4	4	6	6	6	4	4	4	6	6	6	4	4	4	4
PERFORMANCE VARIABLES	DATE PAVED	8/71	7/71	7/71	8/69	6/70	7/72	9/69	7/70	8/70	10/68	8/68	7/69	10/70	9/69	9/69	8/69
	DATE OPENED TO TRAFFIC	12/71	1/72	1/72	8/70	10/70	11/72	12/70	9/71	6/72	4/69	4/69	12/69	11/70	12/70	12/70	12/70
LOAD APPLICATION (TRAFFIC LANE)	Σ 18^k SINGLE AXLES (in millions)	568	.512	512	869	2.500	005	1.050	.721	324	3.059	3.059	1.403	1.088	1.127	1.127	1.053
	LOG (Σ 18^k SINGLE AXLES)	5.754	5.709	5.709	5.939	6.398	3.701	6.021	5.878	5.511	6.486	6.486	6.147	6.038	6.052	6.052	6.022
	NO OF CONCRETE PATCHES	0	12	12	0	0	0	0	0	0	0	0	0	0	1	1	1
	NO OF ASPHALT PATCHES AND BREAKUPS	0	6	8	0	2	0	1	0	0	0	0	0	0	2	2	2
	NO OF DEFECTS	0	18	20	0	2	0	1	0	0	0	0	0	0	3	3	3
NO OF CRACKS	SLIGHTLY SPALLED	4	22	41	1	15	0	1	20	49	27	2	66	13	23	20	71
	MODERATELY SPALLED	5	7	5	0	5	0	2	0	2	2	0	1	0	3	0	6
	HEAVILY SPALLED	1	4	0	0	2	0	0	0	0	0	0	0	0	0	0	0
	LENGTH OF PAVEMENT SECTION WITH CLOSE TRANSVERSE CRACKS (ft)	384	498	838	1590	864	403	599	1106	427	166	438	345	600	712	728	398
	LENGTH OF PAVEMENT SECTION SHOWING EDGE PUMPING (ft)	115	73	168	0	0	0	390	80	0	0	0	422	0	59	59	8
	CONDITION SURVEY PARTY	B	A	C	B	B	E	B	A	C	B	B	B	C	A	C	C

		17	18	19	20*	21	22	23	24	25	26	27	28	29	30	31	32
SECTION IDENTIFICATION	SECTION NO	17	18	19	20*	21	22	23	24	25	26	27	28	29	30	31	32
	HIGHWAY	I-65	I-69	I-65	I-65	I-65	I-65	I-65	I-70	I-94	I-65	I-70	I-65	I-94	I-94	I-94	I-94
	CONTRACT	R7422	R8128	R7714	R7714	R7714	R7714	R8440	R8157	R6553	R8208	R8518	R8208	R7857	R7933	R8181	R8181
	START OF SECTION	1407+00 SBL	94+00 SBL	120+00 NBL	120+00 NBL	270+00 SBL	220+00 SBL	1290+00 NBL	827+00 EBL	198+00 WBL	325+00 NBL	779+00 EBL	445+00 NBL	1201+00 EBL	1373+00 WBL	454+00 EBL	567+00 EBL
	END OF SECTION	1460+00 SBL	144+00 SBL	170+00 NBL	170+00 NBL	320+00 SBL	270+00 SBL	1340+00 NBL	880+25 EBL	250+00 WBL	375+00 NBL	832+00 EBL	465+00 NBL	1237+00 EBL	1430+00 WBL	509+00 EBL	617+00 EBL
	DATE OF CONDITION SURVEY	10/29/72	11/15/72	10/30/72	10/30/72	11/2/72	11/14/72	11/8/72	8/14/72	11/17/72	11/2/72	11/22/72	11/2/72	11/17/72	11/17/72	11/17/72	11/17/72
CONSTRUCTION VARIABLES	SLAB THICKNESS (in)	9	9	9	9	9	9	9	9	9	9	9	9	9	9	9	8
	METHOD OF PAVING	SF	SF	SF	SF	SF	SF	SF	SF	SF	SF	SF	SF	SF	SF	SF	SF
	METHOD OF STEEL PLACEMENT	CH	CH	CH	CH	CH	CH	DP	DP	DP	DP	DP	DP	DP	DP	DP	DP
	TYPE OF STEEL REINFORCEMENT	WF	WF	WF	WF	WF	WF	LB	BM	BM	WF	WF	WF	WF	WF	WF	WF
	TYPE OF SUB-BASE	GR	GR	ST/GR	ST/GR	ST/GR	ST/GR	BS	GR	SL	GR	GR	OR	SL/GR	GR	ST/SL	ST/SL
	SUBGRADE PARENT MATERIAL	F	F	F	F	C	F	F	F	F	F	F	C	F	F	F	C
	SLUMP (in)	1.25	1.75	1.25	1.25	1.25	1.25	2.25	2.0	1.5	1.25	1.75	1.25	2.0	1.5	2.0	2.0
	NO OF LANES	4	6	4	4	4	4	6	6	8	4	6	4	6	6	6	6
PERFORMANCE VARIABLES	DATE PAVED	6/70	8/71	7/70	7/70	8/70	8/70	5/72	6/71	8/72	8/71	11/71	8/71	6/71	10/71	7/72	7/72
	DATE OPENED TO TRAFFIC	12/70	11/71	7/71	7/71	7/71	7/71	6/72	NT	11/72	12/71	NT	12/71	11/72	10/72	11/72	11/72
LOAD APPLICATION (TRAFFIC LANE)	Σ 18^k SINGLE AXLES (in millions)	1.038	1.106	655	655	659	659	320	NT	004	657	NT	567	007	100	004	004
	LOG (Σ 18^k SINGLE AXLES)	6.016	6.044	5.816	5.816	5.819	5.819	5.506	NT	3.618	5.755	NT	5.753	3.848	4.999	3.630	3.630
	NO OF CONCRETE PATCHES	0	0	0	0	0	0	0	0	0	0	0	0	0	0	0	0
	NO OF ASPHALT PATCHES AND BREAKUPS	1	0	0	0	0	1	0	0	0	1	0	1	0	2	0	0
	NO OF DEFECTS	1	0	0	0	0	1	0	0	0	1	0	1	0	2	0	0
NO OF CRACKS	SLIGHTLY SPALLED	155	14	82	63	205	46	27	1	0	67	0	57	0	0	0	0
	MODERATELY SPALLED	5	5	2	2	1	4	1	0	0	1	0	1	0	0	0	0
	HEAVILY SPALLED	0	7	0	0	0	3	0	0	0	0	0	1	0	0	0	0
	LENGTH OF PAVEMENT SECTION WITH CLOSE TRANSVERSE CRACKS (ft)	724	1523	425	412	579	285	280	558	130	945	34	440	229	100	551	257
	LENGTH OF PAVEMENT SECTION SHOWING EDGE PUMPING (ft)	0	16	0	0	0	0	0	0	0	0	0	20	0	20	38	0
	CONDITION SURVEY PARTY	C	B	C	A	C	B	C	B	E	C	B	A	E	E	E	E

TABLE A I, contd.

	SECTION NO	33	34	35	36	37	38*	39	40	41	42	43	44	45	46	47	48*	49	50	51	52	53	54	55	56	57*	58	59	60	61	62	63	64
SECTION IDENTIFICATION	HIGHWAY	I-94	I-94	I-65	I-65	I-65	I-65	I-465	I-465	I-65	I-65	I-65	I-65	I-65	I-65	I-65	I-65	I-94	SR-37	I-65	I-65	I-65	US-30	US-30	US-31	US-31	US-31	US-30	US-30	US-41	US-31	US-31	US-31
	CONTRACT	R7525	R7525	R7715	R7715	R7913	R7913	R7276	R7596	R8208	R7715	R7782	R7782	R7913	R7634	R7634	R7634	R7883	R8776	R8159	R7912	R7674	R7628	R7842	R7859	R7859	R8312	R7915	R7915	R8182	R8750	R8750	R8733
	START OF SECTION	960+00 WBL	925+00 EBL	431+00 SBL	480+00 SBL	580+00 SBL	580+00 SBL	566+00 EBL	720+00 SBL	460+00 SBL	420+00 NBL	110+00 NBL	175+00 NBL	691+00 SBL	680+00 NBL	839+00 NBL	641+00 NBL	1536+00 EBL	1215+00 SBL	210+00 NBL	670+00 NBL	3720+00 SBL	840+00 WBL	903+00 WBL	324+00 SBL	324+00 SBL	191+00 NBL	988+00 EBL	1103+00 EBL	260+00 NBL	1470+00 NBL	1350+00 NBL	1180+00 SBL
	END OF SECTION	1010+00 WBL	975+00 EBL	481+00 SBL	550+00 SBL	630+00 SBL	630+00 SBL	630+30 EBL	770+00 SBL	510+00 SBL	470+00 NBL	160+00 NBL	225+00 NBL	745+00 SBL	730+00 NBL	889+00 NBL	691+00 NBL	1592+00 EBL	1265+00 SBL	260+00 NBL	720+00 NBL	3770+00 SBL	690+00 WBL	953+00 WBL	374+00 SBL	374+00 SBL	241+00 NBL	1038+00 EBL	1153+00 EBL	330+00 NBL	1520+00 NBL	1400+00 NBL	1230+00 SBL
	DATE OF CONDITION SURVEY	12/7/72	12/7/72	11/1/72	11/1/72	10/30/72	10/30/72	11/8/72	11/8/72	10/30/72	11/3/72	11/2/72	11/1/72	10/27/72	11/14/72	11/14/72	11/14/72	11/17/72	11/9/72	11/21/72	11/6/72	11/21/72	11/16/72	11/16/72	11/16/72	11/16/72	11/14/72	11/16/72	11/16/72	11/8/72	11/16/72	11/15/72	11/22/72
CONSTRUCTION VARIABLES	SLAB THICKNESS (in)	9	9	9	9	9	9	9	9	9	9	9	9	9	9	9	9	9	8	8	8	6	6	6	8	6	8	8	6	8	8	8	8
	METHOD OF PAVING	F	F	F	F	F	F	F	F	F	F	F	F	F	F	F	F	F	SF	SF	SF	SF	SF	SF	SF	SF	SF	SF	SF	SF	SF	SF	SF
	METHOD OF STEEL PLACEMENT	CH	CH	CH	CH	DP	DP	DP	DP	DP	DP	DP	DP	DP	DP	DP	DP	DP	CH	CH	CH	CH	CH	CH	CH	CH	CH	CH	CH	CH	DP	DP	DP
	TYPE OF STEEL REINFORCEMENT	BM	BM	WF	WF	WF	WF	WF	WF	WF	WF	WF	WF	WF	WF	WF	WF	WF	LB	LB	LB	BM	BM	BM	WF	WF	WF	WF	WF	WF	LB	LB	LB
	TYPE OF SUB-BASE	ST/SL	ST/SL	GR	GR	GR	GR	GR	GR	GR	GR	GR	GR	GR	ST	ST	ST	SL	BS	BS	GR	BS	GR	GR	GR	GR	GR	GR	GR	ST	BS	BS	BS
	SUBGRADE PARENT MATERIAL	F	C	F	C	F	F	F	F	F	F	F	C	C	F	C	C	F	F	C	F	F	F	F	F	F	F	F	C	F	F	C	C
	SLUMP (in)	3.0	3.0	2.0	2.0	3.67	3.67	2.5	2.5	1.25	2.0	2.5	2.5	3.67	2.50	2.5	2.5	2.5	1.75	1.36	2.25	2.4	1.75	1.75	2.0	2.0	2.0	2.0	2.0	1.5	2.0	2.0	2.0
	NO OF LANES	6	8	4	4	4	4	6	6	4	4	4	4	4	4	4	4	6	4	4	4	4	4	4	4	4	4	4	4	2	4	4	4
PERFORMANCE VARIABLES	DATE PAVED	9/68	8/68	10/69	10/69	10/70	10/70	7/68	5/69	10/70	5/70	8/70	8/70	10/70	6/69	7/69	7/69	8/70	6/72	7/70	6/70	10/69	10/65	5/70	7/70	7/70	5/71	8/70	8/70	9/70	7/72	7/72	7/72
	DATE OPENED TO TRAFFIC	6/69	8/69	9/71	11/71	11/71	11/71	4/69	10/89	12/71	11/71	9/71	9/71	9/71	11/69	11/69	11/69	9/71	9/72	6/72	6/72	6/72	7/70	10/70	8/70	8/70	6/71	11/70	11/70	6/71	NT	NT	NT
LOAD APPLICATION (TRAFFIC LANE)	Σ 18ᴷ SINGLE AXLES (in millions)	3.398	3.398	0.421	0.421	0.670	0.670	6.269	3.967	0.561	0.736	0.721	0.719	0.674	1.129	1.129	1.129	1.076	0.028	0.306	0.308	0.303	0.965	0.873	1.051	1.051	0.613	0.799	0.799	0.193	NT	NT	NT
	LOG (Σ 18ᴷ SINGLE AXLES)	6.531	6.531	5.624	5.624	5.826	5.826	6.799	6.598	5.749	5.867	5.638	5.857	5.629	6.053	6.053	6.053	6.032	4.449	5.485	5.486	5.482	5.985	5.941	6.022	6.022	5.788	5.903	5.903	5.285	NT	NT	NT
	NO OF CONCRETE PATCHES	0	0	0	0	0	0	0	0	0	0	0	0	0	0	0	0	0	0	0	0	0	0	0	0	0	0	0	0	0	0	0	0
	NO OF ASPHALT PATCHES AND BREAKUPS	0	1	1	0	0	0	0	0	0	1	0	0	0	0	0	0	0	0	0	0	0	1	7	0	0	0	2	0	0	0	0	0
	NO OF DEFECTS	0	1	1	0	0	0	0	0	0	1	0	0	0	0	0	0	0	0	0	0	0	1	7	0	0	0	2	0	0	0	0	0
NO OF CRACKS	SLIGHTLY SPALLED	43	51	41	69	0	13	8	16	11	173	91	15	30	73	10	0	0	0	0	8	0	70	36	67	73	32	2	20	5	0	0	0
	MODERATELY SPALLED	1	2	8	3	1	0	0	3	6	1	0	0	6	0	0	0	0	0	0	0	0	14	11	10	0	9	0	5	0	0	0	0
	HEAVILY SPALLED	0	1	17	2	0	0	0	0	1	0	0	0	0	0	0	0	2	0	0	0	0	1	0	0	0	0	0	0	0	0	0	0
	LENGTH OF PAVEMENT SECTION WITH CLOSE TRANSVERSE CRACKS (ft)	911	621	439	279	288	288	1735	660	173	1265	672	750	223	551	420	504	519	137	635	993	703	192	629	423	413	391	694	1014	120	169	6	291
	LENGTH OF PAVEMENT SECTION SHOWING EDGE PUMPING (ft)	0	0	538	0	0	0	20	128	0	10	0	0	0	2	0	0	0	0	0	0	0	470	595	35	110	1210	365	0	0	0	0	0
	CONDITION SURVEY PARTY	C	C	A	B	C	A	B	B	B	C	C	B	B	C	A	B	E	C	A	C	A	B	D	A	C	A	D	D	A	C	C	C

TABLE A 1, contd

		65	66	67	68	69	70	71	72	73	74	75	76	77	78	79	80
SECTION IDENTIFICATION	SECTION NO	65	66	67	68	69	70	71	72	73	74	75	76	77	78	79	80
	HIGHWAY	US-31	US-41	US-31	US-31	US-30	SR-49	SR-49	SR-49	SR-49	SR-42	I-65	SR-67	SR-37	US-31	US-41	US-41
	CONTRACT	R8750	R6515	R8750	R8733	R8296	R7933	R7885	R7885	R7884	R7984	R8221	R8512	R8815	R8312	R8182	R8182
	START OF SECTION	1510+00 SBL	400+00 SBL	1380+00 SBL	1200+00 NBL	1633+00 EBL	340+00 SBL	313+00 NBL	304+00 SBL	226+00 NBL	224+00 SBL	511+00 SBL	678+00 NBL	155+00 SBL	141+00 SBL	180+00 SBL	130+00 SBL
	END OF SECTION	1560+00 SBL	450+00 SBL	1430+00 SBL	1260+00 NBL	1683+00 EBL	423+00 SBL	363+00 NBL	340+00 SBL	280+00 NBL	276+00 SBL	561+00 SBL	728+00 NBL	205+00 SBL	194+00 SBL	230+00 SBL	180+00 SBL
	DATE OF CONDITION SURVEY	11/21/72	11/21/72	11/21/72	11/15/72	11/15/72	11/6/72	11/15/72	11/16/72	11/15/72	11/16/72	11/8/72	11/21/72	11/9/72	11/16/72	11/8/72	11/9/72
CONSTRUCTION VARIABLES	SLAB THICKNESS (in)	8	8	8	8	8	8	8	8	8	8	8	8	8	8	8	8
	METHOD OF PAVING	SF	SF	SF	SF	SF	SF	SF	SF	SF	SF	SF	SF	SF	SF	SF	SF
	METHOD OF STEEL PLACEMENT	DP	DP	DP	DP	DP	DP	DP	DP	DP	DP	DP	DP	DP	DP	DP	DP
	TYPE OF STEEL REINFORCEMENT	BM	BM	BM	BM	BM	BM	BM	BM	BM	BM	WF	WF	WF	WF	WF	WF
	TYPE OF SUB-BASE	BS	BS	BS	BS	GR	SL	SL	SL	SL	SL	BS	BS	BS	GR	ST	ST
	SUBGRADE PARENT MATERIAL	F	F	C	C	C	F	F	F	C	C	F	F	F	F	F	F
	SLUMP (in)	2.0	1.63	2.0	2.0	1.5	1.5	1.75	1.75	1.75	1.75	2.08	1.125	1.25	2.0	1.5	1.5
	NO OF LANES	4	4	4	4	4	4	4	4	4	4	4	4	4	4	4	4
PERFORMANCE VARIABLES	DATE PAVED	7/72	7/72	7/72	7/72	5/72	10/71	8/71	5/71	8/71	10/71	7/71	6/72	8/72	5/71	9/70	9/70
	DATE OPENED TO TRAFFIC	NT	NT	NT	NT	8/72	12/71	12/71	12/71	12/71	12/71	6/72	NT	10/72	8/71	6/71	8/71
LOAD APPLICATION (TRAFFIC LANE)	Σ 18" SINGLE AXLES (in millions)	NT	NT	NT	NT	0.103	0.173	0.145	0.145	0.096	0.096	0.307	NT	0.012	0.613	0.273	0.273
	LOG (Σ 18" SINGLE AXLES)	NT	NT	NT	NT	5.015	5.237	5.161	5.161	4.979	4.979	5.488	NT	4.098	5.787	5.436	5.436
	NO OF CONCRETE PATCHES	0	0	0	0	0	1	0	0	0	0	0	0	0	0	0	0
	NO OF ASPHALT PATCHES AND BREAKUPS	0	0	0	0	2	0	0	0	4	1	0	0	0	3	0	0
	NO OF DEFECTS	0	0	0	0	2	1	0	0	4	1	0	0	0	3	0	0
NO OF CRACKS	SLIGHTLY SPALLED	0	2	1	2	8	1	2	0	0	3	0	0	1	8	18	5
	MODERATELY SPALLED	0	0	0	0	0	0	0	0	5	0	0	0	0	2	2	0
	HEAVILY SPALLED	0	0	0	0	1	1	2	0	1	3	0	0	0	5	0	0
	LENGTH OF PAVEMENT SECTION WITH CLOSE TRANSVERSE CRACKS (ft)	51	117	145	25	42	145	310	288	324	148	212	234	102	428	284	126
	LENGTH OF PAVEMENT SECTION SHOWING EDGE PUMPING (ft)	0	0	0	0	0	0	0	0	0	0	0	0	0	0	0	0
	CONDITION SURVEY PARTY	C	D	C	C	D	E	E	E	E	E	A	E	C	A	A	A

		81	82	83	84	85	86	87	88	89	90	91	92	93	94	95
SECTION IDENTIFICATION	SECTION NO	81	82	83	84	85	86	87	88	89	90	91	92	93	94	95
	HIGHWAY	US-31	I-74	I-65	US-30	US-30	US-31	SR-37	SR-37	SR-37	SR-37	SR-37	SR-46	US-460	US-460	SR-37
	CONTRACT	R7828	R8025	R7780	R7966	R7966	R7858	R8647	R8369	R8525	R8211	R8521	R8233	R7625	R7698	R8212
	START OF SECTION	721+00 SBL	498+00 EBL	405+00 SBL	1229+00 WBL	1409+00 EBL	270+00 NBL	950+00 NBL	700+00 SBL	805+00 SBL	350+00 SBL	600+00 NBL	505+00 WBL	815+00 EBL	1007+00 EBL	462+00 NBL
	END OF SECTION	771+00 SBL	548+00 EBL	455+00 SBL	1279+00 WBL	1459+00 EBL	320+00 NBL	1000+00 NBL	750+00 SBL	855+00 SBL	400+00 SBL	650+00 NBL	553+00 WBL	865+00 EBL	1047+00 EBL	512+00 NBL
	DATE OF CONDITION SURVEY	11/14/72	11/8/72	11/14/72	11/10/72	11/15/72	11/14/72	11/20/72	11/17/72	11/22/72	11/13/72	11/22/72	11/13/72	11/3/72	11/3/72	11/22/72
CONSTRUCTION VARIABLES	SLAB THICKNESS (in)	8	8	8	8	8	8	7	7	7	7	7	7	7	7	7
	METHOD OF PAVING	F	F	F	F	F	F	SF	SF	SF	SF	SF	SF	SF	SF	SF
	METHOD OF STEEL PLACEMENT	CH	CH	CH	DP	DP	DP	CH	CH	CH	CH	CH	CH	CH	CH	DP
	TYPE OF STEEL REINFORCEMENT	WF	WF	WF	BM	BM	WF	LB	LB	LB	LB	LB	LB	BM	BM	WF
	TYPE OF SUB-BASE	GR	GR	GR	GR	GR	GR	ST	ST	ST	ST	ST	ST	GR	GR	ST
	SUBGRADE PARENT MATERIAL	F	F	F	F	C	F	F	F	F	F	F	F	F	F	F
	SLUMP (in)	2.0	2.0	2.5	2.5	2.5	2.0	2.0	1.25	1.75	1.8	2.0	1.5	1.5	1.625	1.0
	NO OF LANES	4	4	8	4	4	4	4	4	4	4	4	4	4	4	4
PERFORMANCE VARIABLES	DATE PAVED	9/68	4/64	7/70	6/70	11/69	11/69	5/72	8/72	5/72	8/71	8/72	6/71	5/70	8/70	6/71
	DATE OPENED TO TRAFFIC	9/68	10/64	11/70	8/72	8/72	4/70	7/72	9/72	8/72	9/72	7/72	6/72	11/70	11/70	11/71
LOAD APPLICATION (TRAFFIC LANE)	Σ 18" SINGLE AXLES (in millions)	1.771	2.701	0.927	0.103	0.103	1.301	0.047	0.022	0.033	0.025	0.039	0.080	0.363	0.876	0.129
	LOG (Σ 18" SINGLE AXLES)	6.248	6.432	5.967	5.013	5.015	6.114	4.670	4.347	4.525	4.370	4.597	4.902	5.583	5.942	5.111
	NO OF CONCRETE PATCHES	0	1	0	0	0	0	0	0	0	0	0	0	0	0	0
	NO OF ASPHALT PATCHES AND BREAKUPS	0	10	0	1	1	0	0	0	0	0	0	0	1	1	1
	NO OF DEFECTS	0	11	0	1	1	0	0	0	0	0	0	0	1	1	1
NO OF CRACKS	SLIGHTLY SPALLED	17	34	8	10	8	38	0	0	0	3	0	3	53	8	4
	MODERATELY SPALLED	0	21	0	0	0	15	0	0	0	0	0	0	3	1	0
	HEAVILY SPALLED	0	6	0	0	0	0	0	0	0	0	0	0	2	1	0
	LENGTH OF PAVEMENT SECTION WITH CLOSE TRANSVERSE CRACKS (ft)	460	1008	366	500	324	498	79	230	230	127	108	225	691	115	306
	LENGTH OF PAVEMENT SECTION SHOWING EDGE PUMPING (ft)	0	0	0	59	441	755	0	0	50	0	0	0	0	212	0
	CONDITION SURVEY PARTY	A	D	B	D	D	A	C	C	A	C	A	C	D	D	A

APPENDIX B

TEST OF ASSUMPTIONS UNDERLYING THE ANALYSIS OF STATEWIDE CRCP CONDITION SURVEY DATA

APPENDIX B

Testing the Covariance Analysis Model Used in the Analysis of Statewide Condition Survey Data for Restrictions on Randomization

The following analysis of covariance model was used for analyzing the statewide condition survey data:

$$Y_{ijk\ell mp} = \mu + A_i + B_j + C_k + D_\ell + F_m + AB_{ij} + AC_{ik} + AD_{i\ell} + AF_{im} + BC_{jk} + BD_{j\ell} + BF_{jm} + CD_{k\ell} + CF_{km} + DF_{\ell m} + \beta_1(S_{ijk\ell mp} - \overline{S}) + \beta_2(T_{ijk\ell mp} - \overline{T}) + \varepsilon_{(ijk\ell m)p} \qquad (B1)$$

where

$Y_{ijk\ell mp}$ = dependent variable, e.g., number of defects per section,

μ = true mean effect for the population,

A_i = true effect of method of paving (slip-formed vs. side-formed),

B_j = true effect of method of steel placement (depressor vs. chairs),

C_k = true effect of method of steel fabrication (bar mats vs. wire fabric vs. loose bars),

D_ℓ = true effect of type of subbase (bituminous stabilized vs. crushed stone vs. slag vs. gravel),

F_m = true effect of subgrade soil (granular vs. fine-grained),

$S_{ijk\ell mp}$ = linear effect of covariate, slump (in),

$T_{ijk\ell mp}$ = linear effect of covariate, number of months of traffic,

β_1, β_2 = regression coefficients,

$\overline{S}, \overline{T}$ = mean values of slump and traffic respectively,

$\varepsilon_{(ijk\ell m)p}$ = true error, NID (o, σ^2)

The other terms denote the two-factor interactions between the factors, A, B, C, D,and F. The subscripts assume the values:

$i = 1,2$

$j = 1,2$

$k = 1,2,3$

$\ell = 1,2,3,4$

$m = 1,2$

$p = 0$ (missing value), or

$1,2.....n_{ijk\ell m}$ (unequal sub-class numbers)

This model was based on a 2x2x3x4x2 completely randomized factorial design (CRD). For the factors included in the model, complete randomization was attained. However, the data derived from the statewide condition survey was collected by five survey parties. Since a factor to represent the variation among parties was not included in the model, it is hypothesized that a restriction on randomization may have been caused by this missing factor.

To test the null hypothesis,

H_o: No restriction error due to the effect of survey parties, a check study was conducted in which each of the five survey parties (designated as A, B, C, D, and E) was required to evaluate four randomly selected test sections in terms of the response variables used in the statewide condition survey. The data resulting from this check study are shown in Table B 1. Next, an analysis of variance (ANOVA) was performed on these data. The ANOVA model and a summary of results, presented in Tables B 2 to B 4 show:

1. No significant difference ($\alpha = 0.05$) among parties was indicated relative to the evaluation of test sections in terms of square root of number of de-

Table B 1. Pavement Condition Data for Testing Variability Among Survey Parties

Condition Survey Party	A				B				C				D				E			
Test Section	1	2	3	4	1	2	3	4	1	2	3	4	1	2	3	4	1	2	3	4
No. of Defects* Per Section	0	5	0	3	0	6	0	3	0	5	0	3	1	7	0	3	0	8	0	3
No. of Moderately Spalled Cracks Per Section	0	3	0	2	4	3	2	12	0	5	0	3	4	5	1	7	0	0	0	0
Length of Close Random Cracks Per Section (Feet)	503	637	478	686	457	487	543	694	487	618	524	722	631	768	609	848	519	580	471	703

*Defects = Asphalt Patches + Breakups (No concrete patches observed on test sections)

Table B 2. Summary of Analysis of Variance of Defects per Section (Survey Party Variability Study)

Source	DF	Sum of Squares	Mean Square	F	$F_{.05}$	Significant at $\alpha = 0.05$
Survey Parties, A_i	4	0.351	0.087	1.46	2.91	--
Test Sections, B_j	3	21.608	7.203	120.32	3.14	yes
Error, $\varepsilon_{(ij)}$	12	0.718	0.060			
Total	19	22.677				

ANOVA Model : $Y_{ij} = \mu + A_i + B_j + \varepsilon_{(ij)}$

where Y_{ij} = square root of number of defects per section
μ = overall mean effect
A_i = effect of ith survey party, $i = 1,2,3,4,5$
B_j = effect of jth test section, $j = 1,2,3,4$
$\varepsilon_{(ij)}$ = error NID $(0, \sigma^2)$

Table B 3. Summary of Analysis of Variance of Length of Random Cracking per Section (Survey Party Variability Study)

Source	DF	Sum of Squares	Mean Square	F	$F_{.05}$	Significant at $\alpha = 0.05$
Survey Parties, A_i	4	70849.5	17712.4	11.34	2.91	yes
Test Sections, B_j	3	147447.4	49149.1	31.48	3.14	yes
Error, $\varepsilon_{(ij)}$	12	18736.9	1561.5			
Total	19	237033.8				

ANOVA Model: $Y_{ij} = \mu + A_i + B_j + \varepsilon_{(ij)}$

where Y_{ij} = length of parallel cracks less than 30 in. spacing plus random bifurcated and intersecting cracks per section (ft/section)

μ = overall mean effect

A_i = effect of ith survey party, i = 1,2,3,4,5

B_j = effect of jth test section, j = 1,2,3,4

$\varepsilon_{(ij)}$ = error, NID $(0, \sigma^2)$

Table B 4. Summary of Analysis of Variance of Spalled Cracks per Section (Survey Party Variability Study)

Source	DF	Sum of Squares	Mean Square	F	$F_{.05}$	Significant at $\alpha = .05$
Survey Parties, A_i	4	12.613	3.153	8.82	2.91	yes
Test Sections, B_j	3	6.234	2.078	5.81	3.14	yes
Error, $\varepsilon_{(ij)}$	12	4.289	0.357			
Total	19	23.137				

ANOVA Model: $Y_{ij} = \mu + A_i + B_j + \varepsilon_{(ij)}$

where Y_{ij} = square root of number of moderately spalled cracks per section

μ = overall mean effect

A_i = effect of ith survey party, $i = 1,2,3,4,5$

B_j = effect of jth test section, $j = 1,2,3,4$

$\varepsilon_{(ij)}$ = error, NID $(0, \sigma^2)$

fects per section (Table B 2). As no concrete patches were observed on any test section, the above conclusion is also valid for the response variable, number of asphalt patches and breakups per section.

2. For the response variables, number of spalled cracks and length of close random cracking per section, a significant difference among parties was indicated at an α level of 0.05 (Tables B 3 and B 4).

Since a restriction error may have resulted in analyzing the statewide condition data pertaining to spalled cracks and length of close random cracking per section, the next approach was to test if a significant difference among parties was indicated for the overall statewide condition survey.

As a first step, the condition survey sections were classified by survey party. This classification is shown in Appendix A, where each survey section is identified by a survey party (A, B, C, D, or E). Then a one-way analysis of variance was made on this classification. The results of the analysis are shown in Tables B 5 and B 6. It is shown by these results that no significant differences among parties was indicated relative to the evaluation of the response variables: number of spalled cracks and length of close random cracking per section, in the statewide condition survey.

On basis of this study the null hypothesis cannot be rejected and the assumption, that no restriction on randomization occurred due to the variation among survey parties, is considered quite valid. As such, the use of a completely randomized design was not unjustified. Nevertheless, the analysis would have been considerably more rigorous if only one survey party had been used in the statewide condition survey.

Table B 5. Summary of Analysis of Variance of Spalled Cracks per Section (Survey Party Variability Study)

Source		Sum of Squares	Mean Square	F	$F_{.05}$	Significant at $\alpha = .05$
Between Parties, A_i	4	9.31	2.33	1.89	2.49	NS
Within Error, $\varepsilon_{(i)j}$	90	110.69	1.23			
Total	94	120.01				

Notes: 1. NS = non-significant

2. Data from statewide condition survey (Appendix 1)

3. ANOVA Model: $Y_{ij} = \mu + A_i + \varepsilon_{(i)j}$

Y_{ij} = square root of number of moderately spalled cracks observed per section.

μ = overall mean effect

A_i = effect of ith survey party, $i = 1,2,3,4,5$

$\varepsilon_{(i)j}$ = error, NID $(0,\sigma^2)$, $j = 1,2,\ldots n_i$

Table B 6. Summary of Analysis of Variance of Length of Random Cracking per Section (Survey Party Variability Study)

Source	DF	Sum of Squares	Mean Square	F	$F_{.05}$	Significant at $\alpha = .05$
Between Parties, A_i	4	1095125.95	273781.49	2.31	2.49	NS
Within Error, $\varepsilon_{(i)j}$	90	10691056.53	118789.52			
Total	94	11786182.48				

Notes: 1. NS = non-significant

2. Data from statewide condition survey (Appendix 1)

3. ANOVA Model: $Y_{ij} = \mu + A_i + \varepsilon_{(i)j}$

Y_{ij} = length of parallel cracks less than 30 in. spacing plus random and bifurcated cracks per section (ft/section)

μ = overall mean effect

A_i = effect of ith survey party, $i = 1,2,3,4,5$

$\varepsilon_{(i)j}$ = error, NID $(0, \sigma^2)$, $j = 1,2,\ldots n_i$

Assumptions Underlying Analysis of Covariance

The analysis of covariance of statewide condition survey data, was based on the following assumptions:

1. Homogeneity of variance within groups.
2. Normality.
3. Normally and independently distributed errors.
4. Additivity among true effects.
5. The regression is linear and the resulting regression coefficient is non-zero.
6. The regression coefficients, within each group, are homogeneous.
7. The independent covariate, X, is not affected by the independent factors or treatments of the experimental design such as method of paving, type of steel or a treatment combination (interaction).

Testing the Assumptions Underlying Analysis of Covariance

Homogeneity of Variance Within Groups: This was tested by the Q-test (7,14). The results of the test have been presented earlier (Table 3). For some response variables, a square root transformation was made to satisfy this requirement.

Normality: Because of insufficient data within groups this assumption could not be tested. A square-root transformation for obtaining homogeneity of variance also tends to normalize the data if non-normality is suspected for the original data. Even otherwise, data in which the effects of the fixed factors are modest, non-normality does not distort the conclusions too seriously (55).

Additivity: Any non-additivity due to two-factor interactions was accounted for in the analysis. Owing to limitations of the computer program, higher order interaction effects could not be tested and were confounded with the error term. It was further assumed that the effect of covariates was additive to the effect of other factors.

Linear Regression: The least squares maximum likelihood procedure used in the analysis permits the user to specify that only the linear effect of the covariate be incorporated in the analysis. Hence the analysis is based on linear regression.

Non-Zero Regression Coefficients: Tests were made to determine if the gression coefficients obtained from the covariance analyses were significantly different from zero. A summary of the test results is shown in Table B 7.

Homogeneity of Regression Coefficients Within Groups: This was established by the test procedures described by Ostle (49). The null hyposhesis for this assumption is:

$$H_0: \beta_1 = \beta_2 = \beta_3 = \dots = \beta_n$$

where β_i = within group regression coefficient, $i=1,2,\dots n$.
n = number of groups.

To test this assumption at least 3 observations per group are required. Homogeneity of regression coefficients within groups was indicated for all covariates. For sake of brevity, typical test results for only one set of data are shown in Table B 8.

Covariates (X's) Not Influenced by Treatments: To test this assumption, analyses of variance were performed using the covariates time and slump as dependent variables. A summary of results is shown in Tables B 9 and B 10.

For the covariate, time, no main effect or interaction was significant at an α-level of 0.05. As expected, the time a pavement section had been open to traffic had no bearing on construction methods or types of material.

On the contrary, the covariate slump was shown to be significantly related to the method of steel placement, the interaction between methods of paving and steel placement, and the interaction between types of steel and subbase.

These results are not too unusual as the slump of concrete used with various types of construction does vary. For instance, a stiffer concrete with a relatively low slump is commonly used in slipform paving as compared to conventional paving with side forms. The variation of slump with method of construction is tabulated in Table B 11.

In the statewide condition study, higher values of slump were shown to have a beneficial effect on performance. This conclusion needs a slight modification as the use of concrete with higher slump may require changing the method of construction.

According to Ostle (49), this assumption is too restrictive. The results of covariance analysis do not need major modification as long as proper care is exercised in interpreting the results.

Table B 7. Hypothesis Tests for Non-Zero Regression Coefficients in Covariance Analysis of Statewide Condition Survey Data

Null Hypothesis $H_o : \beta = 0$

Alternate Hypothesis $H_1 : \beta \neq 0$

No.	Dependent Variable, Y	Covariate X	b	St'd Error of b (s.e.)	DF	$t=\frac{\lvert b \rvert}{s.e.}$	$t_{(\alpha/2, DF)}$	Null Hypothesis
1.	Sq. Root of Number of Defects per Section	Slump (in)	-0.582	0.234	65	2.487	.997	Reject(α=.05)
2.	Sq. Root of Number of Asphalt Patches and Breakups per Section	Time (months)	0.015	0.007	65	2.143	1.997	Reject(α=.05)
3.	Sq. Root of Number of Spalled Cracks per Section	Slump (in)	-0.534	0.315	64	1.724	1.669	Reject(α=.10)
		Time (months)	0.022	0.011	64	2.000	1.998	Reject(α=.C5)
4.	Length of Pavement Sections with Close Random Cracks (ft/section)	Time (months)	6.289	3.159	65	1.991	1.669	Reject(α=.10)*

*Borderline at α = 0.05.

Table B 8. Test for Homogeneity of Regression Coefficients Within Groups

Y = Square root of number of asphalt patches and breakups per section

X = Time (months of traffic since pavement section opened to traffic)

Null Hypothesis $H_o : \beta_1 = \beta_2 = \beta_3 = \ldots\ldots.\beta_7$

(Note: Only groups with at least one non-zero value (y's) were included)

Group	Degrees of Freedom	Σx^2	Σxy	$\Sigma\ ^2$	$\Sigma y^2-(\Sigma xy)^2/\Sigma x^2$	Degrees of Freedom	Mean Square
1	4	393.2	-14.98	7.05	6.48	3	--
2	10	1295.0	-5.41	8.66	8.64	9	--
3	8	252.0	11.60	3.56	3.03	7	--
4	3	175.7	12.36	2.13	1.26	2	--
5	3	4766.0	154.12	6.66	1.68	2	--
6	7	1123.5	-8.25	0.88	0.82	6	--
7	3	181.7	0.38	0.75	0.75	2	--
					22.66	31	0.731
Within Groups Total	38	8187.1	29.69		26.95	37	0.728

$$F = \frac{(26.95-22.66)/(37-31)}{22.66/31} = 0.98$$

$$F_{crit.} = F_{(.05,6,31)} = 3.82$$

Do not reject null hypothesis

$\therefore \beta_1 = \beta_2 = \beta_3 = \ldots\ldots\ \beta_7$

Table B 9. Least Squares Analysis of Variance -- Time*

Source	DF	Sum of Squares	Mean Square	F	$F_{.05}$	Significant at $\alpha = .05$
Total (Uncorrected)	95	21159.04				
Main Effects:						
A_i (Paving)	1	169.07	169.07	1.232	3.99	---
B_j (Placement)	1	368.83	368.83	2.687	3.99	---
C_k (Steel)	2	106.70	53.35	.389	3.14	---
D_ℓ (Subbase)	3	186.70	62.23	.453	2.75	---
F_m (Subgrade)	1	105.84	105.84	.771	3.99	---
Interaction Effects:						
AB_{ij}	1	.34	.34	.002	3.99	---
AC_{ik}	1	64.11	64.11	.467	3.99	---
$AD_{i\ell}$	2	293.24	146.62	1.068	3.14	---
AF_{im}	1	128.22	128.22	.934	3.99	---
BC_{jk}	2	132.45	66.22	.482	3.14	---
$BD_{j\ell}$	2	279.06	139.53	1.016	3.14	---
BF_{jm}	1	49.40	49.40	.360	3.99	---
$CD_{k\ell}$	5	429.08	85.82	.625	2.36	---
CF_{km}	2	51.09	25.54	.186	3.14	---
$DF_{\ell m}$	3	25.71	8.57	.062	2.75	---
Remainder, $\varepsilon_{(ijk\ell m)p}$	66	9060.18	137.28			

Note: Symbols as defined in Equation B1.
*Number of months since pavement section was opened to traffic.

Table B 10. Least Squares Analysis of Variance - Slump (in.)

Source	DF	Sum of Squares	Mean Square	F	$F_{.05}$	Significant at $\alpha = .05$
Total (Uncorrected)	95	28.00				
Main Effects:						
A_i (Paving)	1	.09	.086	.529	3.99	---
B_j (Placement)	1	1.69	1.688	10.421	3.99	yes
C_k (Steel)	2	.25	.123	.759	3.14	---
D_ℓ (Subbase)	3	1.10	.367	2.267	2.75	---
F_m (Subgrade)	1	.002	.002	.013	3.99	---
Interaction Effects:						
AB_{ij}	1	.99	.994	6.132	3.99	yes
AC_{ik}	1	.11	.107	.660	3.99	---
$AD_{i\ell}$	2	.20	.099	.612	3.14	---
AF_{im}	1	.07	.066	.408	3.99	---
BC_{jk}	2	.75	.375	2.313	3.14	---
$BD_{j\ell}$	2	.70	.352	2.173	3.14	---
BF_{jm}	1	.02	.020	.122	3.99	---
$CD_{k\ell}$	5	2.20	.440	2.716	2.36	yes
CF_{km}	2	.17	.087	.538	3.14	---
$DF_{\ell m}$	3	.07	.023	.141	2.75	---
Remainder, $\varepsilon_{(ijk\ell m)p}$	66	10.69	.1620			

Note: Symbols as defined in Equation B1.

Table B 11. Variation of Concrete Slump with Method of Construction

Method of Paving	Slipformed		Sideformed	
Method of Steel Placement	Chairs	Depressor	Chairs	Depressor
Number of Sections	38	30	7	14
Mean **Value** of Slump (in)	1.63	1.72	2.36	2.51
Standard Error of the Mean	0.065	0.073	0.152	0.108

APPENDIX C

SUMMARY OF DETAILED FIELD EVALUATION STUDY DATA

Table Cl. Section and Test Location Identification Data.

Section	Contract	Interstate Highway	Section	Limits	Test Location 1		Test Location 2	
					Number	Station	Number	Station
S1	R-7841	I-465	914+00	— 924+00 EBL	L1-F*	914+25	L2	919+50
S2**	R-7529	I-465	236+00	— 246+00 EBL	L3	239+95	L4	243+89
S3	R-8476	I-94	1789+00	— 1798+00 EBL	L5	1789+67	L6-F	1793+85
S4	R-8232	I-65	202+00	— 212+00 NBL	L7	203+00	L8-F	211+30
S5	R-8001	I-65	1037+00	— 1047+00 NBL	L9	1038+32	L10-F	1040+10
S6	R-7677	I-65	976+00	— 986+00 SBL	L11-F	985+00	L12	980+73
S7	R-7677	I-65	852+00	— 862+00 SBL	L13	853+55	L14	859+63
S8	R-7858	I-65	1332+00	— 1342+00 NBL	L15	1336+92	L16	1333+27
S9	R-7676	I-65	505+00	— 515+00 SBL	L17	505+60	L18	508+13
S10	R-7676	I-65	435+00	— 445+00 SBL	L19-F	442+79	L20	438+00
S11	R-7633	I-65	1240+00	— 1250+00 SBL	L21-F	1247+36	L22	1240+53
S12	R-8128	I-69	121+00	— 131+00 NBL	L23-F	125+63	L24	128+50
S13	R-7422	I-65	1624+00	— 1634+00 SBL	L25	1632+54	L26-F	1628+36
S14	R-7714	I-65	244+00	— 254+00 SBL	L27	251+87	L28-F	245+37
S15	R-8440	I-65	1318+00	— 1328+00 NBL	L29	1319+61	L30	1322+86
S16	R-8137	I-70	807+00	— 817+00 EBL	L31	810+00	L32	814+00

* F = structurally failed location.

** Pavement slab thickness = 8 in. (excluded from analysis of pavement deflections and related variables). Nominal slab thickness on all other sections = 9 in.

Table C1. Continued.

Section	Contract	Interstate Highway	Section	Limits	Test Location 1		Test Location 2	
					Number	Station	Number	Station
S17	R-8553	I-94	255+00	— 265+00 EBL	L33	259+68	L34	258+90
S18	R-7933	I-94	1305+00	— 1315+00 WBL	L35	1306+70	L36	1309+00
S19	R-8208	I-65	384+00	— 394+00 NBL	L37	392+00	——	——
S20	R-8181	I-94	505+00	— 515+00 WBL	L38	506+96	L39	510+80
S21	R-7857	I-94	1180+00	— 1190+00 EBL	L40	1180+64	L41	1184+50
S22	R-7525	I-94	983+00	— 993+00 EBL	L42	986+50	L43	989+00
S23	R-7715	I-65	436+00	— 446+00 SBL	L44	437+00	L45-F*	439+61
S24	R-7715	I-65	485+00	— 495+00 SBL	L46	493+57	——	——
S25	R-7715	I-65	410+00	— 420+00 NBL	L47-S**	415+70	L48	413+00
S26	R-7782	I-65	189+00	— 199+00 SBL	L49	192+55	L50-F	196+00
S27	R-7913	I-65	730+00	— 740+00 SBL	L51	735+00	——	——
S28	R-7913	I-65	598+00	— 608+00 NBL	L52	602+07	——	——
S29	R-7634	I-65	699+00	— 709+00 NBL	L53	701+94	——	——
S30	R-7883	I-94	1485+00	— 1495+00 WBL	L54	1490+05	L55-F	1494+17
S31	R-7677	I-65	976+00	— 986+00 NBL	L56	979+54	——	——

* F = structurally failed location.

** S = location with spalled cracks (incipient failure condition).

Table C2. Construction Variables

Section	Method of Paving	Method of Steel Placement	Type of Steel Reinforcement	Type of Sub-base	Concrete Slump (in.)
S1	Slipformed	Chairs	Loose Bars	Gravel	1.25
S2	Slipformed	Chairs	Loose Bars	Gravel	1.67
S3	Slipformed	Chairs	Loose Bars	Crushed Stone	1.50
S4	Slipformed	Chairs	Loose Bars	Bituminous Stabilized	1.56
S5	Slipformed	Chairs	Bar Mats	Gravel	2.05
S6	Slipformed	Chairs	Bar Mats	Gravel	1.50
S7	Slipformed	Chairs	Bar Mats	Gravel	1.50
S8	Slipformed	Chairs	Bar Mats	Gravel	1.38
S9	Slipformed	Chairs	Bar Mats	Gravel	1.50
S10	Slipformed	Chairs	Bar Mats	Gravel	1.50
S11	Slipformed	Chairs	Wire Fabric	Gravel	1.50
S12	Slipformed	Chairs	Wire Fabric	Gravel	1.75
S13	Slipformed	Chairs	Wire Fabric	Gravel	1.25
S14	Slipformed	Chairs	Wire Fabric	Gravel	1.25
S15	Slipformed	Depressor	Loose Bars	Bituminous Stabilized	2.25
S16	Slipformed	Depressor	Bar Mats	Gravel	2.00

Table C2. Continued.

Section	Method of Paving	Method of Steel Placement	Type of Steel Reinforcement	Type of Sub-base	Concrete Slump (in.)
S17	Slipformed	Depressor	Bar Mats	Slag	1.50
S18	Slipformed	Depressor	Wire Fabric	Gravel	1.50
S19	Slipformed	Depressor	Wire Fabric	Gravel	1.25
S20	Slipformed	Depressor	Wire Fabric	Slag	2.00
S21	Slipformed	Depressor	Wire Fabric	Gravel	2.00
S22	Sideformed	Chairs	Bar Mats	Slag	3.00
S23	Sideformed	Chairs	Wire Fabric	Gravel	2.00
S24	Sideformed	Chairs	Wire Fabric	Gravel	2.00
S25	Sideformed	Depressor	Wire Fabric	Gravel	2.00
S26	Sideformed	Depressor	Wire Fabric	Gravel	2.50
S27	Sideformed	Depressor	Wire Fabric	Gravel	3.67
S28	Sideformed	Depressor	Wire Fabric	Gravel	3.67
S29	Sideformed	Depressor	Wire Fabric	Crushed Stone	2.50
S30	Sideformed	Depressor	Wire Fabric	Slag	2.50
S31	Slipformed	Chairs	Bar Mats	Gravel	1.50

Table C3. Traffic Data

Section	Date of Test	Date Opened to Traffic	No. of Lanes*	Load Applications in Traffic Lane	
				ΣL (Millions)**	Log ΣL
S1	6/28/73	Oct. '70	6	3.213	6.507
S2	6/26/73	Aug. '70	4	1.116	6.048
S3	6/20/73	Nov. '72	6	0.548	5.739
S4	6/14/73	Dec. '71	4	0.974	5.989
S5	6/29/73	Jun. '72	4	0.844	5.927
S6	6/ 6/73	Dec. '70	4	1.383	6.141
S7	6/ 6/73	Dec. '70	4	1.498	6.176
S8	6/13/73	Sep. '71	4	1.112	6.046
S9	5/31/73	Nov. '70	4	1.406	6.148
S10	6/ 1/73	Nov. '70	4	1.405	6.148
S11	6/ 5/73	Dec. '70	4	1.382	6.140
S12	6/28/73	Nov. '71	6	1.781	6.251
S13	6/ 5/73	Dec. '70	4	1.373	6.138
S14	6/ 4/73	Jul. '71	4	0.958	5.981
S15	6/29/73	Jun. '72	6	0.844	5.929
S16	6/26/73	Nov. '71	6	NT***	NT

* Both directions.

** L = equivalent 18-kip, single-axle load application.

*** NT = not opened to traffic.

Table C3. Continued

Section	Date of Test	Date Opened to Traffic	No. of Lanes*	Load Applications in Traffic Lane	
				ΣL (Millions)**	Log ΣL
S17	6/20/73	Nov. '72	6	0.449	5.652
S18	6/21/73	Nov. '72	6	0.658	5.818
S19	6/14/73	Dec. '71	4	0.963	5.984
S20	6/22/73	Nov. '72	6	0.470	5.672
S21	6/19/73	Nov. '72	6	0.765	5.884
S22	6/19/73	Aug. '69	6	3.922	6.594
S23	6/11/73	Sep. '71	4	1.129	6.053
S24	6/ 8/73	Sep. '71	4	1.124	6.051
S25	6/11/73	Sep. '71	4	1.129	6.053
S26	6/13/73	Sep. '71	4	1.112	6.046
S27	6/ 8/73	Sep. '71	4	1.047	6.020
S28	6/12/73	Sep. '71	4	1.040	6.017
S29	6/15/73	Nov. '69	4	1.350	6.130
S30	6/21/73	Sep. '71	6	1.621	6.210
S31	6/12/73	Dec. '70	4	1.393	6.144

* Both directions.

** L = equivalent 18-kip, single-axle load application.

Table C4. Temperature Data

Section	Date Paved	Air Temperature				Estimated Slab Temperature			
		Max*	Min**	24-Hr. Drop	Max. Drop	Max*	Min**	24-Hr. Drop	Max. Drop
S1	***6/--/70	80.7	55.0	25.7	109.0	103.7	71.4	32.3	107.4
S2	8/ 8/69	87.0	60.0	27.0	109.0	110.9	76.5	34.4	114.6
S3	7/20/72	92.0	72.0	20.0	111.0	115.3	85.2	30.1	117.0
S4	8/24/71	76.0	50.0	26.0	98.0	100.9	68.4	32.5	104.6
S5	8/11/70	81.0	65.0	16.0	99.0	106.4	79.7	26.7	107.4
S6	9/15/69	82.0	57.0	25.0	102.0	100.0	69.7	30.3	102.3
S7	10/ 3/69	76.0	56.0	20.0	96.0	90.3	65.5	24.8	92.6
S8	6/27/70	78.0	55.0	23.0	99.0	103.7	72.6	31.1	106.7
S9	5/26/70	71.0	47.0	24.0	88.0	91.9	62.7	29.2	92.2
S10	6/ 8/70	85.0	61.0	24.0	102.0	105.0	74.3	30.7	105.3
S11	8/13/69	83.0	59.0	24.0	103.0	107.6	75.5	32.1	109.9
S12	8/24/71	77.0	50.0	27.0	99.0	101.6	68.3	33.3	105.3
S13	10/21/69	62.0	35.0	27.0	82.0	74.5	47.4	27.1	76.8
S14	8/ 6/70	81.0	59.0	22.0	98.0	106.9	75.9	31.0	107.2
S15	10/ 4/71	81.0	51.0	30.0	96.0	93.5	61.9	31.6	92.5
S16	6/22/71	88.0	62.0	26.0	103.0	109.9	76.8	33.1	108.9

* Max. temperature on the day of paving.

** Min. temperature on the following day.

*** Temperature data are average values for the month.

NOTE: 1. Temperature in degrees Fahrenheit.
2. Air temperature data from Ref. 45.
3. Slab temperatures estimated by the equations in Appendix E.

Table C4. Continued.

Section	Date Paved	Air Temperature				Estimated Slab Temperature			
		Max*	Min**	24-Hr. Drop	Max. Drop	Max*	Min**	24-Hr. Drop	Max. Drop
S17	7/17/72	84.0	66.0	18.0	104.0	109.6	81.1	28.5	111.9
S18	8/ 3/71	74.0	59.0	15.0	91.0	102.3	76.1	26.2	102.6
S19	8/ 7/71	82.0	55.0	27.0	103.0	107.5	73.2	34.3	110.5
S20	5/27/71	50.0	30.0	20.0	69.0	77.4	51.4	26.0	79.1
S21	8/10/71	90.0	55.0	35.0	107.0	112.8	73.0	39.8	113.1
S22	9/23/69	86.0	61.0	25.0	103.0	100.5	70.9	29.6	100.8
S23***	10/--/69	64.2	39.5	24.7	88.0	77.8	51.6	26.2	82.8
S24	10/--/69	64.2	39.5	24.7	88.0	77.8	51.6	26.2	82.8
S25	5/--/70	75.0	52.7	22.3	99.0	91.7	64.6	27.1	96.7
S26	8/11/70	75.0	57.0	18.0	99.0	102.2	74.3	27.9	107.2
S27	10/24/70	69.0	47.0	22.0	93.0	78.4	54.8	23.6	83.4
S28	10/24/70	69.0	47.0	22.0	93.0	78.4	54.8	23.6	83.4
S29	8/20/69	80.0	61.0	19.0	97.0	104.5	76.0	28.5	104.8
S30	7/27/70	90.0	72.0	18.0	109.0	113.8	85.1	28.7	115.5
S31	9/22/69	76.0	50.0	26.0	96.0	93.8	63.7	30.1	96.1

* Max. temperature on the day of paving.

** Min. temperature on the following day.

*** Temperature data are average values for the month.

NOTE: 1. Temperature in degrees Fahrenheit
2. Air temperature data from Ref. 45.
3. Slab temperatures estimated by the equations in Appendix E.

Table C5. Summary of Dynamic Pavement Deflection Data (obtained along the lane center-line at 100 ft. intervals)

Section	Test Position	Dynamic Pavement Deflection at 100 ft. Intervals (milli-in.)										
		1	2	3	4	5	6	7	8	9	10	11
S1	C*	0.51	0.49	0.76	0.47	0.56	0.48	0.43	0.46	0.58	0.34	0.50
	M**	0.47	0.43	0.59	0.50	0.60	0.43	0.39	0.45	0.44	0.34	0.49
S2	C	0.60	0.60	0.68	0.70	0.65	0.64	0.65	0.67	0.59	0.71	----
	M	0.59	0.59	0.70	0.73	0.64	0.60	0.64	0.59	0.59	0.67	----
S3	C	0.99	1.08	0.86	0.90	0.90	1.02	1.02	0.89	1.02	0.85	----
	M	0.93	1.05	0.85	0.90	0.96	0.90	0.93	0.93	0.82	0.83	----
S4	C	0.83	0.96	0.85	0.89	0.75	0.74	0.87	0.78	0.73	0.66	----
	M	0.76	0.99	0.81	0.78	0.70	0.69	0.75	0.72	0.68	0.63	----
S5	C	0.69	0.64	0.67	0.77	0.57	0.61	0.66	0.61	0.54	0.53	----
	M	0.62	0.64	0.63	0.69	0.58	0.57	0.66	0.55	0.52	0.52	----
S6	C	0.50	0.59	0.51	0.48	0.57	0.78	0.60	0.65	0.66	----	----
	M	0.49	0.59	0.54	0.47	0.58	0.77	0.57	0.61	0.65	----	----
S7	C	0.49	0.54	0.65	0.55	0.62	0.51	0.57	0.60	0.52	0.59	0.53
	M	0.51	0.54	0.66	0.56	0.63	0.50	0.61	0.59	0.47	0.50	0.53
S8	C	0.77	0.65	0.63	0.56	0.59	0.49	0.62	0.65	0.69	0.57	0.57
	M	0.77	0.65	0.63	0.52	0.58	0.48	0.54	0.61	0.68	0.56	0.56
S9	C	0.56	0.52	0.67	0.56	0.57	0.63	0.52	0.65	0.56	0.56	----
	M	0.46	0.48	0.46	0.49	0.50	0.56	0.51	0.57	0.52	0.55	----
S10	C	0.55	0.58	0.55	0.48	0.50	0.68	0.50	0.53	0.48	0.54	0.52
	M	0.50	0.49	0.56	0.46	0.45	0.58	0.46	0.51	0.46	0.48	0.48

* Deflection measurement at the crack.

** Deflection measurement at the midspan position between cracks.

Table C5. Continued.

Section	Test Position	Dynamic Pavement Deflection at 100 ft. Intervals (Milli-in.) 1	2	3	4	5	6	7	8	9	10	11
S11	C*	0.62	0.60	0.69	0.68	0.64	0.61	0.54	0.63	0.54	0.62	0.56
	M**	0.52	0.64	0.62	0.60	0.89	0.62	0.54	0.60	0.52	0.58	0.53
S12	C	0.71	0.63	0.62	0.62	0.55	0.64	0.79	0.61	0.75	0.66	0.51
	M	0.71	0.62	0.59	0.57	0.53	0.61	0.74	0.55	0.65	0.64	0.45
S13	C	0.68	0.63	0.70	0.66	0.72	0.71	0.75	0.60	0.62	0.65	0.63
	M	0.70	0.60	0.69	0.68	0.70	0.57	0.72	0.62	0.56	0.64	0.62
S14	C	0.65	0.59	0.68	0.65	0.68	0.69	0.56	0.63	0.68	0.64	0.70
	M	0.66	0.56	0.66	0.60	0.63	0.66	0.61	0.60	0.64	0.65	0.68
S15	C	0.66	0.70	0.62	0.63	0.57	0.73	0.70	0.69	0.72	0.63	0.59
	M	0.65	0.59	0.55	0.60	0.51	0.77	0.67	0.62	0.68	0.61	0.55
S16	C	0.43	0.45	0.43	0.44	0.49	0.51	0.53	0.52	0.43	0.43	0.41
	M	0.40	0.44	0.42	0.44	0.49	0.53	0.50	0.50	0.44	0.42	0.40
S17	C	1.20	1.29	1.23	1.35	1.32	1.38	1.32	1.35	1.17	1.17	----
	M	1.17	1.20	1.23	1.38	1.32	1.32	1.32	1.44	1.05	1.11	----
S18	C	0.73	0.70	0.76	0.75	0.75	0.83	0.76	0.80	0.76	0.73	0.69
	M	0.72	0.64	0.77	0.67	0.67	0.84	0.75	0.77	0.74	0.73	0.69
S19	C	0.68	0.80	0.71	0.81	0.87	0.66	0.63	0.75	0.77	0.67	0.67
	M	0.67	0.74	0.68	0.84	0.82	0.64	0.64	0.77	0.75	0.64	0.67
S20	C	0.65	0.58	0.58	0.64	0.93	0.61	0.70	0.88	0.75	0.68	0.75
	M	0.82	0.49	0.54	0.59	0.90	0.56	0.56	0.78	0.68	0.69	0.78

* Deflection measurement at the crack.

** Deflection measurement at the midspan position between cracks.

Table C5. Continued.

Section	Test Position	Dynamic Pavement Deflection at 100 ft. Intervals (Milli-in.) 1	2	3	4	5	6	7	8	9	10	11
S21	C*	0.82	0.81	0.80	0.87	0.75	0.87	0.83	0.78	0.82	0.79	----
	M**	0.80	0.77	0.79	0.89	0.74	0.82	0.84	0.76	0.80	0.79	----
S22	C	0.82	0.83	0.80	0.66	0.75	0.70	0.65	0.65	0.69	0.59	----
	M	0.71	0.78	0.74	0.78	0.76	0.72	0.66	0.68	0.68	0.61	----
S23	C	0.55	0.63	0.83	0.49	0.42	0.49	0.47	0.57	0.45	0.43	----
	M	0.53	0.63	0.57	0.47	0.40	0.41	0.45	0.46	0.42	0.46	----
S24	C	0.64	0.57	0.69	0.58	0.58	0.65	0.68	0.70	0.67	----	----
	M	0.61	0.52	0.67	0.60	0.56	0.65	0.64	0.69	0.70	----	----
S25	C	0.71	0.71	0.60	0.59	0.73	0.83	0.70	0.75	0.74	0.61	0.63
	M	0.73	0.70	0.60	0.57	0.73	0.81	0.65	0.72	0.67	0.59	0.56
S26	C	0.54	0.59	0.87	1.17	0.55	0.62	0.58	0.67	0.61	0.54	----
	M	0.51	0.55	0.69	0.83	0.56	0.62	0.56	0.75	0.62	0.51	----
S27	C	0.31	0.27	0.32	0.35	0.32	0.42	0.54	0.45	0.48	0.53	0.48
	M	0.30	0.26	0.31	0.37	0.31	0.32	0.39	0.43	0.42	0.54	0.47
S28	C	0.43	0.37	0.39	0.48	0.36	0.47	0.48	0.52	0.56	0.49	0.48
	M	0.44	0.36	0.39	0.46	0.38	0.40	0.41	0.42	0.46	0.43	0.47
S29	C	0.41	0.44	0.41	0.40	0.42	0.45	0.43	0.37	0.41	0.39	----
	M	0.40	0.40	0.35	0.42	0.42	0.57	0.40	0.37	0.40	0.38	----
S30	C	0.66	0.57	0.69	0.96	0.72	0.75	0.79	1.05	0.70	0.83	----
	M	0.63	0.58	0.65	0.72	0.76	0.75	0.72	0.76	0.73	0.83	----
S31	C	0.63	0.64	0.99	0.70	0.58	0.64	0.76	0.62	1.02	0.59	0.79
	M	0.62	0.72	0.50	0.62	0.55	0.56	0.58	0.55	0.90	0.56	0.72

* Deflection measurement at the crack.

** Deflection measurement at the midspan position between cracks.

Table C6. Summary of Subgrade Grain Size Distribution and Consistency Limits Data.

Serial	List Locations	Percent Finer Than Sieve Size					Consistency Limits			Subgrade Class
		No. 4	No. 10	No. 40	No. 100	No. 200	LL	PL	PI	
S1	L1-F	90.9	84.5	69.7	49.5	43.5	16	12	4	SM-SC
	L2	91.7	85.2	65.7	49.9	45.8	23	14	9	SC
S2	L3	95.4	90.5	79.7	64.9	56.3	21	13	8	CL
	L4	89.5	84.4	67.3	53.4	48.7	20	13	7	SM-SC
S3	L5	98.2	96.5	92.5	87.0	85.1	31	16	15	CL*
	L6-F	98.3	96.8	92.6	89.6	87.9	33	17	16	CL
S4	L7	97.8	94.0	83.8	61.2	54.6	21	14	7	ML-CL
	L8-F	94.0	90.0	78.9	58.0	51.8	22	14	8	CL
S5	L9	95.1	92.1	85.5	75.1	68.0	23	15	8	ML-CL
	L10-F	94.1	90.6	83.1	73.3	65.1	28	16	12	CL
S6	L11-F	97.5	95.5	88.6	74.4	66.3	29	14	15	CL
	L12	97.3	94.6	86.1	72.8	63.5	26	14	12	CL
S7	L13	63.4	49.2	20.5	17.0	16.1	48	22	26	SC
	L14-F	92.7	86.8	74.3	60.6	55.6	19	13	6	ML-CL
S8	L15	90.3	85.7	66.4	55.8	51.0	18	12	6	ML-CL
	L16-F	92.7	86.8	73.7	55.5	47.6	17	12	5	SM-SC
S9	L17	94.6	90.4	79.3	62.8	54.5	29	15	14	CL
	L18	96.4	92.9	82.4	68.0	60.7	32	16	16	CL
S10	L19-F	95.5	92.2	82.9	74.8	72.0	29	17	12	CL
	L20	95.0	90.2	77.9	65.1	58.9	24	15	9	CL

* Underlain by a thin layer of sand.

Table C6. Continued.

Serial	List Locations	Percent Finer Than Sieve Size					Consistency Limits			Subgrade Class
		No. 4	No. 10	No. 40	No. 100	No. 200	LL	PL	PI	
S11	L21-F	94.5	90.3	77.9	54.3	43.0	NP	NP	NP	SM
	L22	95.7	90.8	75.9	61.0	51.5	16	NP	NP	SM
S12	L23-F	95.6	90.7	75.9	55.4	45.0	25	15	10	SC
	L24	94.8	90.2	74.9	61.2	56.4	20	13	7	ML-CL
S13	L25	96.8	93.8	79.7	70.7	68.3	27	15	12	CL
	L26-F	93.4	90.1	78.3	65.3	60.5	31	17	14	CL
S14	L27	96.0	93.6	85.4	80.5	78.4	28	16	12	CL
	L28-F	98.8	96.5	89.5	84.3	81.1	31	16	15	CL
S15	L29	90.0	84.6	71.5	51.0	41.0	18	14	4	SM-SC
	L30	78.9	74.8	66.2	53.6	45.8	23	14	9	SC
S16	L31	91.6	82.8	60.9	41.5	37.4	18	12	6	SM-SC*
	L32	92.2	85.5	70.8	51.4	41.6	20	13	7	SM-SC*
S17	L33	98.7	96.9	73.4	9.9	4.9	NP	NP	NP	SP
	L34	----	----	----	----	----	--	--	--	-----
S18	L35	94.4	89.6	67.1	15.1	12.4	NP	NP	NP	SM
	L36	----	----	----	----	----	--	--	--	-----
S19	L37	80.0	74.3	56.8	42.3	35.8	18	13	5	SM-SC
S20	L38	99.5	99.2	96.2	13.4	7.2	NP	NP	NP	SP-SM
	L39	98.8	98.6	43.7	6.3	5.0	NP	NP	NP	SP-SM
S21	L40	99.8	99.3	91.4	87.9	87.3	28	20	8	ML**
	L41	99.8	99.0	95.3	87.8	86.3	30	19	11	CL
S22	L42	100.0	99.9	92.1	31.6	20.0	NP	NP	NP	SM
	L43	99.8	99.7	35.4	9.6	3.7	NP	NP	NP	SP

* Underlain by a thin layer of sand. ** Underlain by a 7" layer of sand.

Table C6. Continued.

Serial	Locations	Percent Finer Than Sieve Size					Consistency Limits			Subgrade Class
		No. 4	No. 10	No. 40	No. 100	No. 200	LL	PL	PI	
S23	L44	95.7	91.9	81.7	67.3	58.4	21	14	7	ML-CL
	L45-F	97.3	93.9	80.6	61.2	59.7	21	14	7	ML-CL
S24	L46	94.0	91.9	86.3	77.4	73.4	33	18	15	CL
S25	L47-S	92.6	83.4	50.2	41.5	36.3	14	NP	NP	SM
	L48	87.5	80.3	64.0	46.7	40.5	18	NP	NP	SM
S26	L49	88.9	83.4	59.6	44.3	38.1	17	11	6	SM-SC
	L50-F	93.6	90.4	80.7	63.6	56.1	25	14	11	CL
S27	L51	95.0	89.4	70.5	47.2	38.7	16	13	3	SM
S28	L52	79.7	68.5	54.3	43.2	39.0	21	13	8	SM-SC
S29	L53	91.5	75.3	55.8	48.3	44.8	31	20	11	SC*
S30	L54	99.0	97.9	92.7	91.2	91.1	34	18	16	CL
	L55-F	98.9	96.2	91.5	87.4	87.0	35	21	14	CL
S31	L56	94.9	89.6	70.7	56.4	52.9	21	14	7	ML-CL

* Subgrade soil consisted of shale fragments.

Table C7. Summary of Subgrade CBR and Density Data

		Field Measurement					Lab Measurement		
		CBR (Percent)		Density (lb/ft^3)					
Section	Test Location	Core	Shoulder	Measured γ_f	Adjusted* γ_f''	Water Content w_f (%)	Max. Density γ_{max} (lb/ft^3)	Opt. Water Content w_{opt}(%)	Percent Compaction γ_f''/γ_{max}
S1	L1-F	36	44	107.4	103.8	17.2	130.4	8.8	79.56
	L2	5	18	124.4	121.6	14.3	125.8	10.5	96.66
S2	L3	32	16	118.1	116.5	12.4	126.5	10.0	91.80
	L4	7	13	117.5	113.7	14.3	126.9	10.1	89.60
S3	L5	9	6	109.3	108.6	20.1	114.7	15.4	94.71
	L6-F	7	5	101.7	101.0	21.1	113.4	15.1	89.05
S4	L7	--	5	-----	-----	----	-----	----	------
	L8-F	--	4	-----	-----	----	123.5	9.8	------
S5	L9	12	25	123.5	122.0	15.9	124.0	11.2	98.36
	L10-F	13	12	113.0	110.8	15.7	122.4	12.4	90.49
S6	L11-F	9	5	112.5	111.6	17.5	120.6	12.8	92.52
	L12	9	7	111.7	110.8	17.8	117.6	12.6	94.21
S7	L13	36	20	119.3	102.8	14.6	-----	----	-----
	L14-F	28	10	130.2	128.0	11.6	129.0	9.0	99.22
S8	L15	37	18	118.9	115.4	11.7	128.8	9.3	89.60
	L16-F	30	30	135.8	133.9	9.5	130.2	8.2	102.86
S9	L17	5	13	126.4	124.7	14.3	118.7	12.5	105.04
	L18	11	12	105.6	104.2	17.4	115.2	13.8	90.45
S10	L19-F	10	16	138.8	137.8	11.5	115.7	15.0	119.09
	L20	15	11	135.4	134.1	13.4	121.8	11.1	110.12

* Adjusted for material retained on No. 4 Sieve.

Table C7. Continued.

		Field Measurement					Lab Measurement		
		CBR (Percent)		Density (lb/ft^3)					
Section	Test Location	Core	Shoulder	Measured γ_f	Adjusted* $\gamma_{f''}$	Water Content w_f (%)	Max. Density γ_{max} (lb/ft^3)	Opt. Water Content w_{opt}(%)	Percent Compaction $\gamma_{f''}/\gamma_{max}$
S11	L21-F	38	23	127.8	126.2	10.0	131.4	7.0	96.09
	L22	25	28	133.8	132.7	10.0	130.4	8.2	101.76
S12	L23-F	16	5	120.5	119.0	14.3	120.1	12.2	99.09
	L24	11	22	97.4	95.3	20.1	107.8	9.0	88.40
S13	L25	9	14	-----	-----	----	114.4	14.3	------
	L26-F	6	15	-----	-----	----	113.3	13.6	------
S14	L27	5	10	124.0	122.7	14.4	114.8	14.3	106.90
	L28-F	4	4	101.1	100.6	19.1	115.9	13.8	86.79
S15	L29	35	31	121.7	118.3	10.1	132.9	7.9	89.00
	L30	4	9	104.0	94.7	18.4	125.8	10.0	75.24
S16	L31	20	19	97.7	94.2	16.9	125.5	10.7	75.06
	L32	19	10	-----	-----	19.7	125.1	8.9	------
S17	L33	26	11	-----	-----	----	109.4	10.5	94.92
	L34	--	--	-----	-----	----	-----	----	------
S18	L35	12	12	123.0	121.7	11.7	119.5	9.8	101.87
	L36	--	--	-----	-----	----	-----	----	------
S19	L37	33	13	124.7	117.5	11.3	126.8	10.0	92.67
S20	L38	31	15	100.2	100.0	21.3	105.4	12.2	94.88
	L39	39	7	103.8	103.4	17.7	102.2	11.0	101.15
S21	L40	13	7	91.4	91.3	23.2	109.4	11.4	83.47
	L41	10	3	97.5	97.4	20.6	110.9	16.4	87.82

* Adjusted for material retained on No. 4 Sieve.

Table C7. Continued.

		Field Measurement					Lab. Measurement		
		CBR (Percent)		Density (lb/ft^3)					
Section	Test Location	Core	Shoulder	Measured γ_f	Adjusted* $\gamma_{f''}$	Water Content w_f (%)	Max. Density γ_{max} (lb/ft^3)	Opt. Water Content w_{opt} (%)	Percent Compaction $\gamma_{f''}/\gamma_{max}$
S22	L42	38	11	95.7	95.7	13.2	106.5	11.8	89.86
	L43	--	16	103.7	103.6	10.2	102.0	7.4	101.55
S23	L44	10	6	114.5	113.0	16.2	124.4	11.2	90.81
	L45-F	7	6	108.9	107.9	17.1	120.9	12.2	89.25
S24	L46	11	4	102.0	99.6	22.1	111.6	13.6	89.21
S25	L47-S	12	13	113.8	111.0	13.0	131.8	8.4	84.25
	L48	4	5	101.1	95.7	17.9	128.6	9.0	74.45
S26	L49	23	9	113.9	109.6	14.0	128.2	9.7	85.48
	L50-F	10	4	122.0	119.8	13.3	124.8	11.2	96.01
S27	L51	13	18	135.1	133.8	10.3	130.5	7.9	102.56
S28	L 52	19	25	103.6	95.6	14.1	128.7	9.8	73.49
S29	L53	20	12	107.2	103.5	17.4	114.2	13.6	90.61
S30	L54	22	11	115.1	114.8	17.7	108.4	16.6	105.86
	L55-F	6	7	110.1	109.7	20.3	108.0	17.4	101.53
S31	L56	12	11	101.1	99.0	19.0	125.7	10.3	78.76

* Adjusted for material retained on No. 4 Sieve.

Table C8. Summary of Subbase Grain Size Distribution and Consistency Limits Data

					Percent Passing Sieve Size								
Section	Location	LL	PI	Dust* Ratio	1"	3/4"	1/2"	3/8"	No. 4	No. 10	No. 40	No. 100	No. 200
S1	L1-F	16	NP	0.60	96.8	91.9	86.3	82.2	67.4	47.0	15.9	10.9	9.6
	L2	18	NP	0.50	87.6	79.5	74.2	67.2	50.9	32.8	15.5	9.0	7.8
S2	L3	NP	NP	0.47	95.5	90.9	86.8	81.9	65.8	46.4	20.8	11.7	9.8
	L4	14	NP	0.44	98.7	96.4	90.1	86.8	74.4	56.9	28.2	15.7	12.4
S3	L5	NP	NP	0.57	96.5	86.1	65.8	56.7	42.1	29.1	15.3	10.8	8.7
	L6-F	NP	NP	0.58	99.1	95.8	85.9	78.3	59.6	37.5	18.0	13.1	10.5
S4	L7**	NP	NP	0.33	99.1	99.1	93.3	87.2	73.0	56.7	27.6	11.9	9.1
	L8-F**	NP	NP	0.34	100.0	99.5	97.3	92.5	78.8	61.2	26.5	12.5	8.9
S5	L9	NP	NP	0.59	95.1	90.6	84.4	79.2	64.6	47.8	10.6	7.4	6.2
	L10-F	NP	NP	0.34	97.3	95.5	89.3	83.5	70.4	53.2	21.1	8.6	7.2
S6	L11-F	NP	NP	0.48	91.1	81.0	69.9	64.5	52.4	39.8	17.9	10.1	8.5
	L12	18	4	0.56	90.5	80.0	72.4	67.8	55.7	42.5	14.9	9.9	8.4
S7	L13	17	NP	0.55	76.1	57.7	46.1	41.7	31.0	22.0	10.2	6.5	5.6
	L14-F	17	NP	0.48	85.5	73.8	63.1	57.1	44.4	32.1	15.0	8.5	7.2
S8	L15	NP	NP	0.44	97.4	91.7	85.6	80.3	65.0	48.1	18.5	9.4	8.2
	L16-F	NP	NP	0.53	92.5	84.7	77.4	72.7	58.6	44.2	13.9	9.4	7.4
S9	L17	NP	NP	0.44	100.0	100.0	96.3	93.8	76.9	57.8	15.6	8.4	6.9
	L18	NP	NP	0.42	100.0	99.5	92.4	88.3	71.5	53.0	26.9	9.6	7.3
S10	L19-F	NP	NP	0.30	100.0	99.6	95.2	91.6	72.7	50.6	26.9	10.3	8.1
	L20	NP	NP	0.64	100.0	98.6	92.6	88.8	72.4	52.7	11.3	8.8	7.2

* Dust Ratio = $\frac{\text{Percent Passing No. 200 Sieve}}{\text{Percent Passing No. 40 Sieve}}$

** Data applies to gravel subbase under the bituminous stablized layer.

Table C8. Continued.

Section	Location	LL	PI	Dust* Ratio	Percent Passing Sieve Size 1"	3/4"	1/2"	3/8"	No. 4	No. 10	No. 40	No. 100	No. 200
S11	L21-F	NP	NP	0.29	100.0	98.7	90.4	85.8	74.0	59.4	27.7	10.3	8.1
	L22	NP	NP	0.50	100.0	98.4	89.0	85.1	73.8	60.2	15.1	9.4	7.6
S12	L23-F	NP	NP	0.46	94.2	90.0	82.5	76.9	62.1	45.3	20.5	10.9	9.4
	L24	16	NP	0.62	97.2	93.2	85.1	79.2	63.4	41.8	13.3	9.3	8.3
S13	L25	NP	NP	0.30	96.9	90.1	81.4	76.2	62.6	48.3	24.3	9.4	7.1
	L26-F	NP	NP	0.49	100.0	95.8	87.9	83.7	71.1	55.6	16.8	10.1	8.2
S14	L27	NP	NP	0.41	100.0	99.7	94.7	88.3	73.8	57.2	17.3	9.3	7.0
	L28-F	NP	NP	0.51	100.0	100.0	93.2	87.2	71.6	55.5	14.9	9.7	7.6
S15	L29**	NP	NP	0.32	96.7	92.1	85.0	80.6	66.0	48.7	19.2	7.7	6.2
	L30**	NP	NP	0.34	93.2	82.4	73.3	69.8	51.5	34.4	14.3	5.9	4.8
S16	L31	NP	NP	0.57	95.3	90.0	81.9	74.8	58.0	39.7	14.4	9.7	8.2
	L32	17	NP	0.57	98.3	93.5	84.9	79.1	61.7	41.0	14.3	9.8	8.2
S17	L33	NP	NP	0.32	100.0	91.3	70.1	56.4	33.8	20.5	10.3	5.4	3.3
	L34	NP	NP	0.33	100.0	93.4	76.9	62.8	36.7	22.7	11.3	5.9	3.7
S18	L35	NP	NP	0.25	-----	-----	99.9	96.5	61.2	48.2	35.1	12.5	8.9
	L36	NP	NP	0.27	99.6	99.6	99.1	96.0	56.2	42.4	30.7	11.7	8.4
S19	L37	NP	NP	0.29	100.0	99.2	94.5	89.7	74.6	56.7	18.9	7.0	5.4
S20	L38	NP	NP	0.34	100.0	97.3	68.7	56.4	39.8	28.6	14.4	7.6	4.9
	L39	NP	NP	0.37	100.0	98.2	79.4	68.5	46.0	30.8	15.2	8.6	5.6

* Dust Ratio = $\frac{\text{Percent Passing No. 200 Sieve}}{\text{Percent Passing No. 40 Sieve}}$

** Data applies to gravel subbase under the bituminous stabilized layer.

Table C8. Continued.

Section	Location	LL	PI	Dust* Ratio	Percent Passing Sieve Size								
					1"	3/4"	1/2"	3/8"	No. 4	No. 10	No. 40	No. 100	No. 200
S21	L40	NP	NP	0.51	100.0	99.3	98.9	93.9	56.7	39.5	27.0	5.6	4.0
	L41	NP	NP	0.22	100.0	100.0	99.6	94.8	55.7	37.9	20.4	5.5	4.37
S22	L42	NP	NP	0.26	100.0	100.0	100.0	100.0	99.9	82.3	40.9	18.5	10.6
	L43	NP	NP	0.28	100.0	99.7	99.7	99.6	99.2	81.4	40.7	18.9	11.2
S23	L44	NP	NP	0.35	97.4	89.3	81.4	77.1	65.8	51.4	19.0	8.1	6.6
	L45-F	NP	NP	0.55	98.7	94.4	88.4	84.2	72.1	55.5	15.6	10.2	8.5
S24	L46	NP	NP	0.36	98.3	92.9	88.6	83.0	71.0	55.1	19.4	8.5	7.0
S25	L47-S	NP	NP	0.48	98.4	94.5	89.3	85.7	74.0	58.9	22.8	13.5	11.0
	L48	NP	NP	0.58	95.0	90.1	83.2	78.5	64.8	49.9	12.6	9.0	7.3
S26	L49	16	NP	0.38	100.0	92.7	79.9	73.7	61.3	47.8	17.0	8.1	6.5
	L50-F	NP	NP	0.43	97.0	92.6	81.4	74.9	61.9	47.9	18.1	9.4	7.8
S27	L51	NP	NP	0.27	100.0	100.0	97.2	91.9	77.7	57.8	16.4	6.2	4.5
S28	L52	NP	NP	0.33	100.0	100.0	97.3	92.6	78.1	58.9	22.6	9.4	7.5
S29	L53	NP	NP	0.53	98.0	92.8	80.0	68.1	47.6	33.3	22.0	15.0	11.6
S30	L54	NP	NP	0.31	99.0	98.0	95.0	94.0	87.3	60.5	6.2	2.9	1.9
	L55-F	NP	NP	0.22	99.7	94.9	91.0	88.6	77.9	57.7	10.8	4.0	2.4
S31	L56	17	2	0.60	95.8	89.7	80.6	76.2	60.6	42.0	11.7	8.5	7.0

$$* \quad \text{Dust Ratio} = \frac{\text{Percent Passing No. 200 Sieve}}{\text{Percent Passing No. 40 Sieve}}$$

Table C9. Summary of Subbase Characteristics, CBR,and Permeability Data

Section	Test Location	Subbase Type And Thickness (in.)	Edge Pumping	CBR (Percent)		Estimated Field Permeability k (ft/day)
				Core	Shoulder	
S1	L1-F	GR* 6.0	No	63	30	811.8
	L2	GR 6.0	No	30	22	403.8
S2	L3	GR 7.0	Yes	52	49	1.8
	L4	GR 6.0	No	19	42	33.4
S3	L5	CS** 6.5	No	41	32	1368.5
	L6-F	CS 7.0	No	38	33	1075.8
S4	L7	BS*** 4.0 GR 3.0	No	--	--	------
	L8-F	BS 4.0 GR 3.0	Yes	--	34	------
S5	L9	GR 6.5	No	48	34	108.7
	L10-F	GR 6.0	No	40	25	11.4
S6	L11-F	GR 6.5	Yes	34	19	122.0
	L12	GR 6.0	No	29	20	36.1
S7	L13	GR 6.0	No	76	47	------
	L14-F	GR 6.0	Yes	50	37	86.3
S8	L15	GR 6.0	No	51	33	9.7
	L16-F	GR 6.5	No	59	31	104.2
S9	L17	GR 6.0	No	20	22	375.4
	L18	GR 6.0	No	38	24	------

* GR = Gravel
** CS = Crushed Stone
*** BS = Bituminous Stabilized

Table C9. Continued.

Section	Test Location	Subbase Type And Thickness (in.)	Edge Pumping	CBR (Percent)		Estimated Field Permeability k (ft/day)
				Core	Shoulder	
S10	L19-F	GR* 6.0	No	54	39	0.84
	L20	GR 6.0	No	41	31	2.6
S11	L21-F	GR 6.0	Yes	54	51	453.1
	L22	GR 6.0	No	53	55	4378.4
S12	L23-F	GR 7.0	Yes	40	31	33.4
	L24	GR 7.0	Yes	38	57	7.3
S13	L25	GR 6.0	Yes	22	38	------
	L26-F	GR 6.0	Yes	26	22	20.7
S14	L27	GR 6.0	No	18	28	------
	L28-F	GR 6.0	No	17	22	6.7
S15	L29	BS** 6.0 GR 3.0	No	52	46	------
	L30	BS 6.5 GR 3.0	No	37	30	------
S16	L31	GR 6.0	No	53	46	135.6
	L32	GR 7.5	No	35	40	330.4
S17	L33	SL*** 7.0	No	90	100	208.4
	L34	SL 6.0	No	90	90	------
S18	L35	GR 6.0	No	46	38	------
	L36	GR 6.0	No	100	100	------

* GR = Gravel
** BS = Bituminous Stabilized
*** SL = Slag

Table C9. Continued.

Section	Test Location	Subbase Type And Thickness (in.)	Edge Pumping	CBR (Percent) Core	CBR (Percent) Shoulder	Estimated Field Permeability k (ft/day)
S19	L37	GR* 6.0	No	46	28	19.1
S20	L38	SL** 6.5	No	100	100	677.3
	L39	SL 6.0	No	100	100	185.3
S21	L40	GR 6.0	No	63	36	77.5
	L41	GR 7.5	No	52	28	36.0
S22	L42	SL 5.0	No	55	42	42.3
	L43	SL 5.0	No	100	43	34.9
S23	L44	GR 6.0	No	42	27	3780.9
	L45-F	GR 5.5	No	33	34	29.3
S24	L46	GR 6.5	No	44	23	4166.2
S25	L47-S	GR 4.0	Yes	38	43	------
	L48	GR 6.0	No	22	21	773.2
S26	L49	GR 6.5	No	34	23	288.9
	L50-F	GR 5.5	Yes	46	23	27.4
S27	L51	GR 6.0	No	35	33	37.0
S28	L52	GR 6.0	No	56	50	252.0
S29	L53	CS*** 6.0	No	59	90	2497.3
S30	L54	SL 7.0	Yes	100	95	30.0
	L55-F	SL 6.0	Yes	58	56	25.6
S31	L56	GR 9.6	No	48	42	1299.8

* GR = Gravel ; ** SL = Slag ; *** CS = Crushed Stone

Table C10. Summary of Subbase Density Data

		Field			Laboratory		Percent
		Dry Density (lb/ft^3)		Water	Maximum	Opt.Water	Compac-
Section	Test Location	Measured γ_f	Adjusted $\gamma_{f'}$	Content w_f (%)	Dry Density γ_{max} (lb/ft^3)	Content w_{opt} (%)	tion $\gamma_{f'}/\gamma_{max}$
S1	L1-F	116.3	113.3	12.7	132.0	6.5	85.8
	L2	125.3	117.9	7.3	136.4	7.2	86.4
S2	L3	142.2	140.2	7.0	132.5	7.6	105.8
	L4	126.1	124.9	9.7	129.5	7.6	96.4
S3	L5	126.3	121.4	8.1	135.0	6.8	89.9
	L6-F	127.7	123.6	12.2	139.5	6.0	88.6
S4	L7	-----	-----	----	-----	---	-----
	L8-F	-----	-----	----	-----	---	-----
S5	L9	126.0	123.0	12.5	132.0	7.9	92.5
	L10-F	131.1	129.9	11.3	132.0	8.0	98.4
S6	L11-F	128.5	122.2	10.6	136.0	7.3	89.8
	L12	133.6	127.5	10.7	135.3	---	94.2
S7	L13	-----	-----	15.3	139.6	7.5	-----
	L14-F	132.8	124.1	10.3	137.0	7.0	90.6
S8	L15	134.8	132.6	8.5	133.0	6.7	99.7
	L16-F	127.6	122.5	9.2	134.7	6.5	90.9

Note:
1. Maximum density for gravel subbases from density control curve.
2. Maximum density for other subbases from laboratory compaction tests.
3. Optimum water content from laboratory compaction tests.
4. Field dry density adjusted for material retained on 3/4 in. sieve.

Table C10. Continued

		Field			Laboratory		Percent Compaction
		Dry Density (lb/ft^3)		Water Content	Maximum Dry Density$_3$ (lb/ft^3)	Opt. Water Content	
Section	Test Location	Measured γ_f	Adjusted $\gamma_{f'}$	w_f (%)	γ_{max}	w_{opt} (%)	$\gamma_{f'}/\gamma_{max}$
S9	L17	114.6	114.6	7.5	128.0	---	89.5
	L18	-----	-----	----	128.5	---	-----
S10	L19-F	141.3	141.2	9.8	130.0	6.7	108.6
	L20	140.2	139.9	13.4	130.3	6.1	107.4
S11	L21-F	113.1	112.6	13.9	129.5	6.5	86.9
	L22	109.9	109.3	12.5	134.5	7.3	81.3
S12	L23-F	130.6	127.6	11.8	134.3	6.3	95.0
	L24	138.6	137.0	9.9	133.5	5.8	102.6
S13	L25	-----	-----	----	132.6	---	-----
	L26-F	129.9	128.7	12.1	130.7	7.0	98.5
S14	L27	-----	-----	----	129.6	---	-----
	L28-F	134.9	133.0	10.1	130.5	6.7	102.0
S15	L29	-----	-----	----	-----	---	-----
	L30	-----	-----	----	-----	---	-----
S16	L31	127.1	123.9	10.4	135.0	6.3	91.8
	L32	121.9	119.7	11.2	134.5	6.8	89.0

Notes:
1. Maximum density for gravel subbases from density control curve.
2. Maximum density for other subbases from laboratory compaction tests.
3. Optimum water content from laboratory compaction tests.
4. Field dry density adjusted for material retained on 3/4 in. sieve.

Table C10. Continued.

Section	Test Location	Field: Dry Density (lb/ft^3) Measured γ_f	Field: Dry Density (lb/ft^3) Adjusted $\gamma_{f'}$	Field: Water Content w_f (%)	Laboratory: Maximum Dry Density γ_{max} (lb/ft^3)	Laboratory: Opt. Water Content w_{opt} (%)	Percent Compaction $\gamma_{f'}/\gamma_{max}$
S17	L33	117.7	116.2	7.7	104.3	4.8	111.4
	L34	-----	-----	----	109.3	6.8	-----
S18	L35	-----	-----	----	134.6	---	-----
	L36	-----	-----	----	135.2	---	-----
S19	L37	126.8	126.6	10.7	129.2	7.0	98.0
S20	L38	104.1	103.4	9.2	109.8	4.9	94.2
	L39	113.6	113.2	6.9	113.1	5.8	100.1
S21	L40	125.3	125.0	10.0	135.1	6.5	92.6
	L41	129.8	129.7	8.6	135.4	6.5	95.8
S22	L42	115.1	115.1	9.4	127.6	6.9	90.2
	L43	115.4	115.4	13.9	127.6	6.9	90.4
S23	L44	107.3	102.9	11.2	132.7	7.5	77.5
	L45-F	128.7	127.0	9.0	130.5	6.6	97.3
S24	L46	117.6	115.1	9.5	130.8	---	88.0

Note: 1. Maximum density for gravel subbases from density control curve.

2. Maximum density for other subbases from laboratory compaction tests.

3. Optimum water content from laboratory compaction tests.

4. Field dry density adjusted for material retained on 3/4 in. sieve.

Table C10. Continued.

Section	Test Location	Field			Laboratory		Percent Compaction γ_f'/γ_{max}
		Dry Density (lb/ft^3)		Water Content w_f (%)	Maximum Dry Density γ_{max} (lb/ft^3)	Opt. Water Content w_{opt} (%)	
		Measured γ_f	Adjusted γ_f'				
S25	L47-S	-----	-----	14.5	129.6	7.3	-----
	L48	117.2	113.8	11.1	133.0	7.1	85.4
S26	L49	120.5	118.0	12.7	134.5	6.0	87.7
	L50-F	131.2	129.1	9.9	134.4	6.1	96.1
S27	L51	122.6	122.6	10.5	127.5	5.8	96.2
S28	L52	114.7	114.7	11.1	127.5	6.9	90.0
S29	L53	122.8	120.3	11.4	141.0	7.0	85.3
S30	L54	98.2	97.6	13.3	83.3	8.2	117.2
	L55-F	99.0	97.6	14.8	84.3	7.8	115.8
S31	L56	116.6	112.8	12.3	134.9	6.0	83.6

Note:
1. Maximum density for gravel subbases from density control curve.
2. Maximum density for other subbases from laboratory compaction tests.
3. Optimum water content from laboratory compaction tests.
4. Field dry density adjusted for material retained on 3/4 in. sieve.

Table C11. Summary of Concrete Data.

Section	Test Location	Bulk Density γ_c (lb/ft^3) Above* Steel	Bulk Density γ_c (lb/ft^3) Below** Steel	Modulus of Elasticity E_c (psi) Above* Steel	Modulus of Elasticity E_c (psi) Below** Steel	Splitting Tensile Strength f_t (psi) Above* Steel	Splitting Tensile Strength f_t (psi) Below** Steel
S1	L1-F	144.7	147.6	4.46	4.42	527.0	582.0
	L2	143.5	140.3	4.73	4.55	522.0	415.0
S2	L3	140.3	141.4	4.64	6.59	470.5	494.5
	L4	142.0	139.8	4.51	6.02	438.6	489.6
S3	L5	142.0	143.9	5.25	4.82	426.0	556.0
	L6-F	141.9	139.6	4.46	3.42	551.0	559.0
S4	L7	140.5	142.1	4.58	4.59	432.0	531.0
	L8-F	140.8	141.8	4.71	4.98	548.0	460.0
S5	L9	141.2	138.7	4.58	4.76	453.0	421.0
	L10-F	140.7	138.1	4.82	4.38	442.0	209.0
S6	L11-F	137.6	139.7	4.79	4.79	462.0	448.0
	L12	142.7	145.4	5.23	5.91	529.0	556.0
S7	L13	139.5	141.3	4.66	5.03	427.0	498.0
	L14-F	140.4	145.7	4.72	5.06	502.0	503.0
S8	L15	146.0	143.0	4.98	4.70	556.0	548.0
	L16-F	141.2	134.7	4.17	4.27	539.0	381.0
S9	L17	134.7	138.1	5.38	5.87	379.7	433.2
	L18	141.0	137.1	3.77	5.71	481.1	518.9
S10	L19-F	140.4	143.0	5.19	5.06	537.0	624.0
	L20	138.6	143.7	6.01	6.34	475.0	565.0

* From segment of concrete core above steel reinforcement.
** From segment of concrete core below steel reinforcement.

Table C11. Continued.

		Bulk Density γ_c (lb/ft^3)		Modulus of Elasticity E_c (psi)		Splitting Tensile Strength f_t (psi)	
Section	Test Location	Above* Steel	Below** Steel	Above* Steel	Below** Steel	Above* Steel	Below** Steel
S11	L21-F	135.3	136.4	4.68	4.73	466.0	427.0
	L22	138.3	138.3	4.78	4.65	408.0	497.0
S12	L23-F	140.9	141.5	4.60	4.56	495.0	521.0
	L24	140.1	141.5	4.77	4.78	480.0	532.0
S13	L25	143.5	146.9	5.02	5.76	334.0	612.5
	L26-F	137.7	141.7	4.83	6.40	447.0	644.5
S14	L27	138.6	141.3	4.88	5.18	550.0	543.0
	L28-F	140.4	137.3	4.74	4.89	478.0	438.0
S15	L29	138.5	136.7	6.57	5.10	432.1	267.3
	L30	141.0	143.8	6.37	8.29	495.9	511.4
S16	L31	138.0	140.7	5.54	6.73	388.4	468.0
	L32	137.6	139.8	5.25	7.09	428.9	370.6
S17	L33	129.8	133.8	4.69	4.80	517.8	581.3
	L34	132.3	133.5	4.55	4.42	561.8	661.8
S18	L35	137.6	136.4	4.50	4.96	490.7	446.0
	L36	136.2	136.3	4.25	4.73	497.3	446.8
S19	L37	138.0	139.0	8.01	7.67	589.1	522.7
S20	L38	139.0	141.6	6.78	7.99	611.6	517.8
	L39	141.7	141.6	6.04	7.02	618.5	682.4

* From segment of concrete core above steel reinforcement.

** From segment of concrete core below steel reinforcement.

Table C11. Continued.

		Bulk Density γ_c (lb/ft^3)		Modulus of Elasticity E_c (psi)		Splitting Tensile Strength f_t (psi)	
Section	Test Location	Above* Steel	Below** Steel	Above* Steel	Below** Steel	Above* Steel	Below** Steel
S21	L40	138.1	145.4	5.13	5.98	551.0	595.9
	L41	137.6	140.5	5.02	4.91	632.2	640.9
S22	L42	139.9	140.9	6.85	7.99	607.9	643.1
	L43	141.3	139.9	7.87	7.88	602.9	584.1
S23	L44	143.9	143.7	4.46	4.79	614.0	606.0
	L45-F	142.6	141.8	5.94	5.11	474.0	572.0
S24	L46	143.3	145.5	6.38	8.29	489.6	616.2
S25	L47-S	140.7	140.2	4.64	4.62	481.0	530.0
	L48	140.6	142.6	5.79	6.01	604.0	565.0
S26	L49	145.4	145.9	5.10	4.96	708.0	611.0
	L50-F	145.2	145.3	4.90	5.13	619.0	642.0
S27	L51	135.4	138.6	6.80	5.87	337.3	489.7
S28	L52	135.0	135.5	5.97	7.81	510.6	522.8
S29	L53	136.2	139.2	6.05	5.74	571.8	644.5
S30	L54	131.8	134.4	4.69	4.69	510.0	634.0
	L55-F	131.2	135.0	4.30	4.74	481.0	602.0
S31	L56	132.8	137.4	5.28	6.63	409.7	486.1

* From segment of concrete core above steel reinforcement.

** From segment of concrete core below steel reinforcement.

Table C12. Summary of Pavement Cracking Data.

Section	Test Location	Crack Width (in.) At Distance From Pavement Edge (ft) 1.0	3.5	6.0	Mean Crack Width (in)	Crack Spacing Mean X_c (ft)	Crack Spacing Variance V_c (ft^2)	No. of Crack Intersections Per 100 ft. Length of Pavement
S1	L1-F	0.022	0.018	0.011	0.017	3.6	4.57	8
	L2	0.011	0.013	0.014	0.013	3.0	3.33	9
S2	L3	0.021	0.010	0.015	0.015	3.2	4.05	13
	L4	-----	-----	-----	-----	---	-----	--
S3	L5	0.009	0.014	0.011	0.011	5.3	8.34	4
	L6-F	0.041	0.032	0.016	0.030	5.5	9.13	3
S4	L7	0.003	0.010	0.015	0.009	6.2	4.20	0
	L8-F	0.011	0.015	0.015	0.014	3.6	6.62	10
S5	L9	0.017	0.021	0.013	0.017	5.9	7.03	3
	L10-F	0.023	0.019	0.019	0.020	4.6	6.58	5
S6	L11-F	0.090	0.040	0.050	0.060	5.1	12.16	2
	L12	0.004	0.015	0.005	0.008	4.2	5.12	2
S7	L13	0.004	0.005	0.009	0.006	4.5	3.67	0
	L14-F	0.025	0.020	0.015	0.020	3.5	3.49	3
S8	L15	0.008	0.010	0.022	0.013	3.7	5.17	5
	L16-F	0.045	0.040	0.020	0.035	2.8	3.51	11
S9	L17	0.013	0.020	0.023	0.020	5.7	8.85	2
	L18	0.009	0.019	0.021	0.016	6.9	8.41	1
S10	L19-F	0.040	0.125	0.030	0.065	9.6	16.08	0
	L20	0.020	0.015	0.030	0.022	7.8	3.78	0
S11	L21-F	0.025	0.035	0.020	0.027	7.4	13.23	5
	L22	0.015	0.020	0.015	0.017	8.3	8.85	1

Table C12. Continued.

Section	Test Location	Crack Width (in.) At Distance From Pavement Edge (ft)			Mean Crack Width (in)	Crack Spacing		No. of Crack Intersections Per 100 ft. Length of Pavement
		1.0	3.5	6.0		Mean X_c (ft)	Variance V_c (ft^2)	
S12	L23-F	0.031	0.030	0.035	0.032	6.6	12.50	3
	L24	0.009	0.013	0.007	0.010	8.3	5.45	1
S13	L25	0.011	0.030	0.025	0.022	9.4	6.72	1
	L26-F	0.110	0.090	0.045	0.082	3.9	9.20	4
S14	L27	0.005	0.015	0.020	0.013	6.9	3.37	0
	L28-F	0.020	0.040	0.030	0.030	4.6	11.74	5
S15	L29	0.009	0.014	0.008	0.010	7.2	29.11	0
	L30	0.004	0.008	0.006	0.006	7.0	34.47	3
S16	L31	0.005	0.009	0.010	0.008	5.5	4.11	1
	L32	0.003	0.006	0.006	0.005	5.0	7.02	1
S17	L33	0.005	0.010	0.006	0.007	3.4	2.87	11
	L34	-----	-----	-----	-----	---	-----	--
S18	L35	0.003	0.003	0.004	0.003	6.0	5.25	0
	L36	-----	-----	-----	-----	---	-----	--
S19	L37	0.004	0.009	0.007	0.007	3.6	3.84	5
S20	L38	0.008	0.012	0.016	0.012	5.1	8.26	6
	L39	0.002	0.004	0.006	0.004	4.8	8.98	2
S21	L40	0.002	0.006	0.014	0.007	5.1	8.92	3
	L41	0.018	0.015	0.020	0.018	6.3	13.40	2
S22	L42	0.006	0.004	0.005	0.005	4.9	3.53	2
	L43	0.002	0.004	0.006	0.004	4.5	4.49	3

Table C12. Continued.

Section	Test Location	Crack Width (in.) At Distance From Pavement Edge (ft) 1.0	3.5	6.0	Mean Crack Width (in)	Crack Spacing Mean X_c (ft)	Crack Spacing Variance V_c (ft^2)	No. of Crack Intersections Per 100 ft. Length of Pavement
S23	L44	0.006	0.011	0.012	0.010	6.4	9.65	2
	L45-F	0.017	0.020	0.015	0.017	5.1	5.75	4
S24	L46	0.005	0.003	0.002	0.003	6.4	5.21	1
S25	L47-S	0.025	0.012	0.015	0.017	5.6	15.22	7
	L48	0.003	0.015	0.008	0.009	5.3	12.51	4
S26	L49	0.009	0.019	0.017	0.015	6.0	4.08	0
	L50-F	0.020	0.030	0.025	0.025	5.1	8.69	5
S27	L51	0.010	0.012	0.020	0.014	6.9	4.88	1
S28	L52	0.002	0.006	0.005	0.004	7.3	8.95	4
S29	L53	0.006	0.010	0.004	0.007	5.2	5.81	1
S30	L54	0.007	0.008	0.008	0.008	4.3	4.15	3
	L55-F	0.015	0.008	0.015	0.013	4.1	4.16	6
S31	L56	0.005	0.004	0.008	0.006	4.3	2.49	0

Table C13. Summary of Dynamic Deflection Data Obtained at Test Locations.

		Dynamic Deflection (10^{-3} in.) at Distance from Pavement Edge (ft)					
		1.0 Test Position		3.5 Test Position		6.0 Test Position	
Section	Test Location	Crack	Midspan	Crack	Midspan	Crack	Midspan
S1	L1-F	0.50	0.54	0.52	0.55	0.46	0.49
	L2	0.54	0.45	0.50	0.45	0.52	0.51
S2	L3	0.99	1.02	0.73	0.76	0.66	0.70
	L4	0.84	0.78	0.66	0.64	0.57	0.55
S3	L5	1.02	1.04	0.93	0.90	0.88	0.87
	L6-F	2.01	2.34	1.59	1.84	1.32	1.77
S4	L7	0.93	1.08	0.63	0.73	0.63	0.65
	L8-F	9.00*	3.40	23.4*	4.00	0.89	0.89
S5	L9	0.59	0.62	0.49	0.49	0.46	0.47
	L10-F	1.53	3.00	0.89	1.47	0.63	0.65
S6	L11-F	0.29	0.42	1.50	0.57	0.88	0.84
	L12	0.90	0.90	0.64	0.54	0.65	0.54
S7	L13	0.56	0.62	0.48	0.49	0.48	0.47
	L14-F	0.90	1.14	0.63	0.66	0.62	0.56
S8	L15	0.60	0.62	0.50	0.49	0.54	0.49
	L16-F	0.63	0.87	0.67	0.71	0.67	0.62
S9	L17	0.85	0.93	0.78	0.76	0.66	0.63
	L18	0.93	0.93	0.62	0.58	0.58	0.58
S10	L19-F	0.99	3.40	0.78	3.10	1.02	2.58
	L20	0.72	0.61	0.50	0.48	0.48	0.48

* Exceedingly high values; test location not included in the analysis.

Table C13. Continued

Section	Test Location	Dynamic Deflection (10^{-3} in.) at Distance from Pavement Edge (ft)					
		1.0 Test Position		3.5 Test Position		6.0 Test Position	
		Crack	Midspan	Crack	Midspan	Crack	Midspan
S11	L21-F	1.38	1.20	1.05	0.96	1.02	0.96
	L22	0.89	0.78	0.60	0.63	0.56	0.63
S12	L23-F	1.71	1.08	0.88	0.87	0.75	0.73
	L24	0.90	0.73	0.72	0.59	0.68	0.59
S13	L25	----	1.08	----	----	0.65	0.67
	L26-F	----	----	----	----	0.65	0.67
S14	L27	1.14	1.05	0.70	0.69	0.65	0.66
	L28-F	3.60	0.98	0.93	0.87	0.60	0.61
S15	L29	0.73	0.75	0.69	0.71	0.70	0.69
	L30	0.90	0.90	0.81	0.82	0.80	0.83
S16	L31	0.96	0.90	0.58	0.57	0.52	0.53
	L32	0.79	0.76	0.48	0.47	0.44	0.44
S17	L33	1.08	1.05	1.02	0.99	0.93	0.90
	L34	1.08	1.11	1.20	1.20	1.11	1.14
S18	L35	0.96	0.90	0.78	0.81	0.77	0.77
	L36	0.69	0.69	0.61	0.62	0.57	0.58
S19	L37	0.74	0.72	0.64	0.66	0.62	0.63
S20	L38	0.86	0.85	0.77	0.75	0.72	0.71
	L39	0.87	0.86	0.59	0.59	0.54	0.55
S21	L40	1.08	1.02	0.78	0.78	0.77	0.76
	L41	1.02	1.05	0.82	0.84	0.80	0.82

Table C13. Continued

Section	Test Location	Dynamic Deflection (10^{-3} in.) at Distance from Pavement Edge (ft)					
		1.0 Test Position		3.5 Test Position		6.0 Test Position	
		Crack	Midspan	Crack	Midspan	Crack	Midspan
S22	L42	0.84	0.76	0.74	0.75	0.72	0.72
	L43	0.77	0.74	0.68	0.68	0.62	0.61
S23	L44	0.65	0.68	0.46	0.48	0.44	0.43
	L45-F	1.50	2.40	----	0.96	0.72	0.75
S24	L46	0.76	0.73	0.62	0.64	0.63	0.64
S25	L47-S	1.17	1.14	----	0.78	0.75	0.76
	L48	0.84	0.83	0.66	0.61	0.61	0.58
S26	L49	0.61	0.62	0.54	0.53	0.54	0.54
	L50	1.53	1.65	1.29	1.35	0.88	0.62
S27	L51	0.56	0.56	0.35	0.44	0.35	0.45
S28	L52	0.53	0.63	0.40	0.42	0.44	0.40
S29	L53	0.61	0.60	0.51	0.49	0.49	0.46
S30	L54	0.89	0.90	0.96	0.96	1.02	1.02
	L55-F	1.59	1.38	1.17	1.20	0.87	0.99
S31	L56	0.90	0.90	0.56	0.56	0.53	0.55

Table C14. Summary of Surface Curvature Index (SCI) Data Obtained at Test Location

		Surface Curvature Index (10^{-3} in.) at Distance from Pavement Edge (ft)					
		1.0		3.5		6.0	
	Test	Test Position		Test Position		Test Position	
Section	Location	Crack	Midspan	Crack	Midspan	Crack	Midspan
S1	L1-F	0.06	0.06	0.04	0.04	0.03	0.03
	L2	0.06	0.04	0.05	0.03	0.04	0.03
S2	L3	0.06	0.05	0.04	0.05	0.04	0.05
	L4	0.06	0.06	0.06	0.06	0.06	0.05
S3	L5	0.06	0.03	0.06	0.04	0.05	0.05
	L6-F	0.69	0.27	0.36	0.76	0.21	0.45
S4	L7	0.30	0.04	0.08	0.04	0.05	0.04
	L8-F	2.08	7.89*	1.43	22.30*	0.03	0.06
S5	L9	0.06	0.04	0.05	0.03	0.04	0.03
	L10-F	0.38	1.20	0.15	0.71	0.05	0.04
S6	L11-F	----	----	0.24	----	0.08	0.07
	L12	0.06	0.05	0.05	0.03	0.06	0.04
S7	L13	0.04	0.05	0.03	0.03	0.04	0.03
	L14-F	0.06	0.32	0.05	0.17	0.06	0.04
S8	L15	0.06	0.06	0.04	0.05	0.05	0.04
	L16-F	0.22	0.19	0.10	0.12	0.06	0.06
S9	L17	0.05	0.08	0.06	0.07	0.07	0.07
	L18	0.12	0.06	0.08	0.06	0.05	0.06
S10	L19-F	0.55	3.08	0.23	2.78	0.50	2.15
	L20	0.10	0.06	0.05	0.04	0.04	0.04

* Exceedingly high values; not included in the analysis.

Table C14. Continued

		Surface Curvature Index (10^{-3} in.) at Distance from Pavement Edge (ft)					
		1.0		3.5		6.0	
		Test Position		Test Position		Test Position	
Section	Test Location	Crack	Midspan	Crack	Midspan	Crack	Midspan
S11	L21-F	0.36	0.03	0.15	0.06	0.12	0.03
	L22	0.05	0.06	0.05	0.05	0.05	0.05
S12	L23-F	2.70	0.50	0.90	0.40	0.60	0.50
	L24	0.10	0.07	0.08	0.05	0.06	0.04
S13	L25	----	----	----	----	----	----
	L26-F	----	----	----	----	----	----
S14	L27	0.12	0.06	0.05	0.04	0.03	0.04
	L28-F	2.34	----	0.08	----	0.06	0.04
S15	L29	0.03	0.05	0.02	0.05	0.03	0.04
	L30	0.04	0.03	0.03	0.03	0.03	0.04
S16	L31	0.06	0.07	0.05	0.03	0.04	0.04
	L32	0.05	0.05	0.04	0.04	0.04	0.03
S17	L33	0.03	0.06	0.06	0.06	0.03	0.01
	L34	0.06	0.06	0.06	0.03	0.03	0.06
S18	L35	0.07	0.05	0.04	0.06	0.04	0.05
	L36	0.05	0.03	0.03	0.03	0.05	0.04
S19	L37	0.05	0.03	0.05	0.05	0.05	0.05
S20	L38	0.06	0.06	0.04	0.04	0.04	0.05
	L39	0.07	0.06	0.04	0.04	0.03	0.05
S21	L40	0.06	0.09	0.04	0.06	0.03	0.05
	L41	0.06	0.09	0.03	0.03	0.05	0.07

Table C14. Continued

		Surface Curvature Index (10^{-3} in.) at Distance from Pavement Edge (ft)					
		1.0		3.5		6.0	
		Test Position		Test Position		Test Position	
Section	Test Location	Crack	Midspan	Crack	Midspan	Crack	Midspan
S22	L42	0.04	0.06	0.06	0.06	0.06	0.03
	L43	0.05	0.03	0.05	0.05	0.03	0.03
S23	L44	0.03	0.05	0.02	0.03	0.02	0.02
	L45-F	0.30	0.25	----	0.08	0.05	0.05
S24	L46	0.05	0.04	0.04	0.04	0.04	0.04
S25	L47-S	0.06	0.06	----	0.02	0.03	0.02
	L48	0.04	0.04	0.03	0.01	0.03	0.02
S26	L49	0.04	0.04	0.03	0.04	0.04	0.04
	L50-F	0.45	0.51	0.69	0.58	0.05	0.19
S27	L51	0.05	0.06	0.05	0.05	0.05	0.05
S28	L52	0.06	0.05	0.04	0.04	0.05	0.05
S29	L53	0.06	0.05	0.05	0.04	0.04	0.04
S30	L54	0.07	0.05	0.03	0.06	0.09	0.06
	L55-F	0.66	0.18	0.45	0.35	0.24	0.30
S31	L56	0.03	0.07	0.05	0.04	0.04	0.04

APPENDIX D

STATISTICAL ATTRIBUTES OF SUBBASE PERMEABILITY MODELS

Note: The models are limited in applicability to graded aggregate subbases conforming to Indiana Standard Specifications (35) Sizes No. 53 and No. 73 coarse aggregate and subbase materials with Top Sizes 1-1/2 in., 1 in., and 1/2 in.

Table D 1. Gravel Subbase Permeability Model

- Dependent variable, $Y = \log_{10} k$
  where k = permeability in ft/day at 25°C
- Mean response = 1.39307
- Standard error of estimate (sq. root of the residual mean square), $S_E = 0.237$
- Coefficient of determination (R^2) = 0.895
- No. of cases = 23

Independent Variable	Regression Coefficient	Standard Error	F*	$F_{(.01,1,19)}$	Variable Description
Constant	16.05572	--	--	--	--
γ_d	-0.09884	0.01163	77.26**	8.18	Dry Density (lb/ft^3)
P4	-0.03435	0.00683	25.28**	8.18	Percent Finer than No. 4 Sieve
DR	1.10754	0.37432	8.75**	8.18	Dust Ratio
					$= \frac{\text{Percent Passing No.200 Sieve}}{\text{Percent Passing No. 40 Sieve}}$

*F-test for significance of regression coefficient, with model containing all independent variables.

**Significant at $\alpha = 0.01$

Table D 2. Crushed Stone Subbase Permeability Model

- Dependent variable, $Y = \log_{10}k$
  where k = permeability in ft/day at 25°C
- Mean response = 2.706
- Standard error of estimate (S_E) = 0.117
- Coefficient of determination (R^2) = 0.956
- No. of cases = 12

Independent Variable	Regression Coefficient	Standard Error	F	$F_{(.01,1,10)}$	Variable Description
Constant	12.56327	--	--	--	--
γ_d	-0.07464	0.00508	215.9*	10.04	Dry Density (lb/ft^3)

*Significant at α = 0.01

Table D 3. Slag Subbase Permeability Model (Based on Data from Pavement Sections with No Distress)

- Dependent variable, $Y = \log_{10} k$
  where k = permeability in ft/day at 25°C
- Mean response = 2.153
- Standard error of estimate (S_E) = 0.120
- Coefficient of determination (R^2) = 0.984
- No. of cases = 11

Independent Variable	Regression Coefficient	Standard Error	F*	$F_{(.01,1,11)}$	Variable Description
Constant	8.68635	--	--	--	--
γ_d	-0.05093	0.00721	49.91 **	9.65	Dry Density (lb/ft^3)
P·200	-0.11301	-0.02063	29.99 **	9.65	Percent Finer than No. 200 Sieve

*F-test for significance of regression coefficient, with model containing all independent variables.

**Significant at $\alpha = 0.01$

Table D 4. Slag Subbase Permeability Model (Based on Data from Pavement Section with Failure)

- Dependent variable, $Y = \log_{10} k$

  where k = permeability in ft/day at 25°C
- Mean response = 2.207
- Standard error of estimate (S_E) = 0.057
- Coefficient of determination (R^2) = 0.974
- No. of cases = 4

Independent Variable	Regression Coefficient	Standard Error	F	$F_{(.05,1,2)}$	Variable Description
Constant	10.07609	--	--	--	--
γ_d	-0.08756	-0.98697	75.27*	18.51	Dry Density (lb/ft^3)

*Significant at $\alpha = 0.05$

APPENDIX E

DEVELOPMENT OF SLAB TEMPERATURE MODELS

APPENDIX E

DEVELOPMENT OF SLAB TEMPERATURE MODELS

Surface temperatures of concrete pavement slabs can be estimated by the theoretical relationship developed by Barber (10). However, the practical use of these deterministic equations requires exact values of the thermal properties of the pavement structure and ambient environmental conditions. As these detailed input parameters were not available for the test sections of the detailed field study, a statistical approach was used for the estimation of surface temperature of the pavement slab as a function of air temperature and radiation effects.

Moulton and Schaub (44) successfully used the following multiple regression analysis model to develop equations for the estimation of pavement surface temperatures in West Virginia:

$$T_p = C_1 + C_2 T_a + C_3 \sin \frac{2\pi t}{365} \qquad \text{(E1)}$$

where T_p = measured pavement surface temperature
T_a = measured air temperature
t = time (in days)
C_1, C_2, C_3 = regression coefficients relating the annual variation in air temperature, the influence of air temperature on the pavement surface temperature and radiation effects (for details, see Ref. 44).

Since geographical and climatic conditions in Indiana are quite different from West Virginia, the slab temperature relationships developed for West Virginia could not be directly used in this study.

Therefore an attempt was made to evolve a slab temperature estimation equation that would be more appropriate for Indiana conditions. It should be noted that the form of the model proposed by Moulton and Schaub was retained, the only exception being the different estimates for the regression coefficients C_1, C_2, and C_3.

A literature search showed a general paucity of data pertaining to the relationship between air temperatures and the corresponding surface temperatures of concrete pavement slabs. A study by Arndt, however, contained a record of daily air and slab surface temperatures for a concrete pavement in Kansas (8). The temperature records, spanning two one-year periods (1936 and 1940) are shown in Figure E1. In order to convert the recorded data of Figure E1 to a form that could be utilized in a multiple regression analysis, the illustrated data were photographically enlarged and then digitized by means of a LARR-V Digital Co-ordinatograph. The resulting daily temperature record consisted of the maximum and minimum air temperatures and the corresponding slab surface temperatures, respectively.

Though the use of Kansas temperature data for the development of slab temperature equations for Indiana pavements may be questioned, it was shown by Arndt that, according to the Weather Bureau records, half of the 48 contiguous states have temperatures similar to Kansas. With respect to the range of summer temperatures, average winter temperatures and amount of sunshine, it was noted that Indiana and Kansas have similar characteristics (8). Hence, as a first approximation, the use of Kansas temperature data for simulating temperature variations in Indiana pavements is quite justified.

The proposed regression analysis model for developing estimation equations for maximum and minimum slab surface temperatures is given as:

$$\begin{aligned} Y = {} & b_0 + b_1x_1 + b_2x_2 + b_3x_3 + b_4x_1 \cdot x_2 \\ & + b_5x_1 \cdot x_3 + \varepsilon \qquad \text{(E2)} \end{aligned}$$

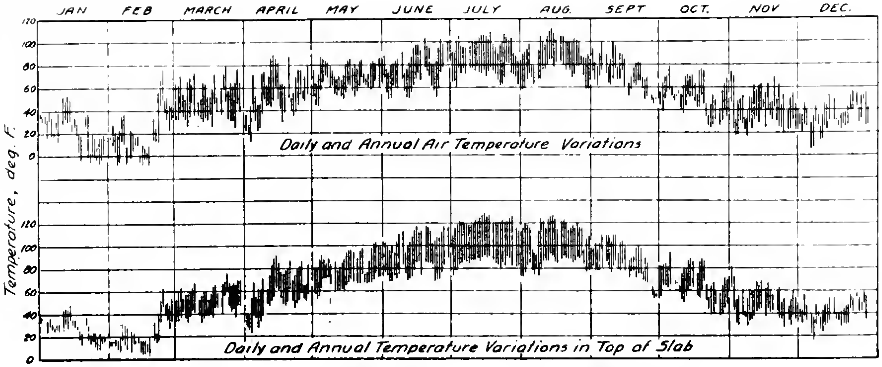

Air and Slab Temperature Data—1936

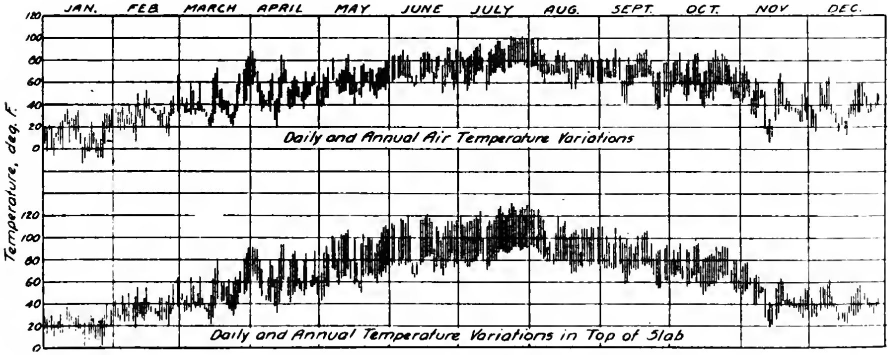

Air and Slab Temperature Data—1940

FIG. E 1. AIR AND SLAB TEMPERATURE
DATA - 1936 AND 1940
(FROM ARNDT)

where Y = slab surface temperature (^{o}F)

x_1 = dummy variable, used to show if 1936 data where significantly different from 1940 data

= 0 for 1936 data

= 1 for 1940 data

x_2 = air temperature (^{o}F)

$x_3 = \sin \frac{2\pi(t-294)}{365}$; radiation effect

t = time (in days); t for Jan. 1 = 0

$\vdots$

t for Dec. 31 = 364; normal yr.

= 365; leap year

$x_1 \cdot x_2$ = interaction of air temperature with years

$x_1 \cdot x_3$ = interaction of radiation effect with years

ε = residual, NID $(0,\sigma^2)$

Notes:

1. The inclusion of the terms x_1, $x_1 \cdot x_2$, $x_1 \cdot x_3$, in the model is a means of testing if the pooling of data observed over the two years, 1936 and 1940, is justified. This also provides an estimate of the temporal stability of the temperature model, although it should be recognized that sufficient data spanning a large number of years was not available. Therefore, the use of the model is justified only as a tool to obtain estimates of slab surface temperatures that are firstorder approximations of the actual slab surface temperatures.
2. The model assumes:
   a. The random errors are normally distributed with mean equal to zero.
   b. The random errors are independent of x's and have a constant variance (σ_E^2).

   These assumptions were found to be valid on examining the residuals obtained from the regression analysis.

The analysis of variance associated with the stepwise regression analysis is given in Tables E1 and E2 for maximum and minimum slab surface temperatures, respectively.

The final estimation equations, as used in this study, are:

$$T_p^{max} = 31.015 + 0.702\ T_a^{max} - 19.755 \sin \frac{2\pi(t-294)}{365} \qquad \text{(E3)}$$

$$T_p^{min} = 23.885 + 0.673\ T_a^{min} - 12.821 \sin \frac{2\pi(t-294)}{365} \qquad \text{(E4)}$$

where T_p^{max} = maximum slab surface temperature (^{o}F) at a given time, t.

T_p^{min} = minimum slab surface temperature (^{o}F) at a given time, t.

T_a^{max} = maximum air temperature (^{o}F) at a given time, t.

T_a^{min} = minimum air temperature (^{o}F) at a given time, t.

t = time (in days); t for Jan. 1 = 0
⋮
t for Dec. 31 = 364; normal yr.
= 365; leap yr.

Statistical attributes of these equations are presented in Tables E3 and E4. It is interesting to note that the regression coefficients of Equations E3 and E4 are approximately of the same order of magnitude as those obtained by Moulton and Schaub (44).

It is cautioned that these equations were developed only to permit approximate estimates of slab surface temperatures for use in this study. No attempt should be made to incorporate these equations in the design of concrete pavements, since these relationships are based on very limited data.

Table E1. Analysis of Variance Associated with Linear Multiple Regression Analysis of Maximum Slab Surface Temperature

*Significant at $\alpha = 0.01$, as tested by the sequential F-test.

Source of Variation	DF	Sum of Squares	Mean Square	F	R^2	Increase in R^2
X_2	1	555777.2	555777.2	16640.0*	0.908	0.908
X_3	1	33204.2	33204.2	994.1*	0.962	0.054
$X_1 \cdot X_2$	1	1506.7	1506.7	45.1*	0.964	0.002
$X_1 \cdot X_3$	1	8.8	8.8	0.3	0.964	0.00001
X_1	1	7.1	7.1	0.2	0.964	0.00001
Residual	656	21880.2	33.4			

Notes:
1. Y = Maximum slab surface temperature (^{o}F).
2. Variables are listed in the order they entered the step-wise regression.
3. X_1, $X_1 \cdot X_2$, $X_1 \cdot X_3$ not included in the final model because of minor increases in R^2 due to these variables.

Table E2. Analysis of Variance Associated with Linear Multiple Regression Analysis of Minimum Slab Surface Temperature

*Significant at $\alpha = 0.01$, as tested by the sequential F-test.

Source of Variation	DF	Sum of Squares	Mean Square	F	R^2	Increase in R^2
X_2	1	332958.1	332958.1	23647.6*	0.938	0.938
X_3	1	12448.1	12448.1	884.1*	0.973	0.035
X_1	1	115.2	115.2	8.2*	0.974	0.0003
$X_1 \cdot X_2$	1	33.8	33.8	2.4	0.974	0.0001
$X_1 \cdot X_3$	1	8.73	8.73	0.6	0.974	0.00002
Residual	656	9239.2	14.08			

Notes: 1. Y = Minimum slab surface temperature (^{o}F).

2. Variables are listed in the order they entered the step-wise regression.

3. X_1, $X_1 \cdot X_2$, $X_1 \cdot X_3$, not included in the final model because of minor increases in R^2 due to these variables.

Table E3. Statistical Attributes of the Regression Equation for the Maximum Temperature of the Concrete Slab Surface

. Dependent variable, T_p^{max} = estimated maximum slab surface temperature (^oF).

. Mean response = 75.01 °F

. Standard error of estimate, (S_E) = 5.96

. Coefficient of determination, (R^2) = 0.962

. No. of cases = 662

Independent Variable	Regression Coefficient	Standard Error	F*	$F_{(.01,1,659)}$	Variable Description
Constant	31.015	-----	------	----	-----------
T_a^{max}	0.702	0.019	1366.7**	6.69	Max. Air Temperature (^oF).
Sin $\frac{2\pi(t-294)}{365}$	-19.755	0.646	935.0**	6.69	Radiation Effects t = time (days)

* F-test for significance of regression coefficient; with model containing all independent variables.

**Significant at $\alpha = 0.01$.

Table E4. Statistical Attributes of the Regression Equation for the Minimum Temperature of the Concrete Slab Surface

. Dependent variable, T_p^{min} = estimated minimum slab surface temperature (^oF).

. Mean response = 53.10 $^\circ F$

. Standard error of estimate (S_E) = 3.78

. Coefficient of determination (R^2) = 0.974

. No. of cases = 662

Independent Variable	Regression Coefficient	Standard Error	F*	$F_{(.01,1,659)}$	Variable Description
Constant	23.885	-----	--------	----	-----------
T_a^{min}	0.673	0.014	2212.0**	6.69	Min. Air Temperature (^oF).
Sin $\frac{2\pi(t-294)}{365}$	-12.821	0.434	873.0**	6.69	Radiation Effects t = time (days)

* F-test for significance of regression coefficient, with model containing all independent variables.

**Significant at $\alpha = 0.01$.

VITA

Asif Faiz was born on January 29, 1947 at Muzaffarabad, Azad Kashmir. He received his secondary education at St. Mary's Cambridge School, Peshawar, Pakistan and graduated with a School Certificate in 1962.

He entered the Engineering College, University of Peshawar in 1964, after a year of pre-engineering studies at Edwardes College, Peshawar. He received his Bachelor of Engineering (Civil) with Honors in 1968.

After a year of graduate studies at the Middle East Technical University, Ankara, Turkey, he came to Purdue University in 1969. In 1971, he received his MSCE degree.

Since 1971, he has been associated with Purdue University in the capacity of a research and teaching graduate instructor. He has taught in the areas of Airport Planning and Design, Pavement and Highway Engineering, and Transportation Engineering Economic Evaluation. In 1974, he was named an outstanding graduate instructor by the School of Civil Engineering, Purdue University and was awarded the Nellie Munson Award.

He has participated actively in professional and extracurricular activities. During 1973-74, he was the President of the ITE Student Chapter at Purdue University. He has won prizes from ASCE and ARBA for outstanding papers.

He is a graduate member of Institute of Engineers (Pakistan), an associate member of the American Society of Civil Engineers, a supporting member of Transportation Research Board, a student member of Institute of Traffic Engineers and a member of Sigma Xi Research Honorary.

He is married.

COVER DESIGN BY ALDO GIORGINI